AD

MEMORANDUM REPORT ARBRL-MR-02949

EFFECTS OF TERRAIN ON BLAST WAVES

John H. Keefer
George T. Watson
George A. Coulter
Vincent L. King

August 1979

US ARMY ARMAMENT RESEARCH AND DEVELOPMENT COMMAND
BALLISTIC RESEARCH LABORATORY
ABERDEEN PROVING GROUND, MARYLAND

Destroy this report when it is no longer needed.
Do not return it to the originator.

Secondary distribution of this report by originating or sponsoring activity is prohibited.

Additional copies of this report may be obtained from the National Technical Information Service, U.S. Department of Commerce, Springfield, Virginia 22151.

The findings in this report are not to be construed as an official Department of the Army position, unless so designated by other authorized documents.

The use of trade names or manufacturers' names in this report does not constitute indorsement of any commercial product.

UNCLASSIFIED

SECURITY CLASSIFICATION OF THIS PAGE *(When Data Entered)*

REPORT DOCUMENTATION PAGE

READ INSTRUCTIONS BEFORE COMPLETING FORM

1. REPORT NUMBER: MEMORANDUM REPORT ARBRL-MR- 02949
2. GOVT ACCESSION NO.:
3. RECIPIENT'S CATALOG NUMBER:

4. TITLE *(and Subtitle)*: EFFECTS OF TERRAIN ON BLAST WAVES
5. TYPE OF REPORT & PERIOD COVERED: Final
6. PERFORMING ORG. REPORT NUMBER:

7. AUTHOR(s): John H. Keefer, George A. Coulter, George T. Watson, Vincent L. King
8. CONTRACT OR GRANT NUMBER(s):

9. PERFORMING ORGANIZATION NAME AND ADDRESS:
USA Ballistic Research Laboratory
ATTN: DRDAR-BLT
Aberdeen Proving Ground, MD 21005
10. PROGRAM ELEMENT, PROJECT, TASK AREA & WORK UNIT NUMBERS: 1L162118AH75

11. CONTROLLING OFFICE NAME AND ADDRESS:
US Army Armament Research and Development Command
US Army Ballistic Research Lab (DRDAR-BL)
Aberdeen Proving Ground, MD 21005
12. REPORT DATE: AUGUST 1979
13. NUMBER OF PAGES: 223

14. MONITORING AGENCY NAME & ADDRESS *(if different from Controlling Office)*:
US Army Harry Diamond Labs
2800 Powder Mill Road
Adelphi, MD 20783
15. SECURITY CLASS. *(of this report)*: UNCLASSIFIED
15e. DECLASSIFICATION/DOWNGRADING SCHEDULE:

16. DISTRIBUTION STATEMENT *(of this Report)*

Approved for public release; distribution unlimited.

17. DISTRIBUTION STATEMENT *(of the abstract entered in Block 20, if different from Report)*

18. SUPPLEMENTARY NOTES

19. KEY WORDS *(Continue on reverse side if necessary and identify by block number)*

Blast waves	Reflection	Rising slopes
Diffraction	Small charges	Falling slopes
Non-ideal blast	Terrain Effects	

20. ABSTRACT *(Continue on reverse side if necessary and identify by block number)* (hib)

The results from a small charge model experiment based on real terrain are presented for various ground zero points. The model simulates a 125 kt weapon burst of a height of 300 m over the prototype terrain. A comparison is shown between the experimental blast waves and those predicted by currently used prediction methods.

DD FORM 1 JAN 73 1473 EDITION OF 1 NOV 65 IS OBSOLETE

UNCLASSIFIED

SECURITY CLASSIFICATION OF THIS PAGE *(When Data Entered)*

TABLE OF CONTENTS

LIST OF ILLUSTRATIONS

LIST OF ILLUSTRATIONS (CONT)

LIST OF TABLES

LIST OF TABLES (CONT)

I. INTRODUCTION

A Blast wave is known to change its typical level-ground peak pressure and waveform characteristics when it travels over hills or through valleys, or whenever the blast wave encounters non-level terrain[1-5]. On rising slopes or in converging valleys, there is an increase in pressure. On falling slopes there is usually the opposite effect - a decay of pressure at the front of the blast wave with some rounding off of the waveform after the initial pressure rise.

Many of the prediction techniques were developed in the mid 1950's[6] with very few verifying tests. The Ballistic Research Laboratory (BRL) has undertaken a program to evaluate the currently accepted prediction techniques[6] when applied to a combination of terrain features which might be present in a real field scenerio.

As a part of this program, a contract, DAA05-77-C-072, was awarded to Scientific Service, Inc (SSI) to design a suitable terrain model, to make instrumentation recommendations, and to make pressure-time predictions of blast wave histories for the test program. A prototype scenerio was furnished to SSI by BRL with a suggested weapon yield of 125 kt at a height of burst (HOB) of 300 m to be simulated by the test. A 1/500 scale was chosen which called for 454 g of bare spherical pentolite charges to be fired above the terrain model at 0.6 m height.

Reference 7 gives the detailed predictions made by SSI for the terrain model to be used. This is described in their contract report. The purpose of this report is to describe the experiment as conducted by BRL at the Socorro, NM test site operated by the New Mexico Institute of Mining & Technology and to compare the results with the predictions of blast waveforms as given by SSI. Differences between predicted blast wave values using current prediction techniques presented in Reference 6 and the test results will be highlighted.

1. *H. Polachek and R. J. Seeger, "Regular Reflection of Shocks in Ideal Gases" Navy Department, February 12, 1944.*
2. *W. Bleakney, "The Diffraction of Shock Waves around Obstacles and the Transient Loading of Structures", Princeton University Dept. of Physics Technical Report II-3, March 16, 1950.*
3. *D. White, "An Experimental Survey of the Mach Reflection of Shock Waves", Princeton University Dept of Physics Technical Report II-10, August 21, 1951.*
4. *K. Kaplan, "Effects of Topography in High Shock Strength Regions", URS Corporation, Burlingame, California, January 1965.*
5. *J. H. Keefer and D. Day, "Terrain Effects on Blast Wave Parameters", Ballistic Research Laboratories Report No. 1319, April 1966.* (AD #488080)
6. *K. Kaplan, N. R. Wallace, and A. B. Willoughby, "Effects of Topography and Shielding", Prepared as Section 501 and 502 "Nuclear Weapons Blast Phenomena (U)", DASA-1200, 1959.*
7. *K. Kaplan, "Effects of Terrain on Blast Prediction Methods and Predictions", Scientific Service, Inc, Report 7636-1 Draft, July 1977; Ballistic Research Laboratory Report ARBRL-CR-00364, January 1, 1978.* (AD #A051569)

II. EXPERIMENT

This Section has been divided into a description of the scaled terrain model and a discussion of the instrumentation used.

A. Terrain Model

The test site chosen was one north of the town of Socorro, NM operated by the New Mexico Institute of Mining and Technology. Construction of the terrain model and support during the test series were furnished to BRL by the New Mexico Institute.

The model to be built was based upon a real world combination of terrain features as given by Figure 1. In order to enhance the blast effects expected from this terrain model the vertical scale, given by Figure 1, was increased by five times before being scaled to the specific model dimensions.

The specific field case chosen was one in which a weapon of 125 kt yield would be fired at a height of 300 m above the ground. By means of cube root scaling[7], and the fact that about half the total weapons yield goes into blast, the weapon yield was scaled down to a 0.454 kg high explosive charge by a scale of 500 :1. The 300 m burst height becomes 0.6 m when scaled for the model. Figure 2 shows the contours for the 1/500th scale model. The 200 metre level of Figure 1 was taken at zero level for the model, Figure 2. The test model was limited to that portion shown with the labeled contours. Figure 3 shows the test site with a portion of the model in view.

The test blast lines were arranged so as to cover as many cases of rising slopes, falling slopes, and channeling as possible. The reference blast lines (nearly flat terrain), were arranged so that a reference station would correspond to each test station on each of the test lines to be recorded. Figure 4 shows a sketch of the location of blast lines A and B. Figures 5 and 6 show some of the transducer stations. Other blast lines are given in Figures 7-11. All blast line stations were measured at horizontal distances from ground zero.

Figure 11-A shows how the bare spherical 50/50 pentolite charges were hung in position from the firing stand over ground zero (GZ). Tie downs were used to restrain the charge to the 0.6 m height. Very light nylon hair nets were used to contain the charge. The detonator was always positioned backwards away from the reference blast line. RP80 exploding bridge wire detonators were used with two disks of 0.042 thick Data Sheet at the bottom of the detonator hole.

Figure 11-B shows the transducer block used at Station 1, directly under the charge. All transducers were electrically insulated with a nylon bushing from the lead mounting blocks. All mounting blocks were buried flush with the ground surface. All transducer cables were

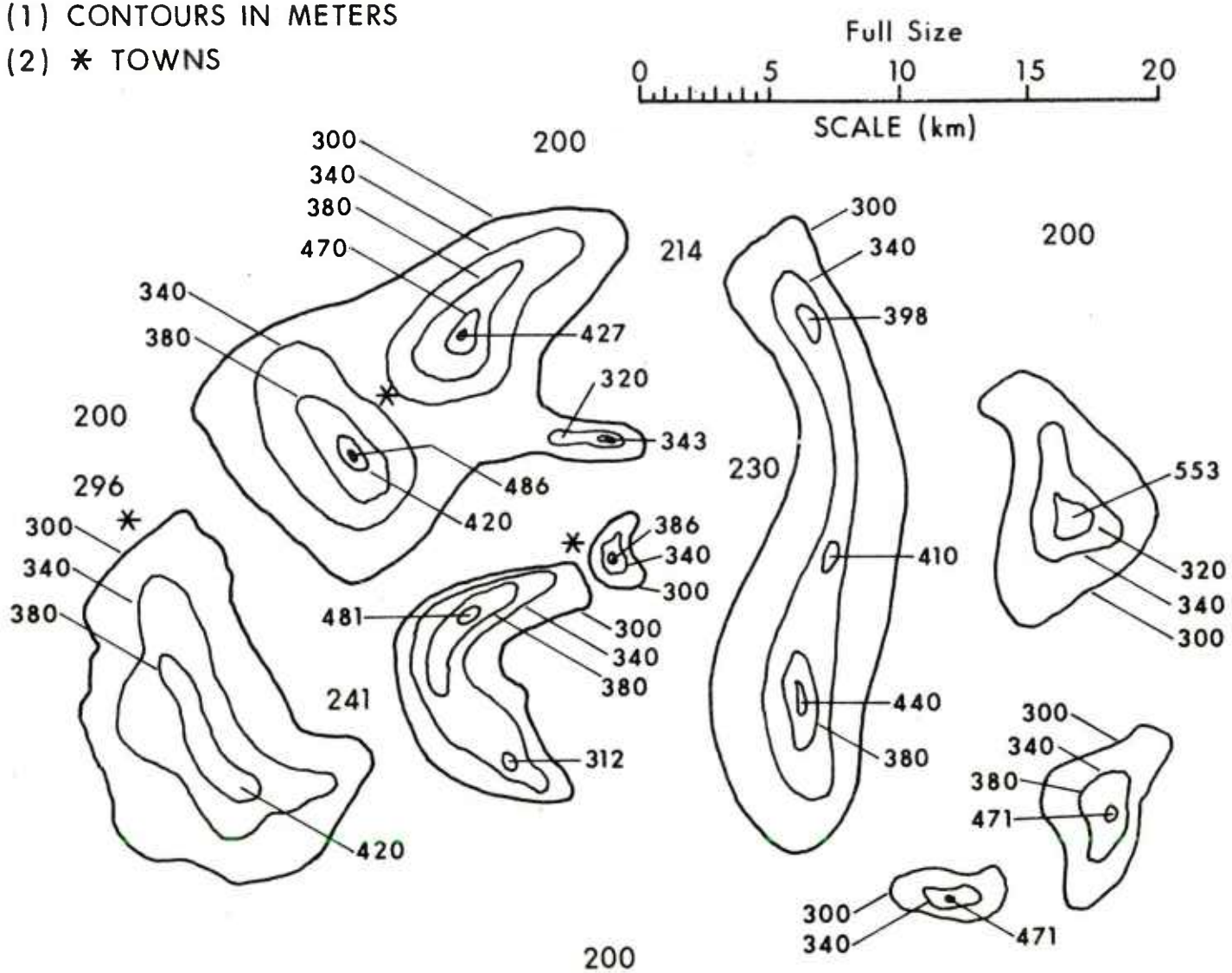

Figure 1. Full Scale Tarrain Contours

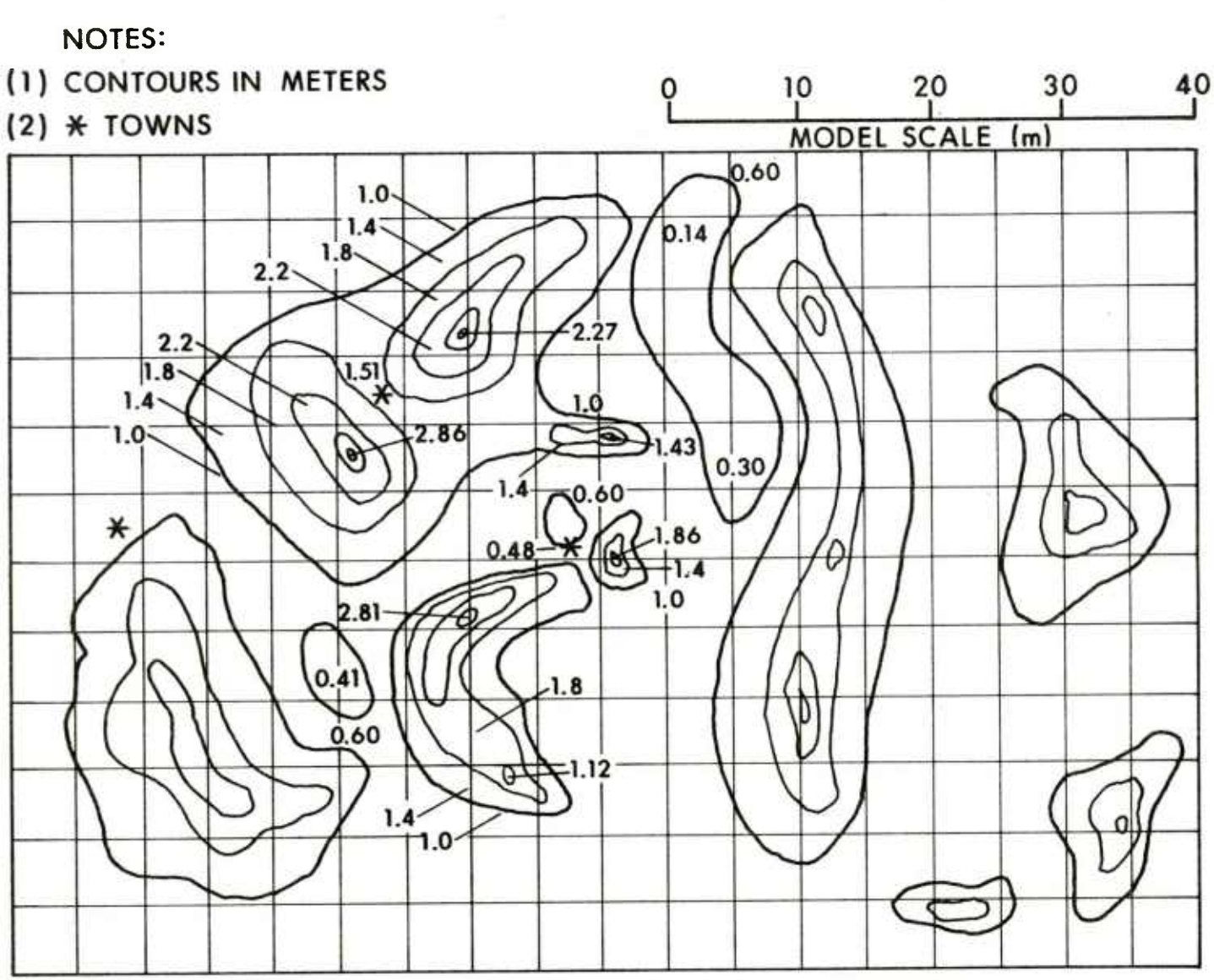

Figure 2. Contours for Tarrain Model (200 m full scale taken as zero level)

(A) VIEW OF SITE

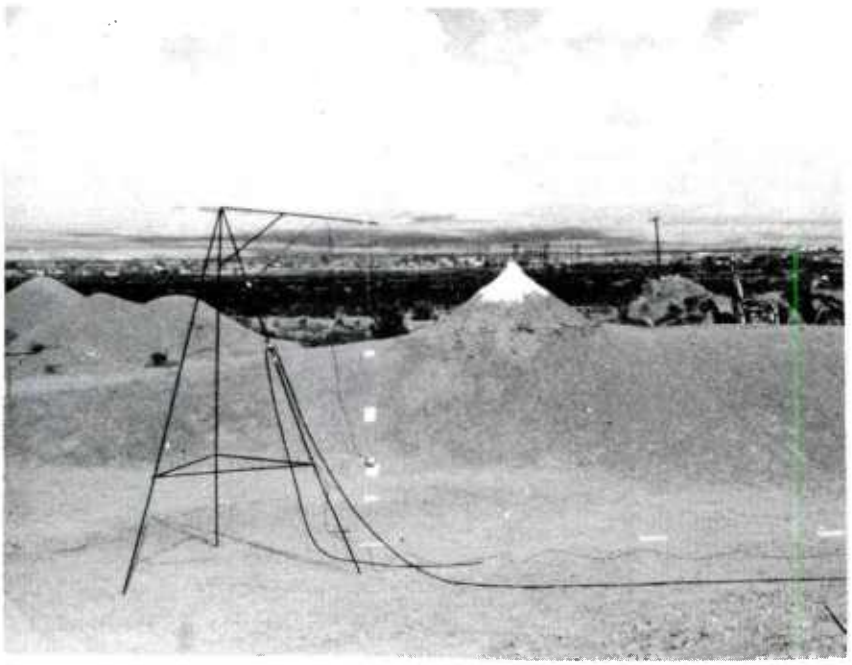

(B) LINES A-1 AND A-2

Figure 3. View of Socorro Test Site - Lines A-1 and A-2

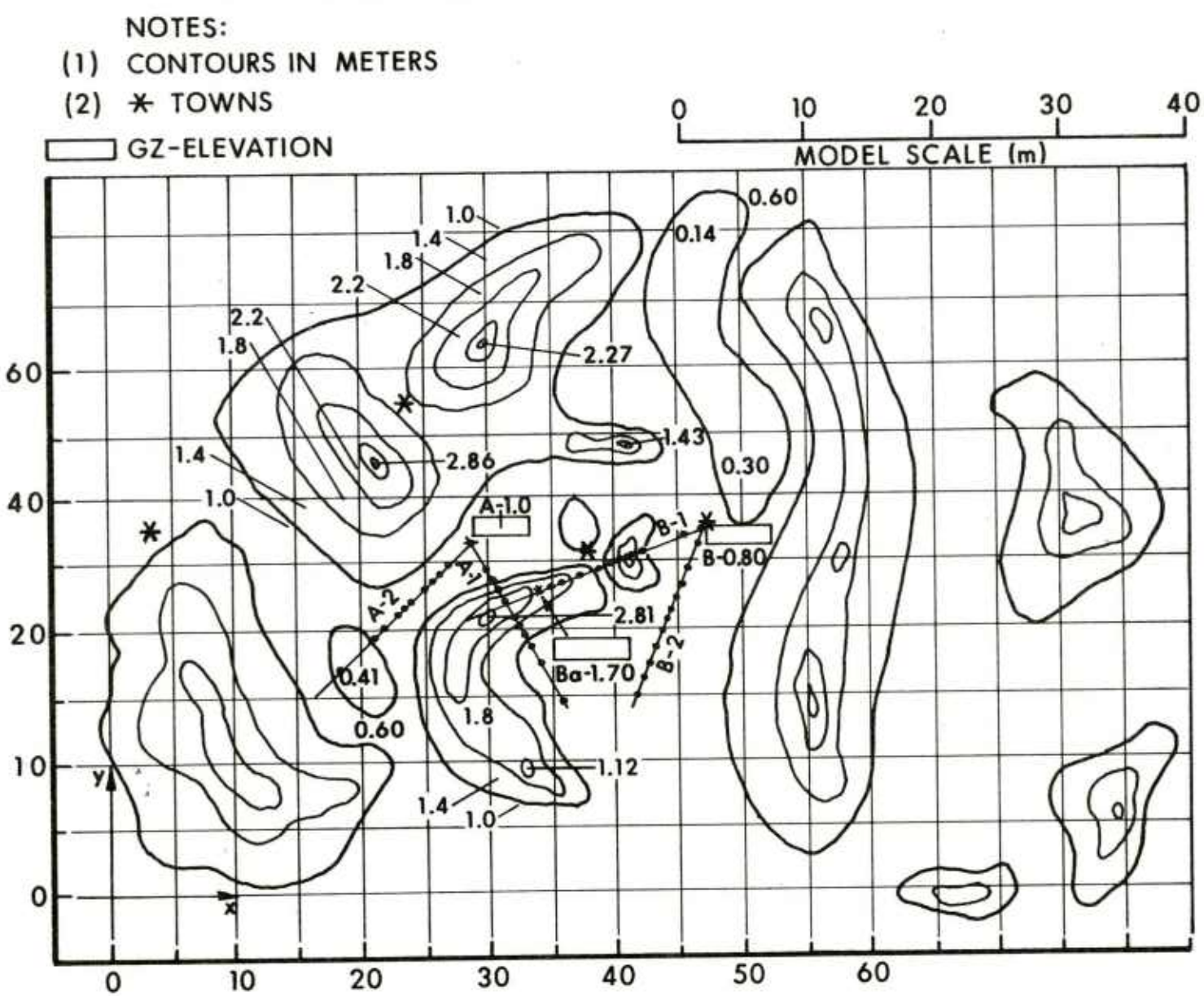

Figure 4. Plan View - Blast Lines A-1, A-2, B-1, and Ground Zeros A, B, and B_a

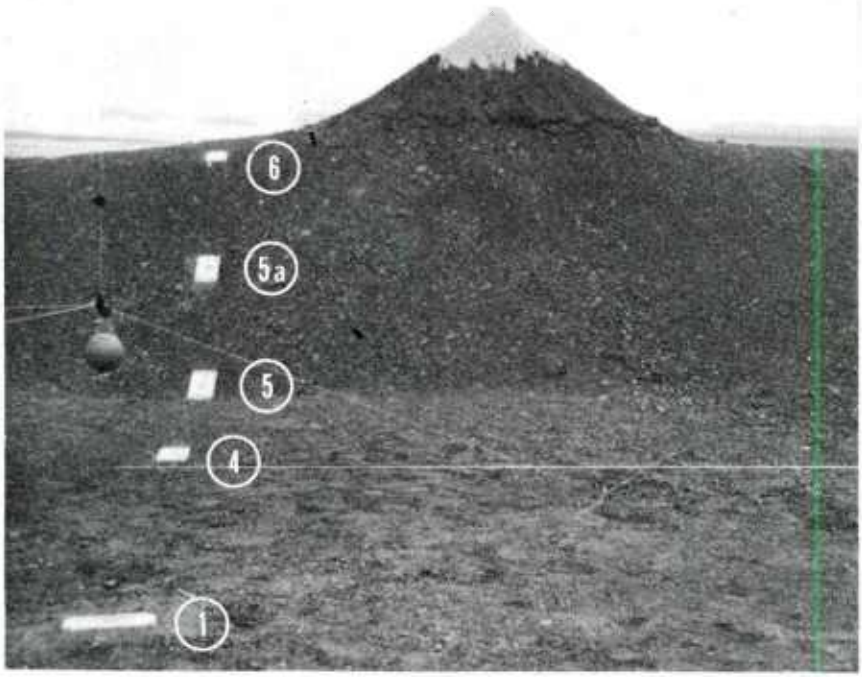

Figure 5. Photograph of Line A-1

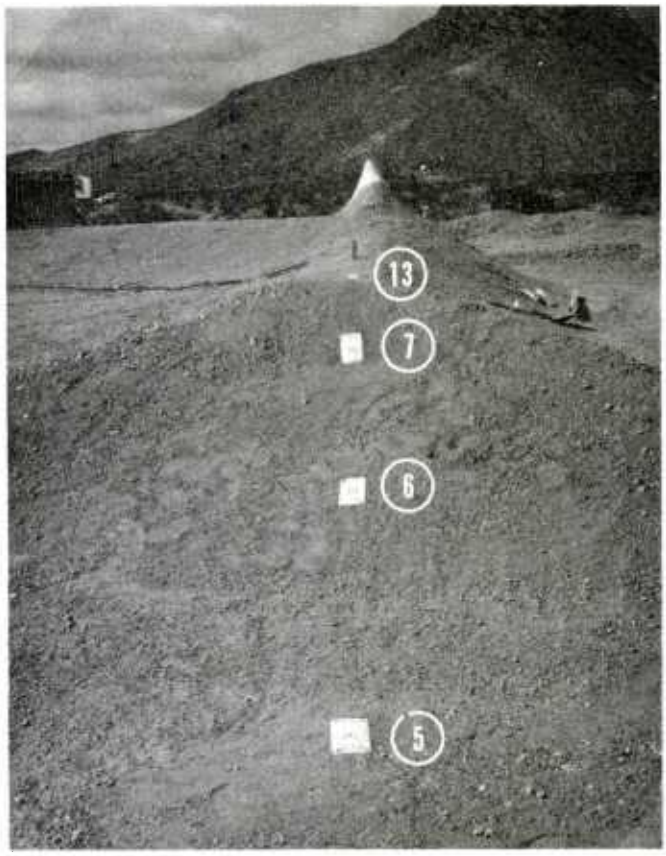

Figure 6. Photograph of Line B-1

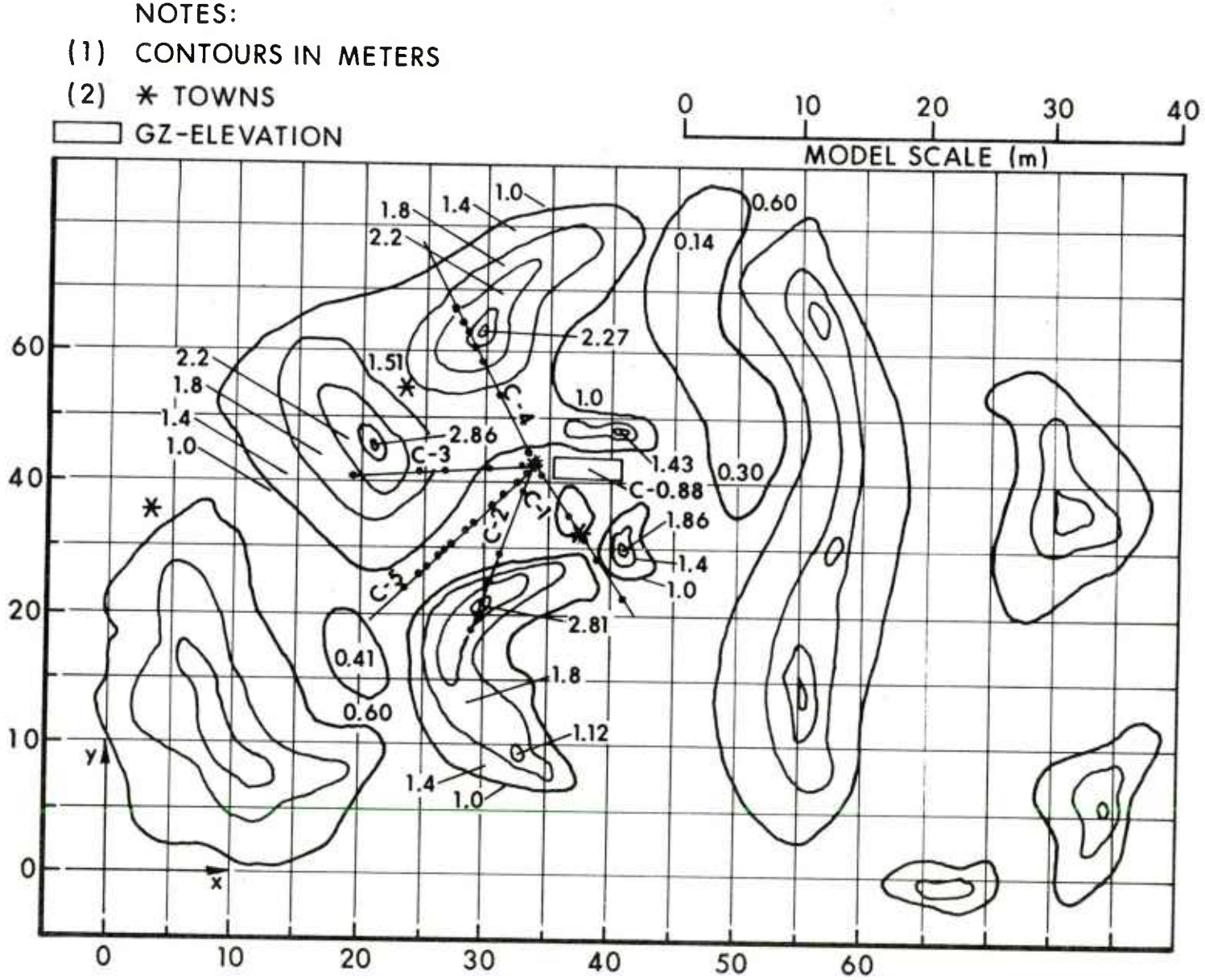

Figure 7. Plan View - Blast Lines C-1, C-2, C-3, C-4, C-5, and Ground Zero C

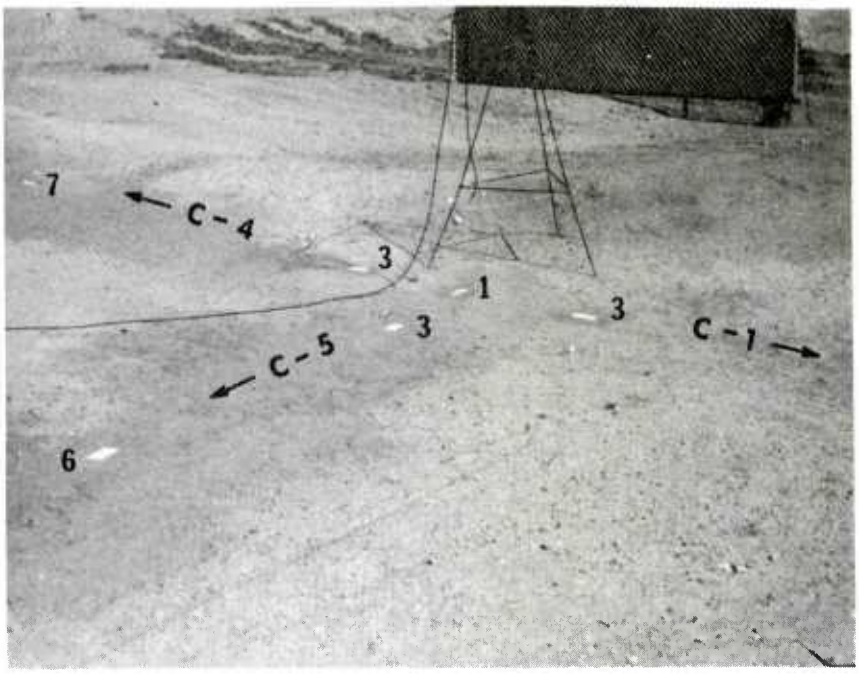

Figure 8. Photograph of Lines C-1, C-4, and C-5

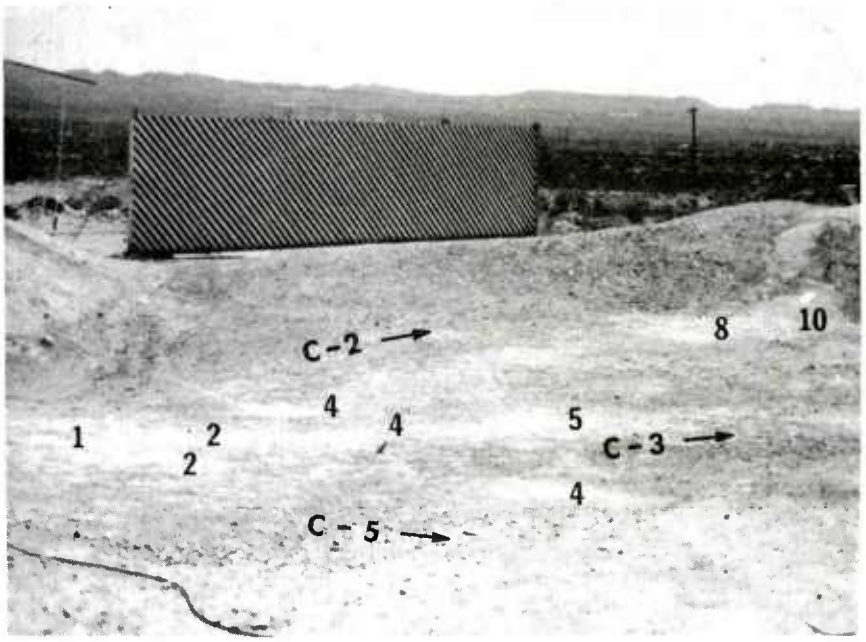

Figure 9. Photograph of Lines C-2, C-3, and C-5

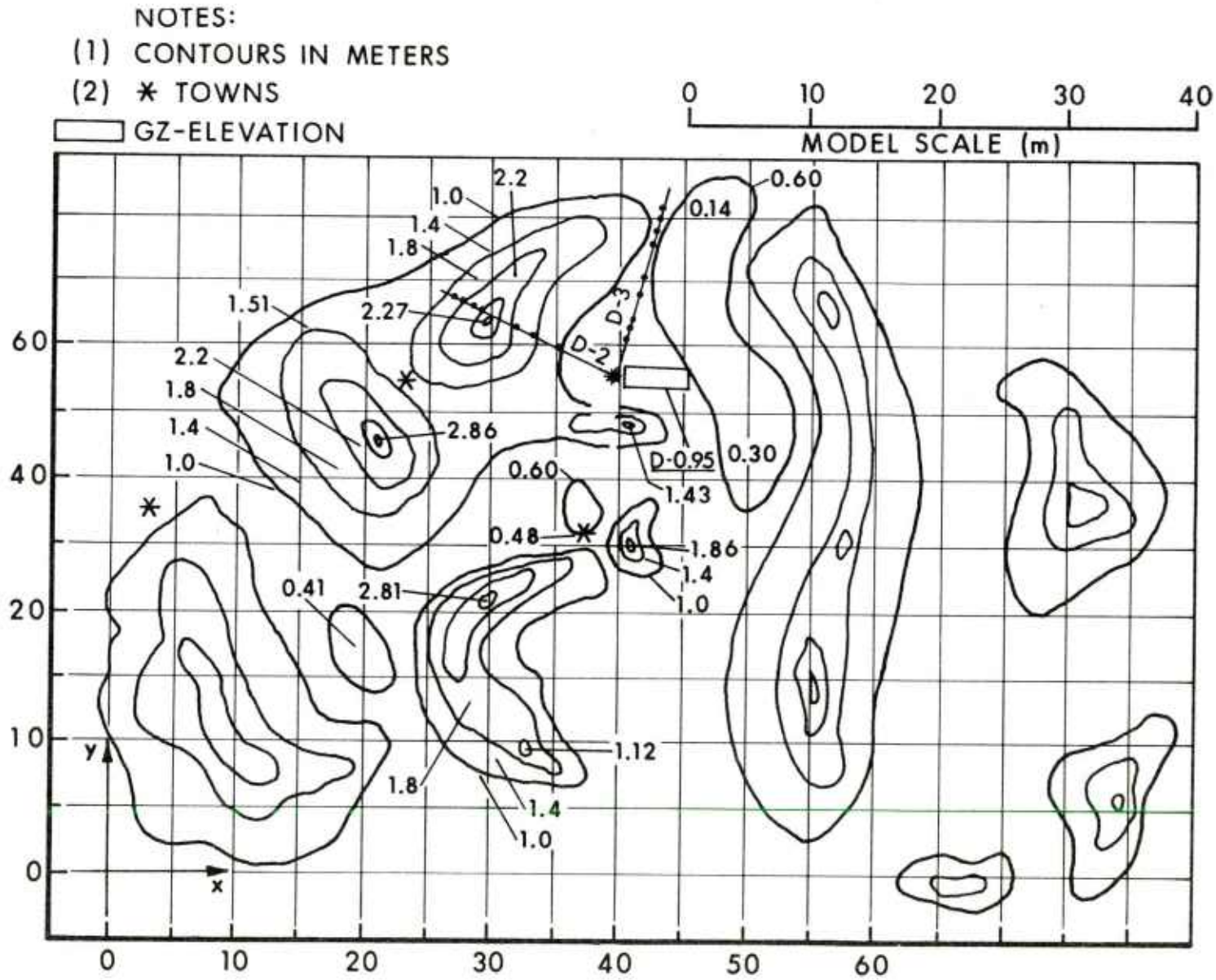

Figure 10. Plan View - Blast Line D-2, D-3, and Ground Zero D

(A) CHARGE

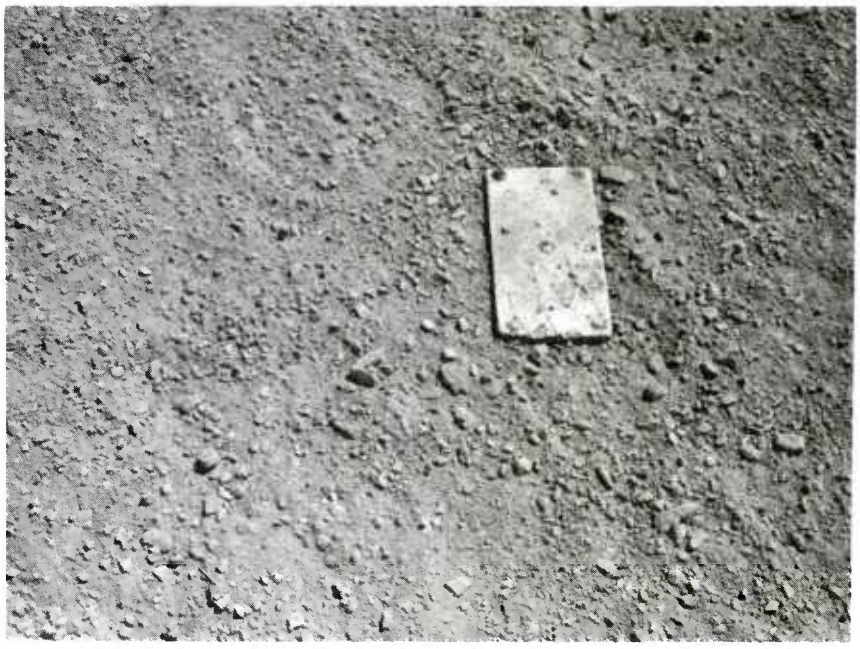

(B) TRANSDUCER BLOCK
POST-SHOT

Figure 11. Photograph of Change and Transducer Block

buried a few inches underground for the length of the blast lines, plus a length two or three metres beyond the last station. Cable noise on the recording channels was kept to a minimum in this way.

Transducer locations for each blast line are indicated in Table I for the shot sequences fired during the test program. All transducers on the test blast lines were matched at equal horizontal distances with those on the flat terrain reference blast lines. Table II gives a listing of pertinent information for the reference stations including predicted peak overpressure and duration of the blast wave.

B. Instrumentation

A block diagram of the data acquisition-reduction system is shown in Figure 12. Two types of high natural frequency crystal transducers were used for the tests. One group of transducers was PCB Piezotronics Series 113A and the other was Susquehanna Instruments Model ST-4, 10,000. Both have crystal elements, quartz and tourmaline, respectively. The PCB series has built-in amplifiers and the ST-4 series uses external ones. All transducers were mounted in lead bricks with nylon bushings to electrically insulate the transducers from the ground. RG-58 coaxial cable was used to connect the transducers to the tape recorders in the recording trailer located about 250 m from the test site.

Honeywell 7600, 80 kHz tape machines were used to record and play-back the pressure-time signals from the transducers. An oscillograph provided a quick look at the analog data at the test site. Final data reduction converted the FM analog signal to digital which was converted by computer to engineering units, listed, and then plotted.

III. RESULTS

The results are presented in two parts, pressure-time traces for each transducer station and tables of blast parameters.

A. Pressure-Time Traces

A total of twenty shots was fired according to the shot sequence given in Table III. Some trouble was experienced by misfires as noted by the missing shot numbers. Initially, the firing line from the field firing set was about 250 m long from the instrumentation trailer to the test site firing position (GZ). The problem of misfires was corrected by moving the firing set to the edge of the test site, about 10 m from GZ. The longer firing line apparently dropped the 5000 VDC firing voltage to a lower value which just allowed the bridge wire to burn and not to explode. The pentolite charge did not detonate but simply shattered into a great many pieces. The shorter firing line, in any case, corrected the problem of misfires.

Table I. Location of Transducers for Each Blast Line and Ground Zero

Station Number	Ground Zero Gauge Line Distance (m)	Shots 1, 2, & 5 A			Shots 8, 9, & 10 B			Shots 11 & 12 B_a	Shots 13, 14, & 15 C			Shots 16, 17, & 18 C			Shots 19 & 20 D		
		A-1		A-2*	B-1		B-2*	B-1	C-1	C-4	C-5*	C-2	C-3	C-5*	D-2		D-3*
		(X Indicates transducer location)															
1	0	X	----	X	X	----	X		X	X		X	X		X	---	X
2	0.8												X	X			
3	1.2						X		X	X	X						
4	2.0	X		X								X		X			X
5	3.3	X		X	X		X						X	X			X
5a	4.1	X		X													
6	5.0	X		X	X		X	X	X		X				X		X
7	6.2	X		X	X		X	X		X	X						
8	7.0	X		X	X		X	X	X		X	X	X	X	X		X
9	7.8	X		X	X		X	X									
10	9.0	X		X	X		X	X	X	X	X	X	X	X	X		X
11	10.7	X		X	X		X	X		X	X	X		X			
12	12				X		X			X	X	X		X	X		X
13	12.8				X		X	X	X	X	X				X		X
14	13.2														X		X
15	14.0	X		X			X	X				X	X	X	X		X
Total Channels Per Shot		22			22			8	21			21			18		

*Reference lines.

Table II. Reference Blast Line

Station Number	Distance from GZ (m)	Distance Between Stations (m)	Flat Terrain Overpressure* (kPa)	Flat Terrain Overpressure* psi)	Positive Pressure Pulse Duration* (m)
1	0		13,800	2000	-
2	0.8	0.8	2,070	300	0.2
3	1.2	0.4	690	100	0.6
4	2.0	0.8	210	30	1.6
5	3.3	1.3	70	10	2.3
5a	4.1	0.8	46	6.7	2.7
6	5.0	0.9	33	5	3.0
7	6.2	1.2	24	3.5	3.2
8	7.0	0.8	21	3	3.4
9	7.8	0.8	17	2.5	3.6
10	9.0	1.2	14	2	3.8
11	10.7	1.7	10	1.5	4.0
12	12.0	1.3	9.0	1.3	4.2
13	12.8	0.8	8.0	1.2	4.2
14	13.2	0.4	7.5	1.1	4.3
15	14.0	0.8	7.0	1.0	4.3

*Predicted values.

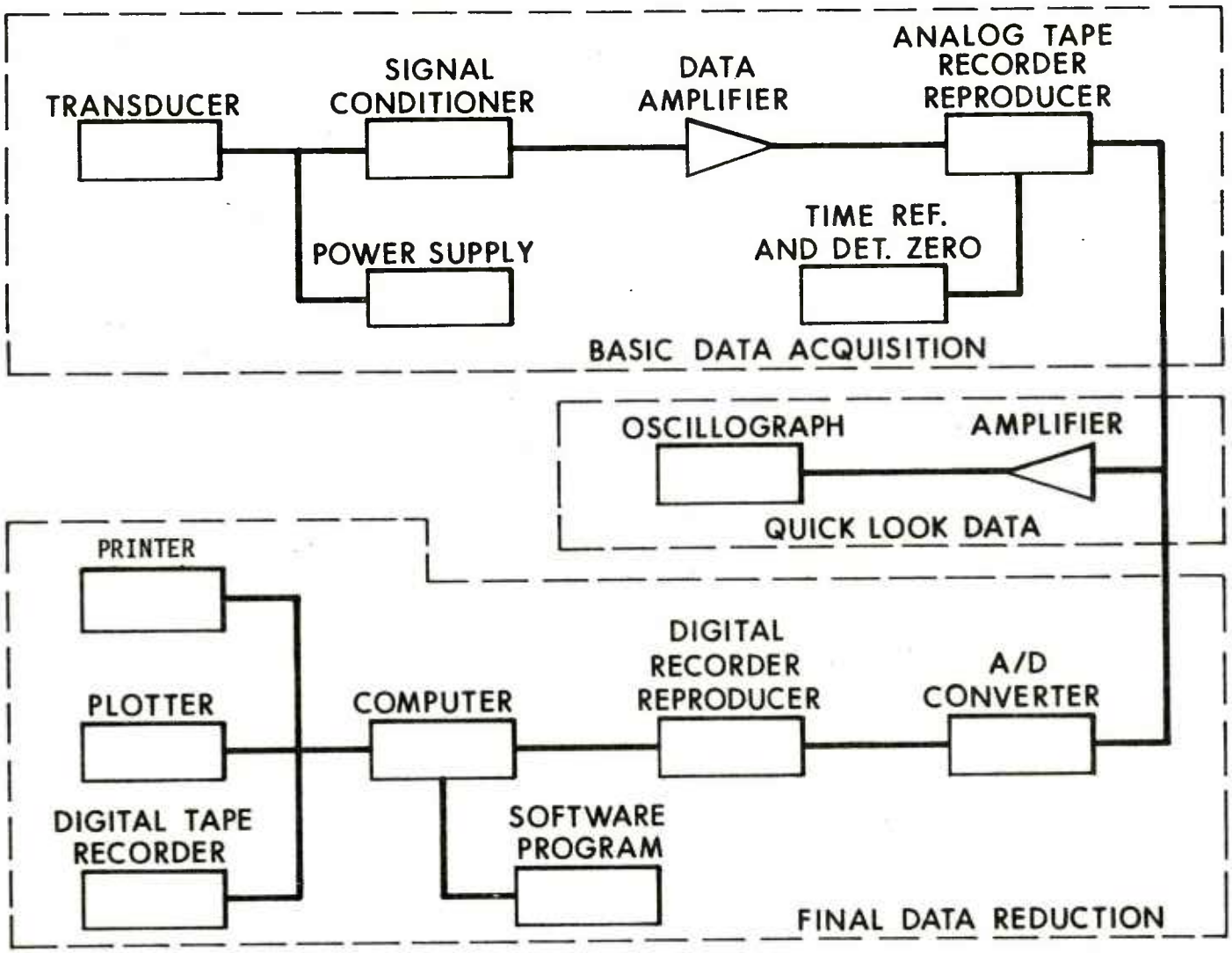

Figure 12. Data Acquisition - Reduction System

Table III lists the successful shots with pertinent charge data, blast line location, and ambient atmospheric conditions at shot time.

Typical pressure-time traces are given in Figures 13-15. Figure 13 and 14 are taken from Line A-1; Figure 15 is from Line C-1. The first group of traces show the narrow reflection peak caused at the beginning of a rising slope and the change with distance as the blast wave travels up the slope.

The second group of traces, Figure 14, illustrates the rounding of the waveform as the blast wave traveled down the falling slope. Note that the initial blast front is strongly degraded for stations just over the crest of the hill. The blast wave tends to recover to a more classical wave shape (as shown by the reference line) as the blast wave moves farther down the slope.

The third set of records, Figure 15, from Line C-1 illustrate what happens when the blast wave is channeled through a valley. The pressure-time trace show peaked waveforms vary similar to the flat terrain reference line. A more complete set of pressure-time traces is presented as Appendix A.

B. Blast Parameters

The measured blast parameters are listed in Tables IV-IX according to blast lines and shot numbers. Ground range was measured horizontally from ground zero, directly under the explosive charge, to the transducer's location. This distance is equal to that of the corresponding transducer on the reference flat terrain blast line. Thus the blast parameters obtained from the two lines can be compared.

Elevation was measured from zero level chosen for the terrain model. It corresponds to the full scale 200 m level of Figure 2 in Section II. The slope angle (θ_s) was measured on a line drawn perpendicular to the contour at the transducer location.

Arrival time was measured from the time the charge was detonated to the arrival of the blast wave at the transducer station. Maximum overpressure was generally the initial peak value. Maximum blast overpressure did occur after the initial rise for blast records from some falling slope stations. The positive duration of the blast wave was measured from the initial rise of the overpressure to a time when it reached a zero value.

It should be noted that overpressure values presented are taken from raw data values, and have not yet been scaled to standard sea level conditions in this group of tables.

Table III. Record of Shots

Shot No.	Date Fired, 1977	Charge Type	Charge Wt, kg	HOB m	HOB ft	Ambient Pressure kPa	Ambient Pressure psi	Ambient Temp. °C	Ambient Temp. °F	Line No.	Wind km/h
1	4 Aug	Pentolite	.489	0.6	1.97	84.89	12.31	34.4	94	A-1 A-2	W @ 6.4
2	5 Aug	Pentolite	.487	0.6	1.97	85.10	12.34	35.6	96	A-1 A-2	SSW @ 1.6
5	9 Aug	Pentolite	.484	0.6	1.97	85.64	12.42	31.1	88	A-1 A-2	W @ 1.6
8	16 Aug	Pentolite	.481	0.6	1.97	85.43	12.39	31.7	89	B-1 B-2	SSW @ 12.5
9	17 Aug	Pentolite	.472	0.6	1.97	85.84	12.45	26.7	80	B-1 B-2	N @ 6.4
10	17 Aug	Pentolite	.472	0.6	1.97	85.64	12.42	31.1	88	B-1 B-2	S @ 6.4
11	17 Aug	Pentolite	.485	0.6	1.97	85.37	12.38	31.1	88	Ba (B-1)	N @ 1.6
12	18 Aug	Pentolite	.472	0.6	1.97	85.30	12.37	29.4	85	Ba (B-1)	SW @ 4.3
13	22 Aug	Pentolite	.472	0.6	1.97	85.16	12.35	26.7	80	C-1 C-4 C-5	NE @ 0.3
14	22 Aug	Pentolite	.485	0.6	1.97	85.16	12.35	31.1	88	C-1 C-2 C-3	SSW @ 8.0
15	22 Aug	Pentolite	.472	0.6	1.97	85.02	12.33	32.2	90	C-1 C-4 C-5	SSW @ 3.2

Table III. Record of Shots (Continued)

Shot No.	Date Fired, 1977	Charge Type	Charge Wt, kg	HOB m	HOB ft	Ambient Pressure kPa	Ambient Pressure psi	Ambient Temp. °C	Ambient Temp. °F	Line No.	Wind km/h
16	24 Aug	Pentolite	.472	0.6	1.97	85.40	12.38	28.9	84	C-2 C-3 C-5	NE @ 4.8
17	24 Aug	Pentolite	.472	0.6	1.97	85.10	12.34	31.1	88	C-2 C-3 C-5	SW @ 11.3
18	25 Aug	Pentolite	.476	0.6	1.97	85.13	12.34	27.8	82	C-2 C-3 C-5	ENE @ 0.8
19	26 Aug	Pentolite	.472	0.6	1.97	85.16	12.35	30.0	86	D-2 D-3	SW @ 1.6
20	26 Aug	Pentolite	.485	0.6	1.97	84.76	12.29	34.4	94	D-2 D-3	SSW @ 16.1

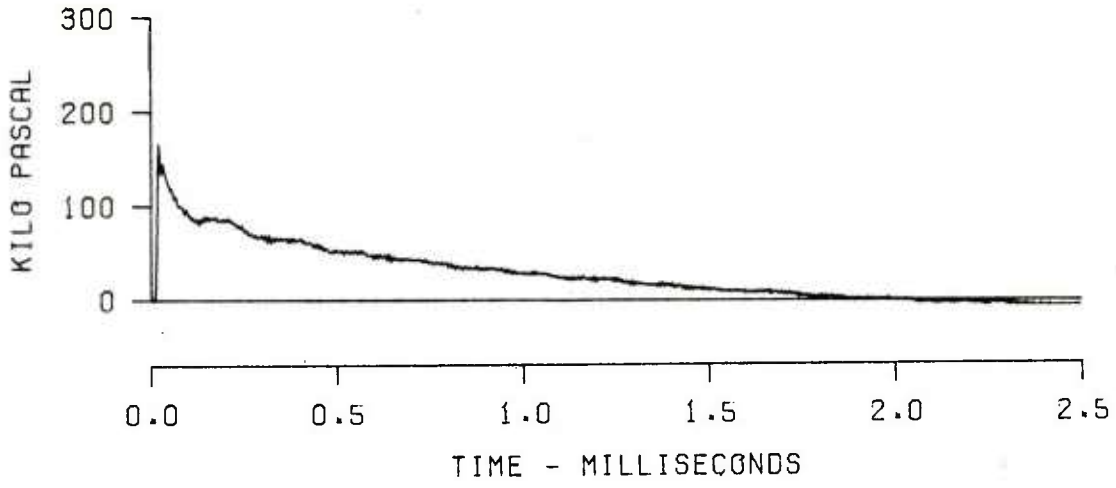

(A) SHOT 2 , LINE A-1 , STATION 5

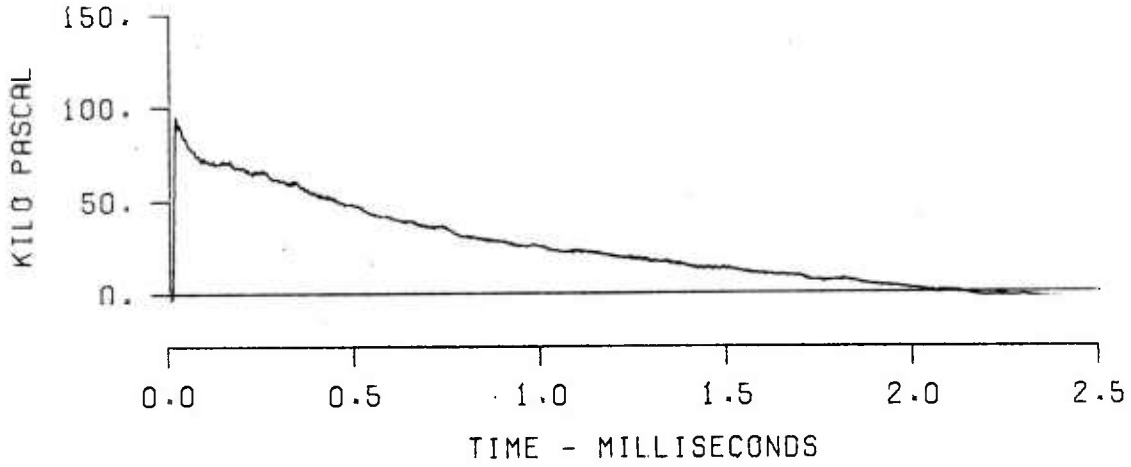

(B) SHOT 2, LINE A-1, STATION 5A

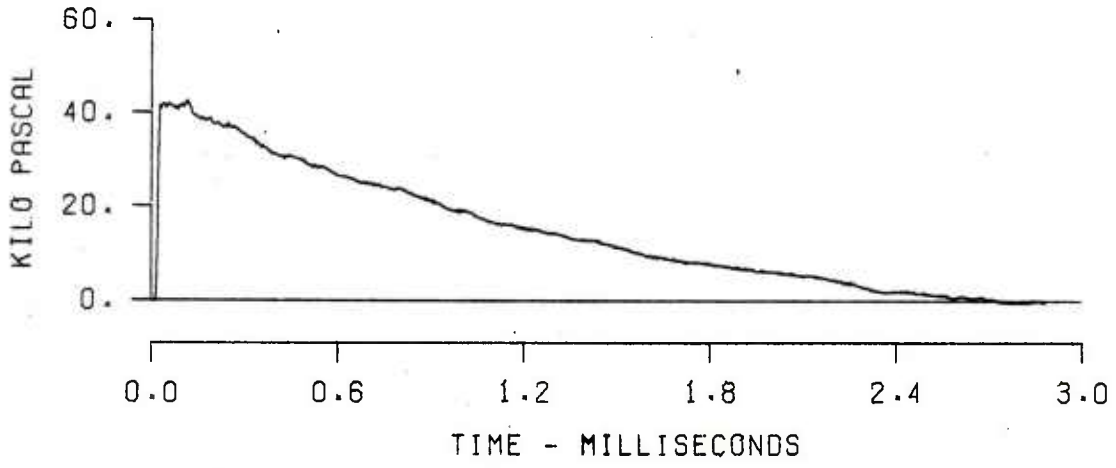

(C) SHOT 2 , LINE A-1, STATION 6

Figure 13. Records from Rising Slopes

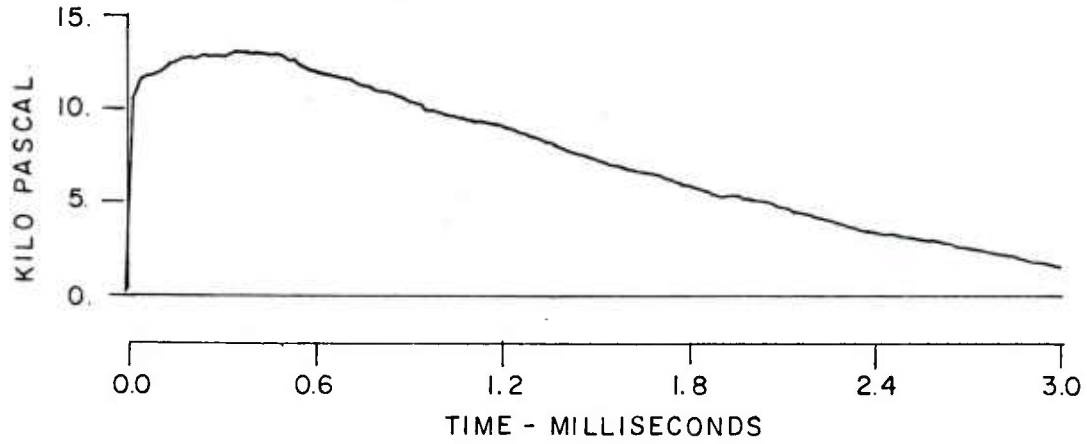

(A) SHOT 2, LINE A-1, STATION 7

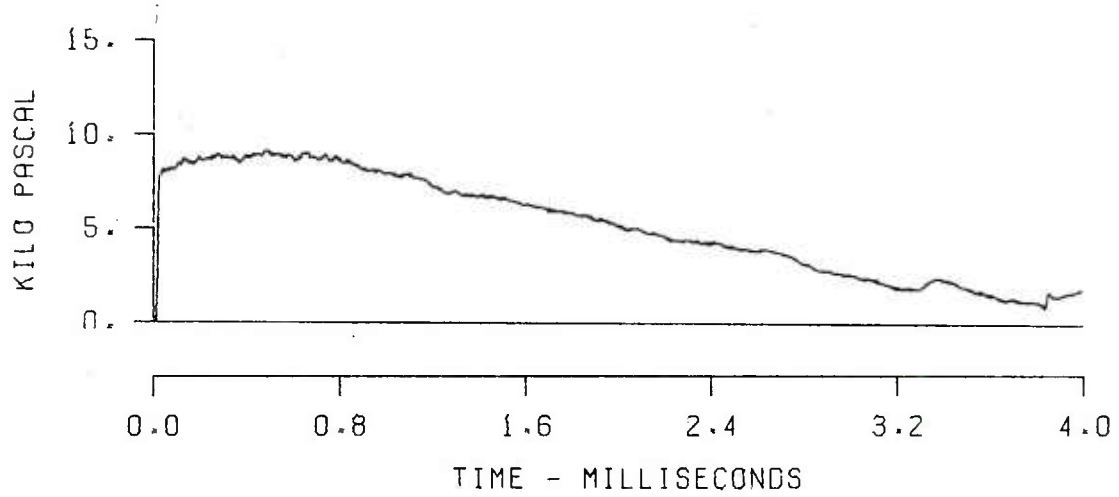

(B) SHOT 2, LINE A-1, STATION 8

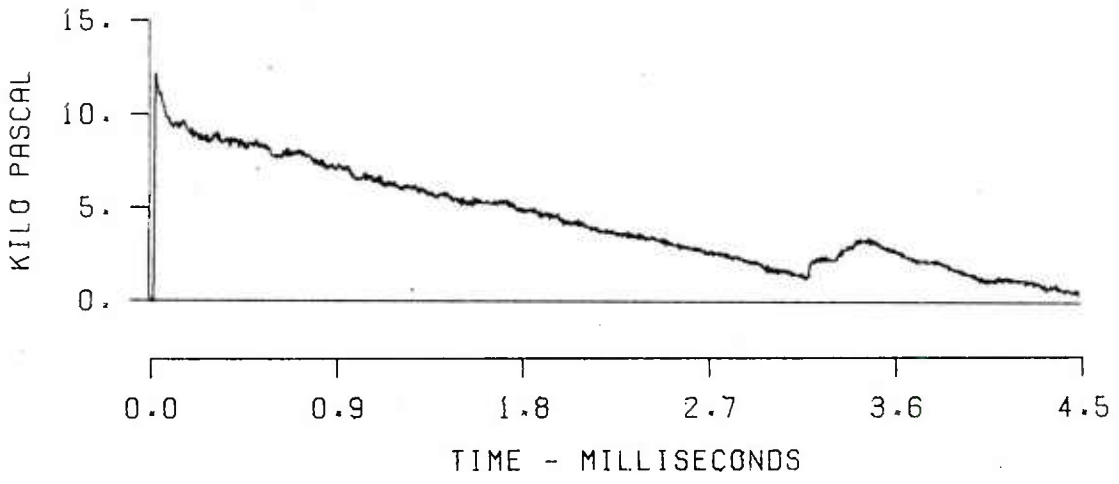

(C) SHOT 2, LINE A-1, STATION 9

Figure 14. Records from Falling Slopes

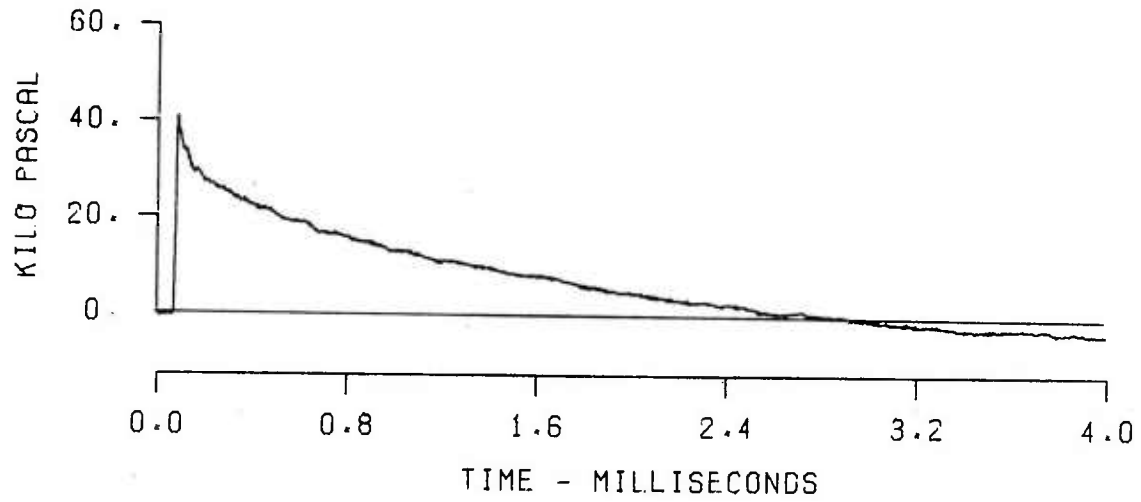

(A) SHOT 14, LINE C-1, STATION 8

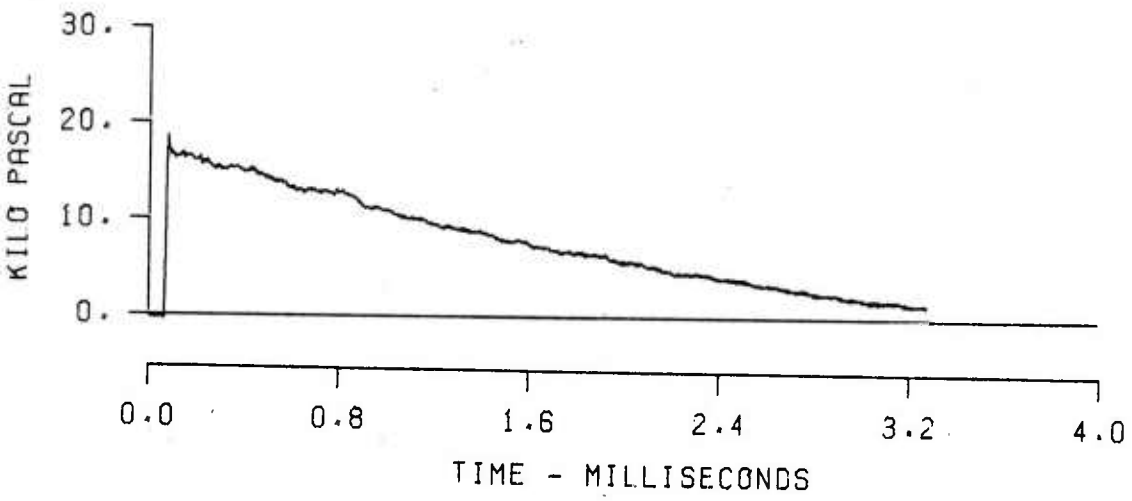

(B) SHOT 14, LINE C-1, STATION 10

Figure 15. Records from Channeling

Table IV. Blast Parameters - Lines A-1 and A-2*; Shots 1, 2 and 5

Station	Ground Range (m)	Elevation (m)	Slope Angle (deg)	Arrival Time (ms)	Overpressure (kPa)	Positive Duration (ms)	Impulse (kPa-ms)
A-2-1	0	1.00	0	.22,.22,.24	-,13000,10500	.23,.19,.18	405,613,428
A-1-4	2.0	1.00	0	2.00,2.00,2.04	222,232,232	1.33,1.45,1.47	89.1,85.4,84.4
A-2-4	2.0	0.97	- 1	2.03,2.05,2.11	226,220, -	1.41,1.41,1.47	89.1,84.2,75.1
A-1-5	3.3	1.04	+29	4.52,4.50,4.79	173,165,162	2.04,2.04,1.95	75.2,71.4,70.4
A-2-5	3.3	0.96	-0.5	4.53,4.56,4.87	77.2,75.2,73.9	2.18,2.19,2.01	57.1,54.3,51.3
A-1-5a	4.1	1.47	+29	6.26,6.30,6.40	96.0,94.5,95.7	2.15,2.13,1.98	62.1,60.6,58.8
A-2-5a	4.1	0.95	-0.5	6.34,6.43,6.57	52.3,50.5,50.6	2.54,2.43,2.27	46.2,43.2,41.2
A-1-6	5.0	1.95	+10	8.51,8.57,8.67	40.7,40.4,38.8** 43.7,42.4,44.9***	2.78,2.72,2.63	45.3,42.3,42.6
A-2-6	5.0	0.93	-1.5	8.50,8.62,8.77	37.9,35.9,36.9	2.79,2.71,2.65	37.1,33.9,33.0
A-1-7	6.2	1.85	-24	12.8,11.8,12.1	10.9,10.0,10.2 14.2,13.3,13.3	3.82,3.85,3.53	- - -
A-2-7	6.2	0.87	- 3	12.1,11.6,12.0	24.6,22.8,22.2	3.35,3.28,3.69	32.0,27.9,28.8
A-1-8	7.0	1.40	-24	14.3,14.4,13.4	7.56,7.45,7.31 9.1, 8.94,9.39	4.72,5.49,4.54	21.5,21.6,20.5
A-2-8	7.0	0.84	- 2	13.6,13.8,14.0	19.7,19.0,19.1	3.36,3.62,3.89	- ,25.5,25.8
A-1-9	7.8	1.22	-16	17.4,16.4,16.8	12.3,12.1,11.1	4.87,5.51,4.79	21.5,19.7,19.2
A-2-9	7.8	0.81	- 2	16.7,15.8,16.2,	- ,14.2,14.3	3.52,3.84,3.81	- ,22.9,21.6
A-1-10	9.0	1.09	- 4	19.6,19.7,18.9	14.1,13.7,11.9	4.70,5.43,4.07	18.5, - , -
A-2-10	9.0	0.73	- 4	18.9,19.1,18.3	14.4,12.9,12.5	3.78,4.05,3.92	22.8, - , -
A-1-11	10.7	1.00	0	24.2,24.3,24.5	10.7,10.9,10.6	4.71,4.64,4.54	17.2,16.3,15.2
A-2-11	10.7	0.63	- 3	23.4,23.8,24.0	11.4,11.1, 9.7	4.84,4.69,4.31	19.5,17.0,16.0
A-1-15	14.0	1.00	0	33.1,33.3,33.6	7.32,7.82,.45	4.85,4.91,4.82	14.1,13.1,12.6
A-2-15	14.0	0.42	-35	- ,32.8,33.1	- ,7.60,6.68	- ,4.92,4.21	- , - , -

* Reference Line
** Initial Peak
*** Maximum Value

Table V. Blast Parameters - Lines B-1 and B-2; Shots 8, 9 and 10

Station	Ground Range (m)	Elevation (m)	Slope Angle (deg)	Arrival Time (ms)	Overpressure (kPa)	Positive Duration (ms)	Impulse (kPa-ms)
B-2-1	0	0.82	0	.22,.22,.22	12300,9600,11100	.24,.23,.24	517,392,491
B-2-3	1.2	0.78	- 2	.96,.97,.96	689,817,735	.76,.81,.83	131,134,127
B-1-5	3.3	0.83	0	4.63,4.65,4.63	76.1,78.6,72.2	2.06,2.11,2.14	52.3,53.1,52.5
B-2-5	3.3	0.67	-5.5	4.74,4.77,4.72	61.1,66.7,63.1	2.10,2.10,2.22	49.0,51.2,51.1
B-1-6	5.0	1.10	+19	8.58,8.61,8.60	55.3,57.8,53.3	2.54,2.54,2.58	40.5,40.6,39.4
B-2-6	5.0	0.56	-3.5	8.80,8.84,8.78	38.8,38.8,36.9	2.57,2.59,2.90	- , - , -
B-1-7	6.2	1.53	+42	11.5,11.6,11.6	65.3,67.6,63.4	2.38,2.34,2.31	39.3,40,6,39.3
B-2-7	5.9	0.45	- 5	11.9,12.0,11.9	20.2,22.4,20.2	3.17,3.17,3.21	26.6,27.1,26.2
B-1-8	7.0	1.66	-34	13.9,13.9,13.9	7.8,9.7,7.8 12.0,13.1,12.6	3.84,3.61,3.70	23.5,24.1,23.6
B-2-8	7.0	0.37	-5.5	14.0,14.1,14.0	18.3,19.7,17.7	3.37,3.30,3.30	22.9,23.3,22.8
B-1-9	7.8	1.27	-22	16.3,16.3,16.3	9.9,11.4,9.4	3.53,3.28,4.10	- ,21.3,20.1
B-2-9	7.8	0.33	- 3	16.1,16.2,16.1	15.9,17.3,15.9	3.41,3.24,3.24	21.8,22.5,21.9
B-1-10	9.0	0.81	+14.5	20.0,20.0,19.9	15.1,18.6,16.9	3.56,3.86,3.62	19.0,20.0,19.3
B-2-10	9.0	0.25	- 4	19.3,19.4,19.3	11.0,13.2,11.8	3.76,4.01,3.57	18.4,19.1,18.7
B-1-11	10.7	1.26	+15	24.1,24.1,23.9	17.0,16.6,17.5	3.80,3.57,3.76	17.5,18.1,17.4
B-2-11	10.7	0.15	-3.5	24.0,24.1,24.1	9.1,11.7,10.0	4.25,4.26,3.75	16.0,16.3,15.9
B-1-12	12.0	1.48	+ 5	27.6,27.5,27.5	10.1,12.8,10.2	4.19,4.06,4.16	14.8,15.3,15.1
B-2-12	12.0	0.07	-3.5	27.6,27.7,27.5	9.1,10.8,10.4	4.33,4.25,3.84	14.2,14.5,14.1
B-1-13	12.8	1.54	+ 6	29.8,29.8,29.7	8.89,10.9,8.39	4.25, - ,4.03	13.4, - ,13.2
B-2-13	12.8	0.01	- 4	29.7,29.9,29.7	6.40,7.94,7.83	- , - , -	- , - , -
B-2-15	14.0	-0.07	- 4	33.1,33.2,33.0	6.29,8.30,7.48	4.44,4.20,4.41	11.3,11.8,10.7

Note: Line B-2 is the reference line.

Table VI. Blast Parameters - Line B_a (B-1);

Shots 11 and 12

Station	Ground Range (m)	Elevation (m)	Slope Angle (deg)	Arrival Time (ms)	Overpressure (kPa)	Positive Duration (ms)	Impulse (kPa-ms)
B-1-15	0	1.67	- 6	.22, .22	[illegible] 000,10 300	.28,.23	512, 405
B-13	1.2	1.54	- 6	1.02, 1.00	700, 701	.77,.82	117, 127
B-1-11	3.3	1.26	-15	4.98, 4.94	53.0, 57.3	2.20, 2.20	43.2, 44.2
B-1-10	5.0	0.81	-14.5	9.37, 9.28	30.3, 30.1	3.25, 3.13	- , 38.7
B-1-9	6.2	1.27	+22	12.2, 12.10	-, 47.1	- , 2.41	- , 31.8
B-1-8	7.0	1.66	+34	14.2, 14.1	34.8 -, 38.4	2.32, 2.09	17.3, 31.1
B-1-7	7.8	1.53	-42	16.2, 16.5	[illegible].9, 6.5 [illegible].0, 11.2	3.90, 3.77	21.4, 21.4
B-1-6	9.0	1.10	-19	20.1, 20.0	.6, 13.8	4.40, 4.00	17.5, 18.1

Table VII. Blast Parameters - Lines C-1, C-4 and C-5 ; Shots 13, 14 and 15

Station	Ground Range (m)	Elevation (m)	Slope Angle (deg)	Arrival Time (ms)	Overpressure (kPa)	Positive Duration (ms)	Impulse (kPa-ms
C-1-1	0	0.90	0	.22,.22,.22	10600,1110,10000	.22,.24,.25	414,497,438
C-1-3	1.2	0.82	- 5	.97,.94,.95	747,727,701	.84,.86,.95	135,123,135
C-4-3	1.2	0.96	+ 2	.92,.90,.88	732,730,771	.77,.81,.89	129,125,134
C-5-3	1.2	0.86	+ 1	.98,.94,.93	645,621,689	.72,.86,.72	- - -
C-1-6	5.0	0.41	- 6	8.9,8.8,8.8	34.4,35.9,40.0	3.02,3.16,2.99	38.9 - ,40.5
C-5-6	5.0	0.95	+ 1	8.8,8.7,7.7	35.2,32.1,35.5	2.80,3.07,2.91	37.7,37.3,38.9
C-4-7	6.2	1.34	+ 6	11.7,11.5,11.5	26.9,27.3,30.5	3.55,3.08,3.21	28.2,28.0,28.0
C-5-7	6.2	0.97	+ 1	11.9,11.2,11.7	29.2,25.2,31.6	2.93,3.26,3.14	- ,29.5,30.3
C-1-8	7.0	0.60	+15	13.9,13.7,13.8	37.4,40.8,42.9	2.81,2.82,2.88	31.8,30.0,32.0
C-5-8	7.0	0.98	0	14.0,13.9,13.8	19.8,19.4,21.6	3.76,3.86,3.86	25.9,25.1,25.6
C-1-10	9.0	0.81	+ 4	19.0,18.9,18.8	19.7,18.6,18.8	3.70,3.71,3.67	26.7,25.8,27.1
C-4-10	9.0	1.95	+13	19.1,18.9,18.9	17.7,18.8,21.2	3.74,3.75,3.74	23.2,22.4,22.8
C-5-10	9.0	0.98	0	19.4,19.3,19.1	15.8, - ,16.0	4.22,4.35,4.09	21.7,21.4,21.5
C-4-11	10.7	2.20	+ 6	23.8,23.4,23.3	9.72,11.6,12.90	3.96,3.90,3.90	17.2,16.5,16.9
C-5-11	10.7	0.95	- 1	24.1,24.0,23.7	13.30,12.3,13.06	4.53,4.48,4.32	22.7,23.0,22.8
C-4-12	12.0	2.18	- 9	27.5,27.1,26.7	3.60,3.52,3.76 6.35,6.40,6.61	4.69,4.55,4.70	15.4,14.6,15.0
C-5-12	12.0	0.93	- 1	27.7,27.6,27.0	8.72,8.39,8.22	4.65,4.59,4.60	16.3,15.8,15.9
C-1-13	12.8	0.86	0	29.5,29.1,29.2	6.73,5.80,7.23 7.75,7.31,7.99	3.78,4.31,4.17	13.0,14.4,14.8
C-4-13	12.8	2.07	- 9	29.8,29.3,29.3	- , - ,5.83 4.45,4.37,6.07	- , - ,4.72	- , - ,14.1
C-5-13	12.8	0.90	- 2	29.9,29.8,29.6	8.31,8.00,8.16	4.67,4.79,4.60	15.5,15.7,15.4

Note: Line C-5 is the reference line.

Table VIII. Blast Parameters - Lines C-2, C-3 and C-5; Shots 16, 17 and 18

Station	Ground Range (m)	Elevation (m)	Slope Angle (deg)	Arrival Time (ms)	Overpressure (kPa)	Positive Duration (ms)	Impulse (kPa-ms)
C-2-1	0	0.90	0	.24,.22,.22	11600,11400,9300	.24,.28,.22	569, 409, 362
C-3-2	0.8	0.88	+ 1	.56,.55,.58	- ,2190,2030	- ,.55,.57	- , 212, 205
C-5-2	0.8	0.88	- 1	.56,.58,.58	- ,2290,1750	- ,.65,.62	- , 185, 192
C-2-4	2.0	0.83	+ 1	2.10,2.09,2.13	196,217,206	1.43,1.38,1.37	83.7,84.6,84.0
C-5-4	2.0	0.87	+ 1	2.10,2.11,2.12	222,207,215	1.29,1.38,1.42	82.1,85.1,73.7
C-3-5	3.3	0.94	+ 1	4.56,4.70,4.64	72.4,74.5,75.5	2.10,2.23,2.20	- - -
C-5-5	3.3	0.91	+ 2	4.57,4.72,4.70	86.1,81.0,85.9	2.05,2.08,2.03	53.5,55.0,56.5
C-2-8	7.0	0.99	0	13.8,13.9,14.0	20.0,21.2,20.8	3.77,3.80,3.88	25.6,25.2,25.7
C-3-8	7.0	1.26	+ 8	13.6,13.9,13.9	24.6,23.8,26.0	3.62,3.61,3.57	27.8,28.2,28.6
C-5-8	7.0	0.98	0	13.8,14.0,14.0	20.6,20.8,23.2	3.63,3.80,3.64	23.8,24.9,25.9
C-2-10	9.0	1.24	+24	19.1,19.3,19.3	32.7,32.3,33.9	3.34,3.30,3.54	23.7,23.2,25.0
C-3-10	9.0	1.60	+10	18.9,19.3,19.2	14.1,12.8,14.2	3.88,3.70,3.84	15.0,14.8,15.4
C-5-10	9.0	0.98	0	19.1,19.4,19.4	15.5,14.8,16.1	4.10,4.18,4.01	21.2,21.2,21.1
C-2-11	10.7	1.98	+24	23.8,24.1,24.1	23.1,20.4,23.6	3.56,3.63,3.53	21.1,20.6,21.1
C-5-11	10.7	0.95	- 1	23.7,24.1,24.1	9.87,9.46,9.96	4.32,4.43,4.38	17.7,17.1,17.5
C-2-12	12.0	2.19	-56	27.2,28.7,28.7	1.20,0.96,0.86 4.33,4.11,4.07 6.15,6.08,6.04	4.93,5.22,5.36	14.2,14.5,14.3
C-5-12	12.0	0.93	- 1	28.3,27.7,27.7	8.52,8.70,9.52	4.54,4.51,4.51	15.5,15.4,16.1
C-2-15	14.0	1.81	- 3	33.3,33.8,33.8	3.09,1.96,2.68 7.88,7.34,7.70	4.96,4.90,3.94	13.2,13.1,11.1
C-3-15	14.0	1.70	-11	32.8,33.7,33.4	1.37,1.26.1.53 4.29,4.23,4.42	5.25,5.29,5.10	11.9,11.7,12.0
C-5-15	14.0	0.83	- 2	32.8,32.7,33.3	6.24,6.09,6.66	5.15,5.11,5.04	14.0,13.5,13.8

Note: Line C-5 is the reference line.

Table IX. Blast Parameters - Lines D-2 and D-3; Shots 19 and 20

Station	Ground Range (m)	Elevation (m)	Slope Angle (deg)	Arrival Time (ms)	Overpressure (kPa)	Positive Duration (ms)	Impulse (kPa-ms)
D-2-1	0	0.92	0	.22, .22	11 200,11 700	.24, .24	420, 480
D-3-4	2.0	0.74	- 5	2.17, 2.12	213, 211	1.38, 1.33	81.8, 80.1
D-3-5	3.3	0.66	- 5	4.80, 4.71	69.8, 69.7	2.08, 1.99	50.9, 50.0
D-2-6	5.0	1.00	+3.5	8.76, 8.65	39.8, 39.2	2.60, 2.71	35.2, 34.9
D-3-6	5.0	0.61	- 2	8.79, 8.65	39.4, 39.7	2.94, 2.66	- , 32.8
D-2-8	7.0	1.20	+ 8	13.8, 13.8	27.1, 26.2	3.02, 3.17	25.4, 25.5
D-3-8	7.0	0.58	- 2	13.90, 13.7	21.9, 22.0	3.70, 3.52	25.7, 25.9
D-2-10	9.0	1.52	+ 9	19.17, 19.1	17.3, 16.3	3.89, -	21.1, -
D-3-10	9.0	0.54	- 1	19.11, 18.9	15.0, 15.8	3.84, 3.85	19.3, 19.2
D-2-12	12.0	2.20	- 2	27.33, 27.3	9.46, 9.24	3.94, 4.04	15.1, 15.1
D-3-12	12.0	0.52	- 1	27.21, 26.9	8.60, 9.84	4.28, 4.15	15.8, 15.8
D-2-13	12.8	2.10	-15	29.58, 29.6	3.35, 3.56 5.96, 6.00	4.58, 4.87	14.2, 14.8
D-3-13	12.8	0.50	0	29.39, 29.1	7.77, 8.80	4.50, 4.37	15.6, 15.1
D-2-14	13.2	1.99	-15	30.75, 30.8	2.21, 1.80 5.00, 4.92	4.80, 4.91	12.8, 12.5
D-3-14	13.2	0.50	- 1	30.52, 30.2	7.80, 8.34	4.36, 4.31	14.9, 14.9
D-2-15	14.0	1.79	-12	33.05, 33.1	3.03, 3.47 4.36, 4.50	5.30, 5.70	12.6, 12.9
D-3-15	14.0	0.52	0	32.66, 32.3	7.50, 8.28	4.48, 4.35	14.5, 14.3

Note: Line D-3 is the reference line.

C. High Speed Photography

High speed photographs were taken by two Fastex framing cameras running at about 2000 pps. Fields of view covered the area from ground zero to the end of the particular blast line being photographed. For this, a black and white diagionally striped backdrop was placed behind the blast line. When a blast wave travels along a terrain feature in front of the backdrops, the change in air density across the blast wave front will cause apparent bending of the straight diagonal lines on the backdrop. The method used is illustrated by the pictures in Figure 16.

The backdrop method worked quite well when the terrain feature was close to ground zero or for Line B-1. When the blast wave became weaker at the greater distances from ground zero, the blast wave was not visible on the backdrop.

Appendix B shows a more complete set of pictures from Shot 8, Line B-1 than given in Figure 16; it also shows a schematic of the camera positions.

IV. ANALYSIS

The analysis section will review briefly the prediction techniques that were used[7] to define the pressure-time records expected from the experiment. After scaling the data from the experiment, the data are compared with those predicted.

A. Prediction Techniques

Free field peak values of blast wave overpressure and positive durations pre-shot predictions were made for each station of the reference blast by means of the graph of Figure 17. The values of peak pressure, P(0), and positive duration τ, were used in Equation 1 to calculate points along the pressure-time profile for the blast wave along the flat reference blast line:

$$P(t) = P(0)\left[1-(t/\tau)\right] e^{-\alpha\, t/\tau}, \qquad (1)$$

where $\alpha = 1$ for $P(0) \leq 140$ k Pa and $\alpha = 0.04\, P(0)^{0.65}$ for $P(0) \geq 140$ kPa. A similar expression from Reference 8, Equation 2, may be used to define the pressure-time profile for a nuclear burst:

8. *H. L. Brode, "A Review of Nuclear Explosion Phenomena Pertinent to Protective Construction", The Rand Corporation, Santa Monica, California, May 1964.*

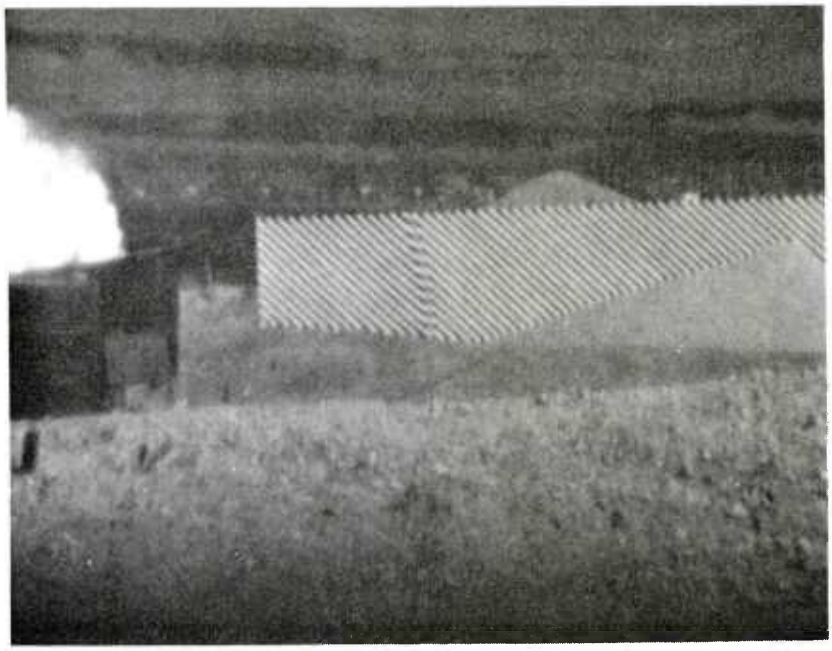

(A) TIME AFTER DETONATION - 6.2 ms

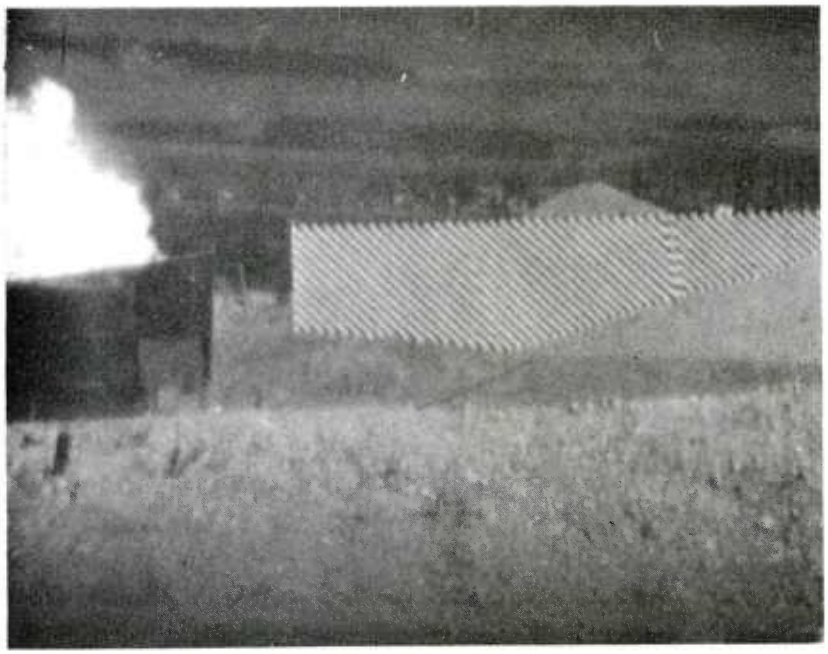

(B) TIME AFTER DETONATION - 10.6 ms

Figure 16. High Speed Photographs - Line B-1, Camera II

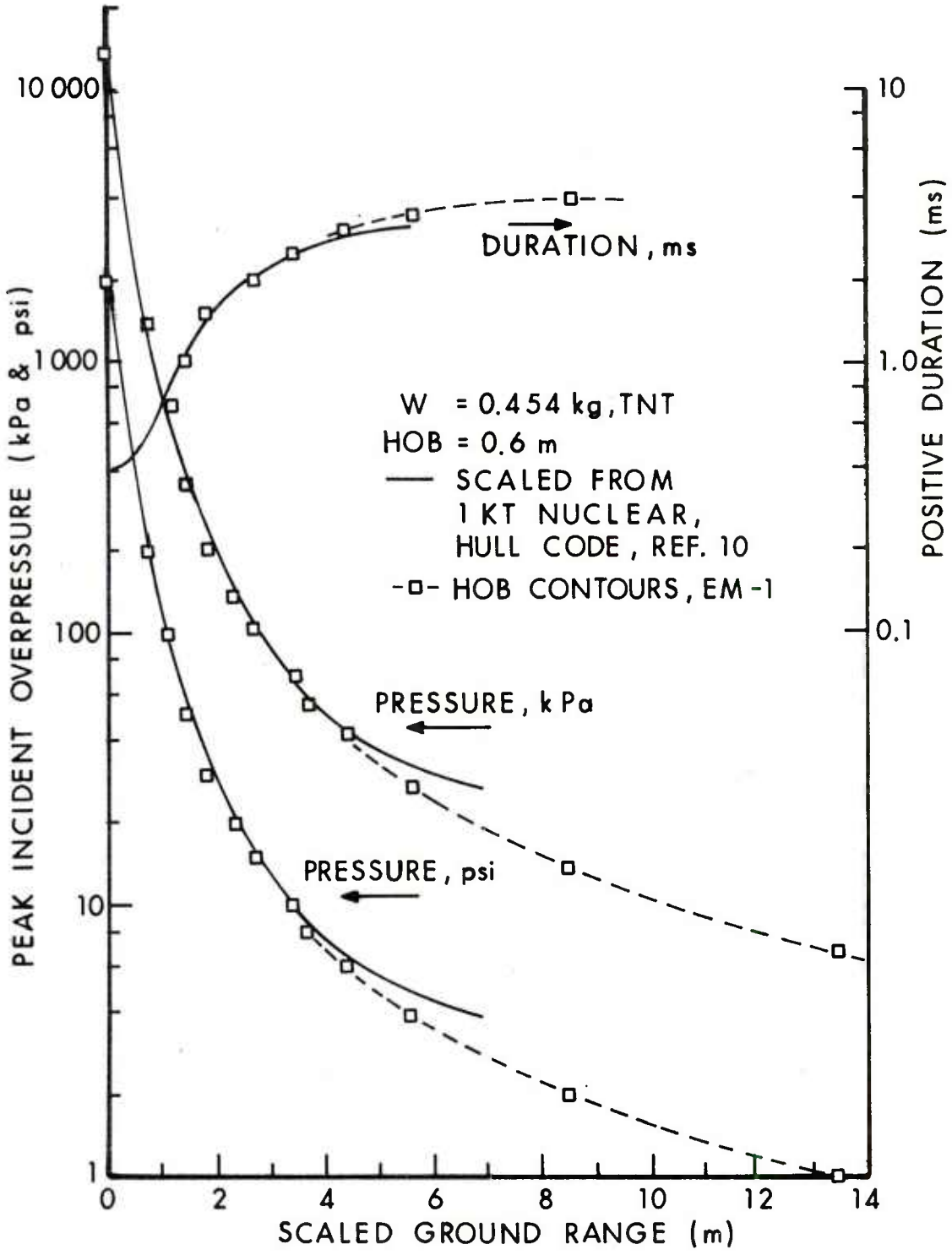

Figure 17. Reference Free-field Blast Parameters vs Ground Range

$$P(t) = P(0)\left[1 - (t/\tau)\right]\left[ae^{-\alpha t/\tau} + be^{-\beta t/\tau} + ce^{-\gamma t/\tau}\right], \quad (2)$$

where a, b, c, α, β, and α are functions of P(0), the initial incident peak overpressure.

The techniques used to predict the blast wave profile when affected by terrain features are divided into effects caused by rising slopes, falling slopes, and by valley channeling. Figure 18-A shows a blast wave approaching a slope from a non-normal direction to the slope contours. A modified slope angle is found for this general case. Figure 18-B shows a cross section of such a slope. ϕ is the angle between the blast wave's direction of travel and the normal to the terrain contour at the target (transducer) location. The slope angle of the terrain feature is defined as θ_s. The true slope angle, θ, as seen by the blast wave, is approximated by the easier to find angle, θ'[7]. The value of tan θ' may be found by combining the triangles of Figure 18-B to give the relationship shown as Equation 3:

$$\tan \theta' = \tan \theta_s \cos \phi, \quad (3)$$

where the angles are those defined in Figure 18. Table X lists some examples of these angles as given in Reference 7.

Figures 19-22 were then used to predict the terrain effect on the peak pressure and pressure-time history at a specific target location. The incident peak overpressure used for each of the figures is the value predicted for the flat terrain reference blast line. The predictions from Reference 7 are taken from two sources: (1) Whitham Theory and (2) results collected from previous small charge experiments. Both techniques are used to create the curves shown. The parameter t/L is calculated for times t, after the blast wave has arrival at the target station, a distance L, measured from the first slope change encountered on the terrain as measured from the level reference area. The wave shape behind the initial blast front was then predicted from a series of t/L values. After a time equivalent to a value of t/L of about 0.1 ms/m a smooth exponential delay was predicted by means of Equation 1 for the remaining postive duration, τ.

The peak pressure caused by the terrain effect of a valley is predicted directly from Figure 23 for a given combination of angles $\theta_1 + \theta_2$. If the direction of propagation is greater than 20 deg, then the terrain feature is to be treated as a series of slopes instead of a valley. The pressure-time history is found again from Equation 1 if the terrain is treated as a valley. Figures 20-22 would be used if the terrain effect is one of slopes combined with a valley.

Station C-1-10 was located in a V-type valley with a combined angle ($\theta_1 = 22°$ and $\theta_2 = 15°$)of 37°. This is somewhat different from that used for the pre-shot prediction for this station given in Reference 7. A new prediction was made for the slope angles as measured from the field model. Table XI lists the actual model slopes for all the stations used.

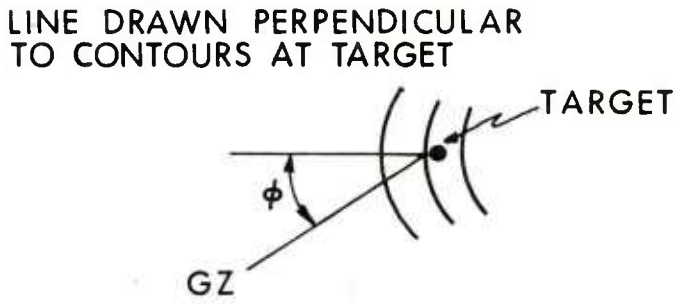

(A) TERRAIN FEATURE

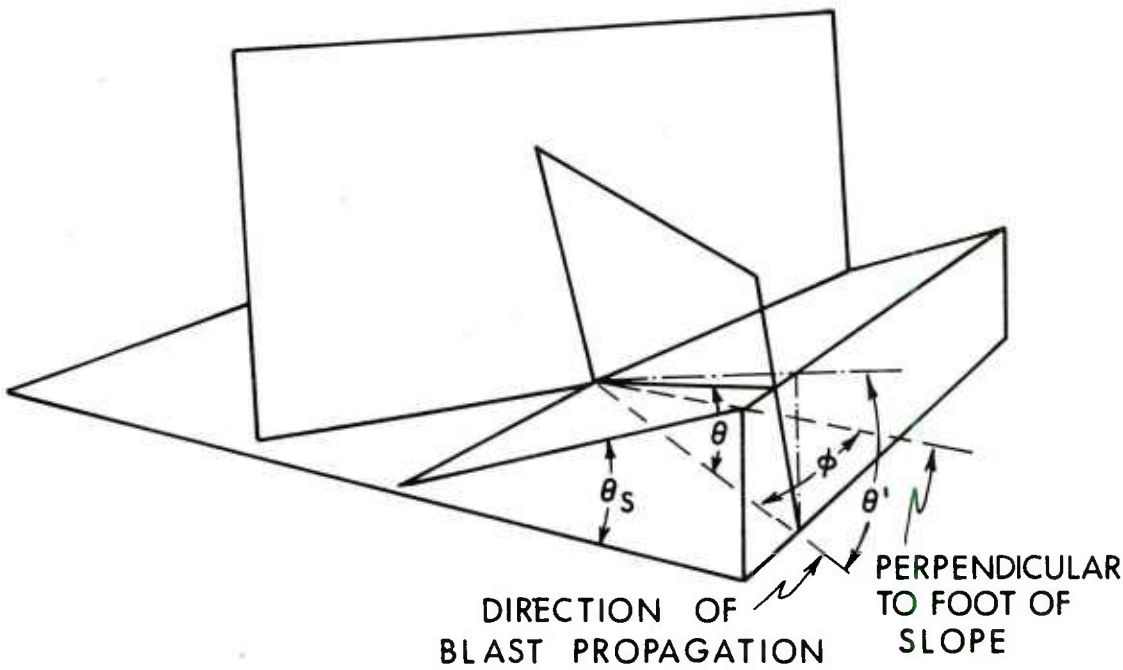

(B) SECTION OF TERRAIN FEATURE

Figure 18. Effective Slope Angle

Table X. Modified Effective Slope Angle θ'

Slope Angle θ_s (deg)	Azimuth Angle φ (deg)	Modified Effective Slope Angle θ' (deg)
10	20	9.4
	40	7.7
	60	5.0
20	20	18.9
	40	15.6
	60	10.3
30	20	28.5
	40	23.9
	60	16.1
40	20	38.3
	40	32.7
	60	22.8

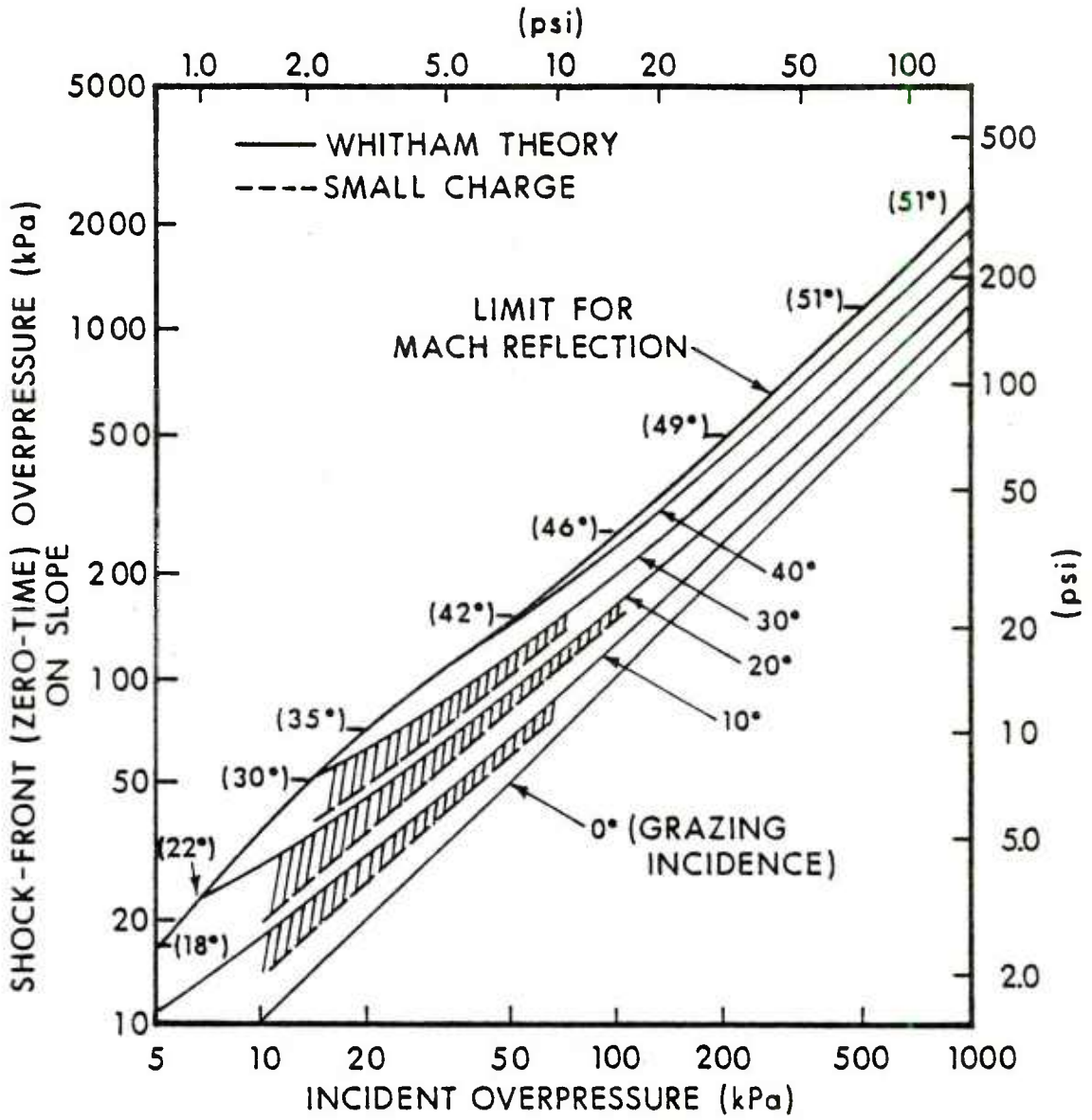

Figure 19. Overpressure at the Shock Front on a Rising Slope

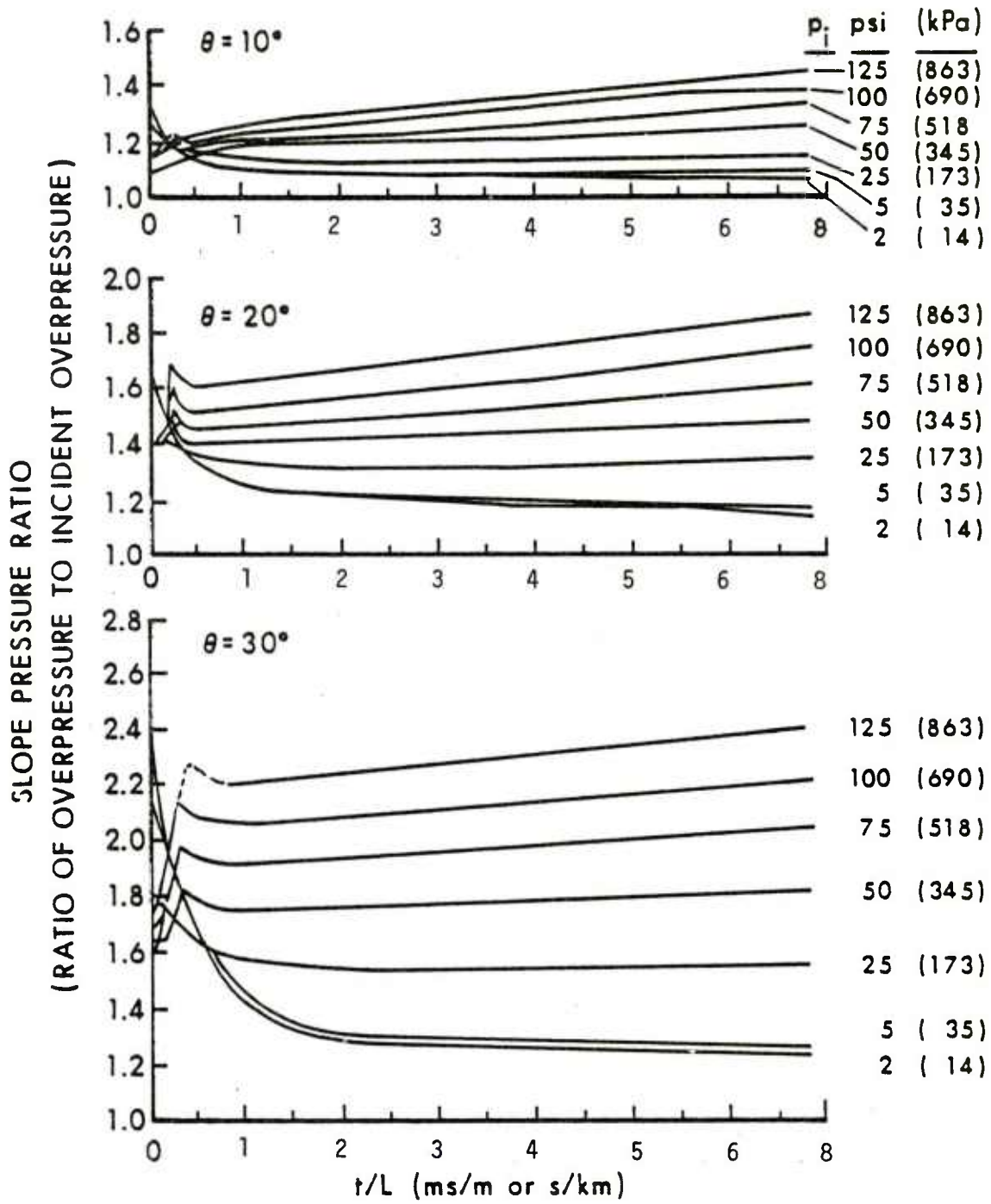

Figure 20. Rising Slope Pressure Ratios as a Function of t/L

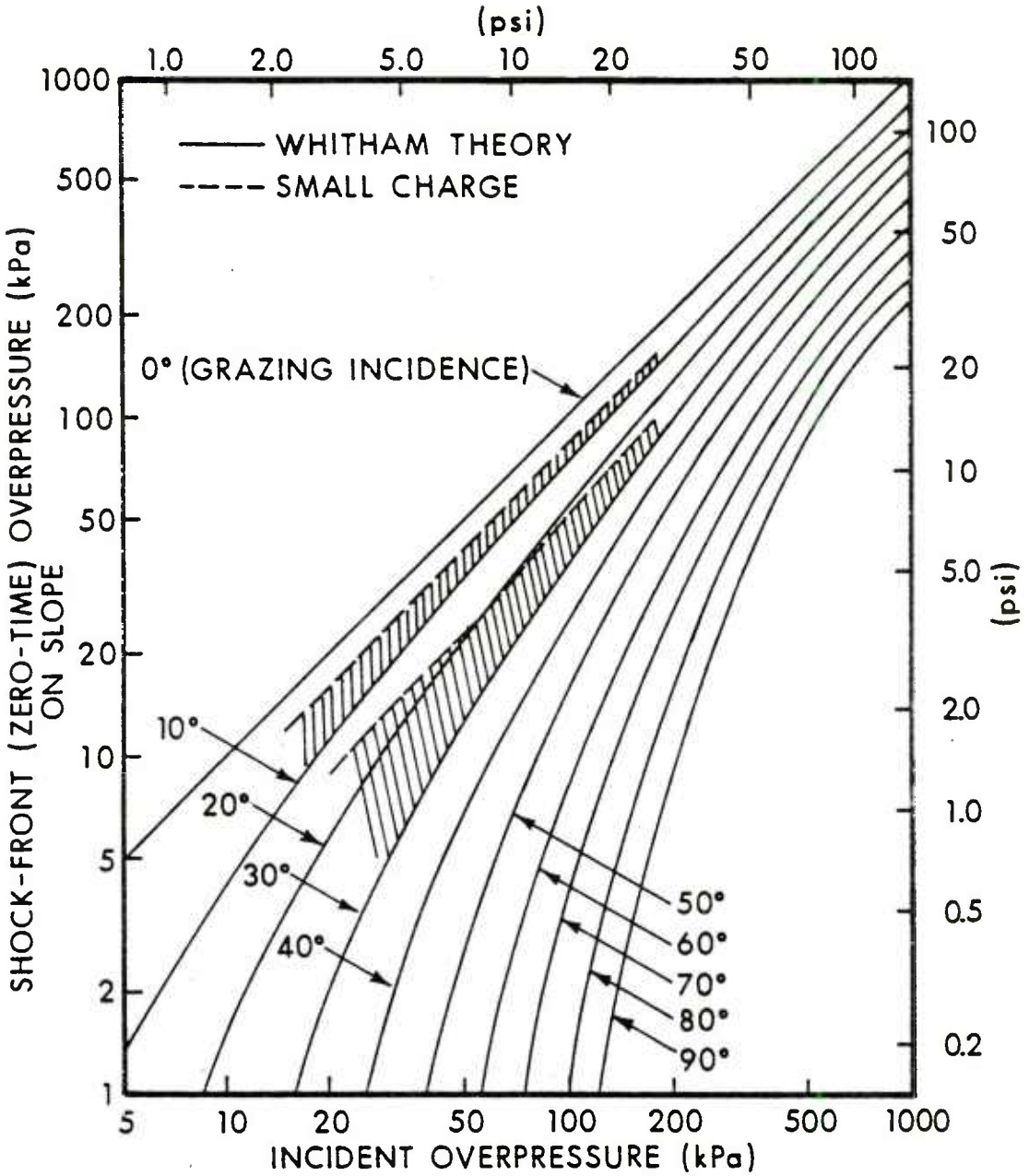

Figure 21. Overpressure at the Shock Front on a Falling Slope

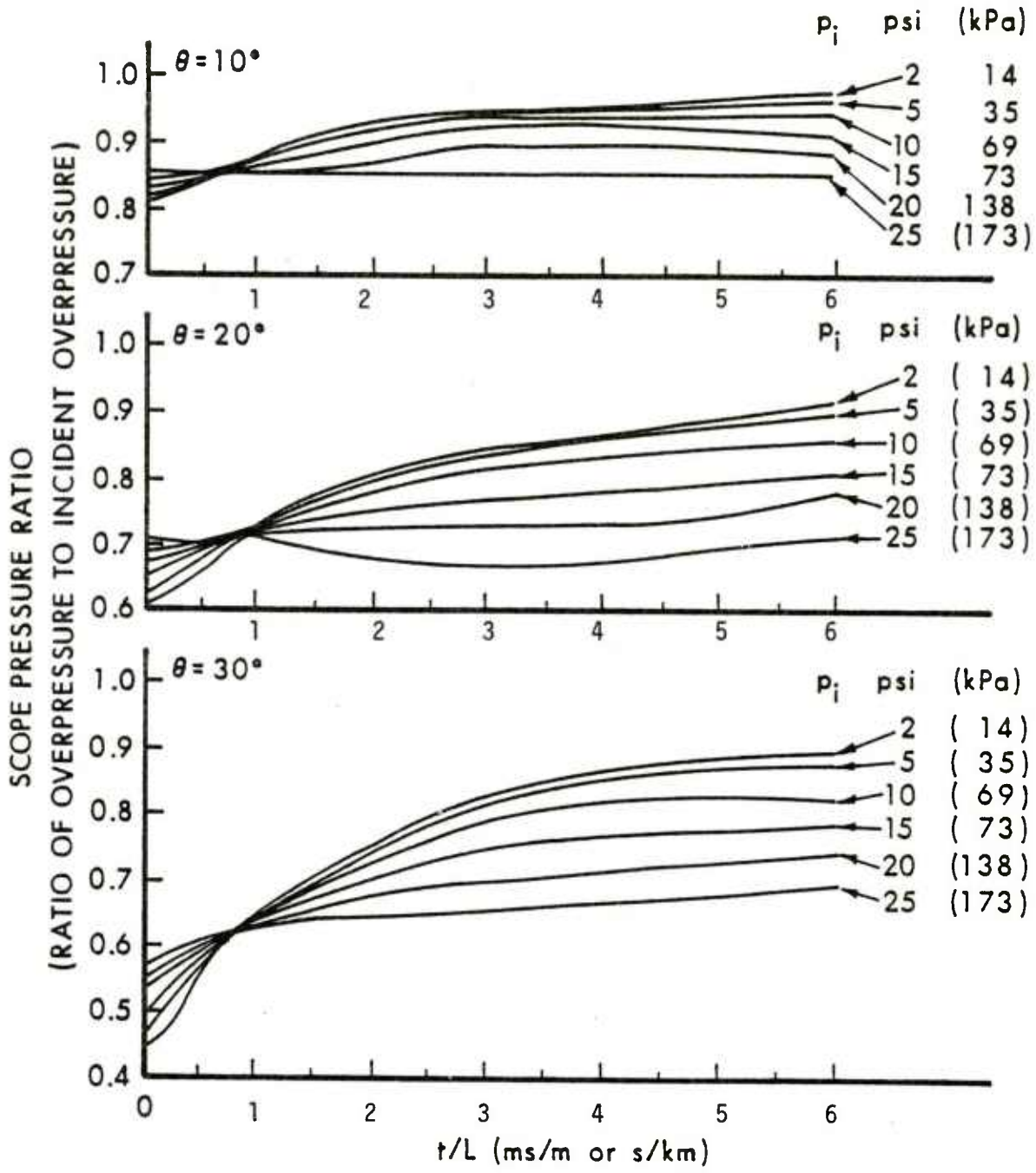

Figure 22. Falling Slope Pressure as a Function of t/L

Table XI. Modified Effective Slope Angle - Field Measurements

Station No.	Blast Line A-1 θ_s	A-1 ϕ	A-1 θ'	B-1 θ_s	B-1 ϕ	B-1 θ'	Ba (B-1) θ_s	Ba (B-1) ϕ	Ba (B-1) θ'	C-1 θ_s	C-1 ϕ	C-1 θ'
1												
2												
3										- 5	0	- 5
4												
5	29	14	28.3									
5a	29	10	28.6									
6	10	19	9.5	19	6	18.9	-19	9	-18.8	- 6	0	- 6
7	-24	4.5	-24	42	5	41.9	-42	3	-42			
8	-24	4.0	-24	-34	20	-32.4	34	19	32.5	15	8	14.9
9	-16	2.5	-16	-22	15	-21.3	22	19	21.5			
10	- 4	3	- 4	14.5	5	14.4	-14.5	0	-14.5	4	0	4
11				15	3	15	-15	0	-15			
12				5	0	5						
13				6	0	6	- 6	0	- 6			
14												
15												

NOTE: All angles are in degrees.

Table XI. Modified Effective Slope Angle - Field Measurements (Continued)

Station No.	Blast Line C-2 θ_s	C-2 ϕ	C-2 θ'	C-3 θ_s	C-3 ϕ	C-3 θ'	C-4 θ_s	C-4 ϕ	C-4 θ'	D-2 θ_s	D-2 ϕ	D-2 θ'
1												
2												
3							2	20	1.9			
4												
5												
6										3.5	5	3.5
7							6	9	5.9			
8				8	45	5.7				8	19	7.6
9												
10	24	36	19.8	10	25	9.1	13	6	12.9	9	22.5	8.3
11	25	31	20.9				6	26	5.4			
12	-56	46	-45.8				- 9	34	- 7.5	- 2	13	- 1.9
13							- 9	34	- 7.5	-15	20	-14.1
14										-15	23	-13.9
15	- 3	67	- 1.2	-11	35	- 9.0				-12	14	-11.7

NOTE: All angles are in degrees.

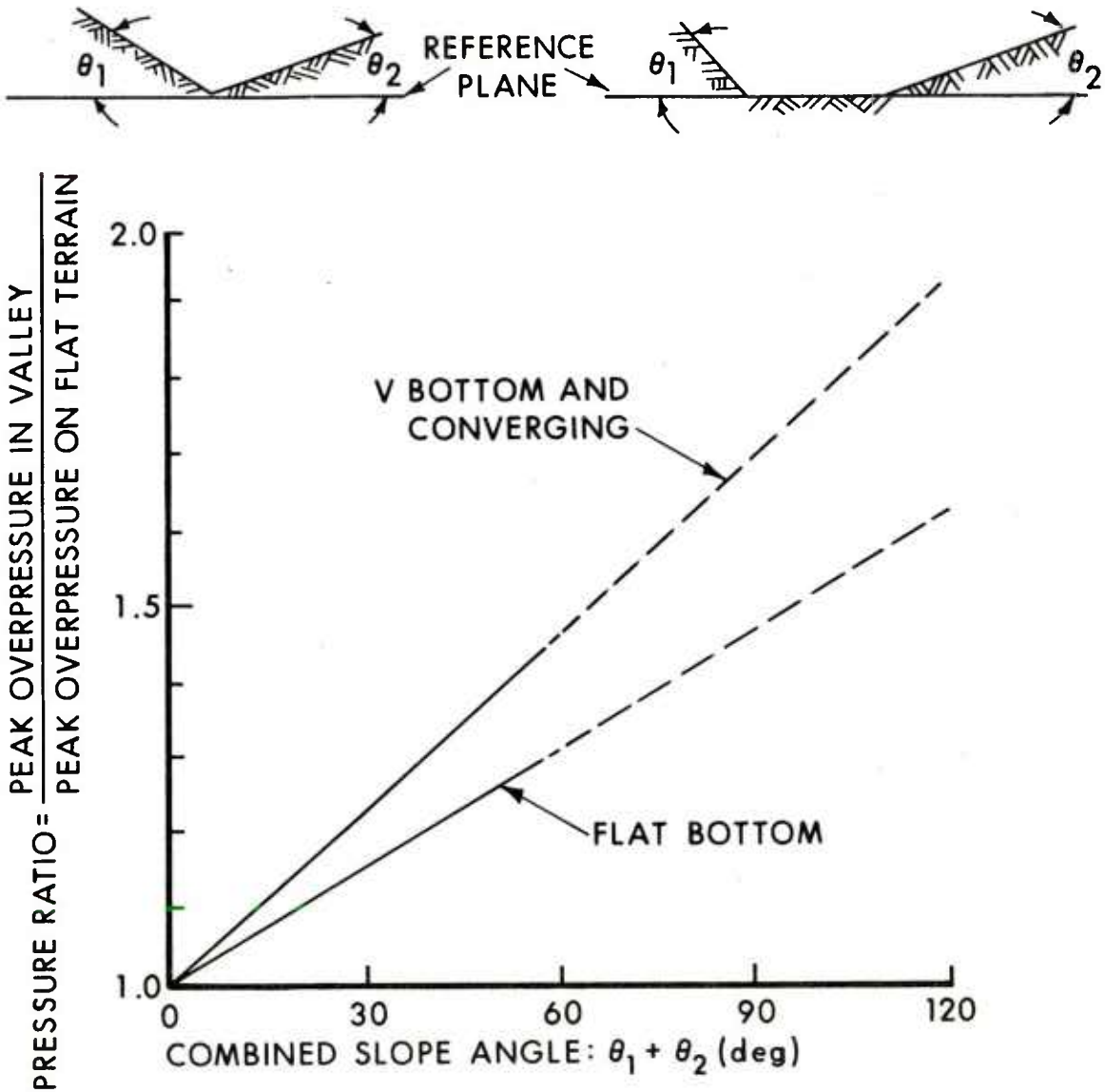

Figure 23. Average Peak Pressure Ratio at the Bottom of Valleys as a Function of Combined Slope Angle

B. Comparison of Data with Predictions

The primary purpose of this test series as stated in the Introduction was to determine how satisfactory the current prediction techniques are for blast wave interaction with terrain features for a real scenerio situation. A comparison will be made in this section of measured pressure-time blast wave histories with those predicted in Reference 7.

Since all the pre-shot predictions were made for sea level standard conditions, all the test data were scaled to conditions of 0.454 kg charge weight (W) of TNT detonated at conditions of ambient pressure P_o = 101.35 kPa and ambient temperature T_o = 288° K. Scaling laws from Reference 9, written in a convenient form as Equations 4-6, were used to adjust the experimental data to standard sea level conditions used for prediction[10]. A conversion factor for the equivalent weight of 50/50 pentolite to TNT was included from Reference 11 in the scaling process. It takes 1.16 times the amount of TNT by weight to equal the pentolite used during the test program.

The scaled sea level (superscript (0)) values of the data parameters measured at the altitude (superscript (h) are found as follows:

Peak pressure,
$$P_S^{(0)} = P_S^{(h)} \left(\frac{101.35}{P_o^{(h)}} \right); \quad (4)$$

distance,
$$D^{(0)} = D^{(h)} \left(\frac{0.454}{1.16\ W^{(h)}} \right)^{1/3} \left(\frac{P_o^{(h)}}{101.35} \right)^{1/3}, \quad (5)$$

and for arrival time or duration,

$$T_A^{(0)} = T_A^{(h)} \left(\frac{0.454}{1.16 W^{(h)}} \right)^{1/3} \left(\frac{P_o(h)}{101.35} \right)^{1/3} \left(\frac{T_o(h)}{288} \right)^{1/2} \quad (6)$$

---

9. *Wilfred E. Baker, "Explosions in Air", University of Texas Press, Austin, Texas, 1973.*
10. *W. McNamara, R. J. Jordano, and P. S. Lewis, "Air Blast from a 1 KT Nuclear Burst at 60 Meters over an Ideal Surface", Ballistic Research Laboratory, CR 353, October 1977.* (AD #B026325L)
11. *"Engineering Design Handbook, "Principles of Explosive Behavior", AMCP 706-180, Hq. USA Materiel Command, April 1972.*

Scaled impulse may be found by multiplication of Equations 4 and 5. The result is Equation 7:

$$I^{(0)} = I^{(h)} \left(\frac{101.35}{p_o^{(h)}} \right)^{2/3} \left(\frac{0.454}{1.16W^{(h)}} \right)^{1/3} \left(\frac{T_o^{(h)}}{288} \right)^{1/2} \quad (7)$$

The scaled experimental data are listed by shot number, and transducer station in Tables XII-XVII. The scaled conditions as noted, are for explosive charges of bare spherical TNT of 0.454 kg weight fired at the ambient sea level conditions of pressure of 101.35 kPa and temperature of 288°C.

Some comparisons of data with predictions are shown in the pressure-time histories in Figure 24. These will serve to illustrate the major differences observed. A more complete set of comparisons are given in Appendix C. The comparisons shown in this appendix are for average values taken from all the shots recorded at the particular station which is compared.

Tables XVIII summarizes two average blast wave parameters - initial overpressure and postive phase duration. An inspection of the average experimential flat terrain pressures shows deviations from the predicted values. Since inaccurate prediction for the flat terrain would give correspondingly inaccurate predictions for the peak pressures from the slopes, a new set of predictions was made for the various stations by using the actual experimental field values of flat terrain reference pressures. Table XIX shows the results for the new predictions.

A comparison was also made of experimental positive impulse as measured on the slopes with that measured on the flat terrain reference lines. See Table XX. Again, average values were used for the comparisons.

A comparison of the scaled blast parameters listed in Tables XVIII-XX is made on the plots shown as Figures 25-27. An overview of all the data from the several blast lines can be seen from the plots. The data appear quite scattered, partly because there were several different slopes and different approach angles. Also, the terrain features varied from line to line for a given ground range. Some trends can be seen in spite of these limitations.

A look at Figure 25 shows the scaled measured blast overpressure from the flat terrain reference lines do fit the prediction curve quite well. An inspection of the data from the several blast lines with terrain features indicates increased pressure on the rising slopes and decreased pressures on the falling slopes. At distances beyond the terrain features the trend is for the pressure to return to the expected flat terrain values.

Table XII. Data Scaled to 0.454 kg TNT at Sea Level Conditions - Lines A-1 and A-2*; Shots 1, 2 and 5

Scaled from Station	Overpressure, kPa	Arrival Time, ms	Positive Duration, ms	Impulse, kPa-ms	Scaled Distance, m	Remarks
A-2-1	- , 15 485, 12 421	0.20, 0.20, 0.22	0.21, 0.17, 0.16	436, 661, 458	0.52, 0.53, 0.52 (HOB)	$W^{(0)}$ = 0.454 kg
A-1-4	265, 276, 274	1.81, 1.81, 1.84	1.20, 1.32, 1.33	95.9, 92.1, 90.2	1.75, 1.75, 1.76	$P_o^{(0)}$ = 101.35 kPa
A-2-4	270, 262, -	1.83, 1.86, 1.91	1.27, 1.28, 1.33	96.0, 90.9, 80.3	1.75, 1.75, 1.76	
A-1-5	206, 196, 192	4.08, 4.08, 4.33	1.84, 1.85, 1.76	81.0, 77.0, 75.2	2.89, 2.89, 2.90	$T_o^{(0)}$ = 288° K
A-2-5	92.1, 89.5, 87.4	4.09, 4.14, 4.40	1.97, 1.99, 1.82	61.5, 58.6, 54.8	2.89, 2.89, 2.90	
A-1-5a	114, 112.4, 113.2	5.65, 5.71, 5.79	1.94, 1.93, 1.79	67.3, 65.4, 62.9	3.59, 3.60, 3.60	
A-2-5a	62.4, 60.1, 59.9	5.73, 5.83, 5.94	2.29, 2.20, 2.05	49.8, 46.6, 44.0	3.59, 3.60, 3.60	
A-1-6	48.6, 48.1, 45.9** 52.1, 50.4, 53.1***	7.68, 7.77, 7.84	2.49, 2.47, 2.38	48.8, 45.6, 45.5	4.38, 4.39, 4.40	
A-2-6	45.2, 42.7, 43.7	7.68, 7.82, 7.93	2.52, 2.46, 2.40	40.0, 36.6, 35.3	4.38, 4.39, 4.40	
A-1-7	13.0, 11.9, 12.1 16.9, 15.8, 15.7	11.6, 10.7, 10.9	3.45, 3.49, 3.19	- , - , -	5.42, 5.44, 5.45	
A-2-7	29.3, 27.1, 26.3	10.9, 10.5, 10.8	3.02, 2.97, 3.34	34.5, 30.1, 30.8	5.42, 5.44, 5.45	
A-1-8	9.0, 8.9, 8.67 10.9, 10.6, 11.13	12.9, 13.1, 12.1	4.26, 4.98, 4.10	23.2, 23.3, 21.9	6.12, 6.14, 6.16	
A-2-8	23.5, 22.6, 22.6	12.3, 12.5, 12.7	3.03, 3.28, 3.52	- , 27.5, 27.6	6.12, 6.14, 6.16	
A-1-9	14.7, 14.4, 13.1	15.7, 14.9, 15.2	4.40, 5.00, 4.33	23.2, 21.2, 20.5	6.82, 6.84, 6.86	
A-2-9	- , 16.9, 16.9	15.1, 14.3, 14.6	3.18, 3.48, 3.44	- , 24.7, 23.1	6.82, 6.84, 6.86	
A-1-10	16.8, 16.3, 14.1	17.7, 17.9, 17.1	4.24, 4.93, 3.68	19.9, - , -	7.88, 7.89, 7.92	
A-2-10	17.2, 15.4, 14.8	17.1, 17.3, 16.5	3.41, 3.67, 3.54	24.6 - , -	7.88, 7.89, 7.92	
A-1-11	12.8, 13.0, 12.5	21.9, 22.0, 22.1	4.25, 4.21, 4.10	18.5, 17.6, 16.2	9.36, 9.38, 9.41	
A-2-11	13.6, 13.2, 11.5	21.1, 21.6, 21.7	4.37, 4.25, 3.90	21.0, 18.3, 17.1	9.36, 9.38, 9.41	
A-1-15	8.7, 9.3, 7.6	29.9, 30.2, 30.4	4.38, 4.45, 4.36	15.2, 14.1, 13.5	12.2, 12.3, 12.3	
A-2-15	- , 9.0, 7.9	- , 29.7, 29.9	- , 4.46, 3.81	- , - , -	12.2, 12.3, 12.3	

*Reference Line ** Initial Peak *** Maximum Value

Table XI11. Data Scaled to 0.454 kg TNT at Sea Level Conditions - Lines B-1 and B-2*; Shots 8, 9 and 10

Scaled from Station	Overpressure, kPa	Arrival Time, ms	Positive Duration, ms	Impulse, kPa-ms	Scaled Distance, m	Remarks
B-2-1	14 588, 11328,13 131	.19, .19, .20	.21, .20, .21	554, 418, 529	.52, .53, .53 (HOB)	$W^{(0)}$= 0.454 kg
B-2-3	817, 964, 870	.86, .87, .87	.68, .73, .75	140, 143, 137	1.05, 1.06, 1.06	$P_o^{(0)}$= 101.35 kPa
B-1-5	93.2, 92.7, 85.4	4.18, 4.19, 4.21	1.86, 1.90, 1.94	56.1, 56.7, 56.5	2.90, 2.93, 2.92	
B-2-5	72.5, 78.7, 74.6	4.28, 4.31, 4.29	1.89, 1.90, 2.02	52.5, 54.6, 55.0	2.90, 2.93, 2.92	$T_o^{(0)}$= 288° K
B-1-6	65.6, 68.2, 63.1	7.75, 7.79, 7.83	2.29, 2.29, 2.35	43.4, 43.3, 42.4	4.40, 4.40, 4.43	
B-2-6	46.0, 45.8, 43.7	7.95, 8.00, 7.99	2.32, 2.34, 2.64	- , - , -	4.40, 4.40, 4.43	
B-1-7	77.4, 79.8, 75.0	10.4, 10.5, 10.6	2.15, 2.11, 2.10	42.1, 43.3, 42.3	5.46, 5.50, 5.49	
B-2-7	24.0, 26.4, 23.9	10.8, 10.9, 10.8	2.86, 2.86, 2.92	28.5, 28.9, 28.2	5.46, 5.50, 5.49	
B-1-8	9.3, 11.4, 9.2 14.2, 15.4, 14.9	12.6, 12.6, 12.7	3.37, 3.26, 3.37	25.2, 25.7, 25.4	6.16, 6.21, 6.20	
B-2-8	21.7, 23.2, 20.9	12.7, 12.7, 12.8	3.04, 2.98, 3.00	24.5, 24.9, 24.6	6.16, 6.21, 6.20	
B-1-9	11.7, 13.4, 11.1	14.7, 14.8, 14.8	3.19, 2.96, 3.73	- , 22.7, 21.6	6.87, 6.92, 6.91	
B-2-9	18.9, 20.4, 18.8	14.6, 14.7, 14.7	3.08, 2.93, 2.95	23.4, 24.0, 23.6	6.87, 6.92, 6.91	
B-1-10	17.9, 21.9, 20.0	18.1, 18.1, 18.1	3.21, 3.49, 3.29	20.4, 21.3, 20.8	7.92, 7.99, 7.98	
B-2-10	13.0, 15.6, 14.0	17.4, 17.6, 17.6	3.39, 3.62, 3.22	19.7, 20.4, 20.1	7.92, 7.99, 7.98	
B-1-11	20.2, 19.6, 20.7	21.8, 21.8, 15.9	3.43, 3.23, 3.42	18.8, 19.3, 18.7	9.42, 9.50, 9.49	
B-2-11	10.8, 13.8, 11.8	21.7, 21.8, 22.0	3.84, 3.85, 3.41	17.2, 17.4, 17.1	9.42, 9.50, 9.49	
B-1-12	12.0, 15.0, 12.1	25.0, 24.9, 25.1	3.78, 3.67, 3.78	15.9, 16.3, 16.3	10.5, 10.7, 10.6	
B-2-12	10.8, 12.7, 12.3	25.0, 25.1, 25.1	3.91, 3.84, 3.49	15.2, 15.5, 15.2	10.5, 10.7, 10.6	
B-1-13	10.5, 12.9, 9.9	26.5, 27.0, 27.1	3.84, - , 3.67	14.4, - , 14.2	11.3, 11.4, 11.4	
B-2-13	7.6, 9.4, 9.3	26.8, 27.1, 27.1	- , - , -	- , - , -	11.3, 11.4, 11.4	
B-2-15	7.4, 9.8, 8.8	29.9, 30.0, 30.1	4.01, 3.80, 4.01	12.1, 12.6, 11.5	12.3, 12.4, 12.4	

*Reference Line

Table XIV. Data Scaled to 0.454 kg TNT at Sea Level Conditions - Line B_a (B-1); Shots 11 and 12

Scaled from Station	Overpressure, kPa	Arrival Time, ms	Positive Duration, ms	Impulse, kPa-ms	Scaled Distance, m	Remarks
B-1-15	14 244, 12 236	.20, .20	.25, .21	548, 436	.53, .53	$W^{(0)}$=0.454 kg
B-1-13	831, 833	.92, .91	.70, .74	125, 137	1.05, 1.06	$P_o^{(0)}$=101.35 kPa
B-1-11	62.9, 68.1	4.50, 4.48	1.99, 2.00	46.3, 47.6	2.90, 2.92	$T_o^{(0)}$=288° K
B-1-10	36.0, 35.8	8.46, 8.42	2.93, 2.84	- , 41.7	4.40, 4.43	
B-1-9	- , 56.0	11.0, 11.0	- , 2.19	- , 34.2	5.45, 5.49	GZ over α 15
B-1-8	- , 41.3 - , 45.6	12.8, 12.8	2.09, 1.90	- , 33.5	6.15, 6.20	
B-1-7	7.0, 7.7 13.1, 13.3	14.6, 15.0	3.52, 3.42	22.9, 23.0	6.86, 6.91	
B-1-6	13.8, 16.4	18.2, 18.1	3.97, 3.63	18.7, 19.5	7.90, 7.97	

Table XV. Data Scaled to 0.454 kg TNT at Sea Level Conditions - Lines C-1, C-4 and C-5; Shots 13, 14 and 15

Scaled from Station	Overpressure, kPa	Arrival Time, ms	Positive Duration, ms	Impulse, kPa-ms	Scaled Distance, m	Remarks
C-5-1	12 614,13 209,11 920	.20, .20, .20	.20, .22, .23	445, 533, 475	.53, .53 .53(HOB)	$W^{(0)}$= 0.454 kg
C-1-3	889, 865, 836	.88, .85, .87	.76, .78, .87	145, 132, 146	1.06, 1.05, 1.06	
C-4-3	871, 869, 919	.83, .81, .80	.70, .73, .81	138, 134, 145	1.06, 1.05, 1.06	$P_o^{(0)}$= 101.35 kPa
C-5-3	768, 739, 821	.88, .85, .85	.65, .78, .66	- , - , -	1.06, 1.05, 1.06	
C-1-6	40.9, 42.7, 47.7	8.04, 7.93, 8.02	2.73, 2.85, 2.72	40.8, - , 43.9	4.43, 4.39, 4.42	$T_o^{(0)}$= 288° K
C-5-6	41.9, 38.2, 42.3	7.95, 7.85, 7.92	2.53, 2.77, 2.65	40.5, 40.0, 42.2	4.43, 4.39, 4.42	
C-4-7	32.0, 32.5, 36.4	10.6, 10.6, 10.4	3.21, 2.78, 2.92	30.3, 30.0, 30.4	5.49, 5.44, 5.49	
C-5-7	34.7, 30.0, 37.7	10.7, 10.1, 10.7	2.64, 2.94, 2.86	- , 31.7, 32.9	5.49, 5.44, 5.49	
C-1-8	44.5, 48.6, 51.1	12.6, 12.4, 12.3	2.54, 2.55, 2.62	34.2, 32.2, 34.7	6.20, 6.15, 6.20	
C-5-8	23.6, 23.1, 25.7	12.6, 12.5, 12.3	3.40, 3.49, 3.52	27.8, 26.9, 27.8	6.20, 6.15, 6.20	
C-1-10	23.4, 22.1, 22.4	17.2, 17.0, 17.1	3.34, 3.35, 3.34	28.7, 27.7, 29.4	7.97, 7.90, 7.97	
C-4-10	21.1, 22.4, 25.3	17.2, 17.0, 17.2	3.38, 3.39, 3.41	24.9, 24.0, 24.7	7.97, 7.90, 7.97	
C-5-10	18.8, - , 19.1	17.5, 17.4, 17.4	3.81, 3.93, 3.73	23.3, 23.0, 23.3	7.97, 7.90, 7.97	
C-4-11	11.5, 13.8, 15.4	21.5, 21.1, 21.2	3.58, 3.52, 3.55	18.5, 17.7, 18.3	9.48, 9.39, 9.47	
C-5-11	15.8, 14.6, 15.6	21.8, 21.6, 21.6	4.09, 4.04, 3.74	24.4, 24.7, 24.7	9.48, 9.39, 9.47	
C-4-12	4.28, 4.19, 4.48 7.56, 7.6, 7.87	24.8, 24.4, 24.3	4.24, 4.11, 4.28	16.5, 15.7, 16.3	10.6, 10.5 ,10.6	
C-5-12	10.4 ,11.2, 9.79	25.0, 24.9, 24.6	4.20, 4.14, 4.19	17.5, 17.0, 17.2	10.6, 10.5, 10.6	
C-1-13	8.01, 6.90, 9.79 9.22, 8.70, 9.52	26.6, 26.2, 26.6	3.41, 3.89, 3.80	14.0, 15.4, 16.1	11.3, 11.2, 11.3	
C-4-13	- , - , 6.94 5.30, 5.20, 7.23	26.9, 26.4, 26.7	- , - , 4.30	- , - , 15.3	11.3, 11.2, 11.3	
C-5-13	9.89, 9.52, 9.72	27.0, 26.9, 27.0	4.22, 4.32, 4.19	16.6, 16.8, 16.7	11.3, 11.2, 11.3	

*Reference Line

Table XVI. Data Scaled to 0.454 kg TNT at Sea Level Conditions - Lines C-2, C-3 and C-5*; Shots 16, 17 and 18

Scaled from Station	Overpressure, kPa	Arrival Time, ms	Positive, Duration, ms	Impulse, kPa-ms	Scaled Distance, m	Remarks
C-5-1	13 757,13 566,11 067	.22, .20, .20	.22, .25, .20	612, 442, 388	.53, .53, .53 (HOB)	$W^{(0)}$= 0.454 kg
C-3-2	- , 2606 , 2416	.51, .50, .52	- , .50, .51	- , 229, 220	.71, .71, .71	
C-5-2	- , 2725 , 2082	.51, .53, .52	- , .59, .56	- , 200, 206	.71, .71, .71	$P_o^{(0)}$= 101.35 kPa
C-2-4	232 , 258, 245	1.90, 1.90, 1.92	1.30, 1.25, 1.23	90.0, 91.4, 90.1	1.77, 1.77, 1.77	
C-5-4	263 , 246, 256	1.90, 1.92, 1.91	1.17, 1.25, 1.28	88.3, 92.0, 79.1	1.77, 1.77, 1.77	$T_o^{(0)}$= 288° K
C-3-5	85.9, 88.7, 89.8	4.14, 4.27, 4.19	1.90, 2.03, 1.98	- , - , -	2.92, 2.92, 2.91	
C-5-5	102, 96.4,102.2	4.14, 4.29, 4.24	1.86, 1.89, 1.83	57.5, 59.4, 60.6	2.92, 2.92, 2.91	
C-2-8	23.7, 25.2, 24.8	12.5, 12.6, 12.6	3.42, 3.45, 3.50	27.5, 27.2, 27.8	6.20, 6.20, 6.18	
C-3-8	29.2, 28.3, 30.9	12.3, 12.6, 12.5	3.28, 3.28, 3.22	29.9, 30.5, 30.7	6.20, 6.20, 6.18	
C-5-8	24.4, 24.8, 27.6	12.5, 12.7, 12.6	3.29, 3.45, 3.28	25.6, 26.9, 27.8	6.20, 6.20, 2.18	
C-2-10	38.8, 38.4, 40.3	17.3, 17.5, 17.4	3.03, 3.00, 3.19	25.5, 25.1, 26.8	7.97, 7.97, 7.95	
C-3-10	16.7, 15.2, 16.9	17.1, 17.5, 17.3	3.51, 3.36, 3.46	16.1, 16.0, 16.5	7.97, 7.97, 7.95	
C-5-10	18.4, 17.6, 19.2	17.3, 17.6, 17.5	3.72, 3.80, 3.62	22.8, 22.9, 22.6	7.97, 7.97, 7.95	
C-2-11	27.4, 24.3, 28.1	21.6, 21.9, 21.7	3.23, 3.30, 3.18	22.7, 22.3, 22.6	9.48, 9.47, 9.45	
C-5-11	11.7, 11.2, 11.9	21.5, 21.9, 21.7	3.92, 4.03, 3.95	19.0, 18.5, 18.8	9.48, 9.47, 9.45	
C-2-12	1.42, 1.14, 1.02 5.14, 4.89, 4.84 7.29, 7.24, 7.19	24.7, 26.1, 25.9	4.47, 4.74, 4.83	15.3, 15.7, 15.3	10.6, 10.6, 10.6	
C-5-12	10.1, 10.4, 11.3	25.7, 25.2, 25.0	4.12, 4.10, 4.07	16.7, 16.6, 17.3	10.6, 10.6, 10.6	
C-2-15	3.66, 2.33, 3.19 9.34, 8.73, 9.16	30.2, 30.7, 30.5	4.50, 4.45, 3.55	14.2, 14.2, 11.9	12.4, 12.4, 12.4	
C-3-15	1.62, 1.50, 1.82 5.09, 5.03, 5.26	29.7, 30.6, 30.1	4.75, 4.81, 4.60	12.8, 12.6, 12.9	12.4, 12.4, 12.4	
C-5-15	7.40, 7.25, 7.93	29.7, 29.7, 30.0	4.67, 4.64, 4.55	15.1, 14.6, 14.8	12.4, 12.4, 12.4	

*Reference Line

Table XVII. Data Scaled to 0.454 kg TNT at Sea Level Conditions - Lines D-2 and D-3*; Shots 19 and 20

Scaled from Station	Overpressure, kPa	Arrival Time, ms	Positive Duration, ms	Impulse, kPa-ms	Scaled Distance, m	Remarks
D-3-1	13 328, 13 981	.20, .20	.22, .22	454, 519	.53, .53	$W^{(0)}$ = 0.454 kg
D-3-4	253, 252	1.97, 1.92	1.25, 1.20	88.3, 86.6	1.77, 1.75	$P_o^{(0)}$ = 101.35 kPa
D-3-5	83.1, 83.3	4.36, 4.26	1.89, 1.80	55.0, 54.1	2.92, 2.89	
D-2-6	47.4, 46.8	7.95, 7.83	2.36, 2.45	38.0, 37.7	4.43, 4.39	$T_o^{(0)}$ = 288° K
D-3-6	46.9, 47.4	7.98, 7.83	2.67, 2.41	- , 35.4	4.43, 4.39	
D-2-8	32.2, 31,3	12.3, 12.3	2.74, 2.87	27.4, 27.6	6.20, 6.14	
D-3-8	26.1, 26.3	12.6, 12.4	3.36, 3.19	27.8, 28.0	6.20, 6.14	
D-2-10	22.7, 19.5	17.4, 17.3	3.53, -	22.8, -	7.97, 7.89	
D-3-10	17.9, 18.9	17.4, 17.1	3.49, 3.48	20.8, 20.8	7.97; 7.89	
D-2-12	11.2, 11.0	24.8, 24.7	3.58, 3.66	16.3, 16.3	10.6 , 10.5	
D-3-12	10.2, 11.8	24.7, 24.3	3.89, 3.76	17.1, 17.1	10.6 , 10.5	
D-2-13	3.99, 4.25 7.09, 7.17	26.9, 26.8	4.16, 4.41	15.3, 16.0	11.3 , 11.2	
D-3-13	9.2 , 10.5	26.7, 26.3	4.09, 3.95	16.8, 16.3	11.3 , 11.2	
D-2-14	2.63, 2.15 5.95, 5.88	27.9, 27.9	4.36, 4.44	13.8, 13.5	11.7 , 11.6	
D-3-14	9.28, 9.97	27.7, 27.3	3.96, 3.90	16.1, 16.1	11.7 , 11.6	
D-2-15	3.60, 4.15 5.19, 5.38	30.0, 30.0	4.81, 5.16	13.1, 13.9	12.4 , 12.3	
D-3-15	8.92, 9.89	29.7, 29.2	4.07, 3.94	15.7, 15.4	12.4 , 12.3	

*Reference Line

Table XVIII. Comparison of Scaled Experimental[1] Blast Parameters with Pre-Shot Predicted[2] Values

Station	Ground Range, m	Flat Terrain: Overpressure, kPa Predicted	Flat Terrain: Overpressure, kPa Experiment[4]	Flat Terrain: Positive Duration, ms Predicted	Flat Terrain: Positive Duration, ms Experiment	θ' deg	Line A-1: Overpressure, kPa Predicted	Line A-1: Overpressure, kPa Experiment	Line A-1: Positive Duration[3], ms Predicted	Line A-1: Positive Duration[3], ms Experiment
1	0	13 800	13 100	-	0.21		13 800	13 900		
2	0.8	2 070	2 400	0.2	0.58	Flat				
3	1.2	690	830	0.6	0.71					
4	2.0	210	257	1.5	1.25		210	272	1.5	1.28
5	3.3	70	87.3	2.3	1.89	28.3	150(150)	198	2.3	1.82
5a	4.1	46	60.8	2.7	2.18	28.6	120(110)	113	2.7	1.89
6	5.0	33	44.0	3.0	2.52	9.5	45(42)	47.5	3.0	2.45
7	6.2	24	28.8	3.2	2.93	-24.0	5.2(13)	12.3	3.2	3.88
8	7.0	21	24.0	3.4	3.27	-24.0	4.2(11.5)	8.8	3.4	4.45
9	7.8	17	18.4	3.6	3.25	-16.0	5.2(11.5)	14.1	3.6	4.58
10	9.0	14	16.9	3.8	3.60	-4.0	14.0	15.7	3.8	4.28
11	10.7	10	13.0	4.0	3.97		10.0	12.8	4.0	4.19
12	12.0	9.0	11.0	4.2	3.97	Flat				
13	12.8	8.0	9.4	4.2	4.15					
14	13.2	7.5	9.7	4.3	3.93					
15	14.0	7.0	8.4	4.3	4.14		7.0	8.5	4.3	4.40

Notes:

1 Experimental values for individual shots were scaled to 0.454 kg TNT at sea level and averaged.

2 Predicted values were taken from Reference 7, Tables 2 and B-2, Whitham Theory; values in parenthesis are from small charge studies.

3 Positive durations from the terrain features were predicted to be the same as for the flat reference durations.

4 These values are averages for all the flat terrain data.

Table XVIII. Comparison of Scaled Experimental Blast Parameters with Pre-Shot Predicted Values (Cont)

Station	Ground Range, m	Line B-1 θ' deg	Line B-1 Pressure, kPa Predicted	Line B-1 Pressure, kPa Experiment	Line B-1 Positive Duration, ms Predicted	Line B-1 Positive Duration, ms Experiment	Line B_a (B-1 backwards) θ' deg	Line B_a Overpressure, kPa Predicted	Line B_a Overpressure, kPa Experiment	Line B_a Positive Duration, ms Predicted	Line B_a Positive Duration, ms Experiment
1	0		13 800	13 000	-	0.21					
2	0.8										
3	1.2	Flat									
4	2.0										
5	3.3		70	90.4	2.3	1.90					
5a	4.1										
6	5.0	18.9	63(53)	65.6	3.0	2.31	-18.8	5.0(10)	15.1	3.8	3.80
7	6.2	41.9	60	79.0	3.2	2.12	-42	<1(7.5)	7.35	3.6	3.47
8	7.0	-32.4	1.0(7.0)	10.7	3.4	3.37	32.5	52	41.3	3.4	2.00
9	7.8	-21.3	1.1(10)	12.1	3.6	3.29	21.5	62(48)	56	3.2	2.19
10	9.0	14.4	28(22)	19.9	3.8	3.33	-14.5	23(29)	35.9	3.0	2.89
11	10.7	15	23(16)	20.2	4.0	3.36	-15	55(60)	65.5	2.3	2.00
12	12.0	5	13(11)	13.1	4.2	3.74					
13	12.8	6	11(10)	11.1	4.2	3.76	-6	690	832	0.6	0.72
14	13.2										
15	14.0						Flat	13 800	13 200	-	0.23

Table XVIII. Comparison of Scaled Experimental Blast Parameters with Pre-Shot Predicted Values (Cont)

Station	Ground Range, m	Line C-1 θ^1 deg	Line C-1 Overpressure, kPa Predicted	Line C-1 Overpressure, kPa Experiment	Line C-1 Positive Duration, ms Predicted	Line C-1 Positive Duration, ms Experiment	Line C-2 θ' deg	Line C-2 Overpressure, kPa Predicted	Line C-2 Overpressure, kPa Experiment	Line C-2 Positive Duration, ms Predicted	Line C-2 Positive Duration, ms Experiment
1	0		13 800	12 600	-	0.22		13 800	12 800	-	0.21
2	0.8	Flat					Flat				
3	1.2	-5.0	690	863	0.60	0.80					
4	2.0							210	245	1.5	1.26
5	3.3										
5a	4.1										
6	5.0	-6.0	33	43.8	3.0	2.77					
7	6.2										
8	7.0	14.9	48(39)	48.1	3.4	2.57		21	24.6	3.4	3.46
9	7.8										
10	9.0	4.0	30(25)	22.6	3.8	3.34	19.8	42(29)	39.2	3.8	3.07
11	10.7	Flat					20.9	30(20)	26.6	4.0	3.24
12	12.0						-45.8	8.7	1.19	4.2	4.68
13	12.8		12(10)	8.23	4.2	3.70					
14	13.2										
15	14.0						-1.2	6.9	3.06	4.3	4.12

Table XVIII. Comparison of Scaled Experimental Blast Parameters with Pre-Shot Predicted Values (Cont)

Station	Ground Range, m	Line C-3 θ' deg	Line C-3 Overpressure, kPa Predicted	Line C-3 Overpressure, kPa Experiment	Line C-3 Positive Duration, ms Predicted	Line C-3 Positive Duration, ms Experiment	Line C-4 θ' deg	Line C-4 Overpressure, kPa Predicted	Line C-4 Overpressure, kPa Experiment	Line C-4 Positive Duration, ms Predicted	Line C-4 Positive Duration, ms Experiment
1	0		13 800	12 800	-	0.22	Flat	13 800	12 600	-	0.22
2	0.8		2 070	2 511	0.2	0.50					
3	1.2						1.9	690	886	0.6	0.75
4	2.0	Flat									
5	3.3		70	88.1	2.3	2.06					
5a	4.1										
6	5.0										
7	6.2						5.9	24	33.6	3.2	2.97
8	7.0	5.7	26(24)	29.5	3.4	3.26					
10	9.0	9.1	22(18)	16.3	3.8	3.34	12.9	23(19)	22.9	3.8	3.50
11	10.7						5.4	12(12)	13.6	4.0	3.55
12	12.0						-7.5	2.2(6.6)	4.32	4.2	4.21
13	12.8						-7.5	1.9(6.1)	6.94	4.2	4.30
14	13.2										
15	14.0	-9.0	2.0(5.5)	1.65	4.3	4.72					

Table XVIII. Comparison of Scaled Experimental Blast Parameters with Pre-Shot Predicted Values (Cont)

Station	Ground Range, m	θ' deg	Line D-2 Overpressure, kPa Predicted	Overpressure, kPa Experiment	Positive Duration, ms Predicted	Positive Duration, ms Experiment
1	0		13 800	13 700	-	0.22
2	0.8					
3	1.2	Flat				
4	2.0					
5	3.3					
5a	4.1					
6	5.0	3.5	42(40)	47.1	3.0	2.41
7	6.2					
8	7.0	7.6	29(25)	31.8	3.4	2.81
9	7.8					
10	9.0	8.3	22(18)	21.1	3.8	3.53
11	10.7					
12	12.0		-	11.1	4.2	3.62
13	12.8		-	4.12	4.2	4.02
14	13.2		-	2.39	4.3	4.40
15	14.0	-16.7	1.1(5.0)	3.88	4.3	4.99

Table XIX. Comparison of Scaled Blast Pressures on the Terrain Features with Post-Shot Predicted Values

Equivalent Station	Scaled Distance, m	Flat Terrain Measured Overpressure, kPa	Line A-1 θ' deg	Line A-1 Blast Pressure, kPa Predicted	Line A-1 Blast Pressure, kPa Experiment	Line B-1 θ' deg	Line B-1 Blast Pressure, kPa Predicted	Line B-1 Blast Pressure, kPa Experiment	(Line B_a (B-1 backwards) θ' deg	(Line B_a (B-1 backwards) Blast Pressure, kPa Predicted	(Line B_a (B-1 backwards) Blast Pressure, kPa Experiment
1	0.53 (HOB)	13 100									
2[3]	0.71	2 400									
3	1,06	830									
4	1.77	257									
5	2.92	87.3	28.3	165[2](160)	198						
5a	3.60	60.8	28.6	135(122)	113						
6	4.42	44.0	9.5	57(54)	47.5	18.9	78(68)	65.6	-18.8	3.8(10.6)	15.1
7	5.46	28.8	-24	7.6(15.5)	12.3	41.9	98(96)	79.0	-42	<1(5.6)	7.4
8	6.19	24.0	-24	9.4(10.5)	8.8	-32.4	2.2(10)	10.7	33.5	75(58)	41.3
9	6.88	18.4	-16	14(16.5)	14.1	-21.3	4.2(14)	12.1	21.5	64(53)	56
10	7.95	16.9				14.4	25(33)	19.9	-14.5	23(32)	35.9
11	9.46	13.0				15	26(20)	20.2	-15	52(64)	65.5
12	10.6	11.0				5	14.5(13)	13.1			
13	11.3	9.4				6	13(12	11.1	-6	750	832
14	11.6	9.7									
15	12.4	8.4									

Notes:

1 Post-shot predictions in this table were made for field values of input blast pressures as measured on the flat terrain lines. All pressure values were scaled to 0.454 kg TNT at sea level and averaged as noted above in Table XVIII.

2 Predicted values were read from graphs in Reference 7, Whitham Theory; values in parenthesis are from small charge studies.

3 Distances from Stations 2-15 are the scaled horizontal ground distances. Station 1 is scaled height-of-burst (HOB).

Table XIX. Comparison of Scaled Blast Pressures on the Terrain Features with Post-Shot Predicted Values (Cont)

Equivalent Station	Scaled Distance, m	Flat Terrain Measured Overpressure, kPa	Line C-1 θ' deg	Line C-1 Blast Pressure, kPa Predicted	Line C-1 Blast Pressure, kPa Experiment	Line C-2 θ' deg	Line C-2 Blast Pressure, kPa Predicted	Line C-2 Blast Pressure, kPa Experiment	Line C-3 θ' deg	Line C-3 Blast Pressure, kPa Predicted	Line C-3 Blast Pressure, kPa Experiment
1	0.53(HOB)	13 100									
2	0.71	2 400									
3	1.06	830	-5	750	863						
4	1.77	257									
5	2.92	87.3									
5a	3.60	60.8									
6	4.42	44.0	-6	22(37)	43.8						
7	5.46	28.8									
8	6.19	24.0	14.9	43(36)	48.1				5.7	30(28)	29.5
9	6.88	18.4									
10	7.95	16.9	4	25(23.8)	22.6	19.6	39(28)	39.2	9.1	27(24)	16.3
11	9.46	13.0				20.9	34(24)	26.6			
12	10.6	11.0				-45.8	<1	1.19			
13	11.3	9.4	0	14(11.6)	8.2						
14	11.6	9.7									
15	12.4	8.4							-9	3.6(8.3)	1.65

Table XIX. Comparison of Scaled Blast Pressures on the Terrain Features with Post-Shot Predicted Values (Cont)

Equivalent Station	Scaled Distance, m	Flat Terrain Measured Overpressure, kPa	Line C-4 θ' deg	Line C-4 Blast Pressure, kPa Predicted	Line C-4 Blast Pressure, kPa Experiment	Line D-2 θ' deg	Line D-2 Blast Pressure, kPa Predicted	Line D-2 Blast Pressure, kPa Experiment
1	0.53(HOB)	13 100						
2	0.71	2 400						
3	1.06	830	1.9	840	886			
4	1.77	257						
5	2.92	87.3						
5a	3.60	60.8						
6	4.42	44.0				3.5	48(47)	47.1
7	5.46	28.8	5.9	36(35)	33.6			
8	6.19	24.0				7.6	33(28)	31.8
9	6.88	18.4						
10	7.95	16.9	12.9	29(24)	22.9	8.3	23.5(21)	21.1
11	9.46	13.0	5.4	17(15)	13.6			
12	10.6	11.0	-7.5	5.6(9.2)	4.32	-1.9	9.4(10.3)	11.1
13	11.3	9.4	-7.5	4.6(8.4)	6.94	-14.1	2.6(6.8)	4.12
14	11.6	9.7				-13.9	2.6(6.8)	2.39
15	12.14	8.4				-11.7	2.5(6.4)	3.88

Table XX. Comparison of Scaled[1] Positive Impulse on the Sloping Terrain with Impulse on the Flat Terrain

Equivalent Station	Ground Range, m	Flat Terrain	Impulse, kPa-ms															
			θ' deg	Line A-1	θ' deg	Line B-1	θ' deg	Line B_a[2] (Line B-1 backwards)	θ' deg	Line C-1	θ' deg	Line C-2	θ' deg	Line C-3	θ' deg	Line C-4	θ' deg	Line D-2
1	0(.53 HOB)	466																
2	0.71	203	Flat		Flat						Flat		Flat	244				
3	1.06	140							-5	141					1.9	139		
4	1.77	87.7		92.7								90.5						
5	2.92	56.7	28.3	77.7		56.4												
5a	3.60	46.8	28.6	65.2														
6	4.42	38.6	9.5	46.6	18.9	43.0	-18.8	19.5	-6	42.4							3.5	37.9
7	5.46	30.7	-24	-	41.9	42.6	-42	23.0							5.9	30.2		
8	6.19	26.7	-24	22.8	-32.4	25.4	32.5	33.5	14.9	33.7		27.4	5.7	30.4			7.6	27.5
9	6.88	23.8	-16	21.6	-21.3	22.2	21.5	34.2										
10	7.95	22.0	Flat	19.9	14.4	20.8	-14.5	41.7	4	28.6	19.8	25.8	9.1	16.2	12.9	24.5	8.3	22.8
11	9.46	19.9		17.4	15.1	18.9	-15	47.0			20.9	22.5			5.4	18.2		
12	10.6	16.6			5	16.2					-45.8	15.4			-7.5	16.2	-1.9	16.3
13	11.3	16.6			6	14.3	-6	131	Flat	15.2					-7.5	15.3	-14.1	15.7
14	11.6	16.1			Flat		Flat										-13.9	13.7
15	12.4	14.0		14.3		12.1		492			-1.2	13.4	-9	14.8			-11.7	13.7

1 Scaled to 0.454 kg TNT at sea level.

2 Charges were fired over Station 15 for Line B_a. Station 15 should be compared with flat terrain value at Station 1, Station 13 with Station 3, and so on.

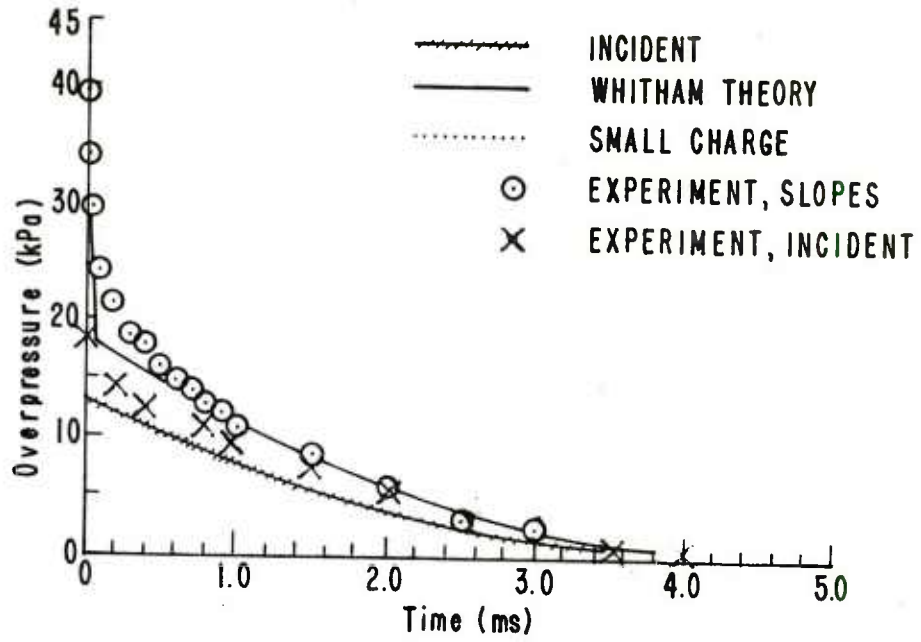

(A) RISING SLOPE - SHOT 18, LINE C-2, STATION 10

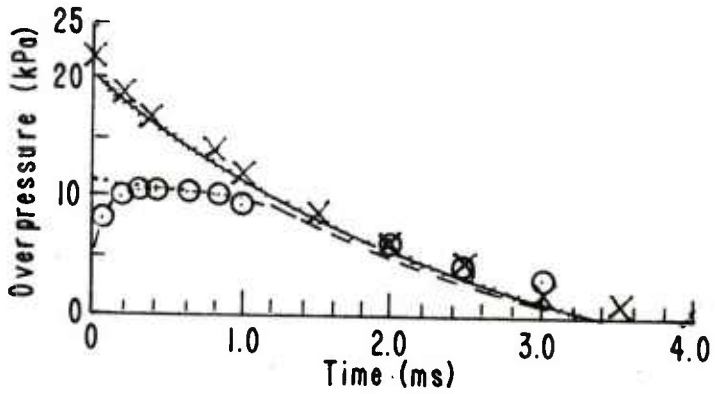

(B) FALLING SLOPE-SHOT 5, LINE A-1, STATION 8

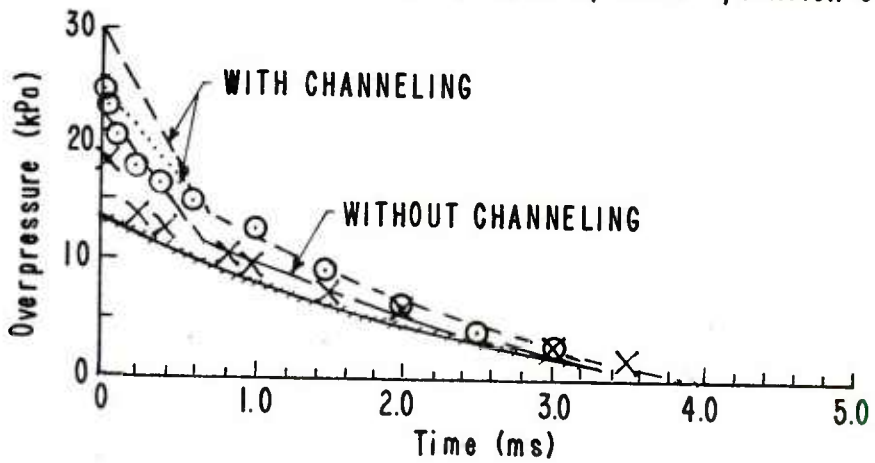

(C) CHANNELING - SHOT 13, LINE C-1, STATION 10

Figure 24. Comparison of Experimental Data with Predicted Waveforms

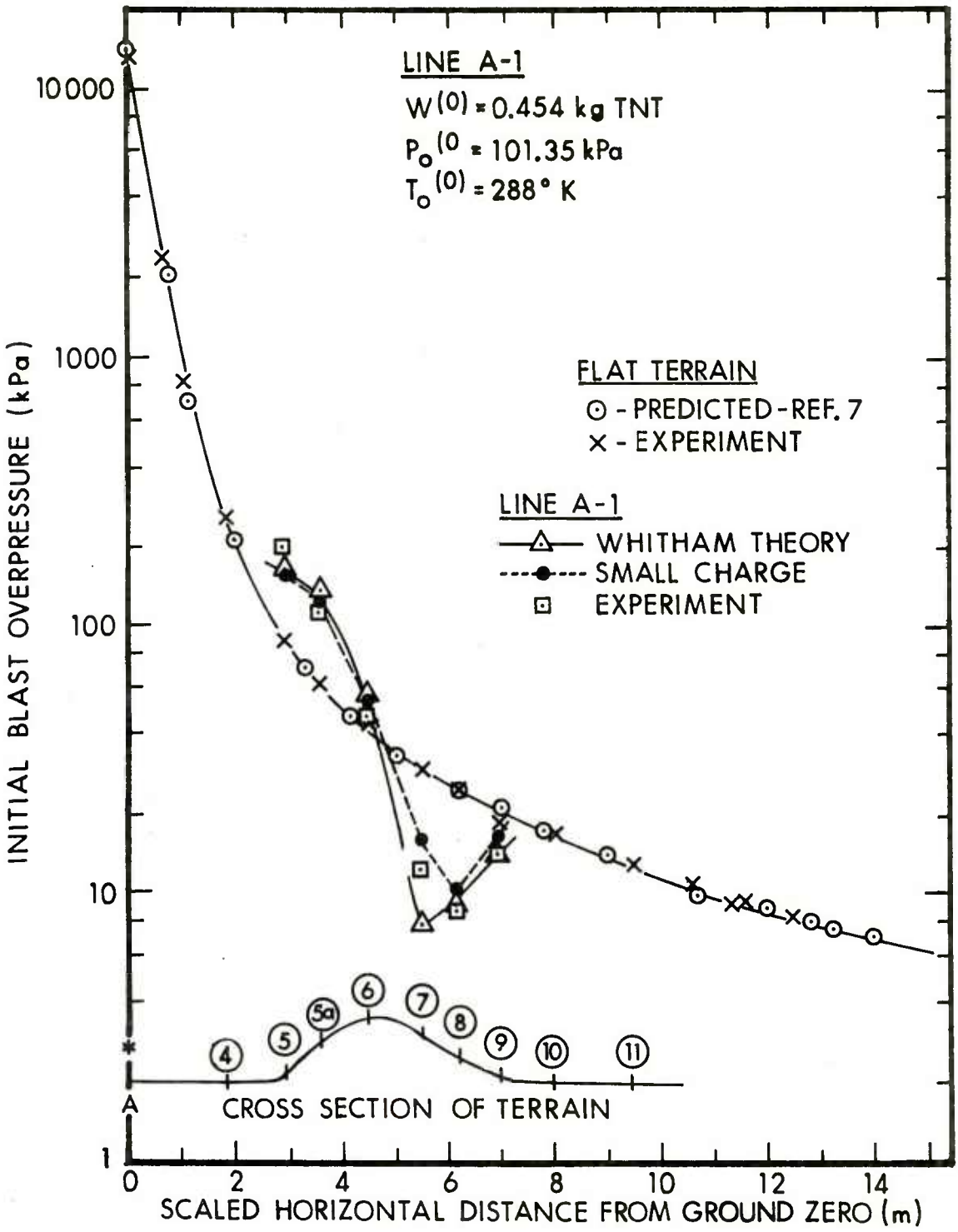

Figure 25-A. Scaled Blast Pressure as a Function of Ground Range

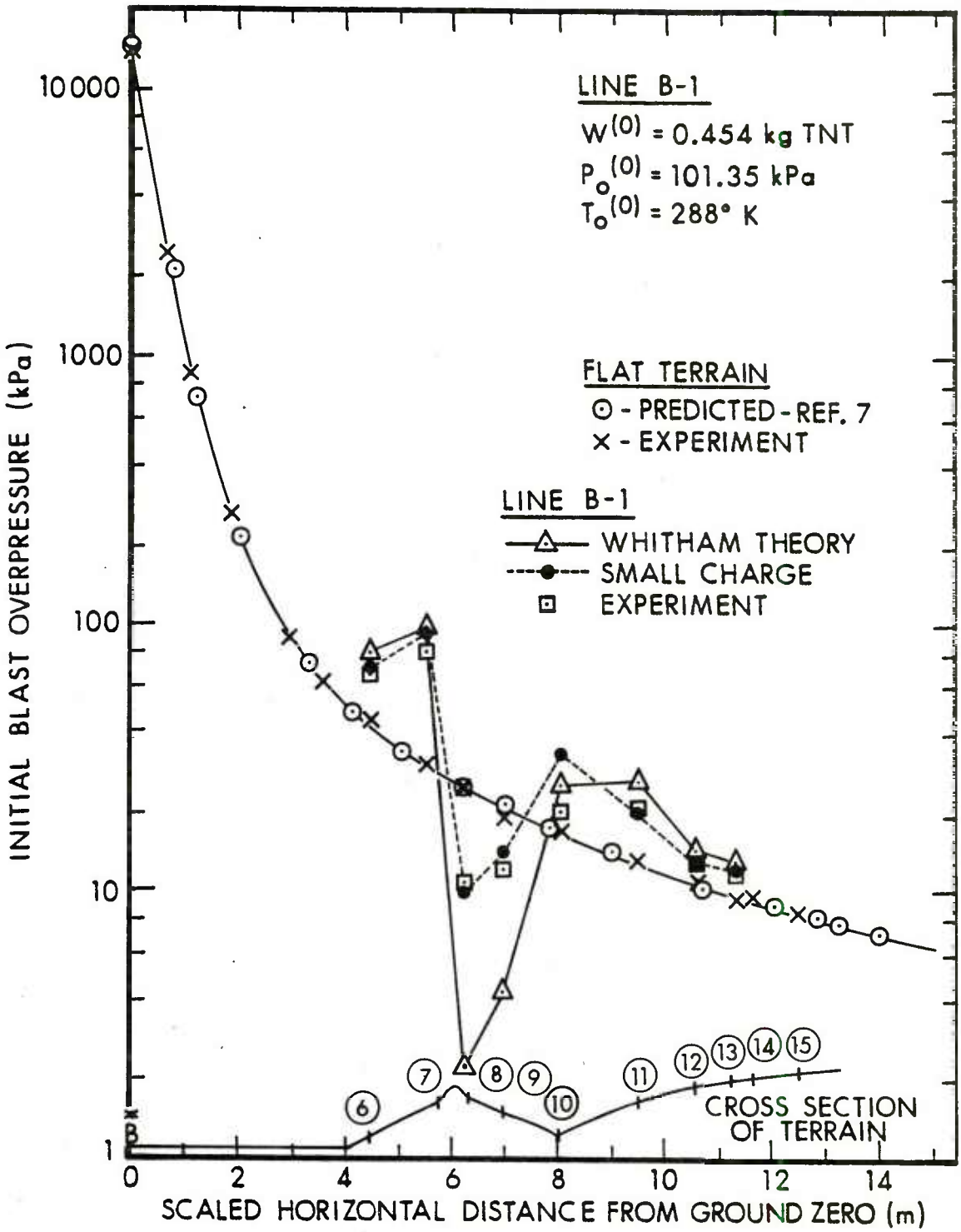

Figure 25-B. Scaled Blast Pressure as a Function of Ground Range

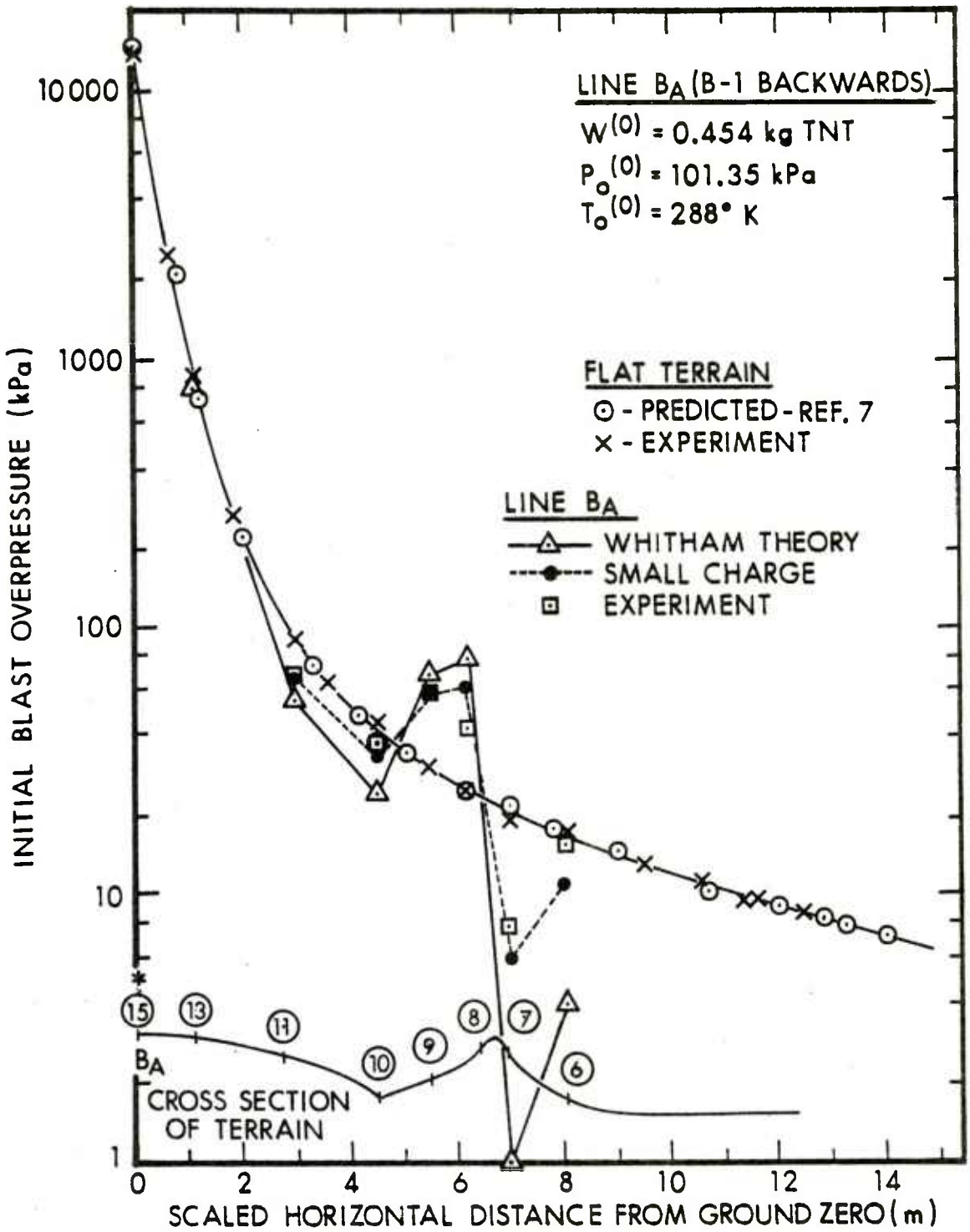

Figure 25-C. Scaled Blast Pressure as a Function of Ground Range

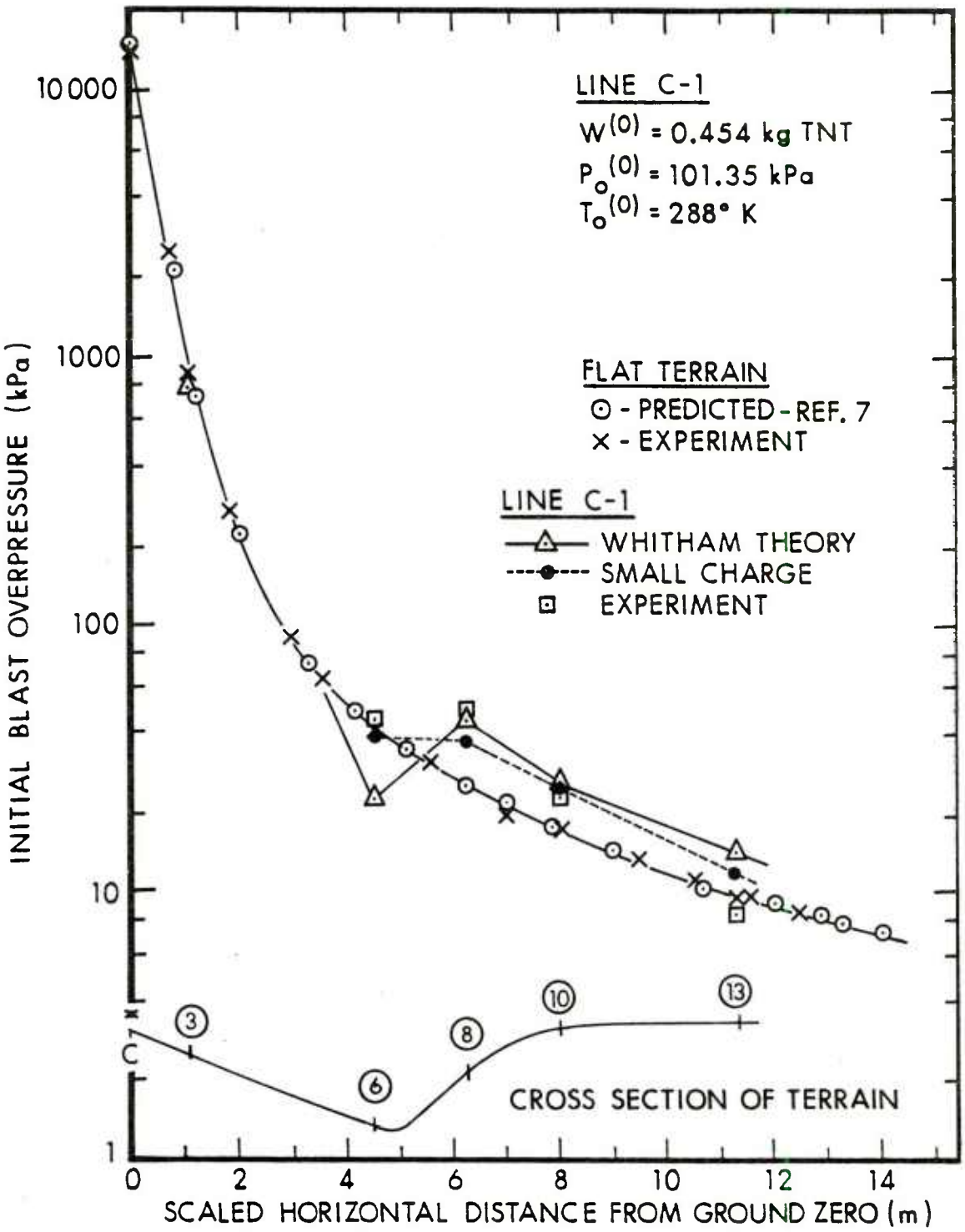

Figure 25-D. Scaled Blast Pressure as a Function of Ground Range

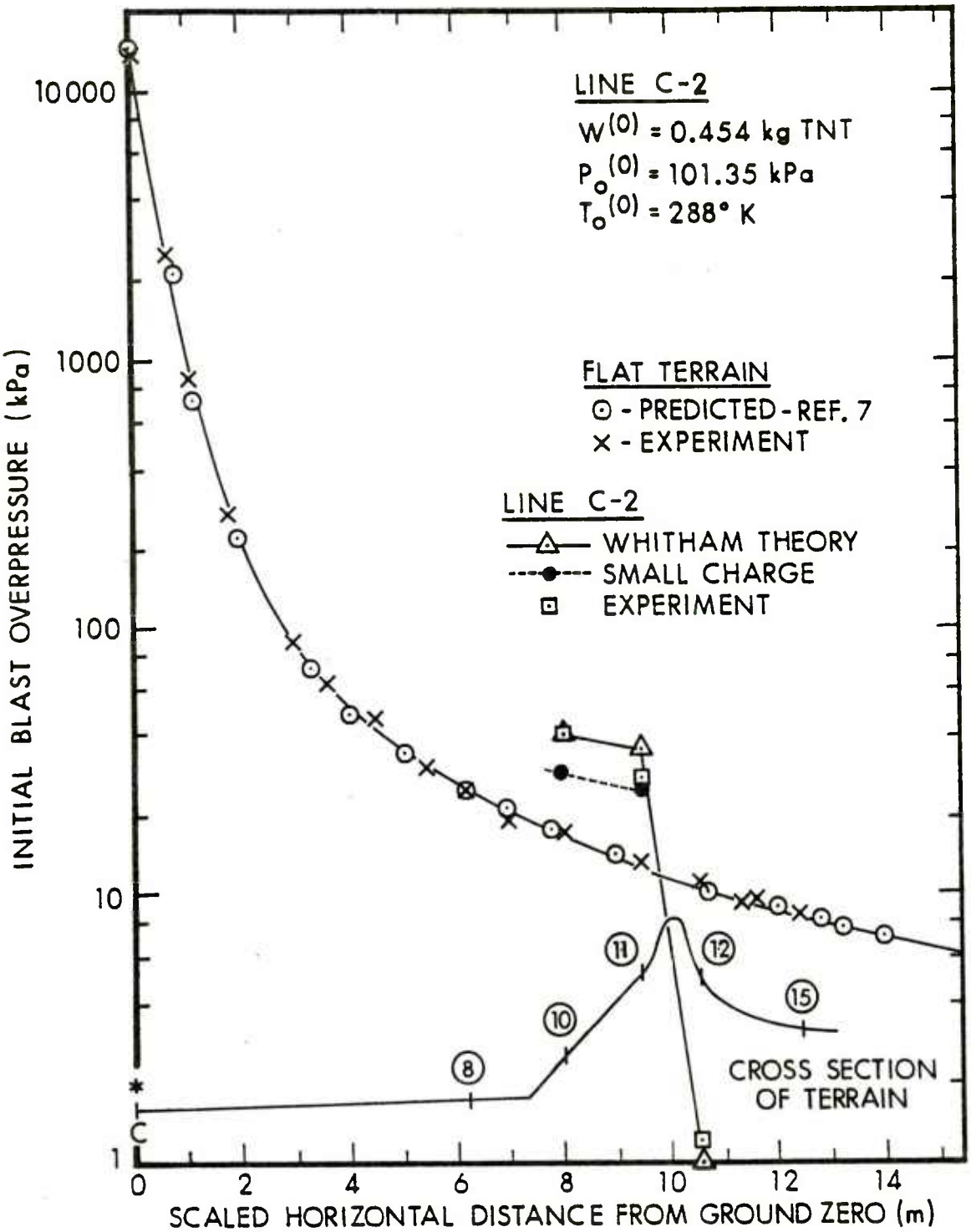

Figure 25-E. Scaled Blast Pressure as a Function of Ground Range

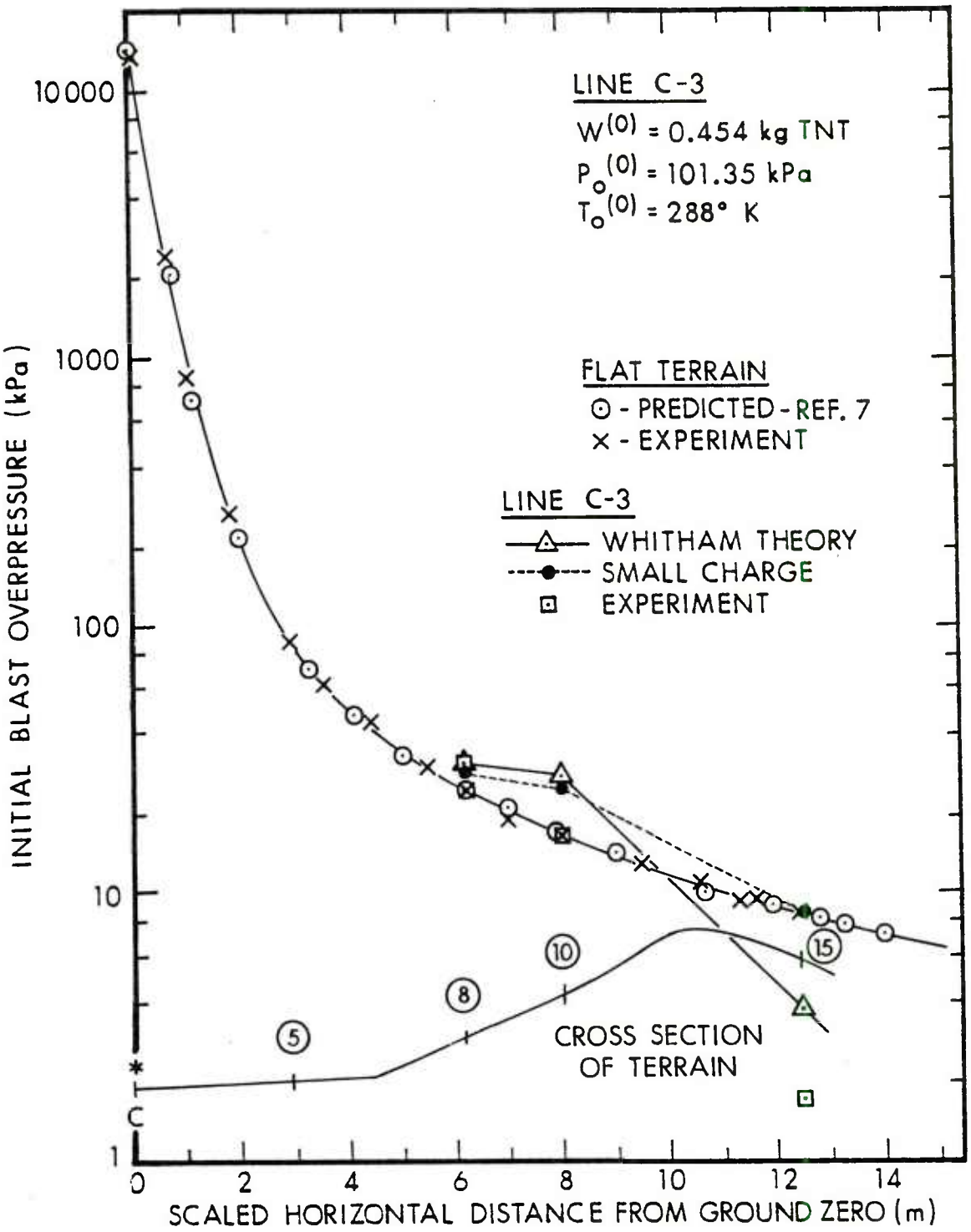

Figure 25-F. Scaled Blast Pressure as a Function of Ground Range

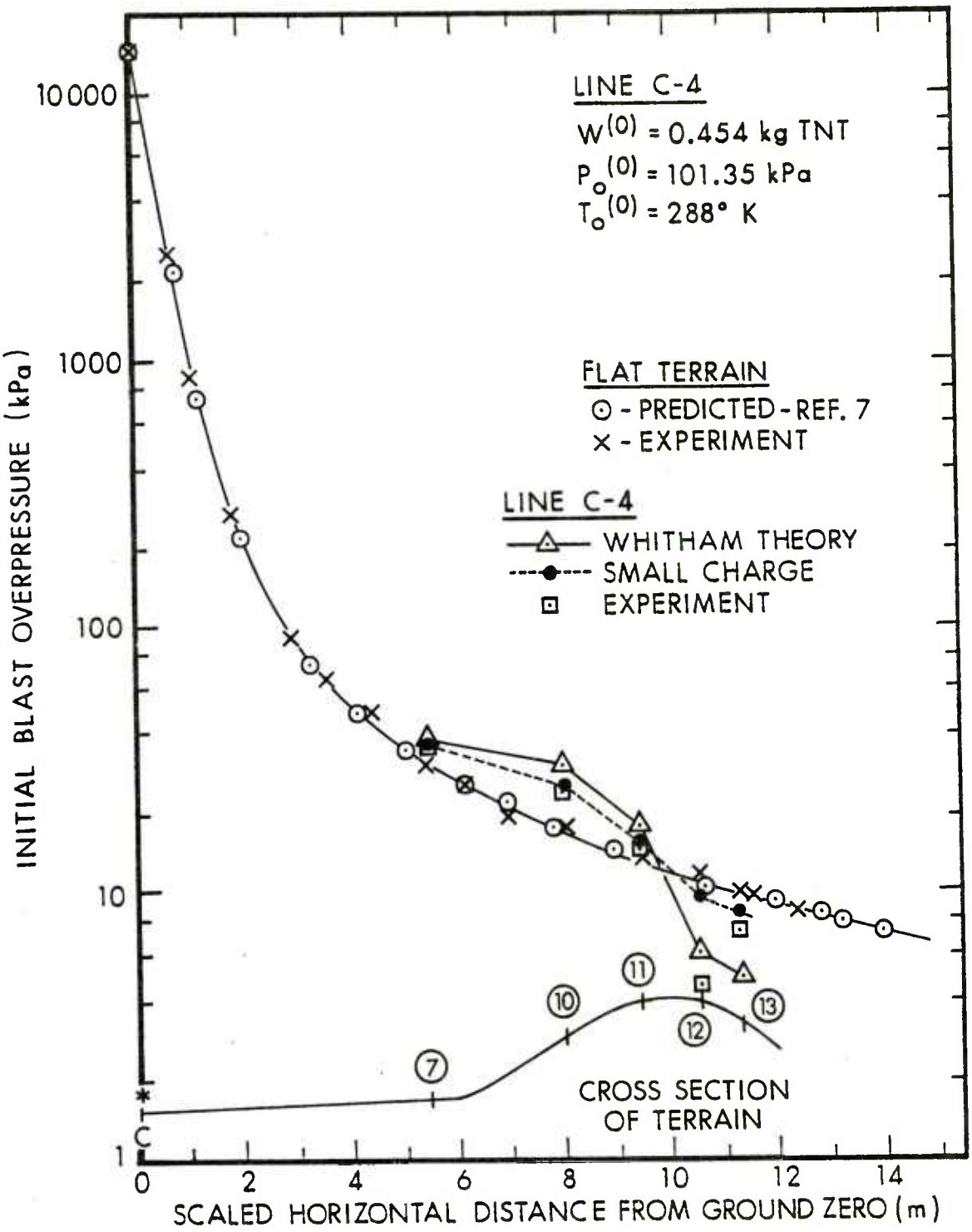

Figure 25-G. Scaled Blast Pressure as a Function of Ground Range

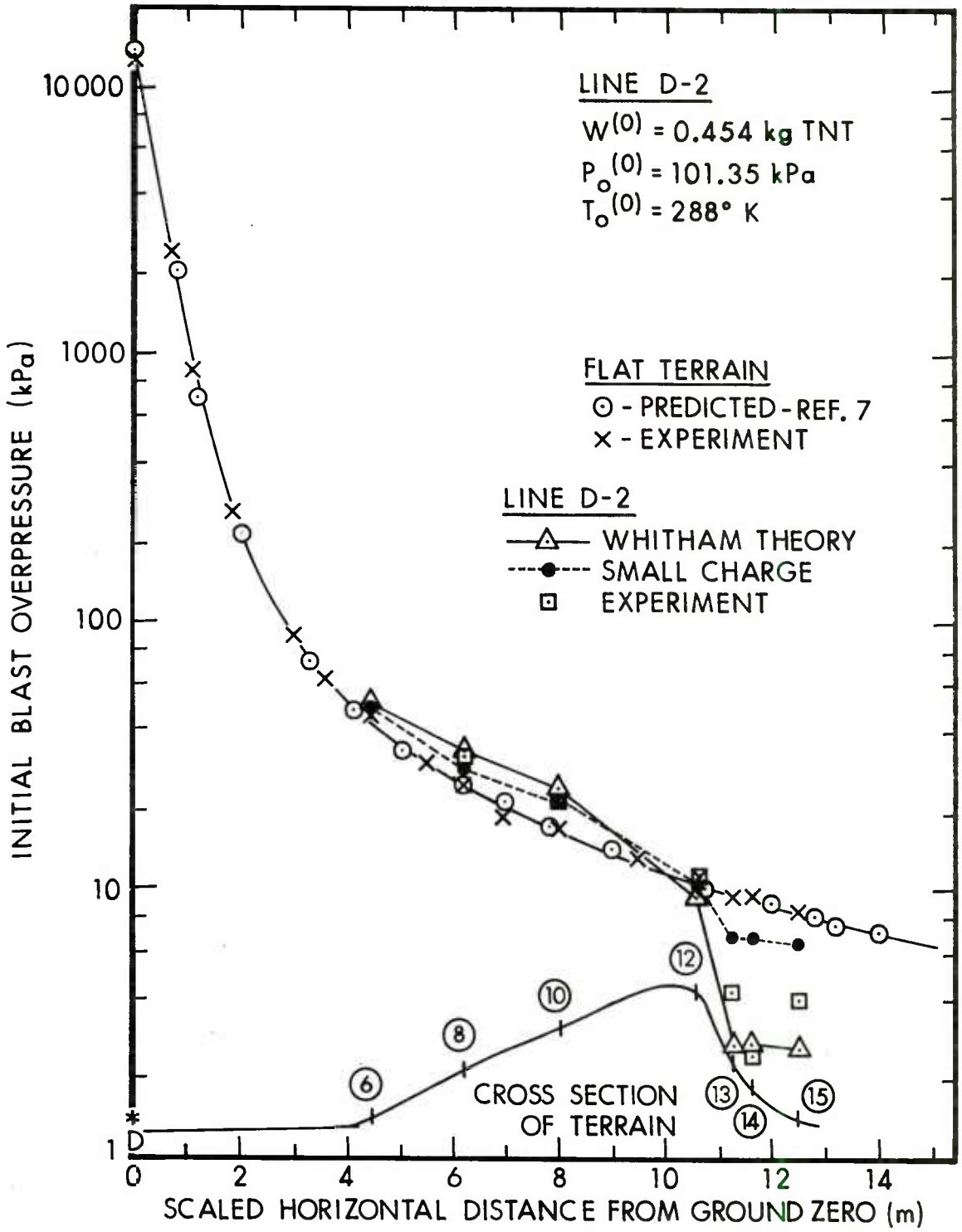

Figure 25-H. Scaled Blast Pressure as a Function of Ground Range

Figure 26 shows a comparison of the scaled positive duration obtained from the terrain features with those from the flat terrain. Predictions from Reference 7 listed the positive durations the same for the terrain stations as for the level reference stations. The positive duration is seen from Figure 26, however, to decrease on rising slopes and to increase on the falling slopes when compared to the durations measured at the flat reference stations.

Figure 27 shows two plots illustrating the combined effects of pressure and duration on the positive blast wave impulse. The net effect is an increase in impulse on the rising slopes and a decrease in impulse on the falling slopes. At the greater distant stations the impulse values are close to those obtained on the flat terrain reference line.

No channeling effect was observed at Station 10, Line C-1 located in the V-bottom valley. Only the expected increased pressure from the rising slope was noted experimentally.

The Summary and Conclusion Section will summarize these differences as a function of terrain features.

V. SUMMARY AND CONCLUSIONS

An experimental shot series was fired at the Socorro, NM site to determine the effect of combined terrain features on a blast wave crossing the terrain. The test was designed to represent a real situation scenerio which included hills and valleys combined.

The test with the terrain model was conducted with a nominal 0.454 kg of bare spherical 50/50 pentolite fired over the model at a burst height of 0.6 m. The specific simulation was for a weapon with a yield of 125 kt exploded at a burst height of 300 m. Blast lines and ground zeros were chosen so as to observe the different effects on the blast wave by rising slopes, falling slopes, and channeling of valleys.

Pressure-time histories were recorded at several stations on sets of test and flat terrain reference blast lines by means of piezolectric pressure transducers. The experimental data were compared to pre-shot predictions[7]. Detailed sets of these comparisons are grouped in Appendix C.

These graphic comparisons show that in some cases the flat terrain pre-shot predictions of Reference 7 did not agree with the experimental field values obtained. This was primarily because of needed altitude corrections. Therefore, new initial blast pressure predictions were made and used as input pressures for the pressure prediction curves for the rising and falling terrain features.

Table XXI highlights the major differences between these post-shot predictions and the experimentally measured pressures. A study of this table indicates that the small charge method of Reference 7 predicted the initial pressure for the rising slopes to ±15% in at a little over half of the stations. The Whitham Theory predicted with the same accuracy (±15%) on the rising slopes in about a third of the cases.

Neither of the prediction methods predicted very satisfactorily the initial pressure on the falling slopes. The apparent difficulty was to correctly determine the expected shape in rounding of the blast waveform caused by the falling slopes. In some instances a peaked wave occurred instead of the predicted rounded wave. As indicated in Table XXI, percentage error can become quite large (>100%) for such a case of wrong waveform.

Durations were predicted[7] to be the same for all types of terrain features - the same as for the flat terrain reference lines. Table XXII shows the errors in positive duration by predicting in this manner. The durations were predicted as much as 30% too high for the rising slopes and about the same amount too low on the falling slopes.

No pre-shot predictions were made for impulse. Table XXIII shows, however, the changes observed in impulse on the slopes when compared to the impulse on the flat terrain. The pressure increases combined with the duration decreases on the rising slopes to give a net increase of impulse over the flat line. As much as a 39% increase was measured for Line A-1-5a. The falling slopes produced a corresponding decrease in impulse. For example, this was about a 17% decrease for Line B_a, Station 11. There were impulse variation in between these extremes depending on the previous terrain features.

In conclusion, neither of the two prediction methods (Whitham or Small Charge) used to obtain the blast parameters over multiple terrain features was found experimentally to give completely satisfactory answers. Another important consideration in making predictions over multiple terrain features is that the predictions should consider altitude of scenerio to be studied. The present set of experiments for example, were moved from a near - zero elevation to one of about 1,370 m. This corresponded to a change in ambient pressure of 101.35 kPa at sea level to about 85 kPa at the elevated New Mexico test site. The blast overpressure was directly proportional to these values of ambient pressure and new post-shot predictions were needed. Predictions of blast over any given terrain should, therefore, use the altitude of the specific scenerio in order to obtain the most accurate results.

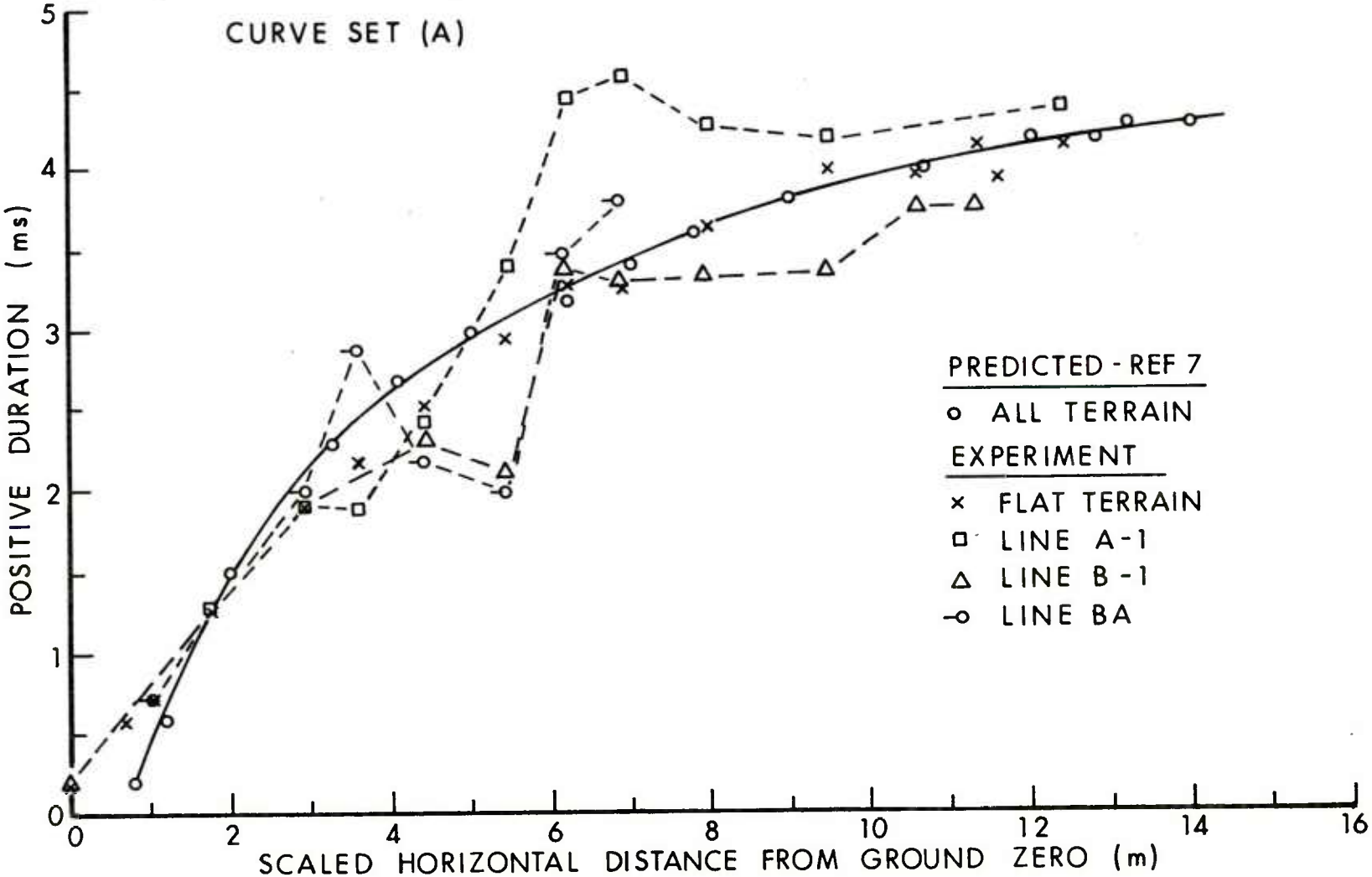

Figure 26. Scaled Positive Duration as a Function of Ground Range

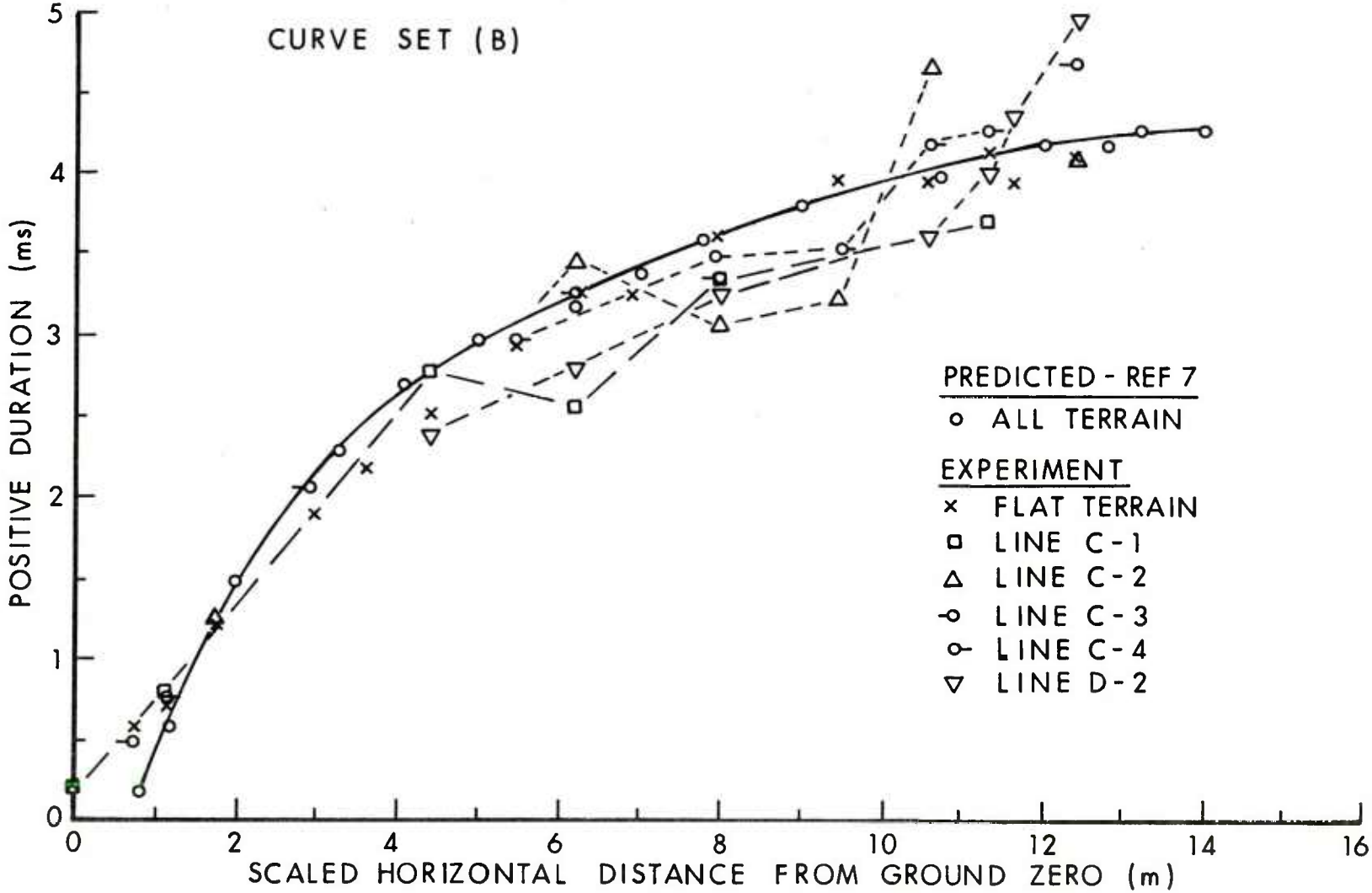

Figure 26 (Cont). Scaled Positive Duration as a Function of Ground Range

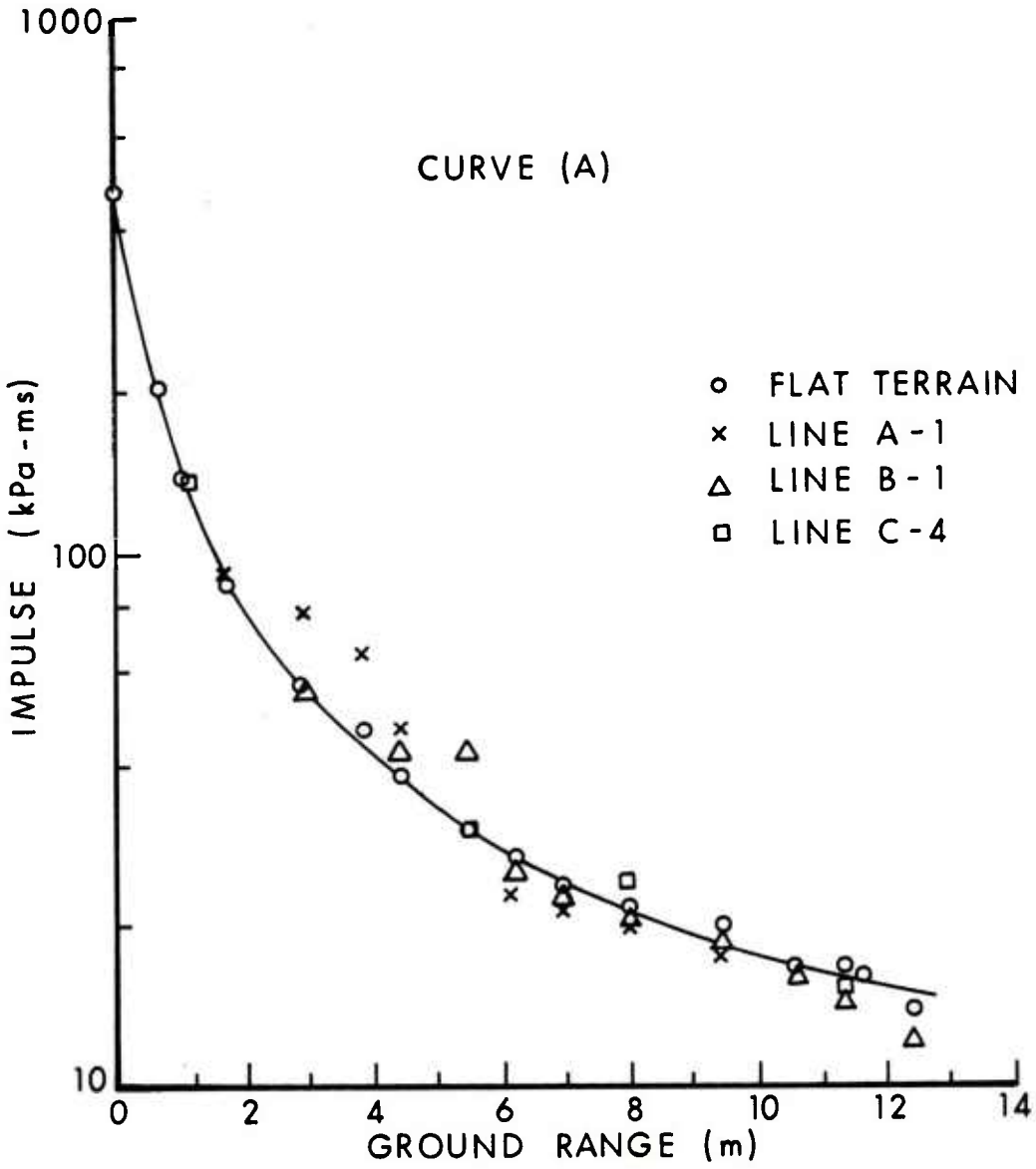

Figure 27. Scaled Impulse as a Function of Ground Range

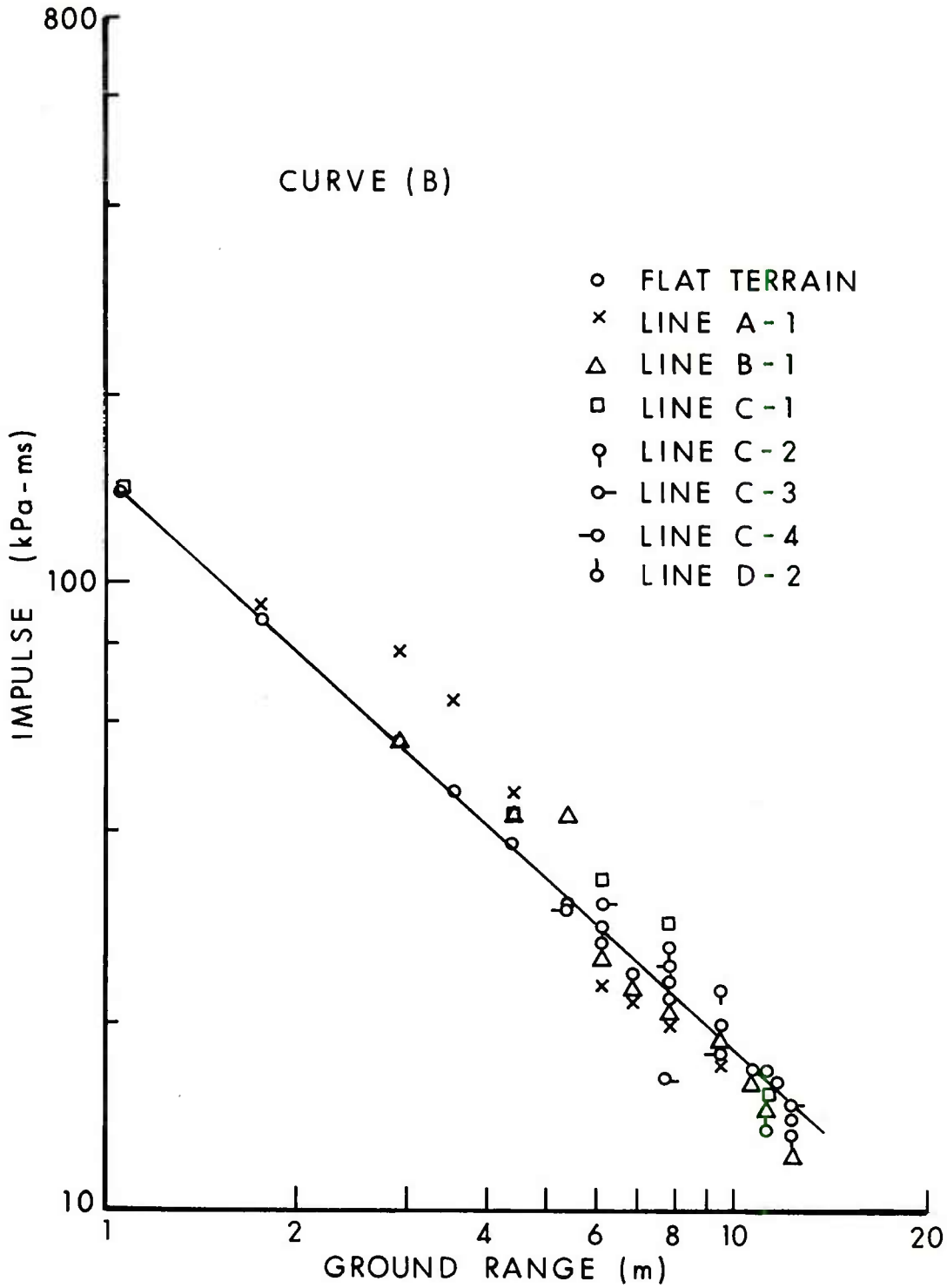

Figure 27 (Cont). Scaled Impulse as a Function of Ground Range

Table XXI. Comparison of Blast Pressure as a Function of Terrain

Blast Line and Station	Terrain Slope Characteristics	Waveform			Predicted Initial Blast Overpressure	
		Whitham	Small Charge	Experiment	Whitham	Small Charge
Line A-1						
S	Rising, bottom	Steeply peaked	-	Steeply peaked	17% Low	19% Low
Sa	Rising, middle	Peaked	Peaked	Slightly peaked	19% High	8% High
6	Rising, top	Slightly peaked	Slightly peaked	Slightly rounded	20% High	14% High
7	Falling, top	Rounded	Peaked	Rounded	38% Low	26% High
8	Falling, middle	Rounded	Peaked	Rounded	7% High	19% High
9	Falling, bottom	Rounded	Peaked	Peaked	1% Low	17% High
Line 8-1						
6	Rising , bottom	Steeply peaked	Steeply peaked	Peaked	19% High	4% High
7	Rising, top	Peaked	-	Slightly rounded	24% High	22% High
8	Falling, top	Rounded	Rounded	Rounded	79% Low	2% Low
9	Falling, middle	Rounded	Peaked	Slightly rounded	65% Low	16% High
10	Valley, V-bottom	Peaked	Peaked	Peaked	26% High	66% High
11	Rising, middle	Peaked	Peaked	Peaked	29% High	1% Low
12	Rising, top	Slightly peaked	Slightly peaked	Slightly peaked	11% High	1% Low
13	Rising, top	Slightly peaked	Slightly peaked	Slightly peaked	17% High	8% High
Line 8_a(8-1)						
11	Falling middle	Slightly peaked	Slightly peaked	Slightly peaked	21% Low	2% Low
10	Valley, V-bottom	Slightly rounded	Slightly peaked	Slightly peaked	36% Low	11% Low
9	Rising, middle	Steeply peaked	Steeply peaked	Peaked	14% High	S% Low
8	Rising, top	Peaked	-	Peaked,then rounded	82% High	40% High
7	Falling, top	Rounded	Peaked	Rounded	>100% Low	24% Low
6	Falling, bottom	Slightly rounded	Peaked	Peaked	7S% Low	30% Low
Line C-1						
8	Rising, middle	Steeply peaked	Steeply peaked	Peaked	10% Low	25% Low
10	Rising, top	Peaked	Peaked	Peaked	11% High	S% High
13	Rising, top	Slightly peaked	Slightly peaked	Slightly rounded	71% High	41% High
Line C-2						
10	Rising, middle	Steeply peaked	Steeply peaked	Steeply peaked	1% Low	29% Low
11	Rising, top	Peaked	Peaked	Peaked	28% High	10% Low
12	Falling, top	Slightly peaked	-	Rounded, twice	>16% High	-
Line C-3						
8	Rising, bottom	Peaked	Peaked	Peaked	2% High	5% Low
10	Rising, middle	Peaked	Peaked	Peaked	66% High	47% High
1S	Falling, middle	Rounded	Peaked	Slightly rounded	118% High	403% High
Line C-4						
10	Rising, middle	Peaked	Peaked	Peaked	27% High	5% High
11	Rising, top	Peaked	Peaked	Slightly rounded	2S% High	10% Low
12	Falling, top	Rounded	Peaked	Rounded	30% High	113% High
13	Falling, bottom	Rounded	Peaked	Slightly rounded	34% Low	21% High
Line D-2						
6	Rising, bottom	Steeply peaked	-	Peaked	2% High	0%
8	Rising, bottom middle	Peaked	Peaked	Peaked	4% High	12% Low
10	Rising, middle	Peaked	Peaked	Peaked	11% High	0.S% Low
1S	Falling, bottom	Rounded	Peaked	Rounded	36% Low	65% High

Table XX1. Comparison of 8last Pressure as a Function of Terrain (Cont)

8last Line and Station	θ', deg	Experimental Initial Pressure, kPa		Overpressure Ratio
		Sloping	Flat	Sloping/Flat
5	28.3	198	87.3	2.27
5a	28.6	113	50.8	1.86
6	9.5	47.5	44.0	1.08
7	-24	12.3	28.8	0.43
8	-24	8.8	24.0	0.37
9	-16	14.1	18.4	0.77
Line 8-1				
6	18.9	65.6	44.0	1.49
7	41.9	79.0	28.8	2.74
8	-32.4	10.7	24.0	0.44
9	-21.3	12.1	18.4	0.66
10	14.4	19.9	16.9	1.18
11	15	20.2	13.0	1.55
12	5	13.1	11.0	1.19
13	6	11.1	9.4	1.18
Line 8_a(8-1)				
11	-18.8	65.5	87.3	0.75
10	-42	35.9	44.0	0.82
9	32.5	56.0	28.8	1.94
8	21.5	41.3	24.0	1.72
7	-14.5	7.4	18.4	0.40
6	-15	15.1	16.9	0.89
Line C-1				
8	14.9	48.1	24.0	2.00
10	4	22.6	16.9	1.34
13	0	8.2	9.4	0.87
Line C-2				
10	19.8	39.2	16.9	2.32
11	20.9	26.6	13.0	2.05
12	-45.8	1.19	11.0	0.11
Line C-3				
8	5.7	29.5	24.0	1.23
10	9.7	16.3	16.9	0.96
15	-9	1.65	8.4	0.20
Line C-4				
10	12.9	22.9	16.9	1.36
11	5.4	13.6	13.0	1.05
12	-7.5	4.32	11.0	0.39
13	-7.5	6.94	9.4	0.74
Line 0-2				
6	3.5	47.1	44.0	1.07
8	7.6	31.8	24.0	1.32
10	8.3	21.1	16.9	1.25
12	-1.9	11.1	11.0	1.01
13	-14.1	4.1	9.4	0.44
14	-13.9	2.39	9.7	0.25
15	-11.7	3.88	8.4	0.46

Table XXII. Comparison of Positive Duration as a Function of Terrain

Blast Line and Station	Terrain Slope Characteristic	θ', deg	Predicted Flat or Sloping	Duration, ms Experimental Flat	Duration, ms Experimental Sloping	Sloping Pred/Exp Durations	Sloping/Flat Ratio of Exp Durations
Line A-1							
5	Rising, bottom	28.3	2.3	1.89	1.82	1.26	0.96
5a	Rising, middle	28.6	2.7	2.18	1.89	1.43	0.87
6	Rising, top	9.5	3.0	2.52	2.45	1.22	0.97
7	Falling, top	-24	3.2	29.3	3.38	0.95	1.15
8	Falling, middle	-24	3.4	3.27	4.45	0.76	1.36
9	Falling, bottom	-16	3.6	3.25	4.58	0.79	1.41
Line 8-1							
6	Rising, bottom	18.9	3.0	2.52	2.31	1.30	0.92
7	Rising, top	41.9	3.2	2.93	2.12	1.51	0.72
8	Falling, top	-32.4	3.4	3.27	3.37	1.01	1.03
9	Falling, middle	-21.3	3.6	3.25	3.29	1.09	1.01
10	Valley, V-Bottom	14.4	3.8	3.60	3.33	1.14	0.93
11	Rising, middle	15	4.0	3.97	3.36	1.18	0.85
12	Rising, top	5	4.2	3.97	3.74	1.12	0.94
13	Rising, top	6	4.2	4.15	3.76	1.12	0.91
Line B_a(B-1)							
11	Falling, middle	-18.8	2.3	1.89	2.00	1.15	1.06
10	Valley, V-bottom	-42	3.0	2.52	2.89	1.04	1.15
9	Rising, middle	32.5	3.2	2.93	2.19	1.46	0.75
8	Rising, top	21.5	3.4	3.27	2.00	1.70	0.61
7	Falling, top	-14.5	3.6	3.25	3.47	1.04	1.07
6	Falling, bottom	-15	3.8	3.60	3.80	1.00	1.06
Line C-1							
8	Rising, middle	14.9	3.4	3.27	2.57	1.32	0.79
10	Rising, top	4	3.8	3.60	3.34	1.14	0.93
13	Rising, top	0	4.2	4.15	3.70	1.14	0.89
Line C-2							
10	Rising, middle	19.8	3.8	3.60	3.07	1.24	0.85
11	Rising, top	20.9	4.0	3.97	3.24	1.23	0.82
12	Falling, top	-45.8	4.2	3.97	4.68	0.90	1.18
Line C-3							
8	Rising, Bottom	5.7	3.4	3.27	3.26	1.04	1.00
10	Rising, middle	9.1	3.8	3.60	3.34	1.14	0.93
15	Falling, middle	-9	4.3	3.14	4.72	0.91	1.14
Line C-4							
10	Rising, middle	12.9	3.8	3.65	3.50	1.09	0.97
11	Rising, top	5.4	4.0	3.97	3.55	1.13	0.89
12	Falling, top	-7.5	4.2	3.97	4.21	1.00	1.06
13	Falling, bottom	-7.5	4.2	4.45	4.30	0.98	1.04
Line D-2							
6	Rising, bottom	3.5	3.0	2.52	2.41	1.24	0.96
8	Rising, bottom middle	7.6	3.4	3.27	2.81	1.21	0.86
10	Rising, middle	8.3	3.8	3.60	3.53	1.08	0.98
15	Falling, bottom	-11.7	4.3	4.14	4.99	0.86	1.21

Table XXIII. Comparison of Positive Impulse as a Function of Terrain Impulse

Blast Line and Station	Terrain Slope Characteristic	θ', deg	Experimental Impulse, kPa-ms		Sloping/Flat Ratio of Impulse
			Sloping Terrain	Flat Terrain	
5	Rising, bottom	28.3	77.7	56.7	1.37
5a	Rising, middle	28.6	65.2	46.8	1.39
6	Rising, top	9.5	46.6	38.6	1.21
7	Falling, top	-24	-	30.7	-
8	Falling, middle	-24	22.8	26.7	0.85
9	Falling, bottom	-16	21.6	23.8	0.91
Line B-1					
6	Rising, bottom	18.9	43.0	38.6	1.11
7	Rising, top	41.9	42.6	30.7	1.39
8	Falling, top	-32.4	25.4	26.7	0.95
9	Falling, middle	-21.3	22.2	23.8	0.93
10	Valley, V-bottom	14.4	20.8	22.0	0.94
11	Rising, middle	15	18.9	19.9	0.95
12	Rising, top	5	16.2	16.6	0.98
13	Rising, top	6	14.3	16.6	0.86
Lines 8_a (B-1)					
11	Falling, middle	-18.8	47.0	56.7	0.83
10	Valley, V-bottom	-42	41.7	38.6	1.08
9	Rising, middle	32.5	34.2	30.7	1.11
8	Rising, top	21.5	33.5	26.7	1.25
7	Falling, top	-14.5	23.0	23.8	0.97
6	Falling, bottom	-15.0	19.5	22.0	0.89
Line C-1					
8	Rising, middle	14.9	33.7	26.7	1.26
10	Rising, top	4	28.6	22.0	1.30
13	Rising, top	0	15.2	16.6	0.92
Line C-2					
10	Rising middle	19.8	25.8	22.0	1.17
11	Rising, top	20.9	22.5	19.9	1.13
12	Falling, top	-45.8	15.4	16.6	0.93
Line C-3					
8	Rising, bottom	5.7	30.4	26.7	1.14
10	Rising, middle	9.1	16.2	22.0	0.74
15	Falling, middle	-9	14.8	14.0	1.06
Line C-4					
10	Rising, middle	12.9	24.5	22.0	1.11
11	Rising, top	5.4	18.2	19.9	0.91
12	Falling, top	-7.5	16.2	16.6	0.98
13	Falling, bottom	-7.5	15.3	16.6	0.92
Line D-2					
6	Rising, bottom	3.5	37.9	38.6	0.98
8	Rising, bottom middle	7.6	27.5	26.7	1.03
10	Rising, middle	8.3	22.8	22.0	1.04
15	Falling, bottom	-11.7	13.7	14.0	0.98

ACKNOWLEDGEMENTS

The authors wish to thank all the people in the TERRA Group at the New Mexico Institute of Mining and Technology, Socorro, New Mexico, for their excellent field support of these experiments. Analog to digital data processing was done at the Waterway Experimental Station.

APPENDIX A

PRESSURE-TIME TRACES

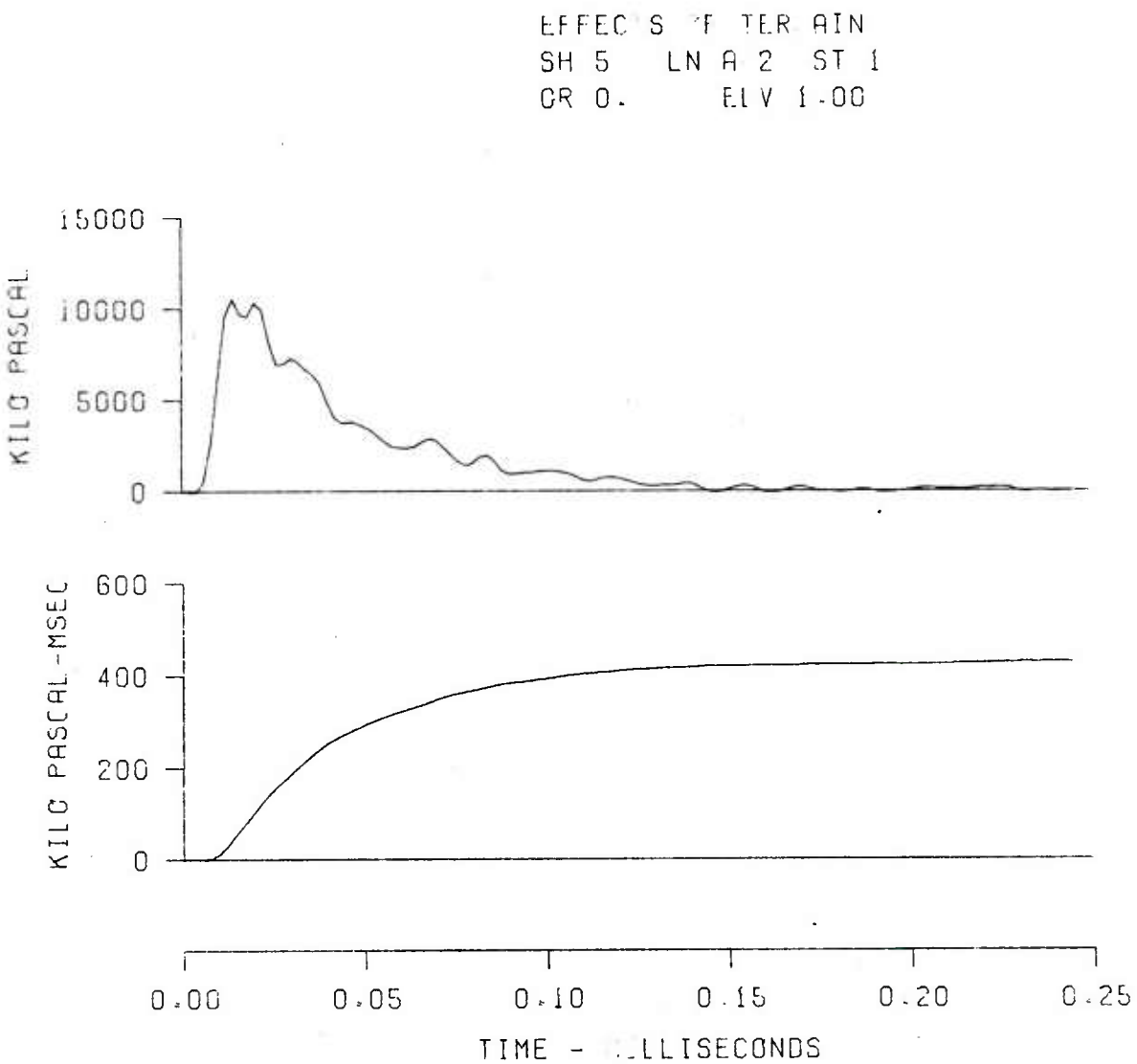

Figure A-1. Pressure-Time Traces for Lines A-1 and A-2

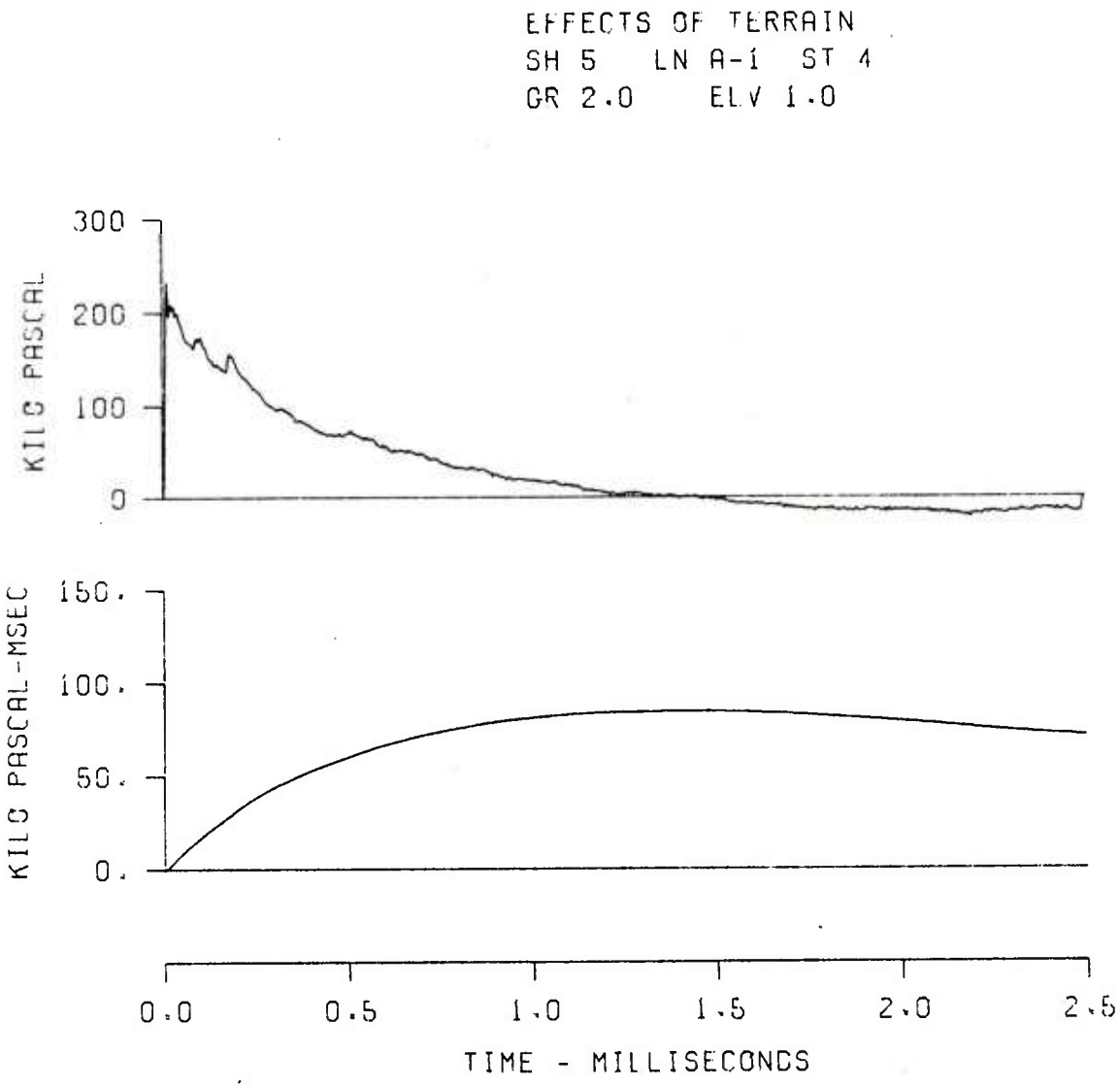

Figure A-1 (Cont). Pressure-Time Traces for Lines A-1 and A-2

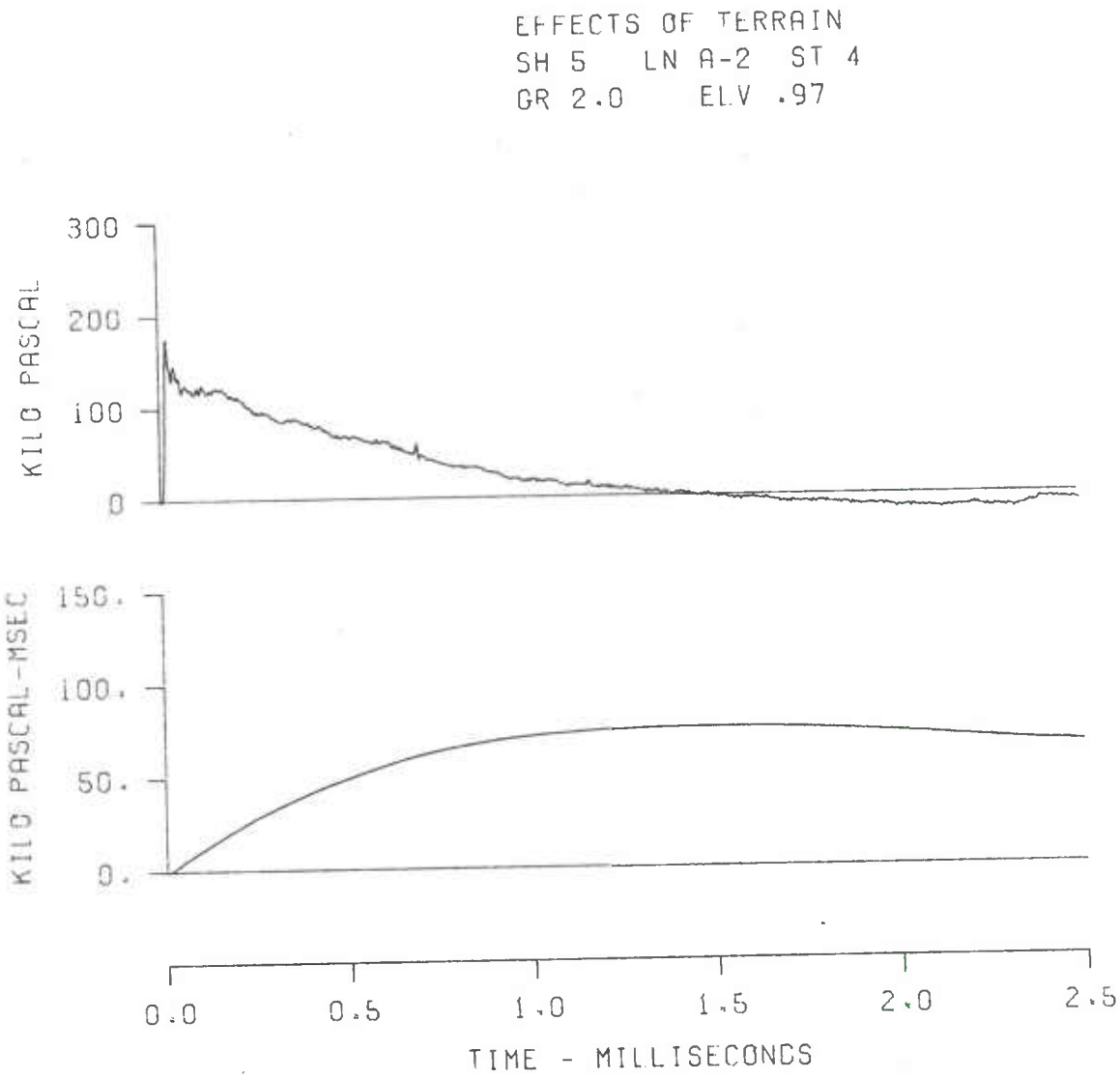

Figure A-1 (Cont). Pressure-Time Traces for Lines A-1 and A-2

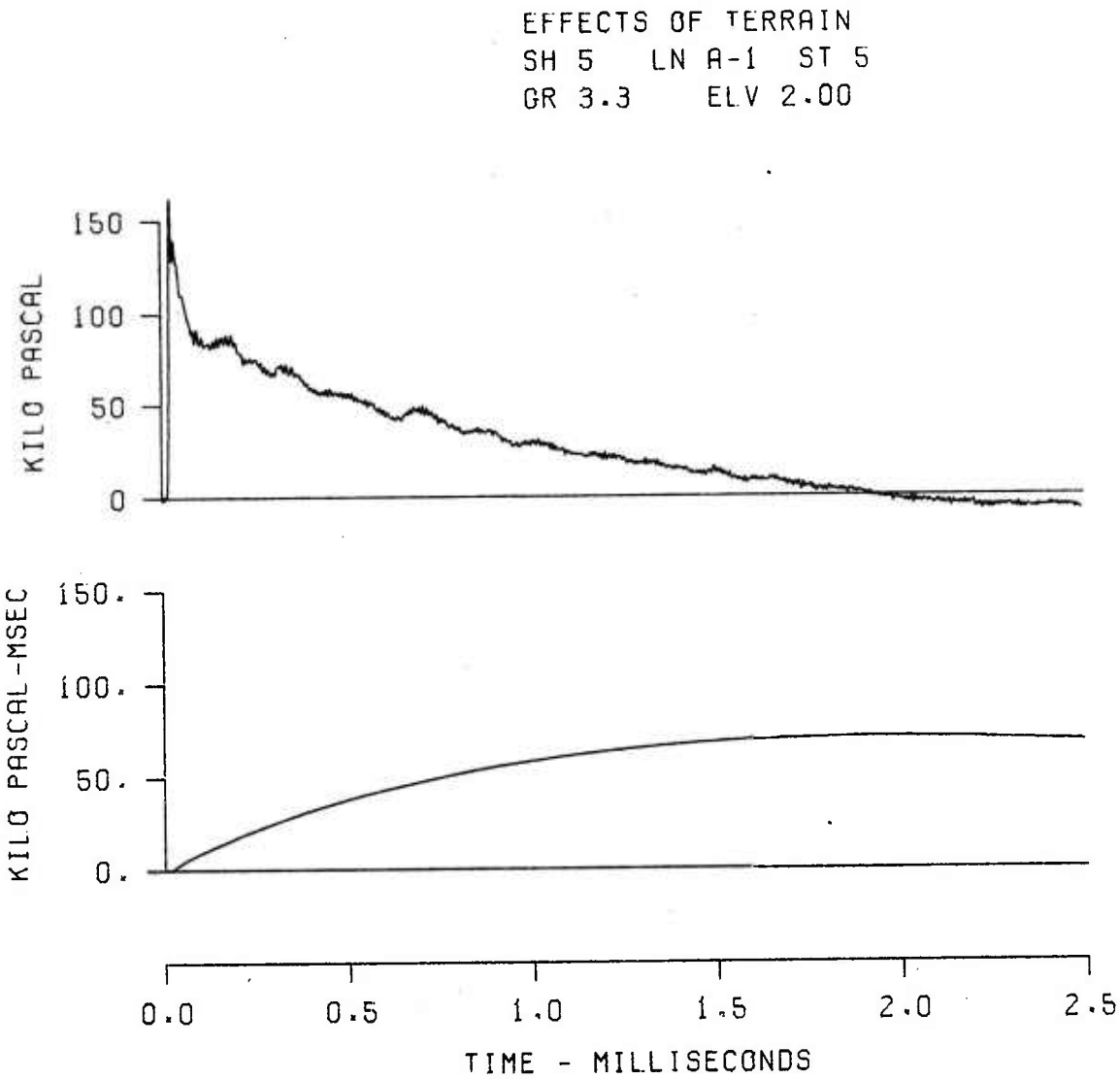

Figure A-1 (Cont). Pressure-Time Traces for Lines A-1 and A-2

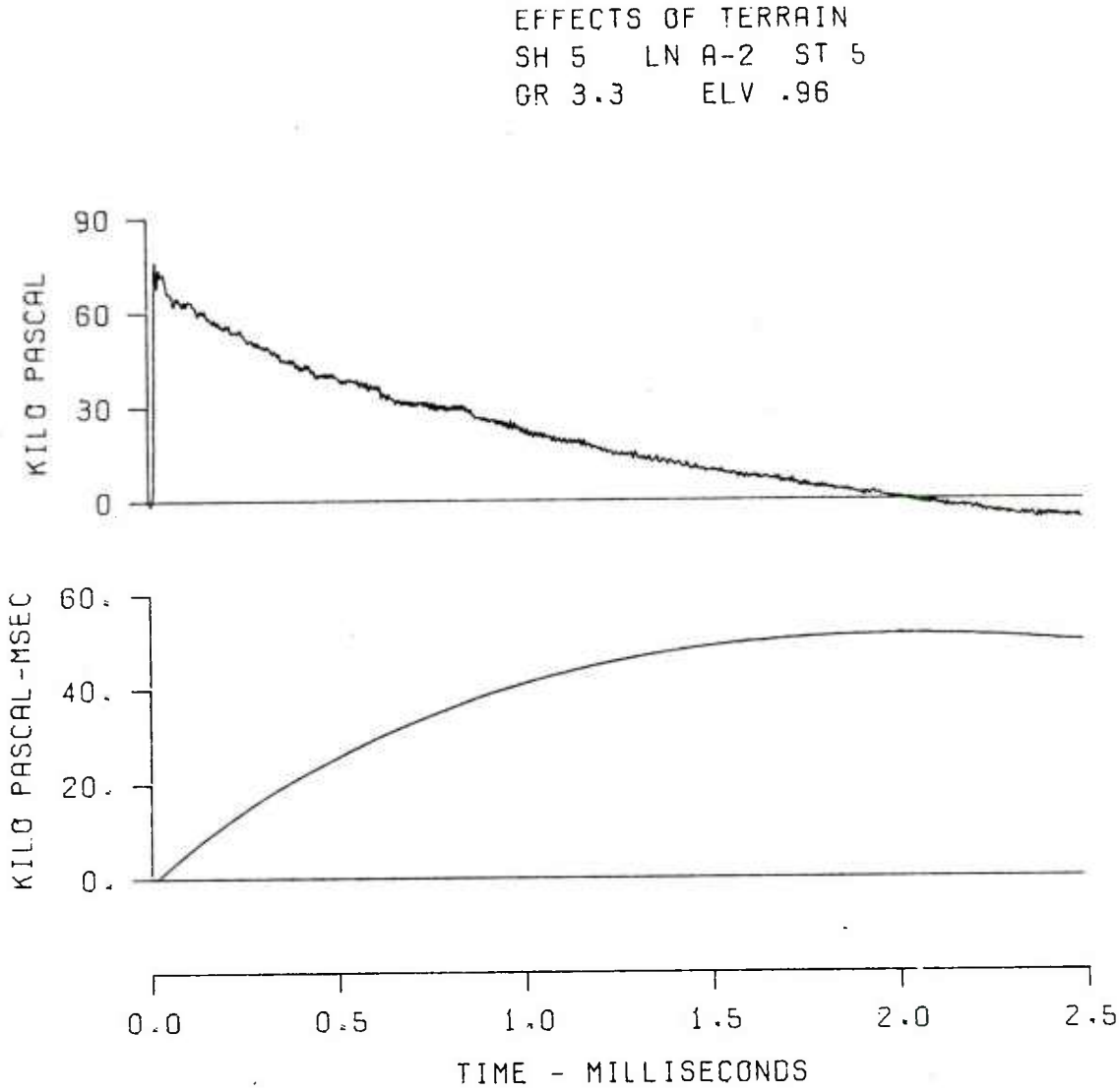

Figure A-1 (Cont). Pressure-Time Traces for Lines A-1 and A-2

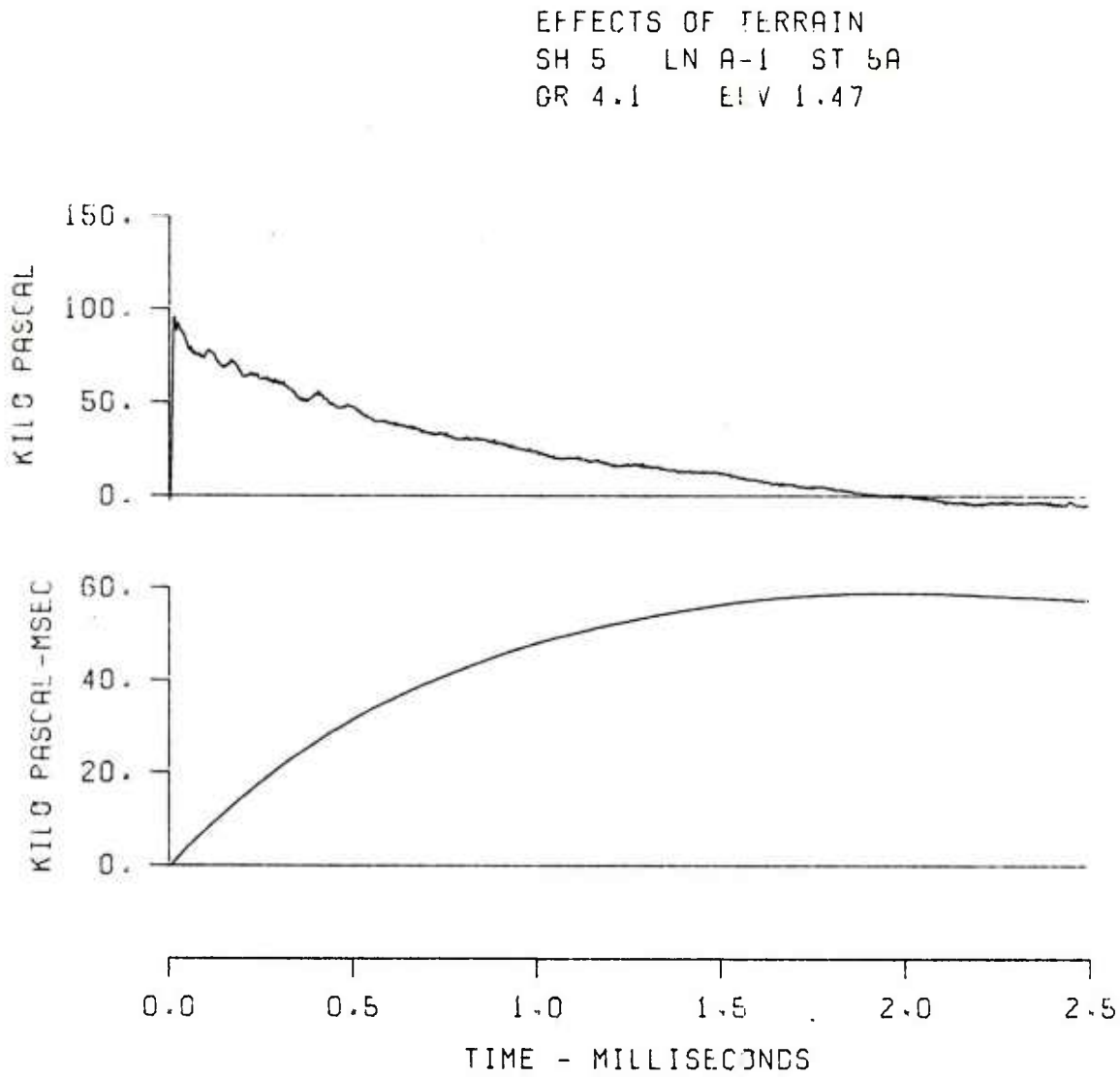

Figure A-1 (Cont). Pressure-Time Traces for Lines A-1 and A-2

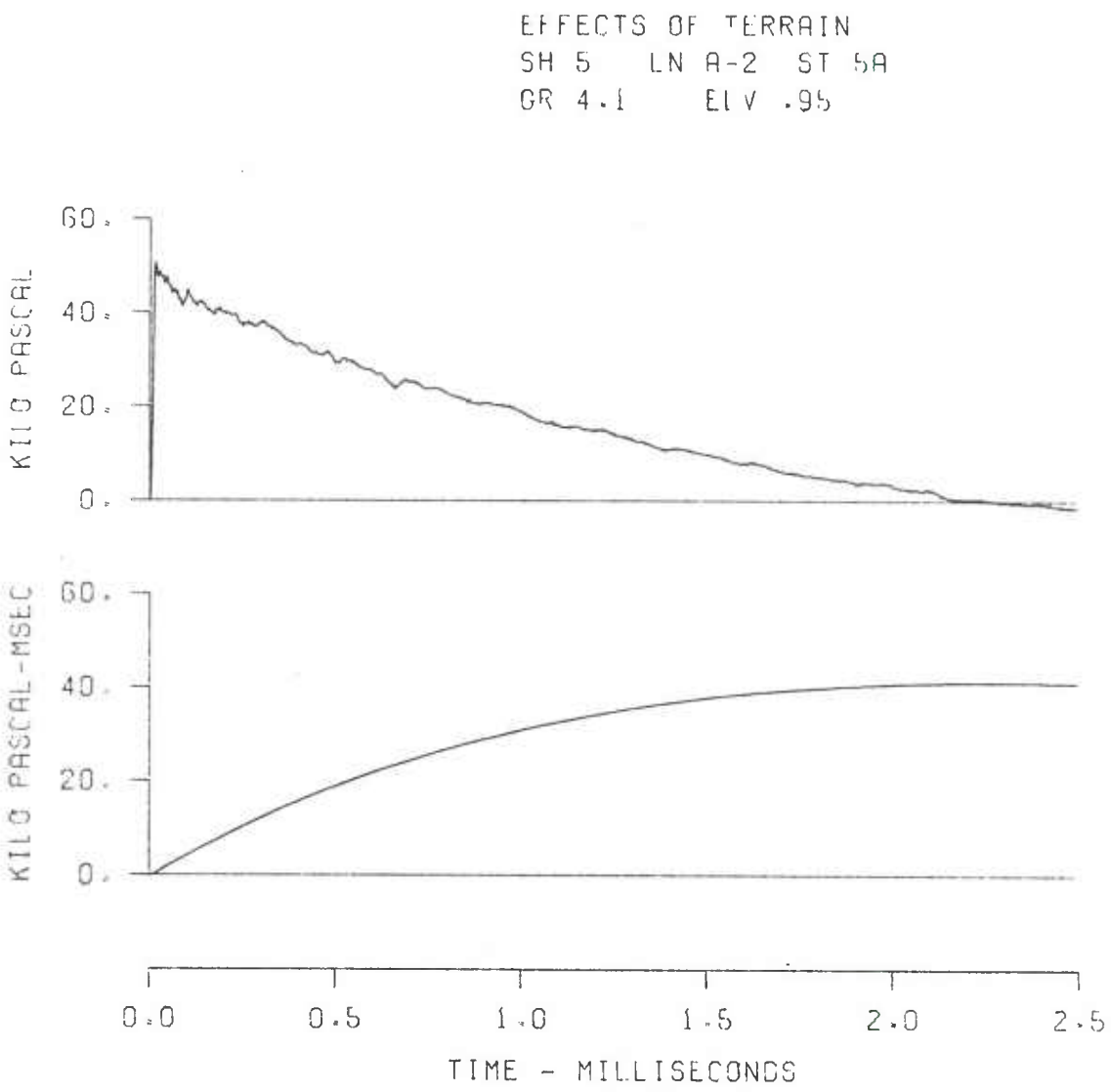

Figure A-1 (Cont). Pressure-Time Traces for Lines A-1 and A-2

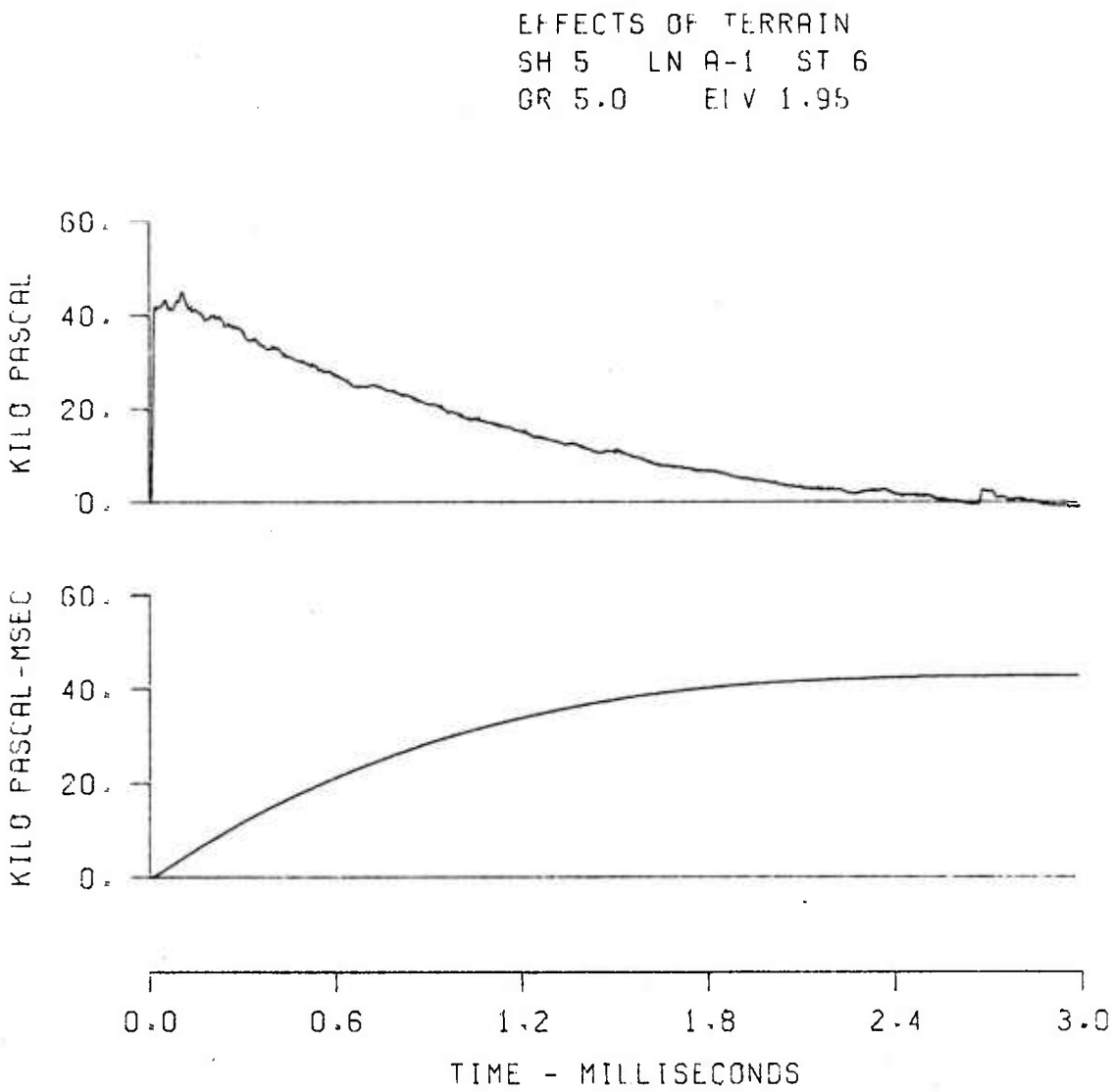

Figure A-1 (Cont). Pressure-Time Traces for Lines A-1 and A-2

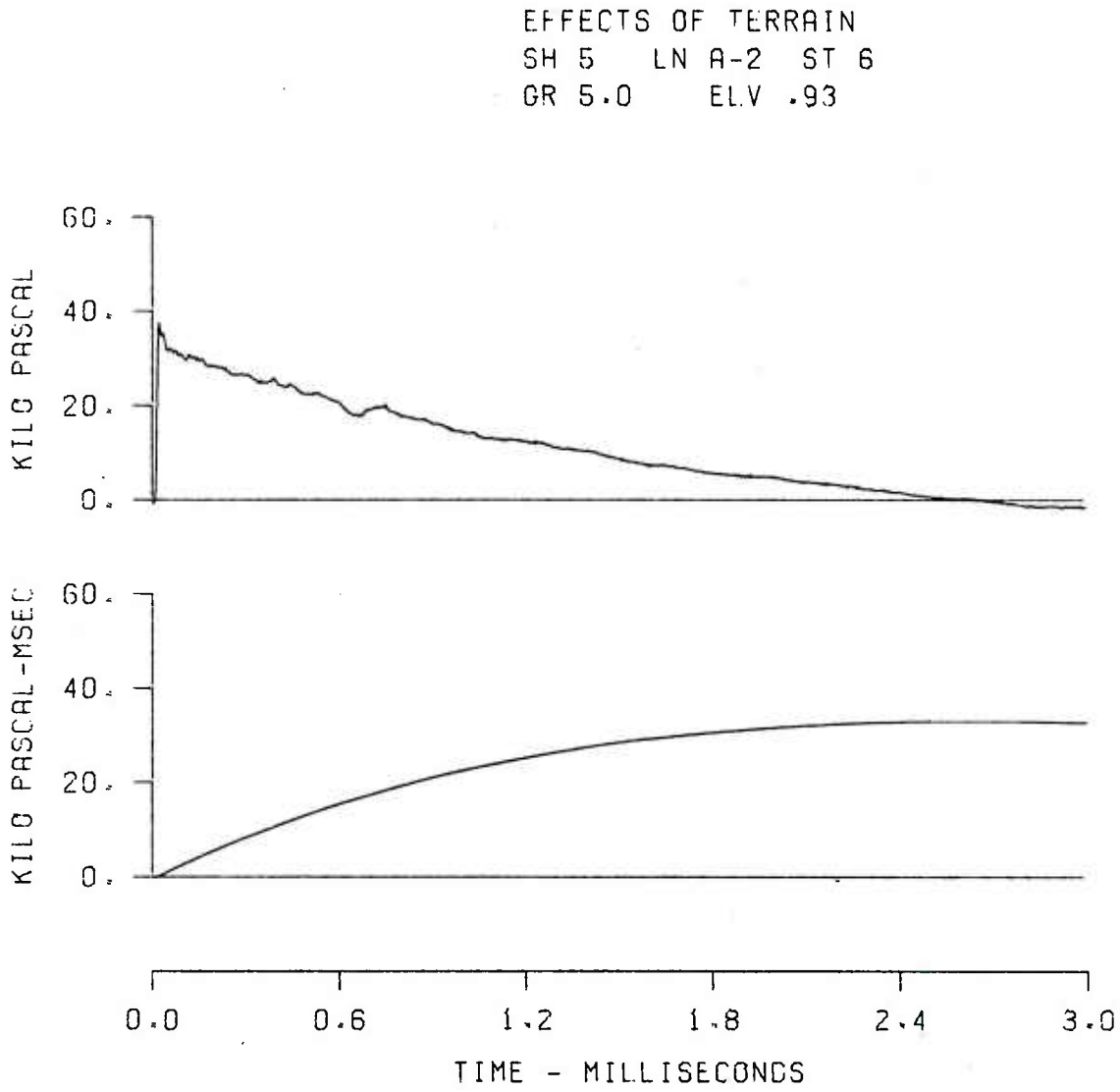

Figure A-1 (Cont). Pressure-Time Traces for Lines A-1 and A-2

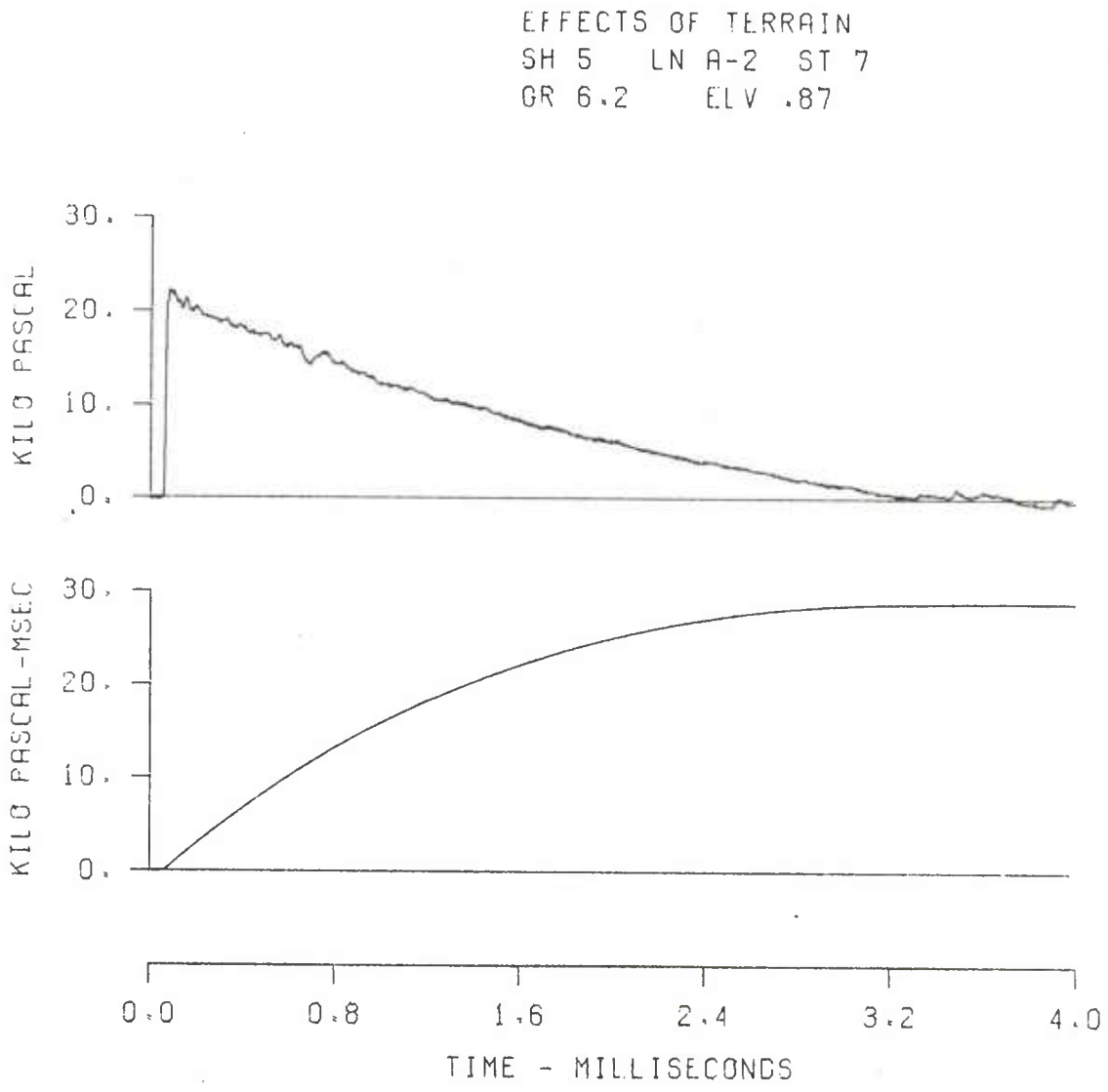

Figure A-1 (Cont). Pressure-Time Traces for Lines A-1 and A-2

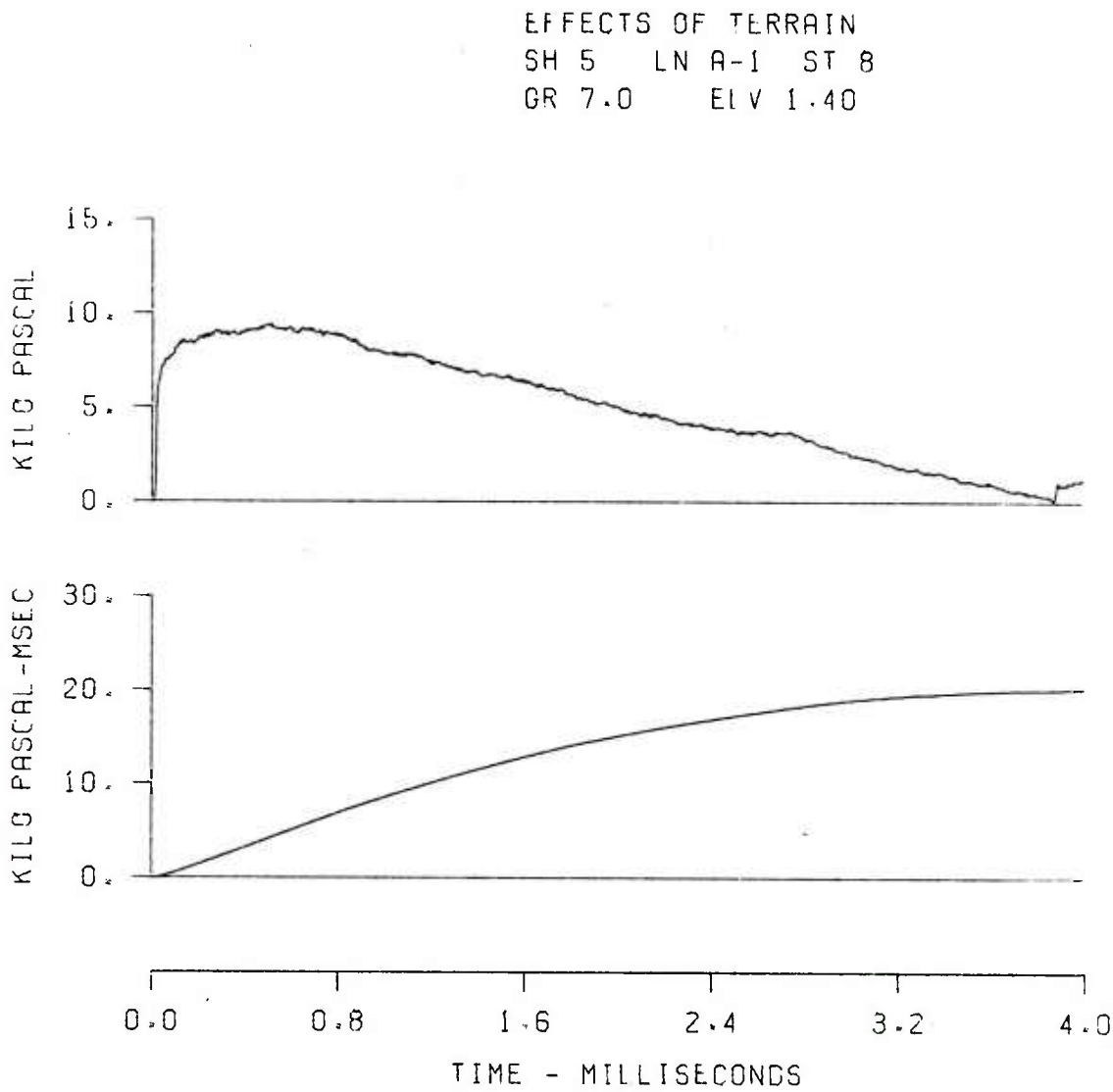

Figure A-1 (Cont). Pressure-Time Traces for Lines A-1 and A-2

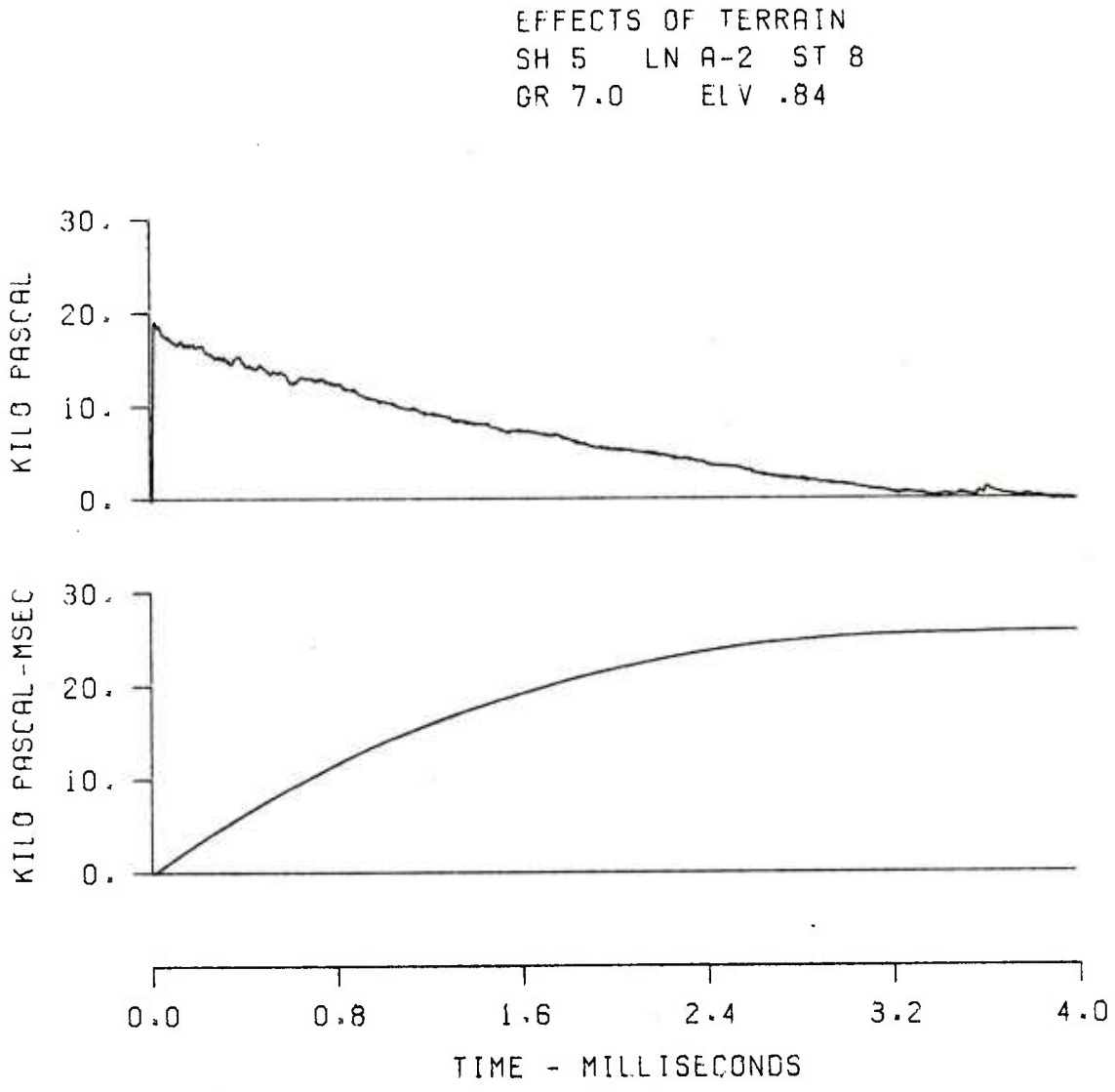

Figure A-1 (Cont). Pressure-Time Traces for Lines A-1 and A-2

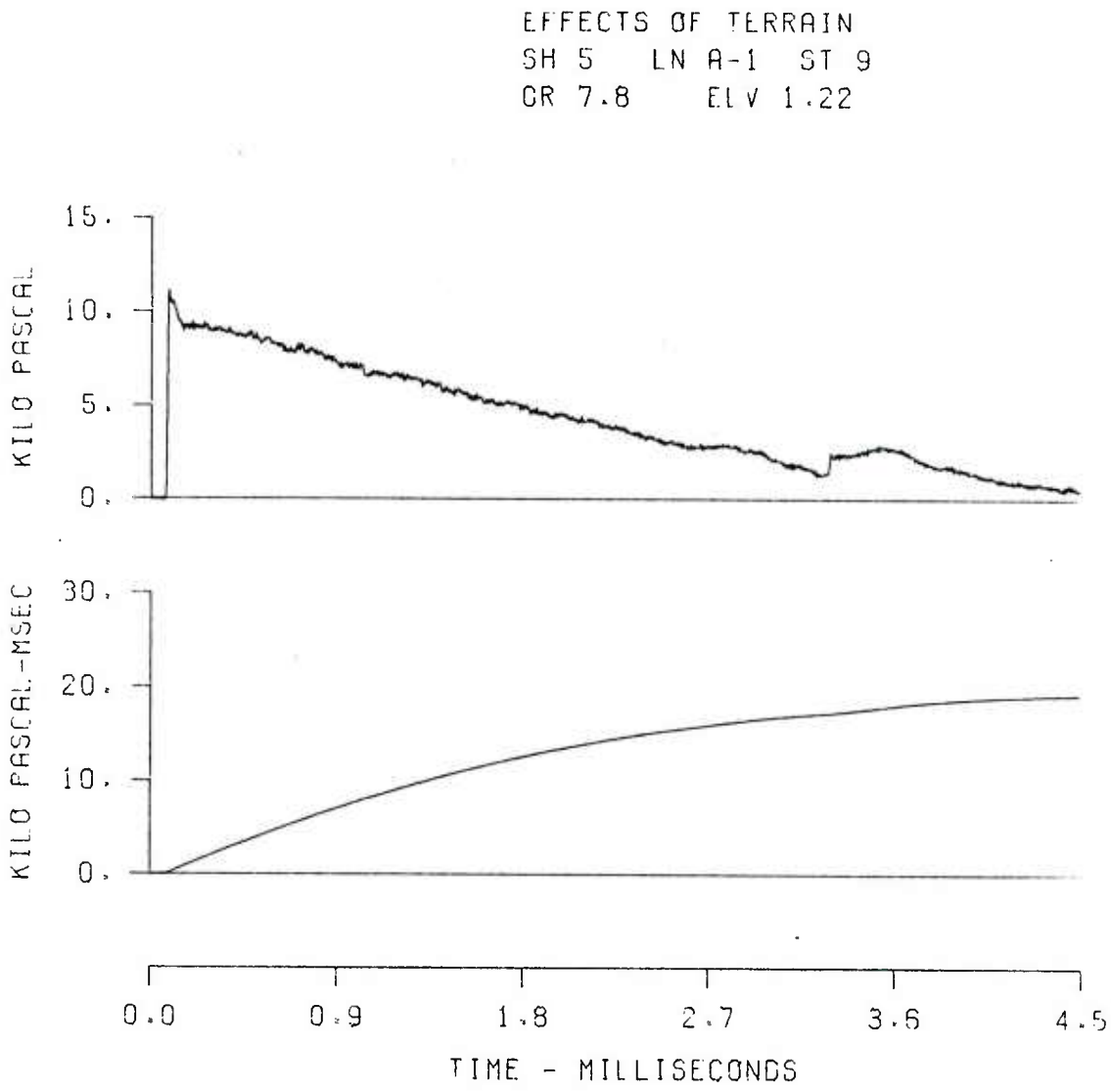

Figure A-1 (Cont). Pressure-Time Traces for Lines A-1 and A-2

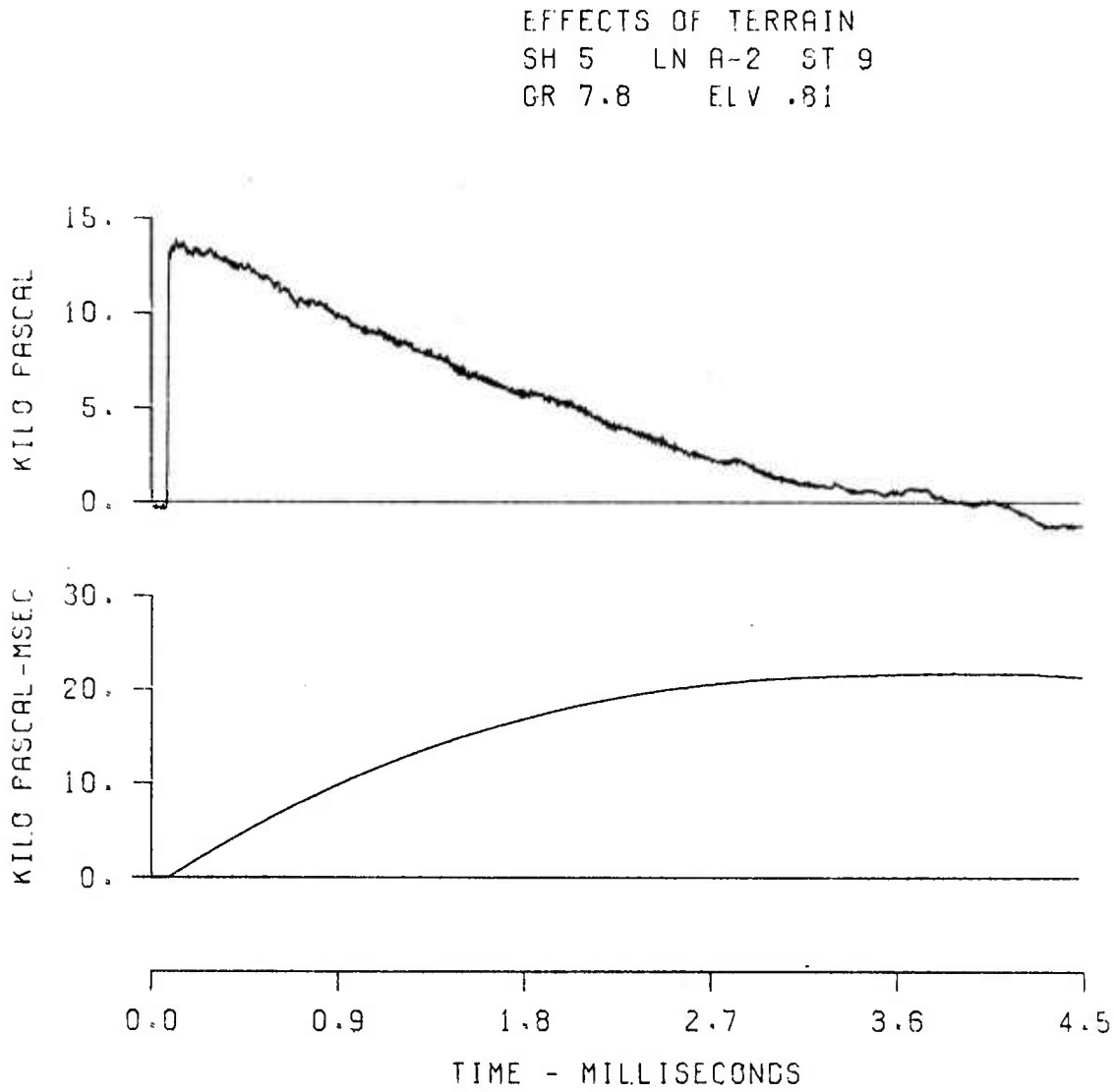

Figure A-1 (Cont). Pressure-Time Traces for Lines A-1 and A-2

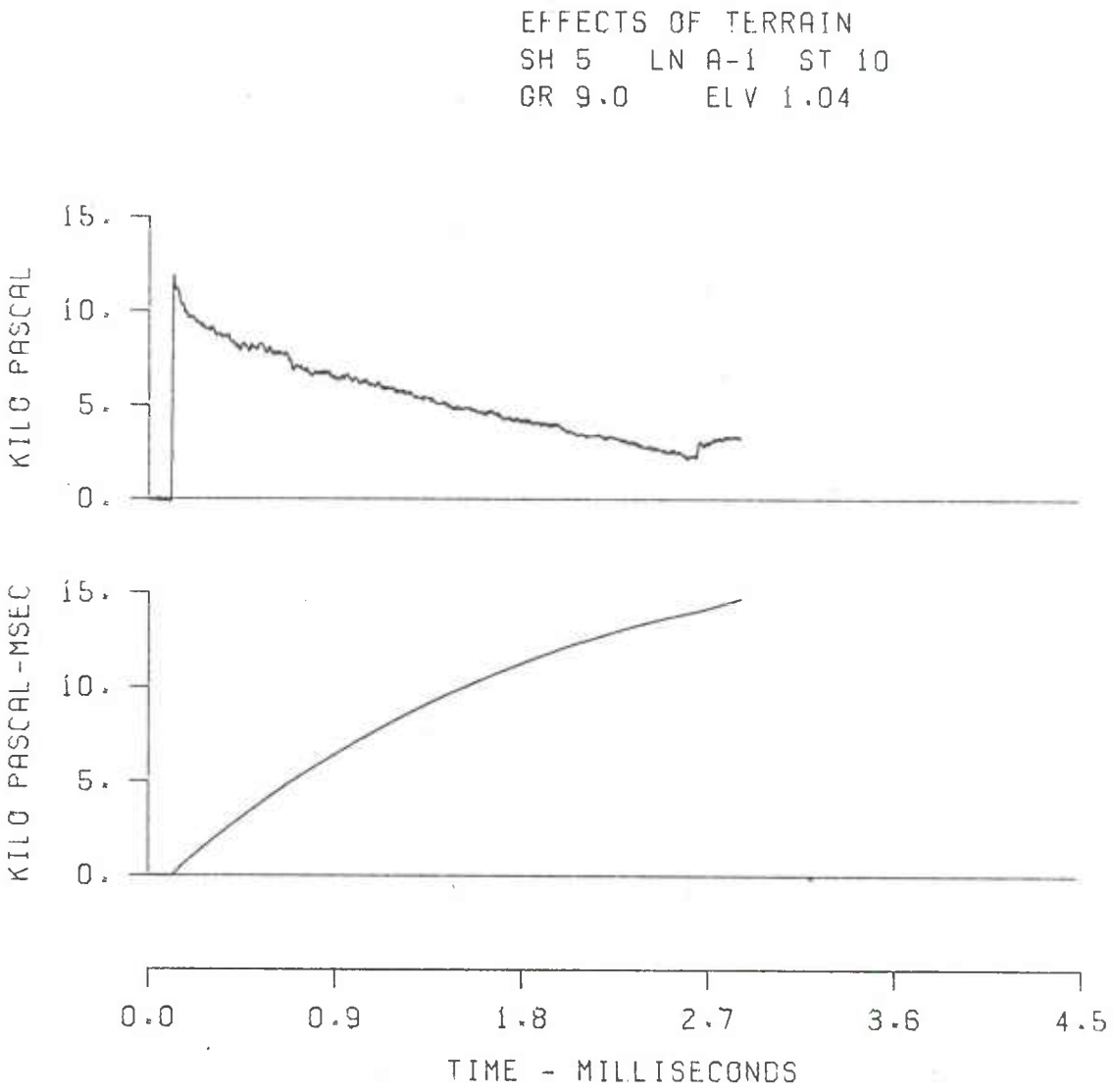

Figure A-1 (Cont). Pressure-Time Traces for Lines A-1 and A-2

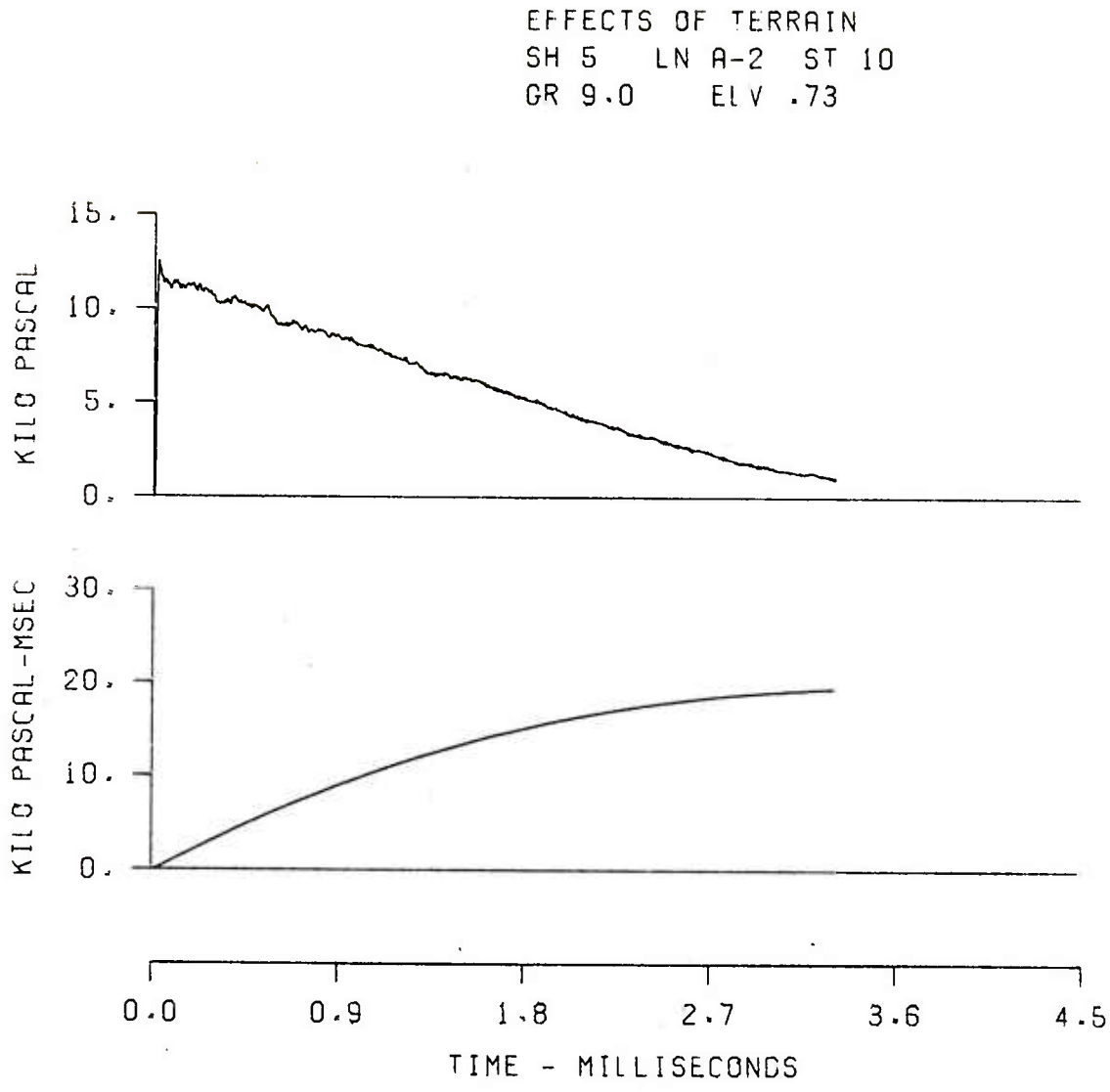

Figure A-1 (Cont). Pressure-Time Traces for Lines A-1 and A-2

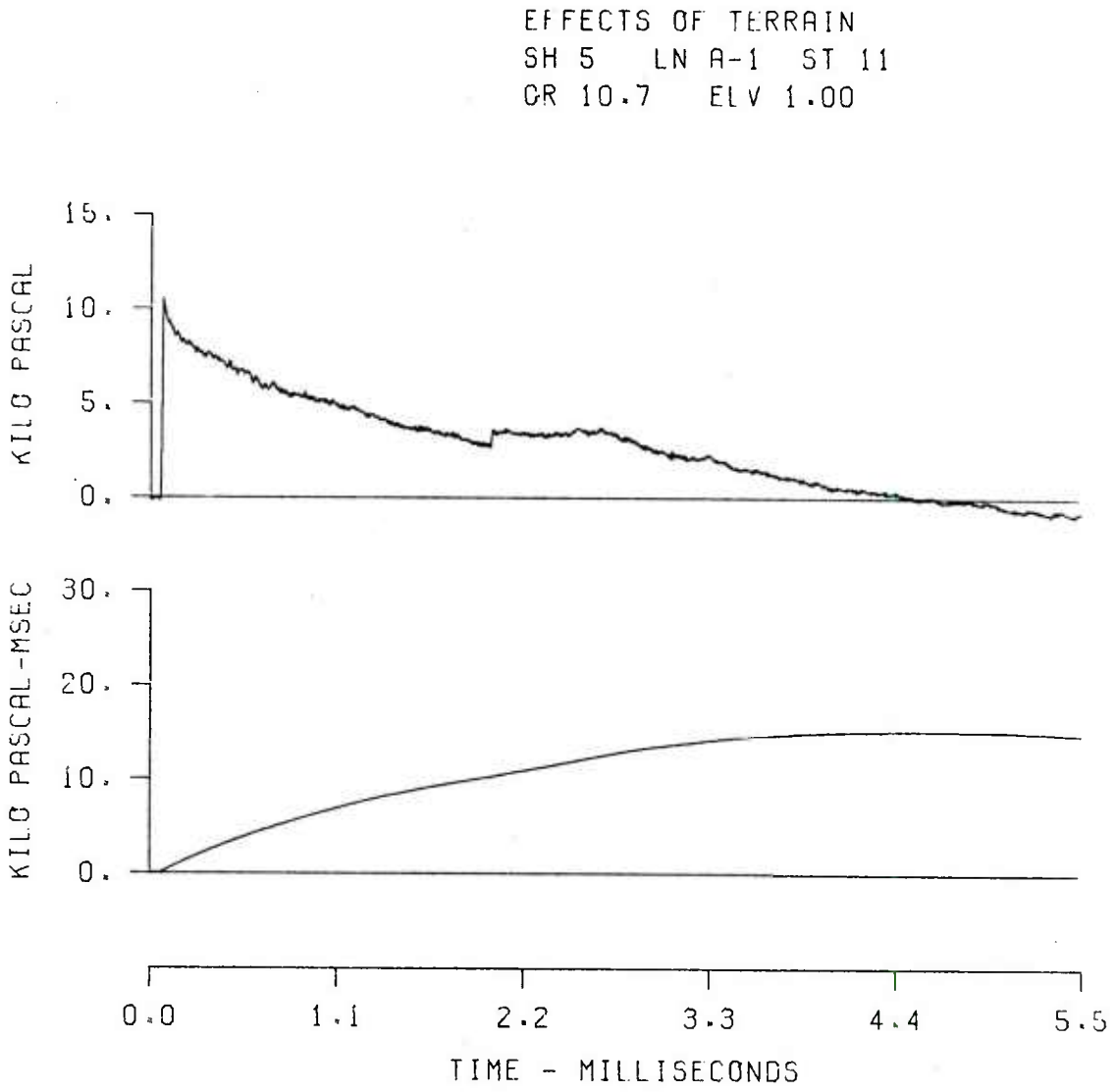

Figure A-1 (Cont). Pressure-Time Traces for Lines A-1 and A-2

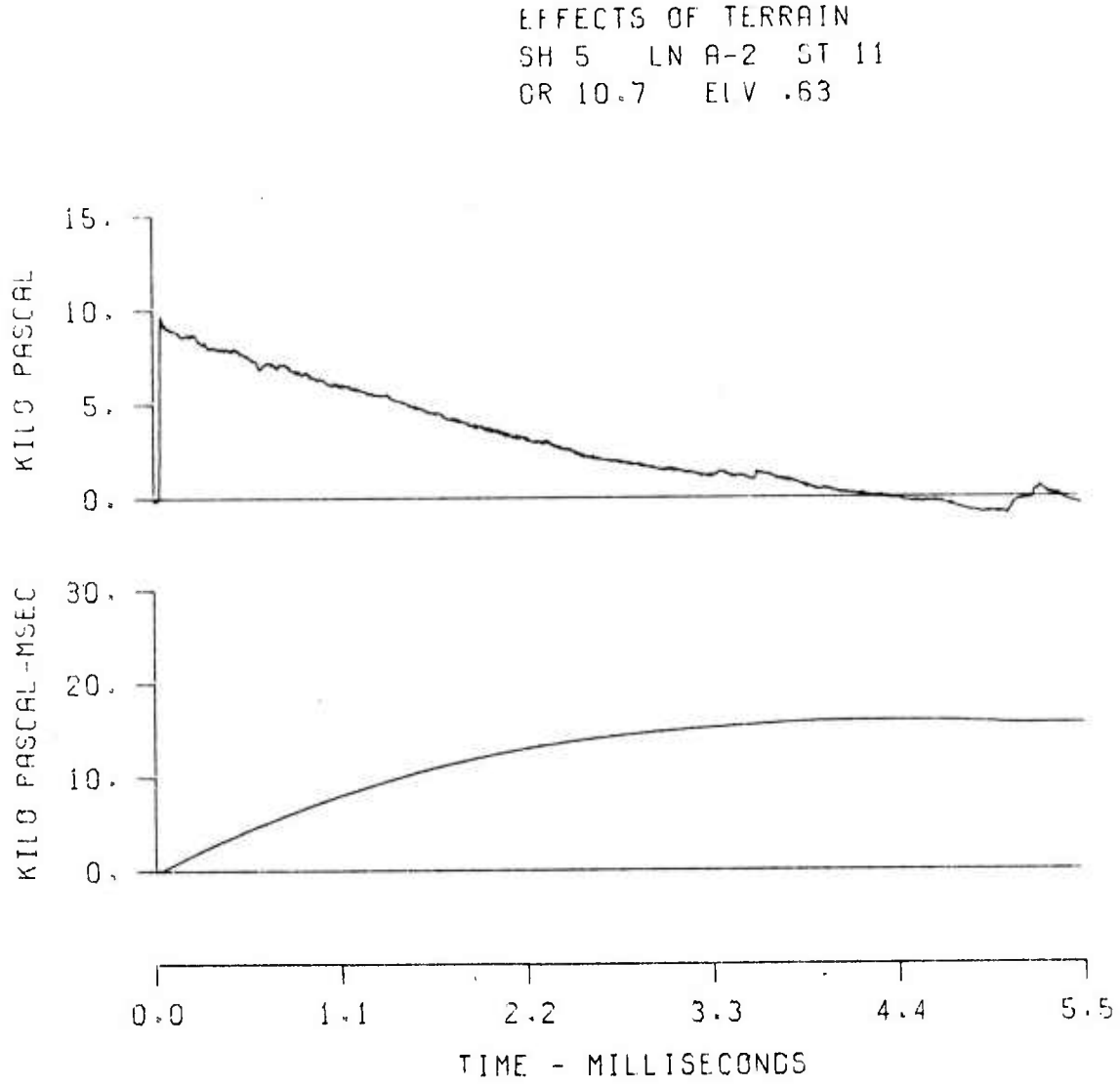

Figure A-1 (Cont). Pressure-Time Traces for Lines A-1 and A-2

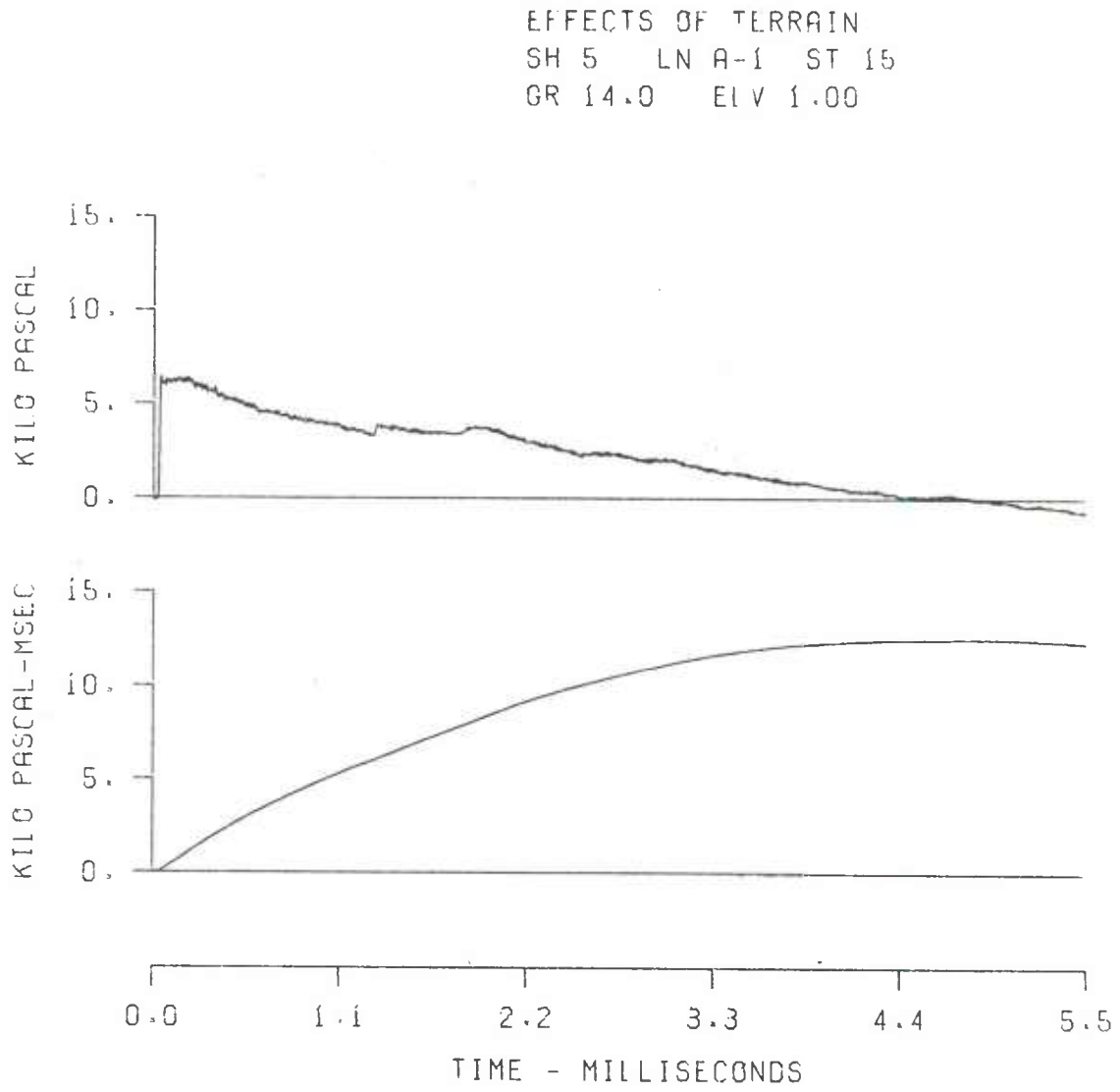

Figure A-1 (Cont). Pressure-Time Traces for Lines A-1 and A-2

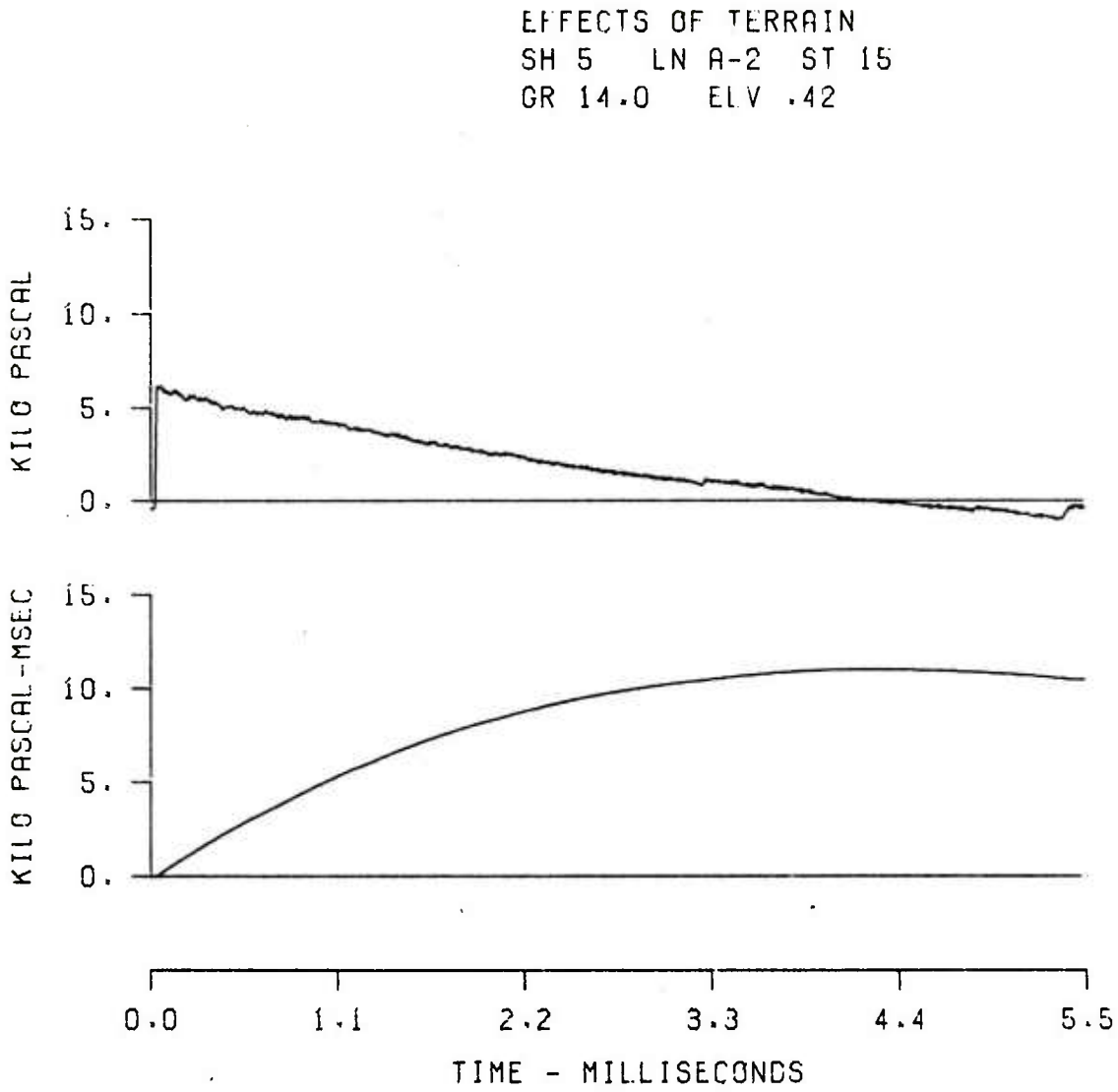

Figure A-1 (Cont). Pressure-Time Traces for Lines A-1 and A-2

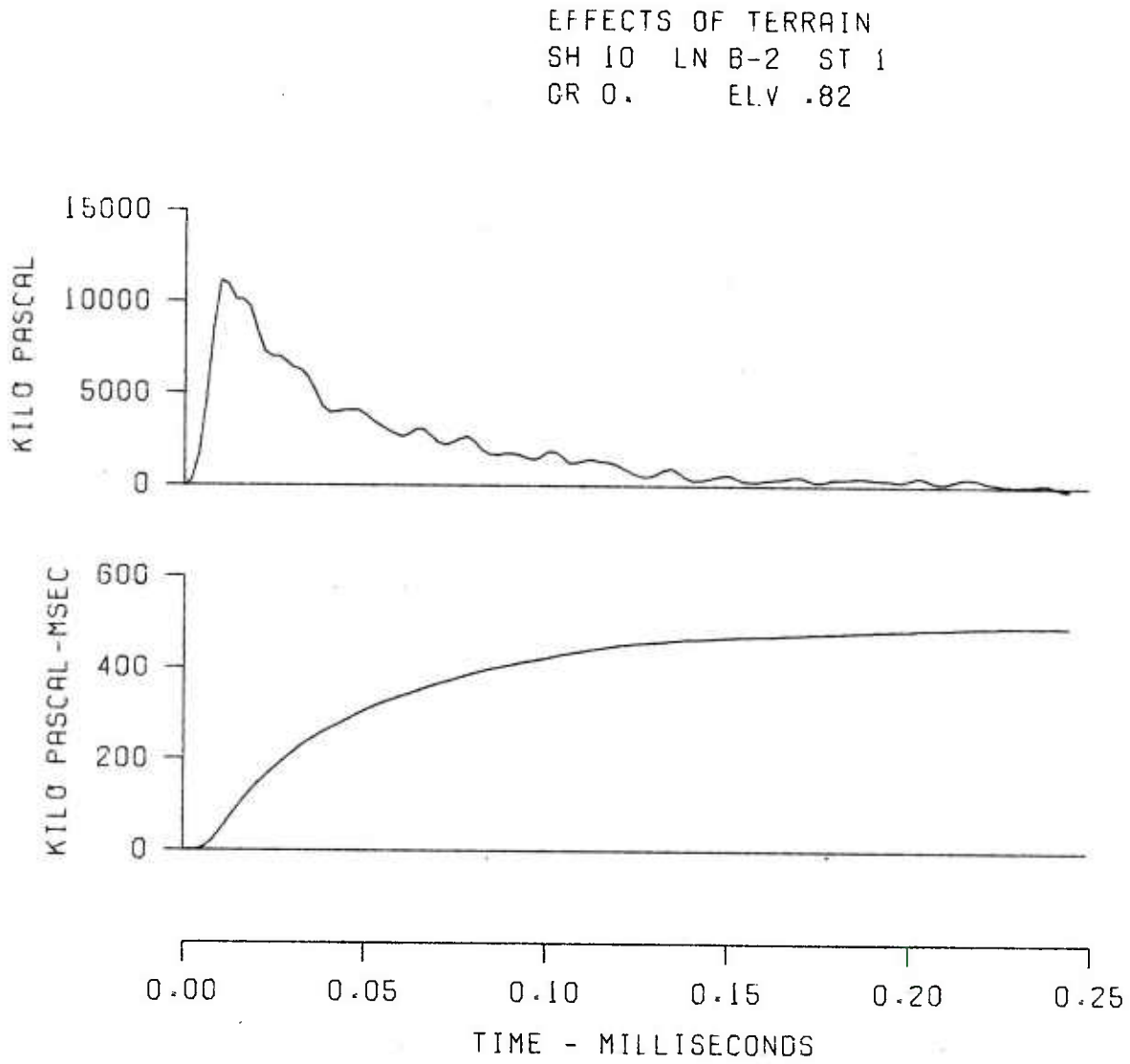

Figure A-2. Pressure-Time Traces for Lines B-1 and B-2

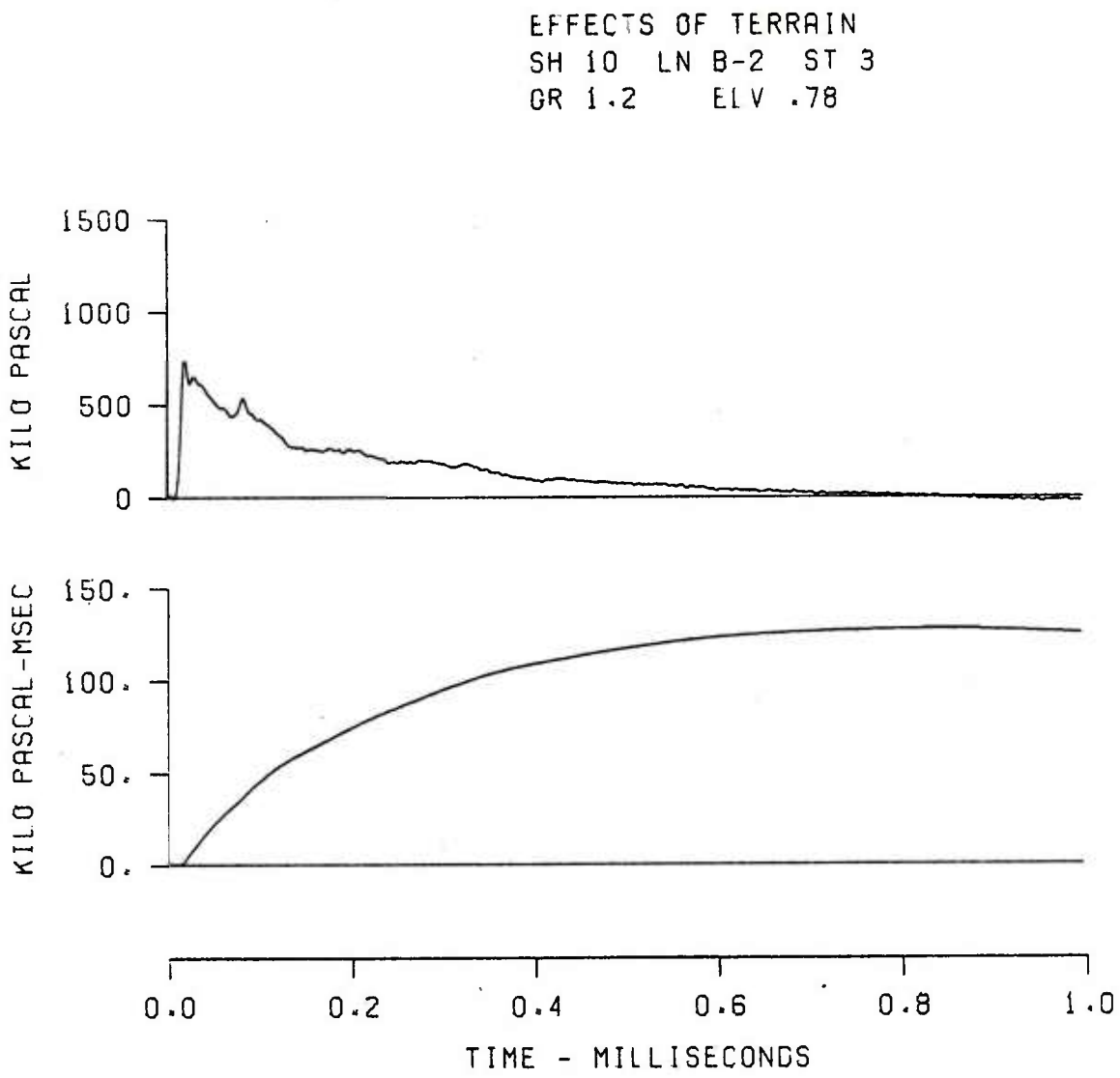

Figure A-2 (Cont). Pressure-Time Traces for Lines B-1 and B-2

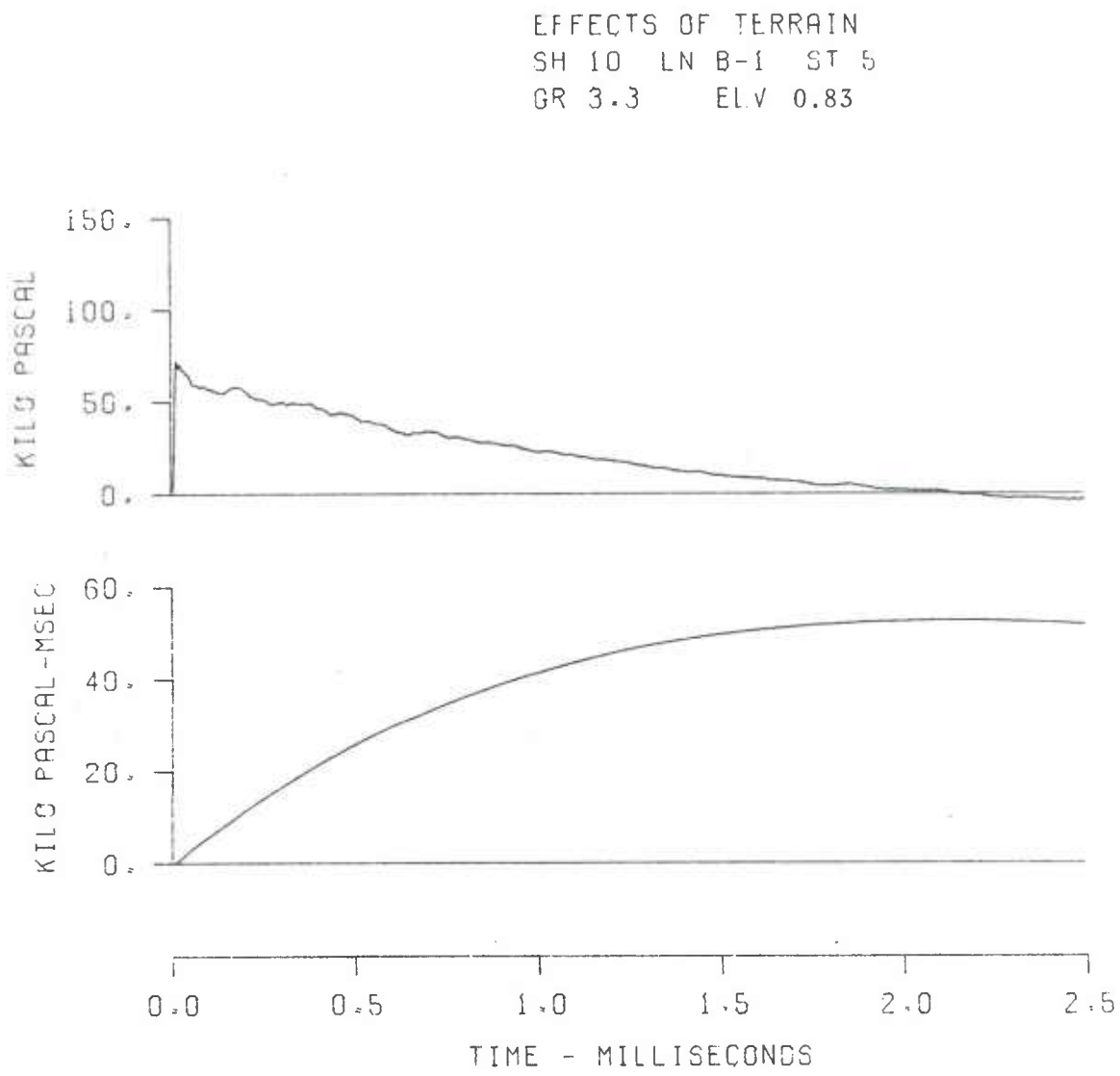

Figure A-2 (Cont). Pressure-Time Traces for Lines B-1 and B-2

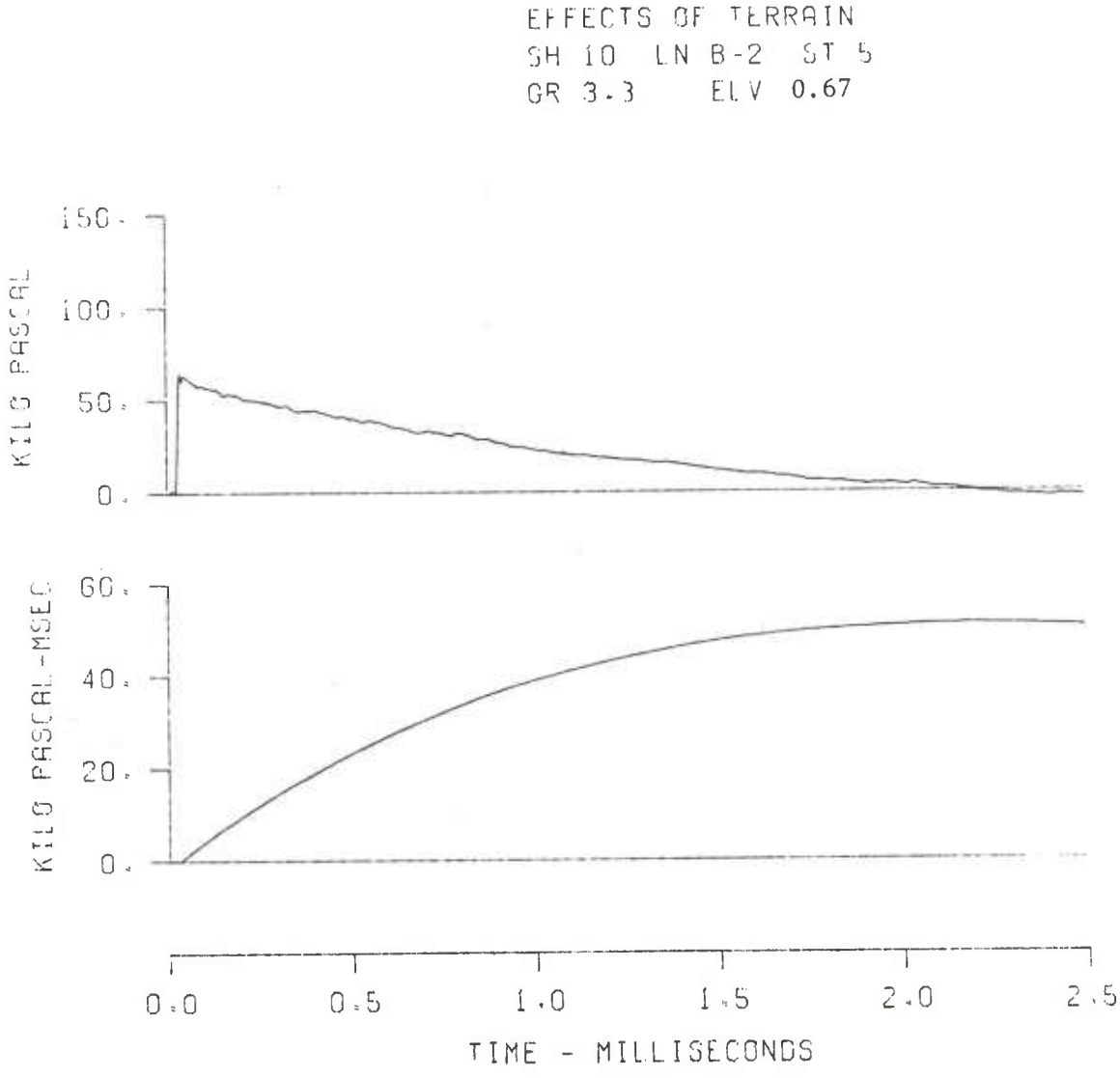

Figure A-2 (Cont). Pressure-Time Traces for Lines B-1 and B-2

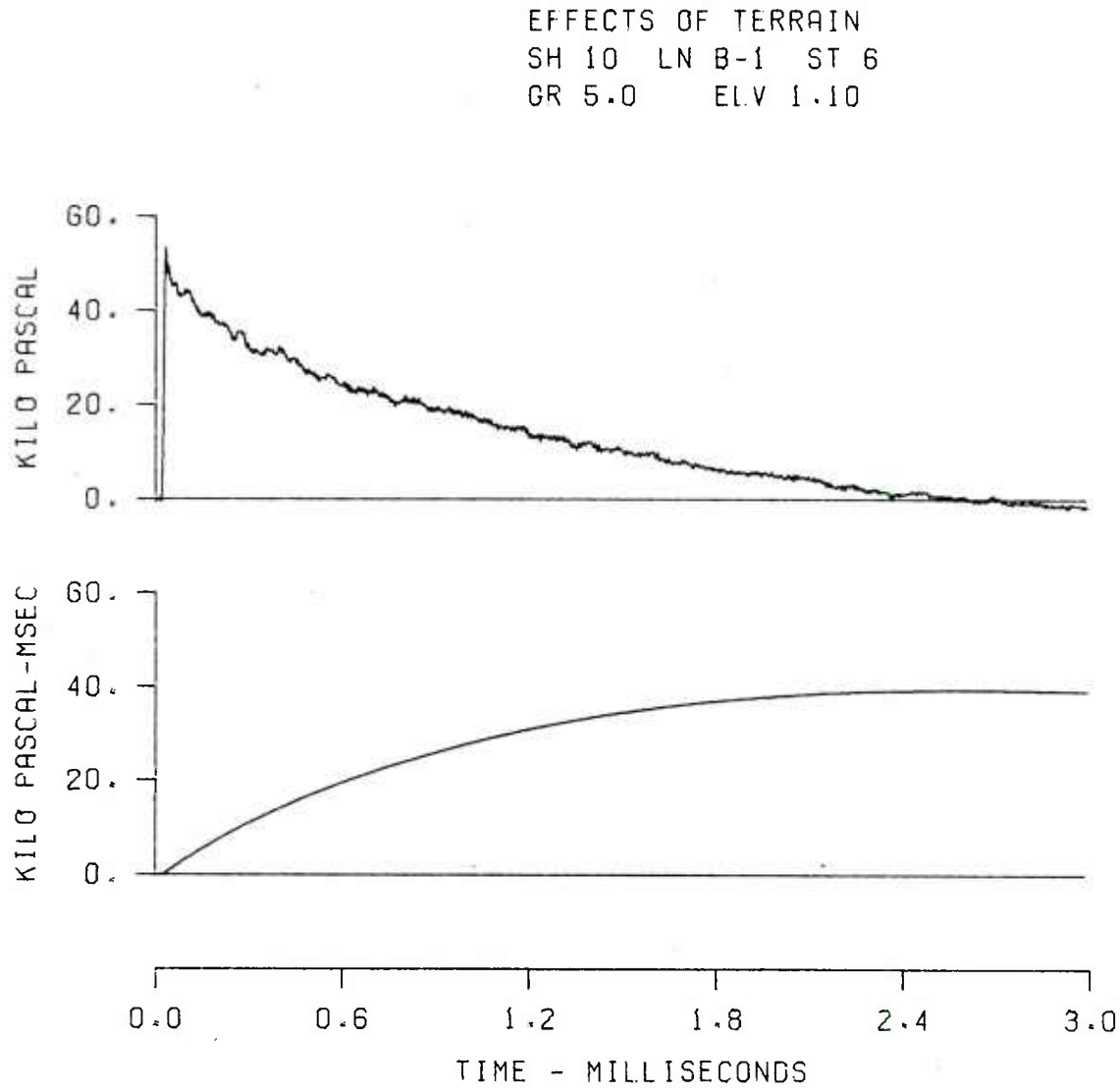

Figure A-2 (Cont). Pressure-Time Traces for Lines B-1 and B-2

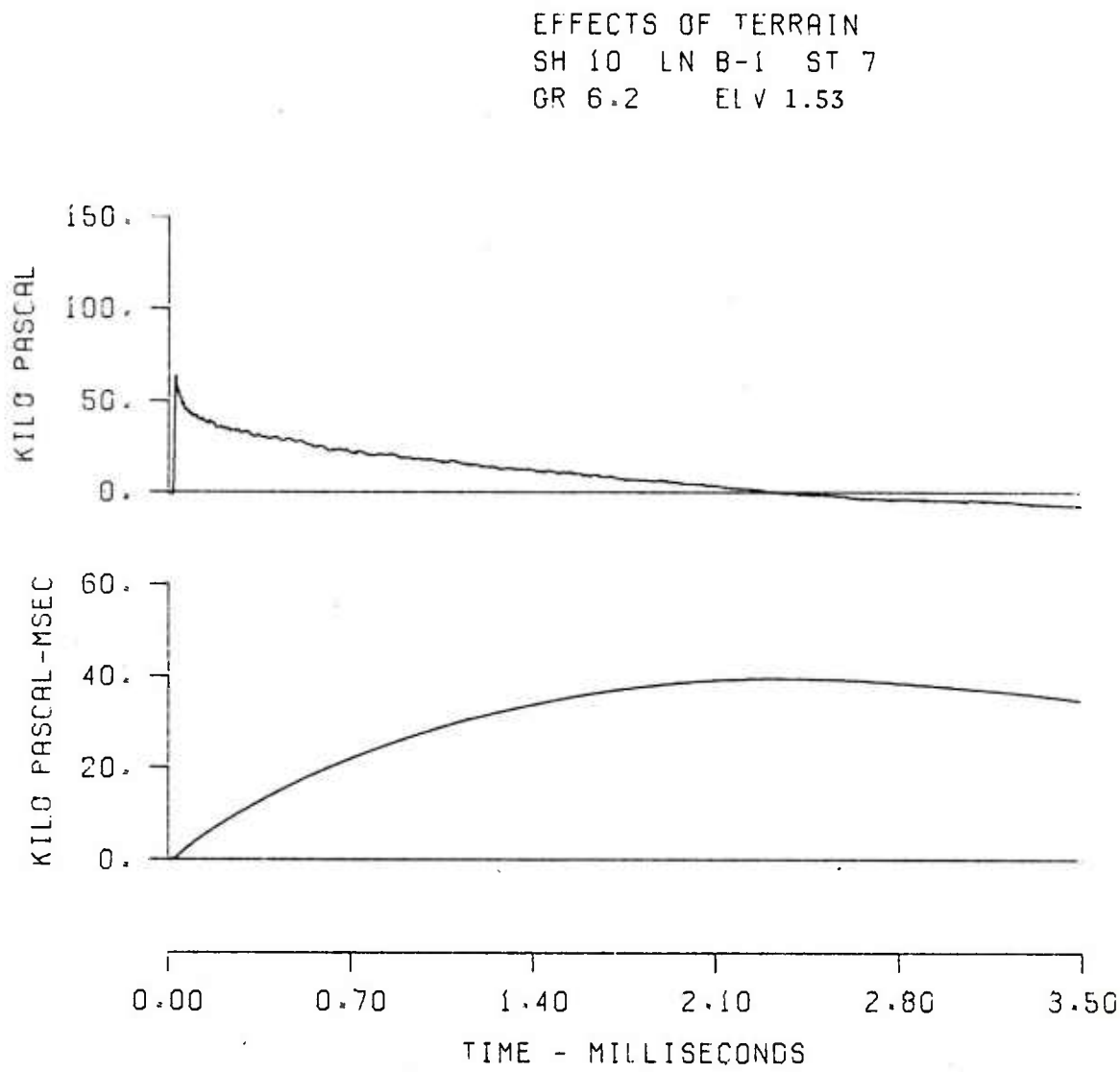

Figure A-2 (Cont). Pressure-Time Traces for Lines B-1 and B-2

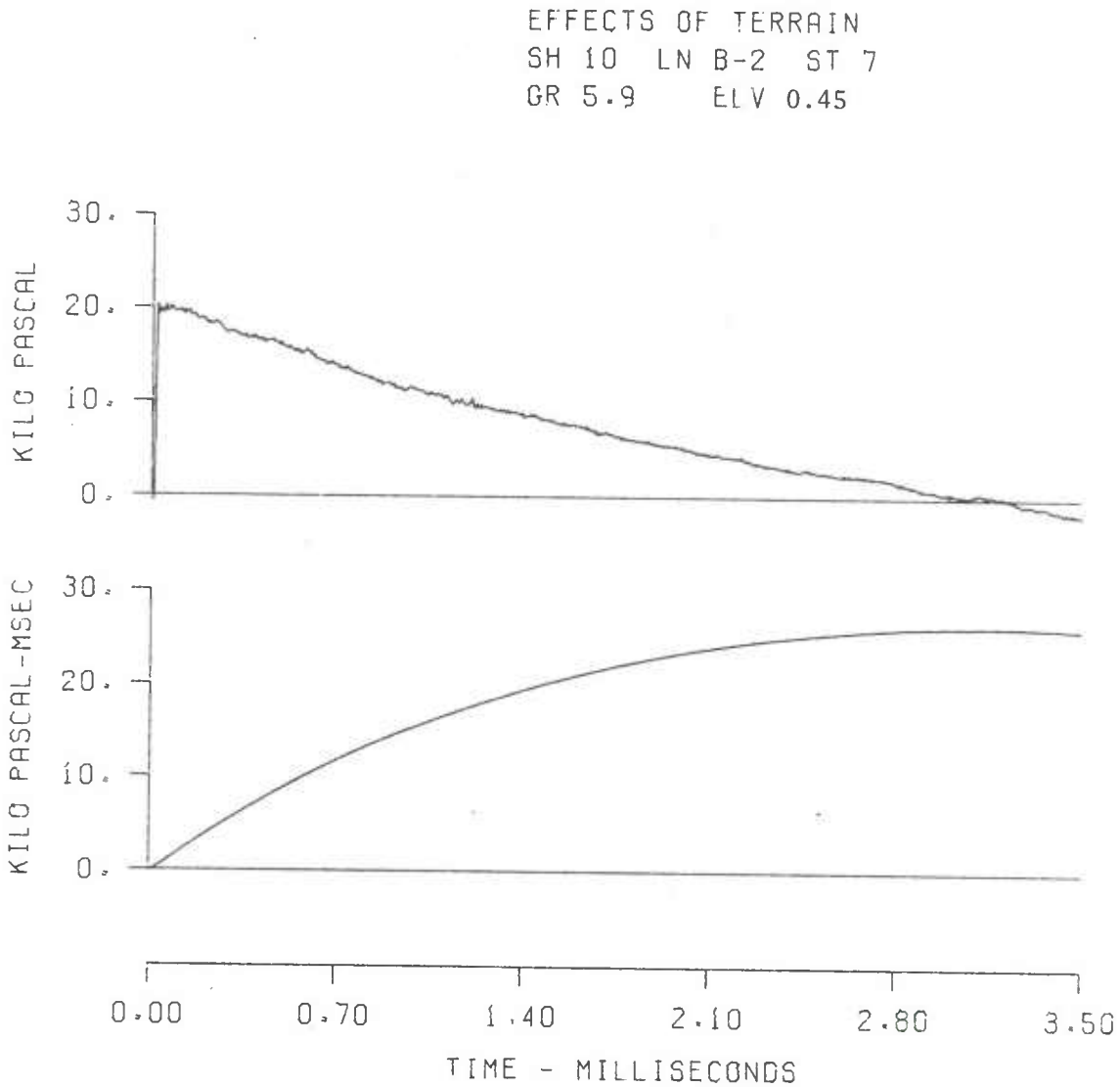

Figure A-2 (Cont). Pressure-Time Traces for Lines B-1 and B-2

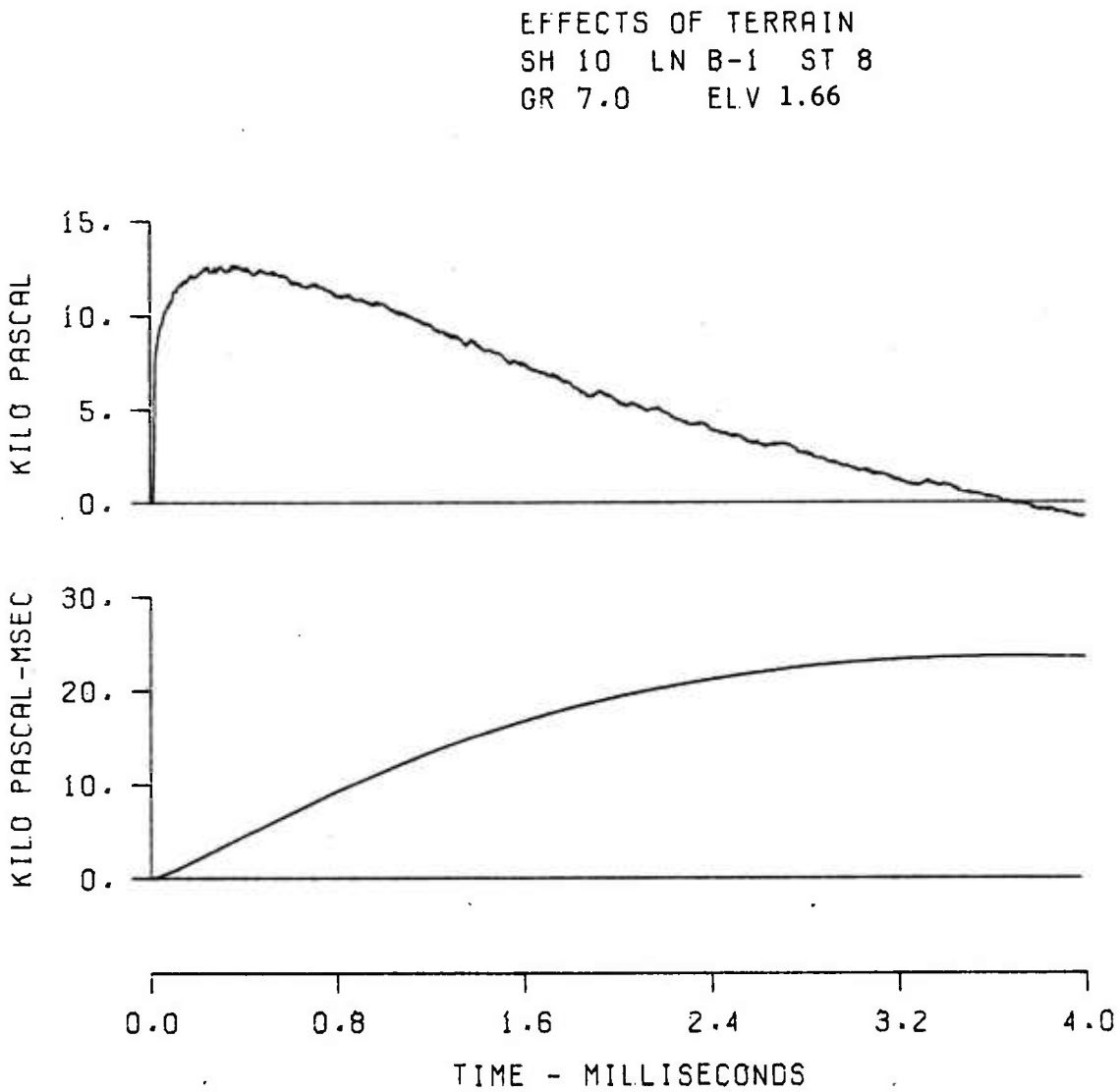

Figure A-2 (Cont). Pressure-Time Traces for Lines B-1 and B-2

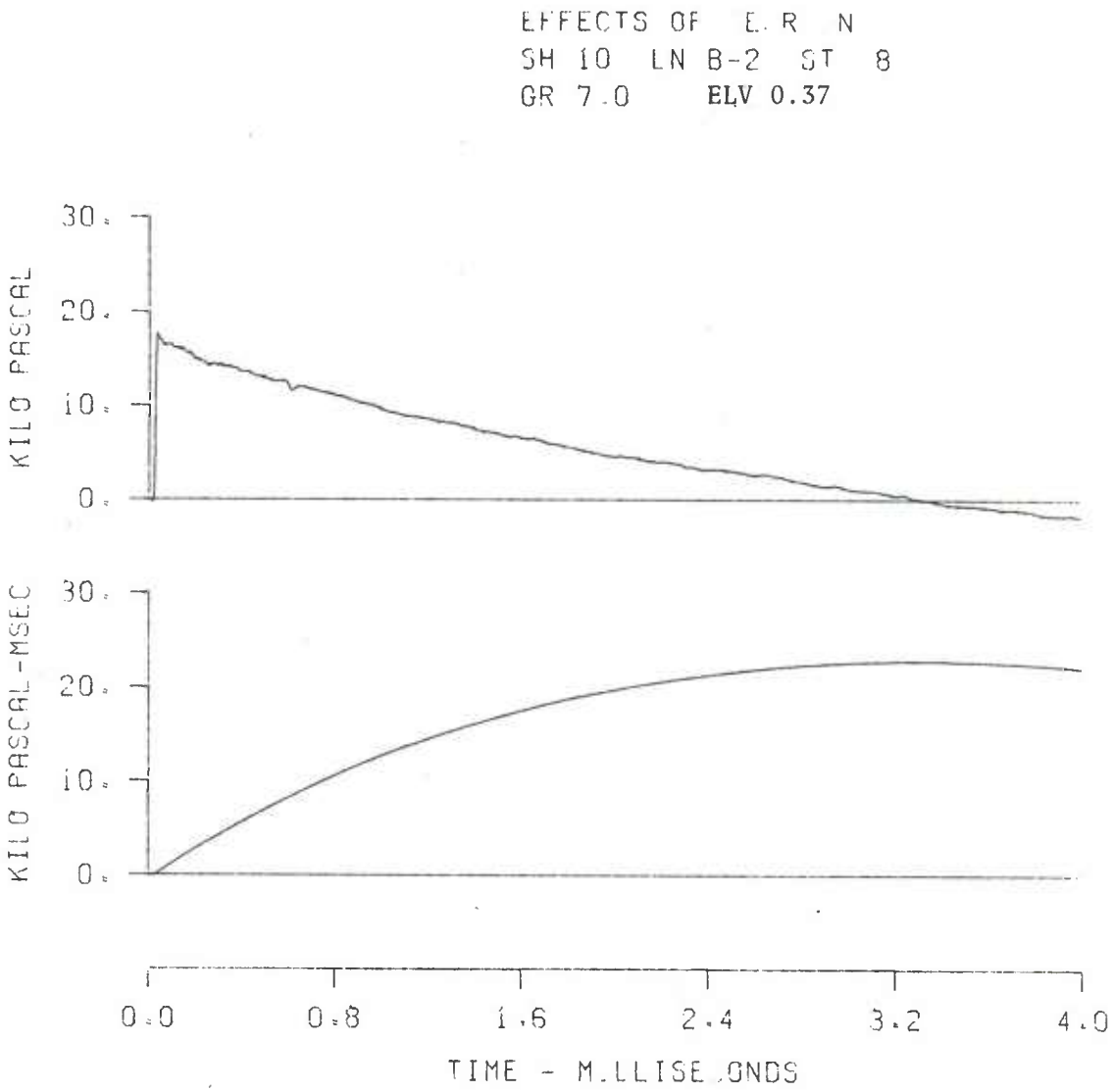

Figure A-2 (Cont). Pressure-Time Traces for Lines B-1 and B-2

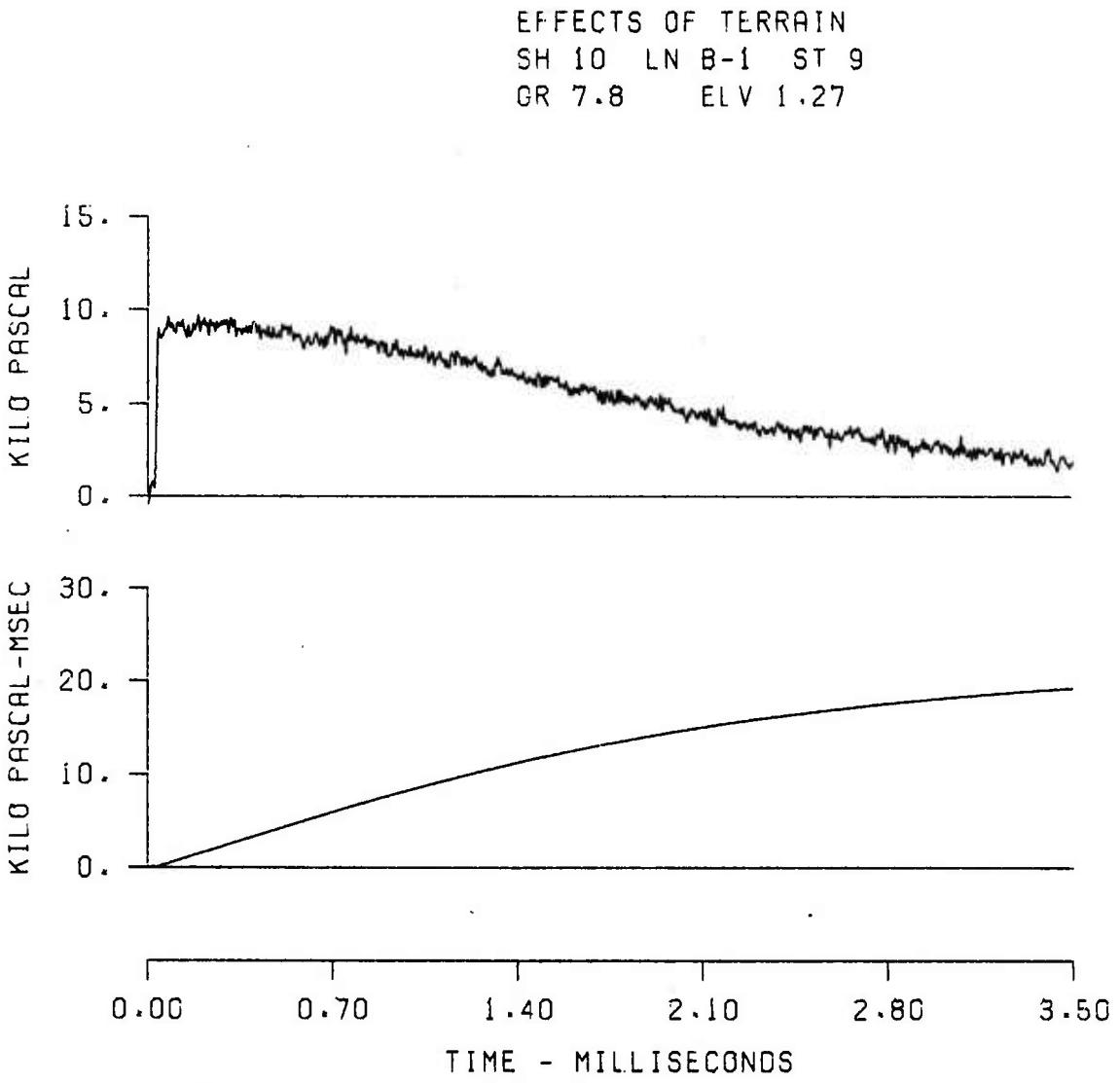

Figure A-2 (Cont). Pressure-Time Traces for Lines B-1 and B-2

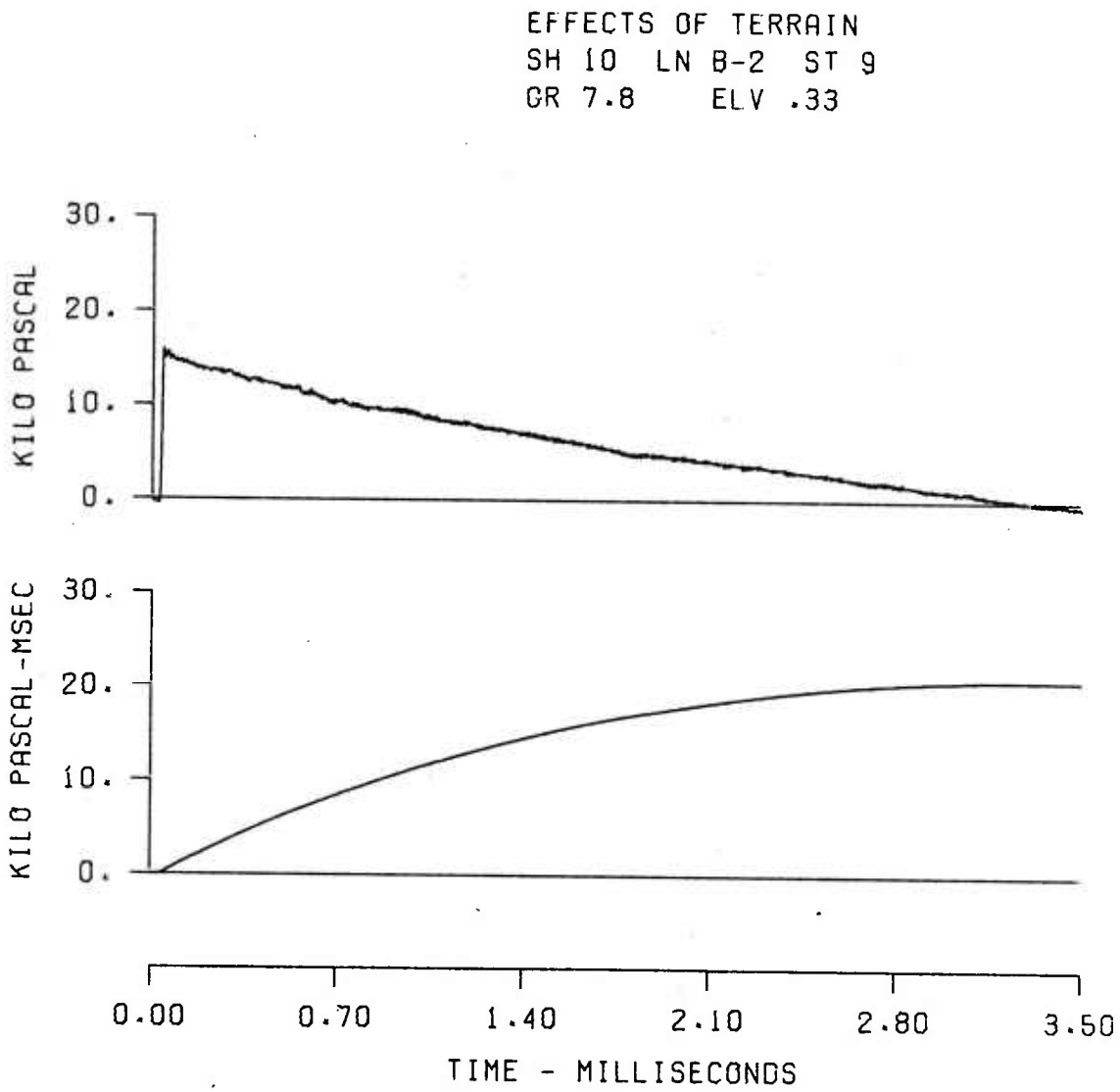

Figure A-2 (Cont). Pressure-Time Traces for Lines B-1 and B-2

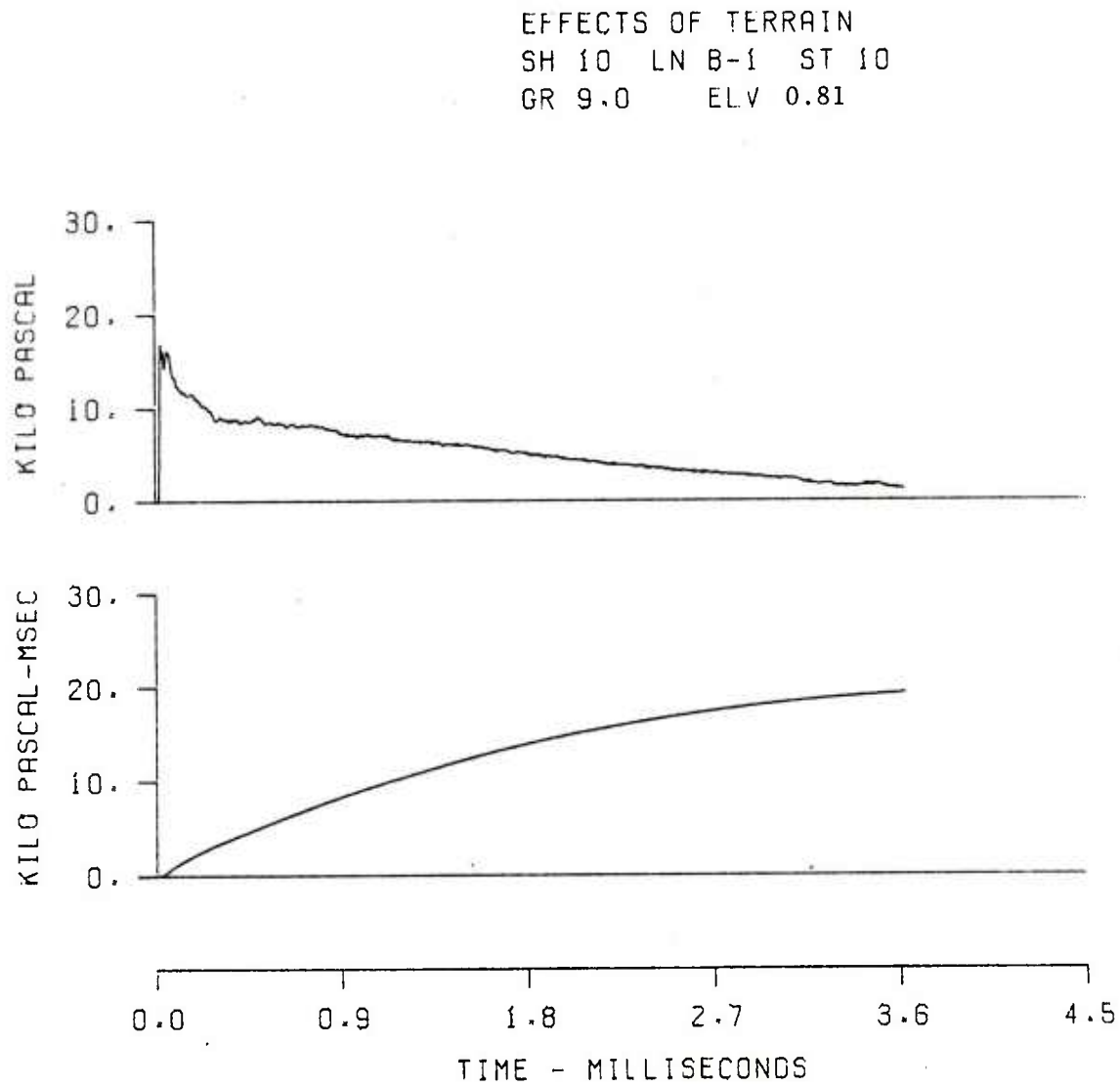

Figure A-2 (Cont). Pressure-Time Traces for Lines B-1 and B-2

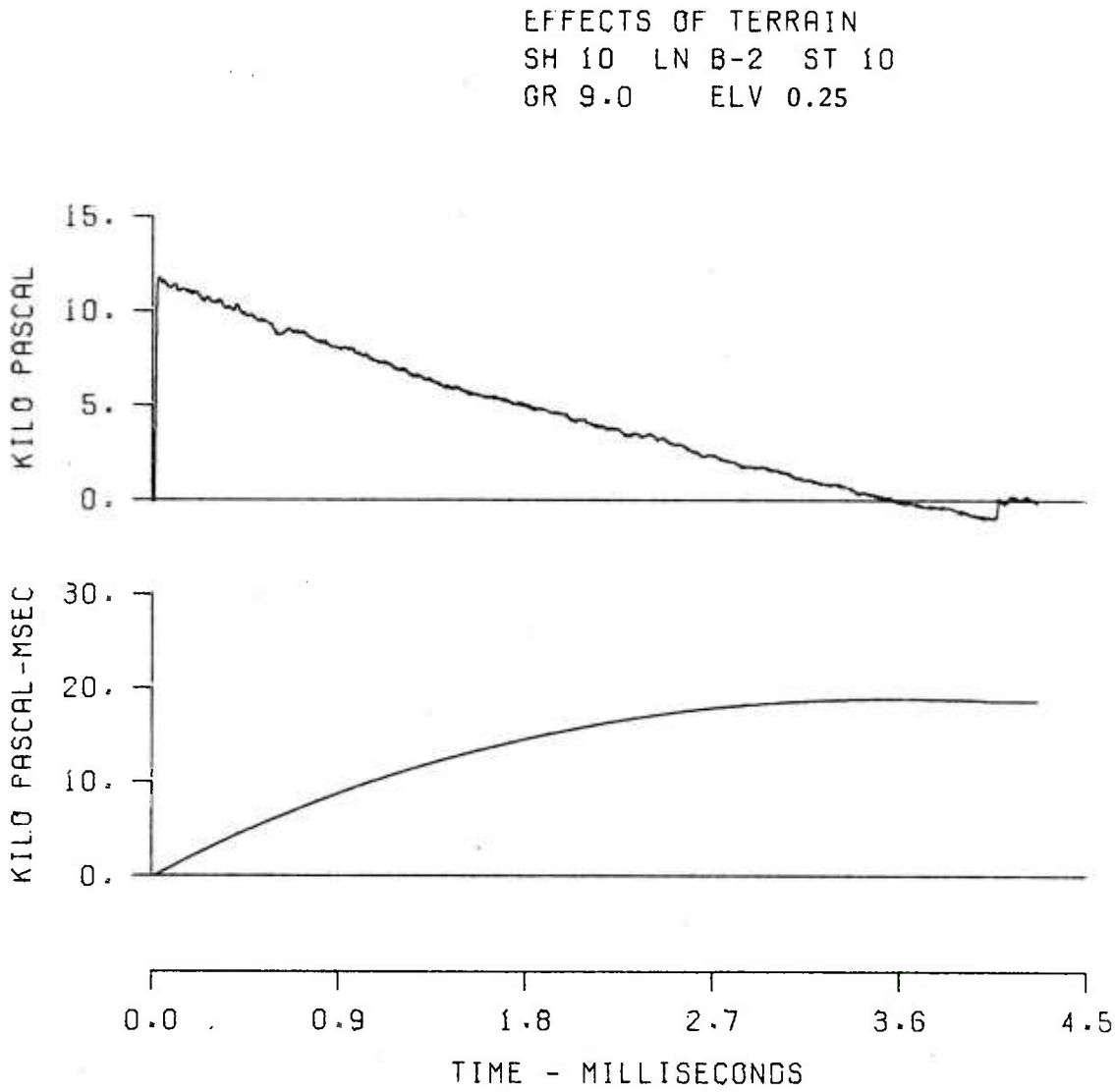

Figure A-2 (Cont). Pressure-Time Traces for Lines B-1 and B-2

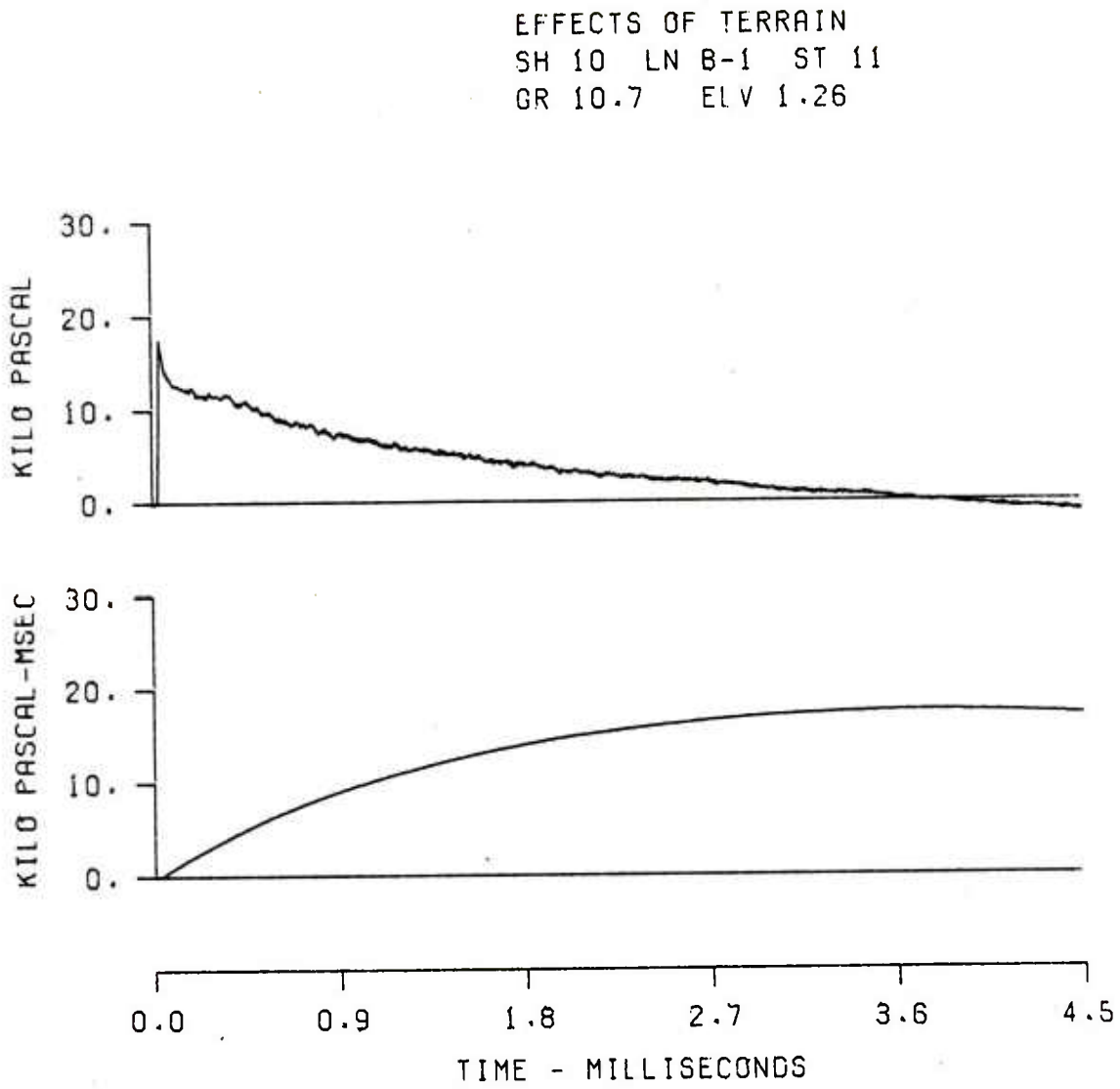

Figure A-2 (Cont). Pressure-Time Traces for Lines B-1 and B-2

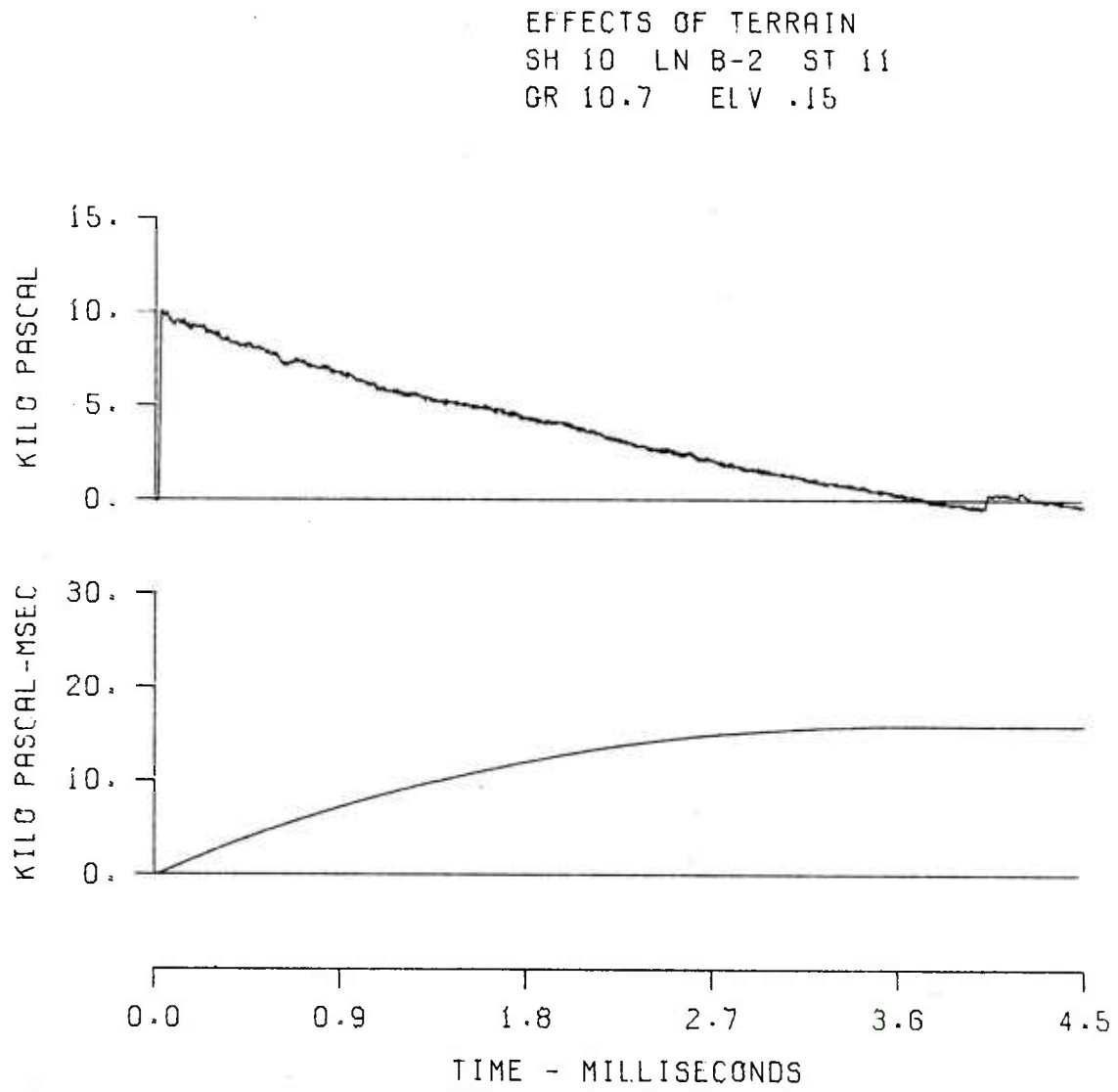

Figure A-2 (Cont). Pressure-Time Traces for Lines B-1 and B-2

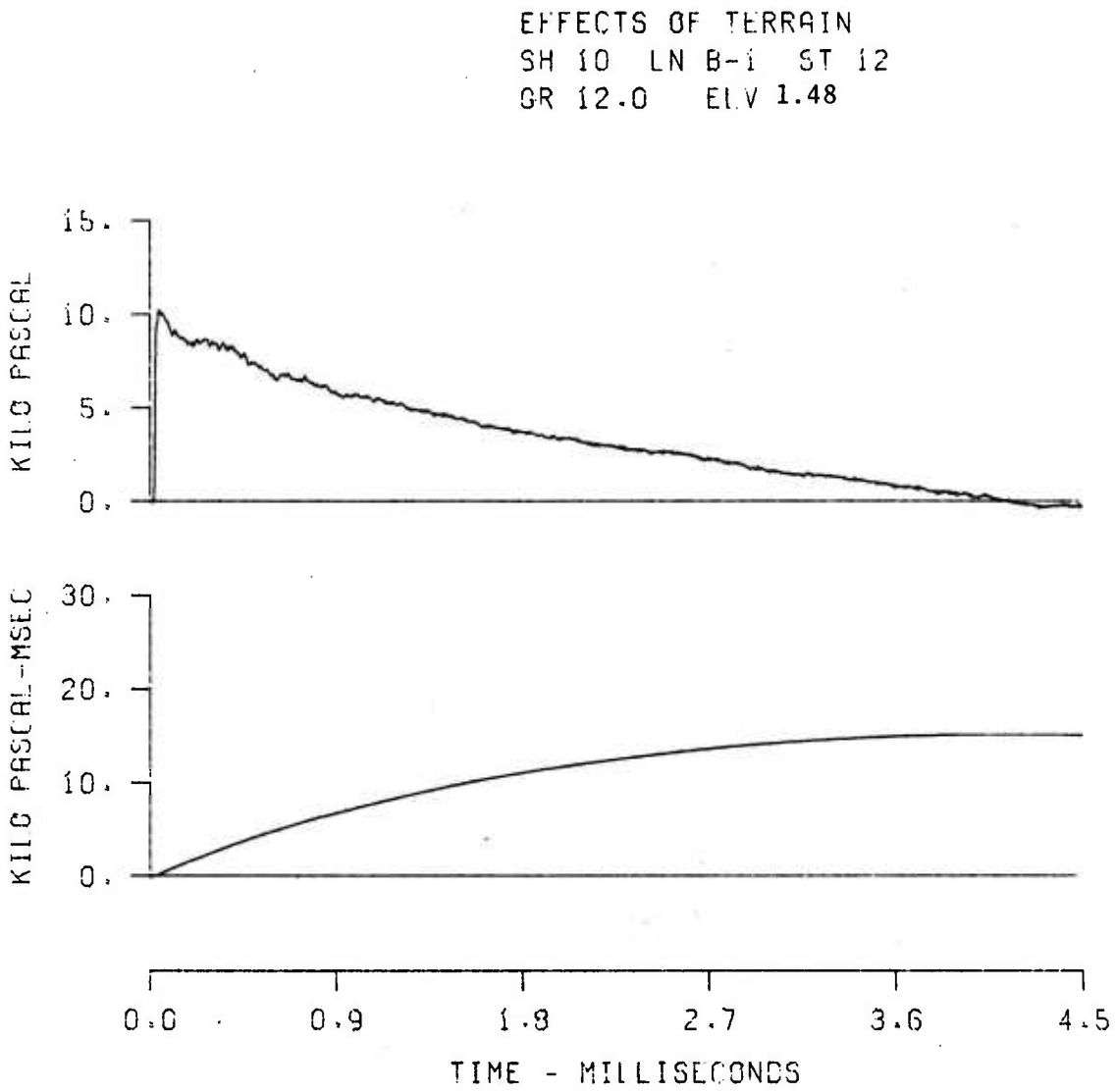

Figure A-2 (Cont). Pressure-Time Traces for Lines B-1 and B-2

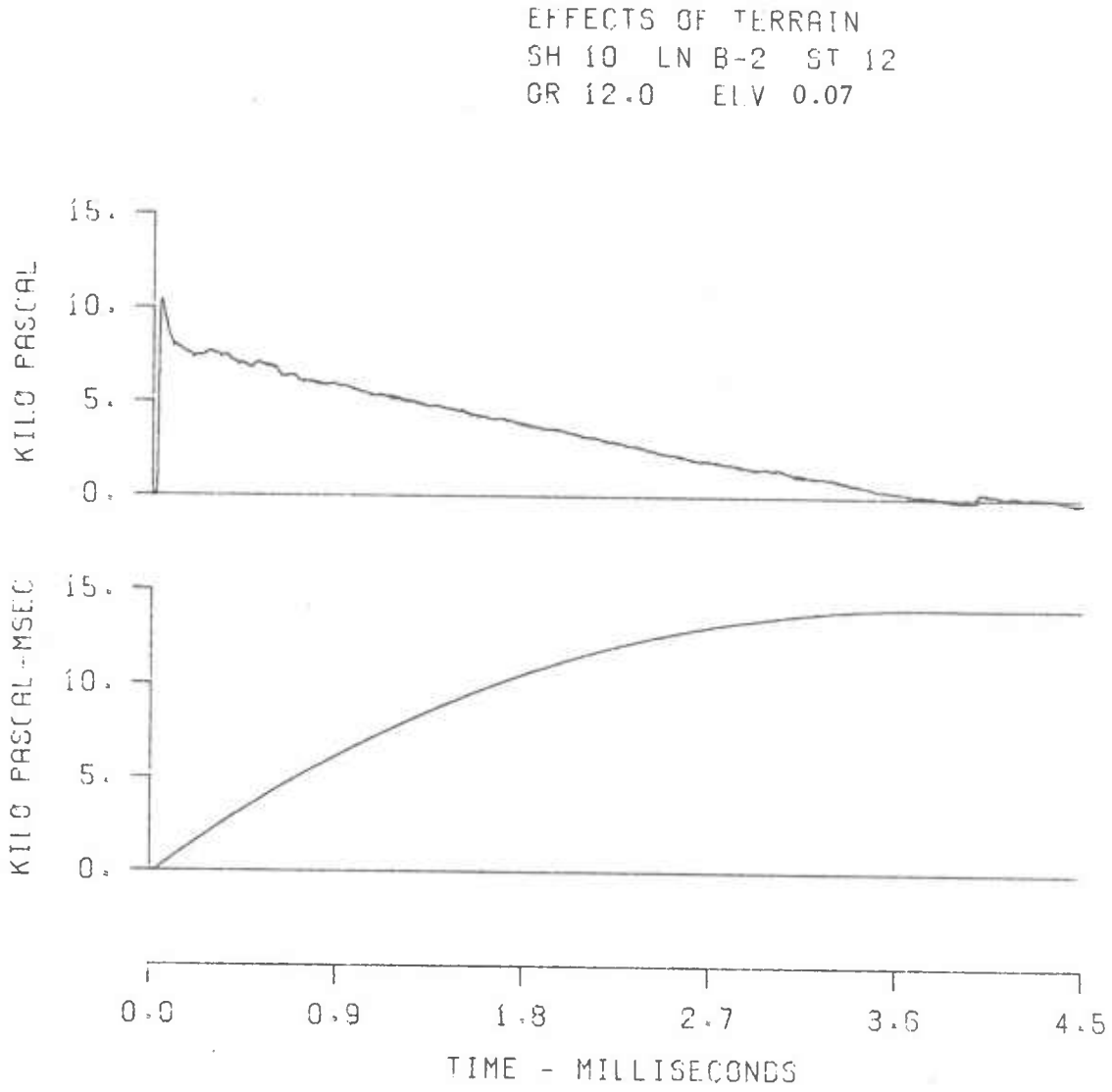

Figure A-2 (Cont). Pressure-Time Traces for Lines B-1 and B-2

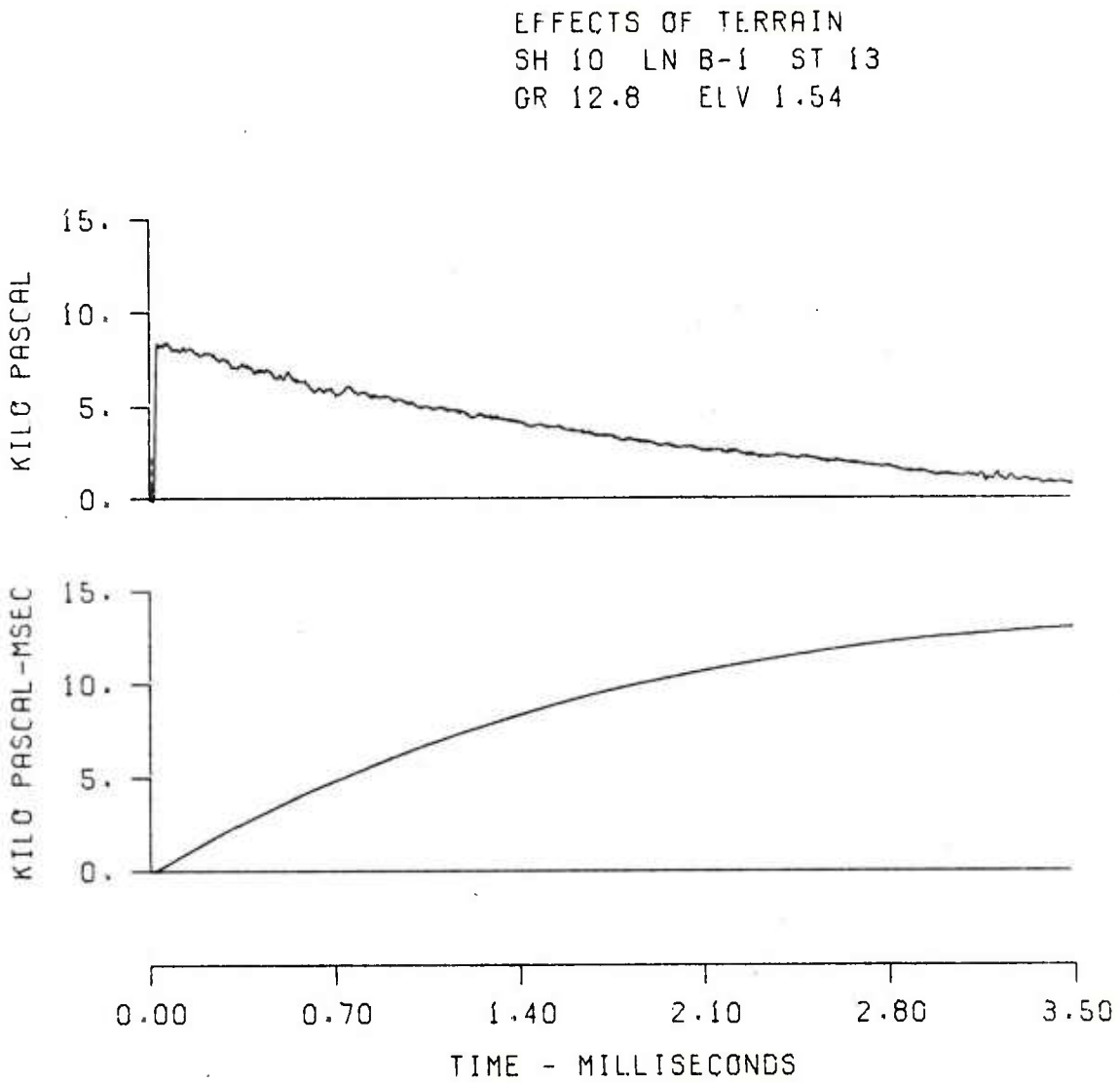

Figure A-2 (Cont). Pressure-Time Traces for Lines B-1 and B-2

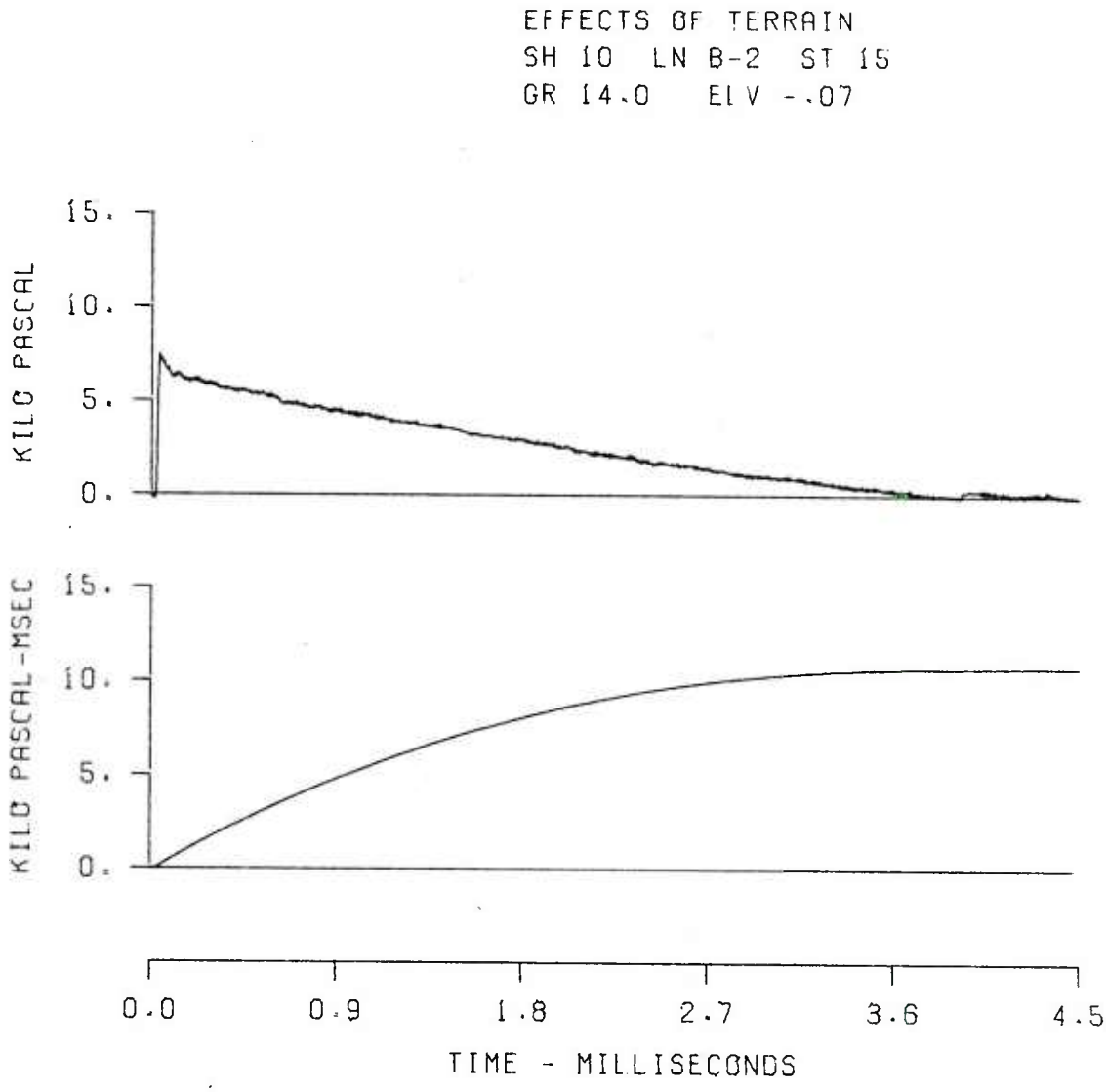

Figure A-2 (Cont). Pressure-Time Traces for Lines B-1 and B-2

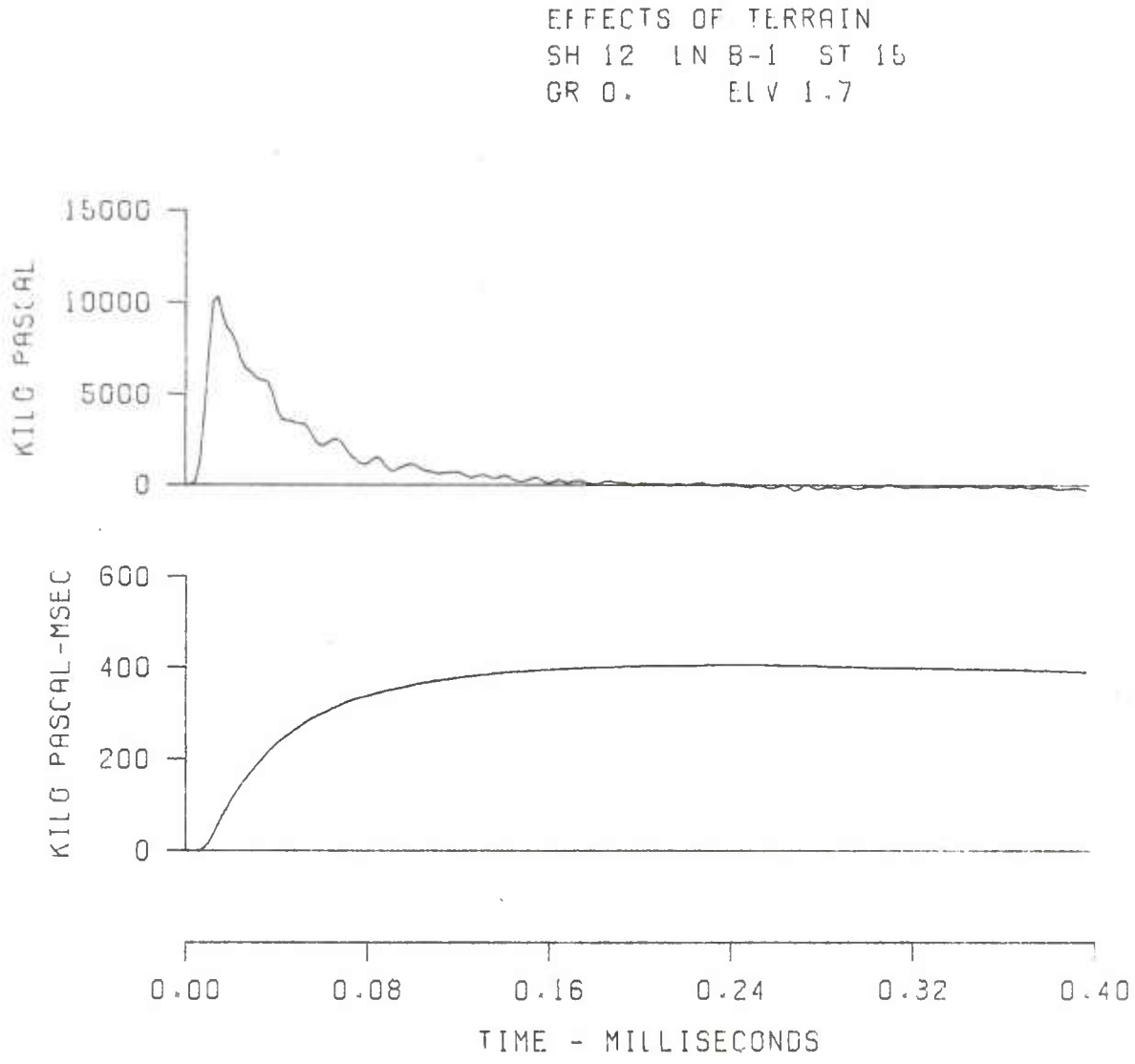

Figure A-3. Pressure-Time Traces for Line B_a (B-1)

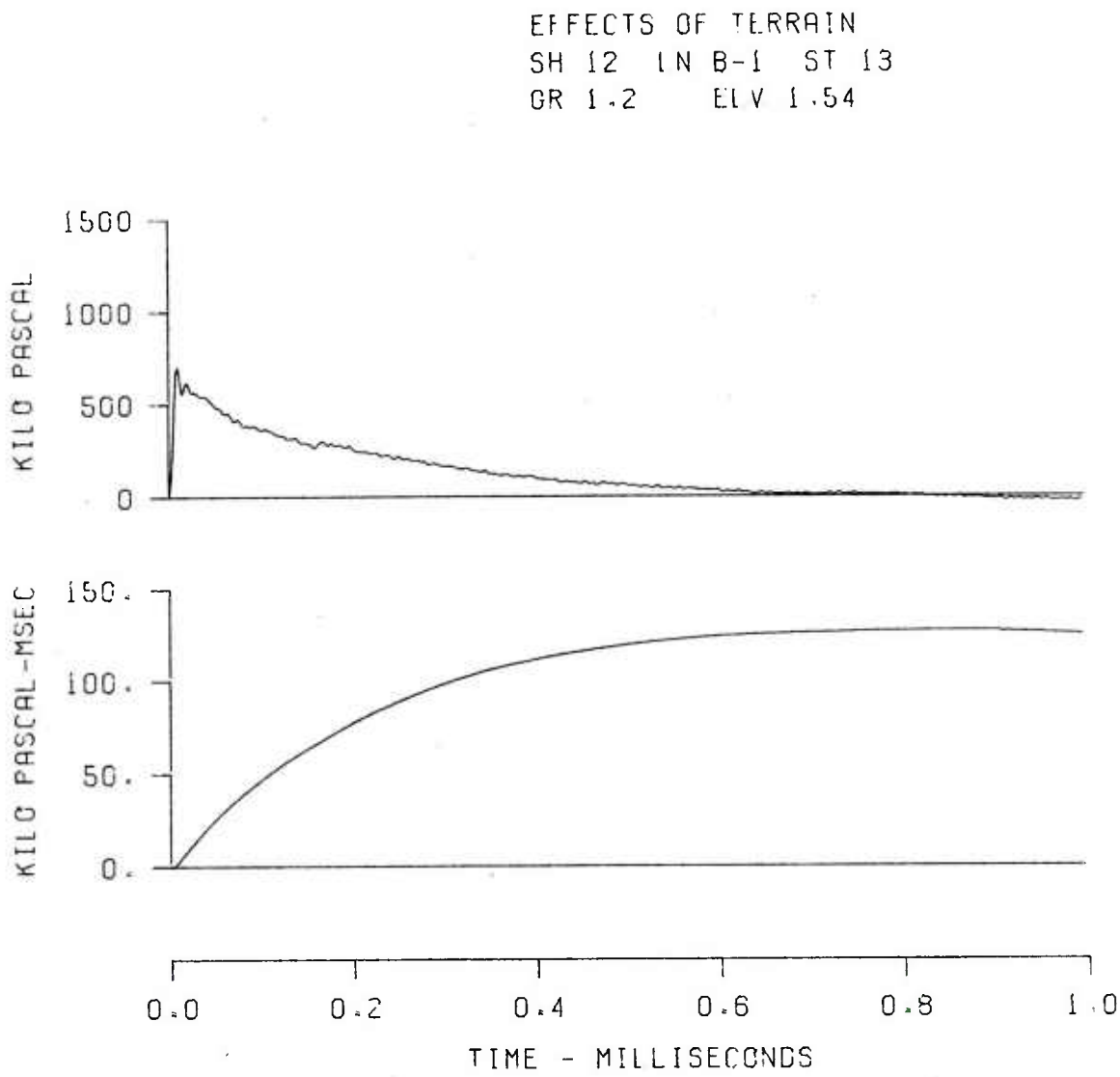

Figure A-3 (Cont). Pressure-Time Traces for Line B_a (B-1)

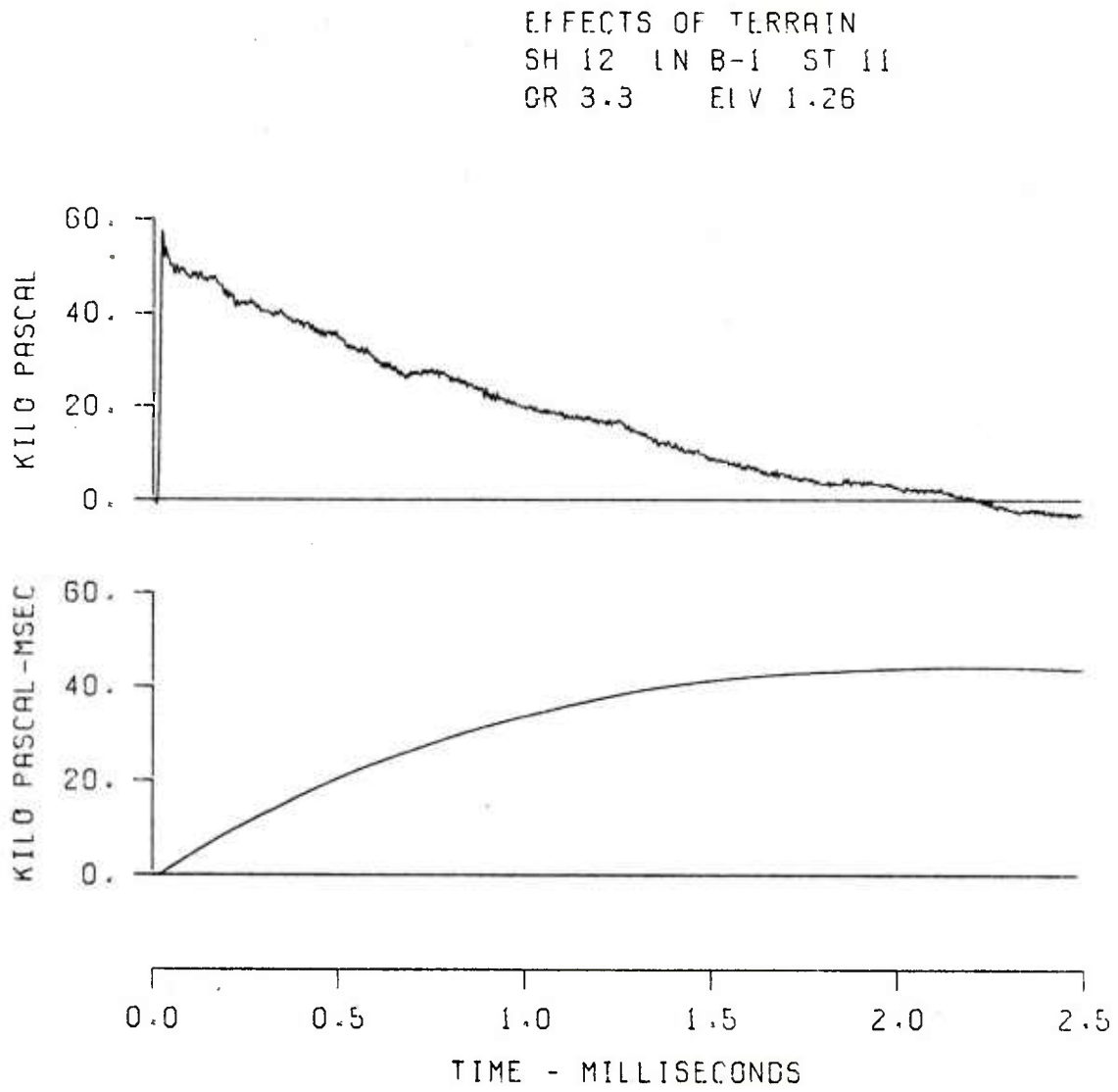

Figure A-3 (Cont). Pressure-Time Traces for Line B_a (B-1)

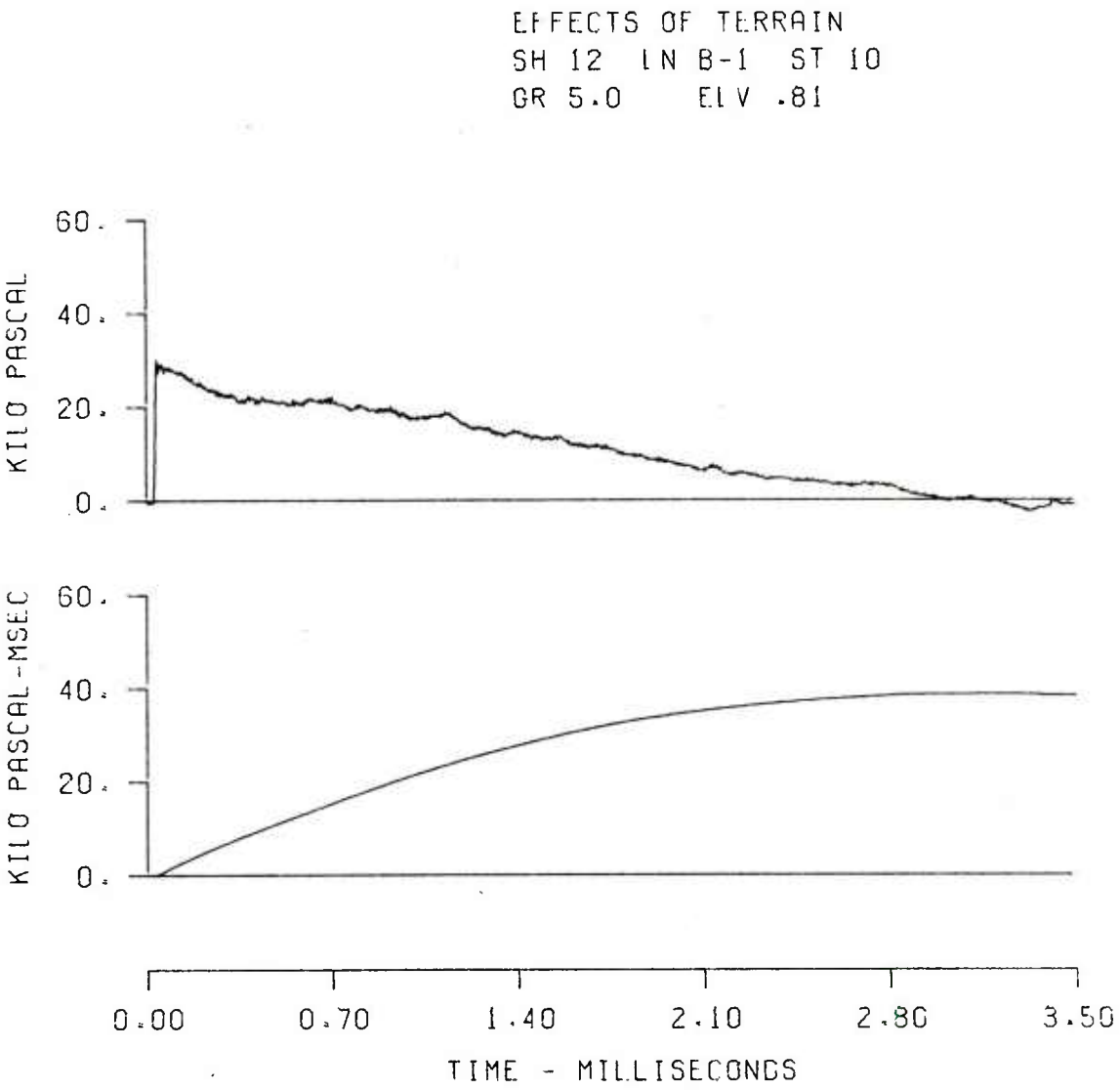

Figure A-3 (Cont). Pressure-Time Traces for Line B_a (B-1)

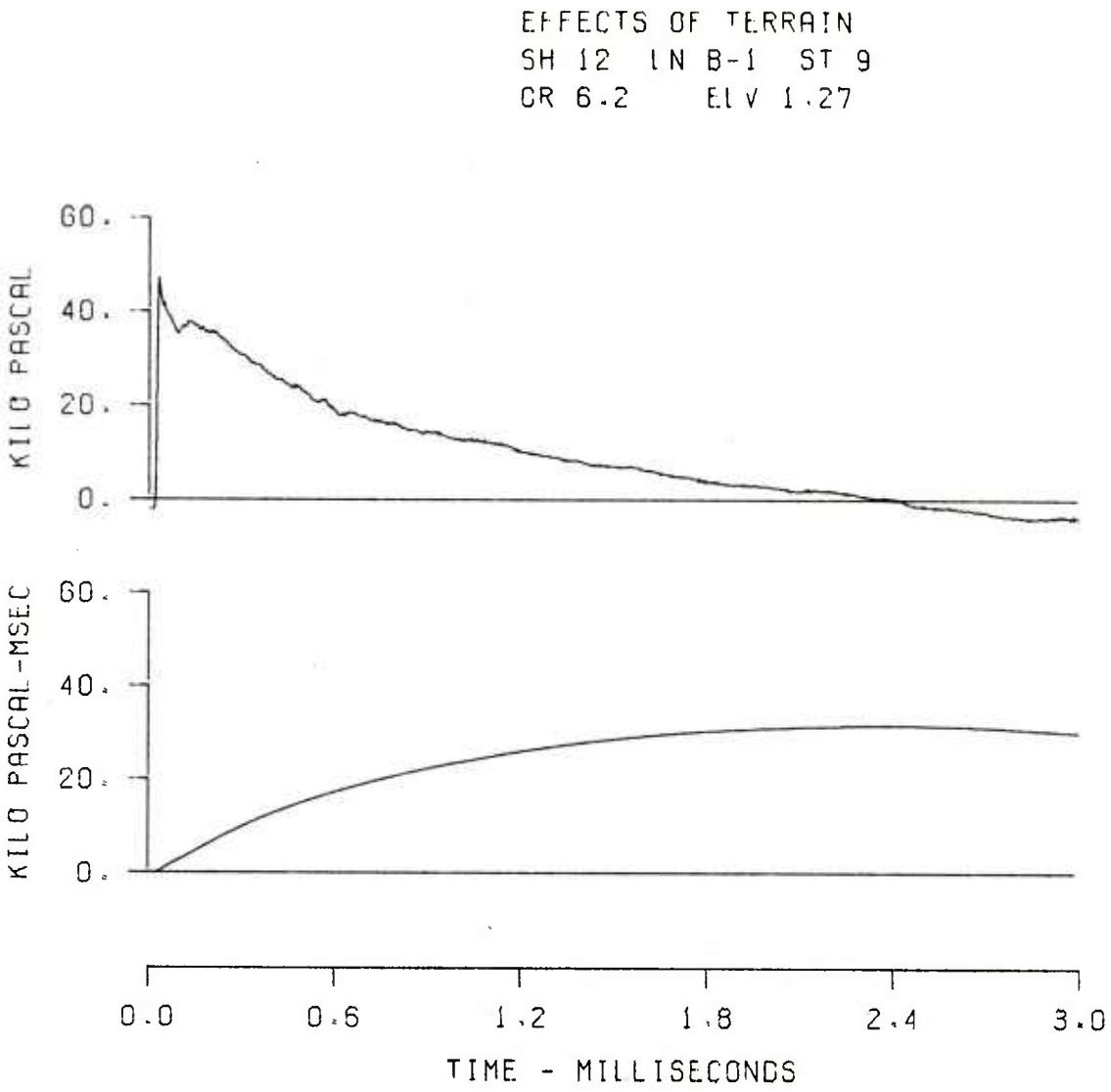

Figure A-3 (Cont). Pressure-Time Traces for Line B_a (B-1)

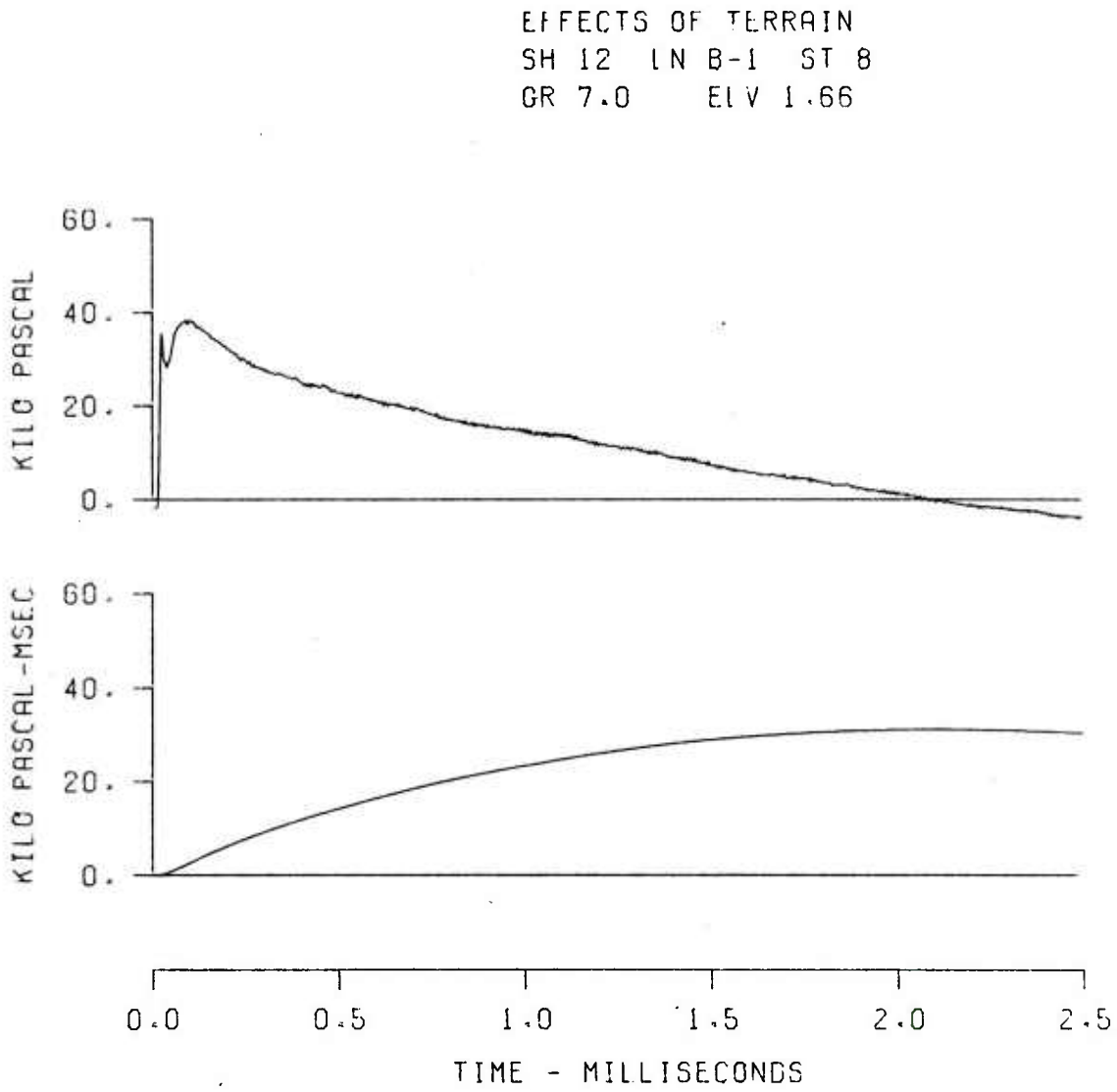

Figure A-3 (Cont). Pressure-Time Traces for Line B_a (B-1)

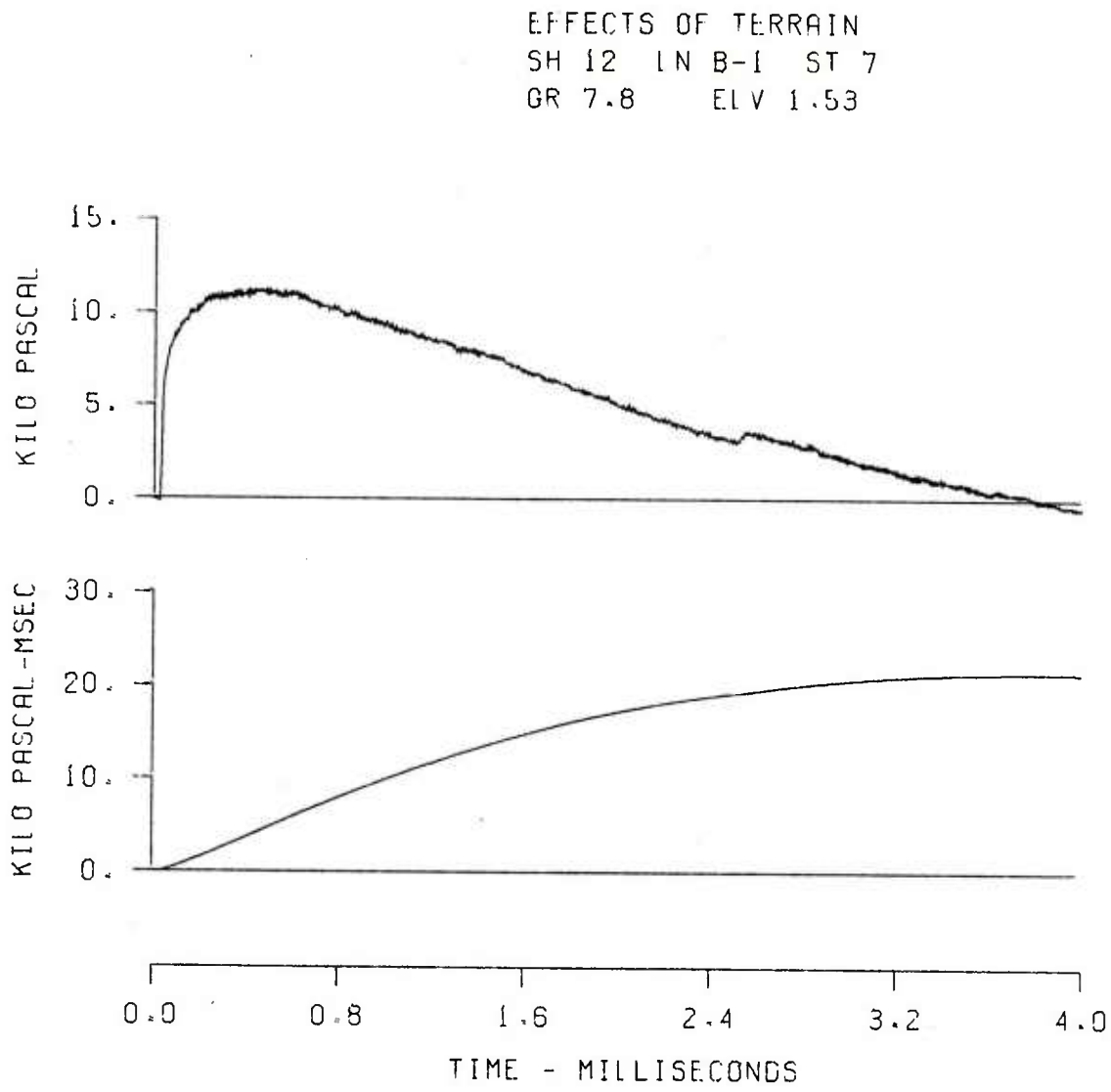

Figure A-3 (Cont). Pressure-Time Traces for Line B_a (B-1)

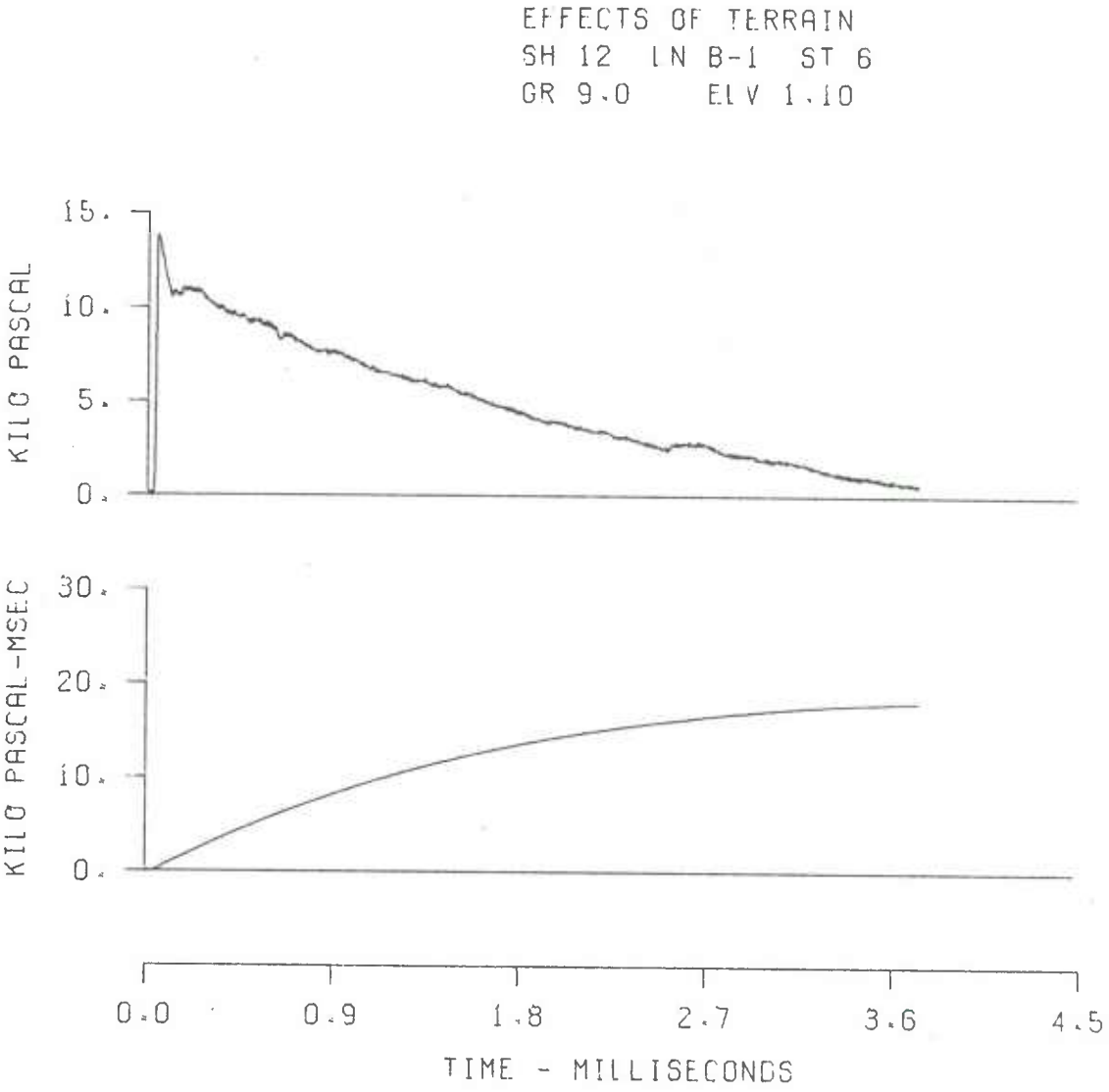

Figure A-3 (Cont). Pressure-Time Traces for Line B_a (B-1)

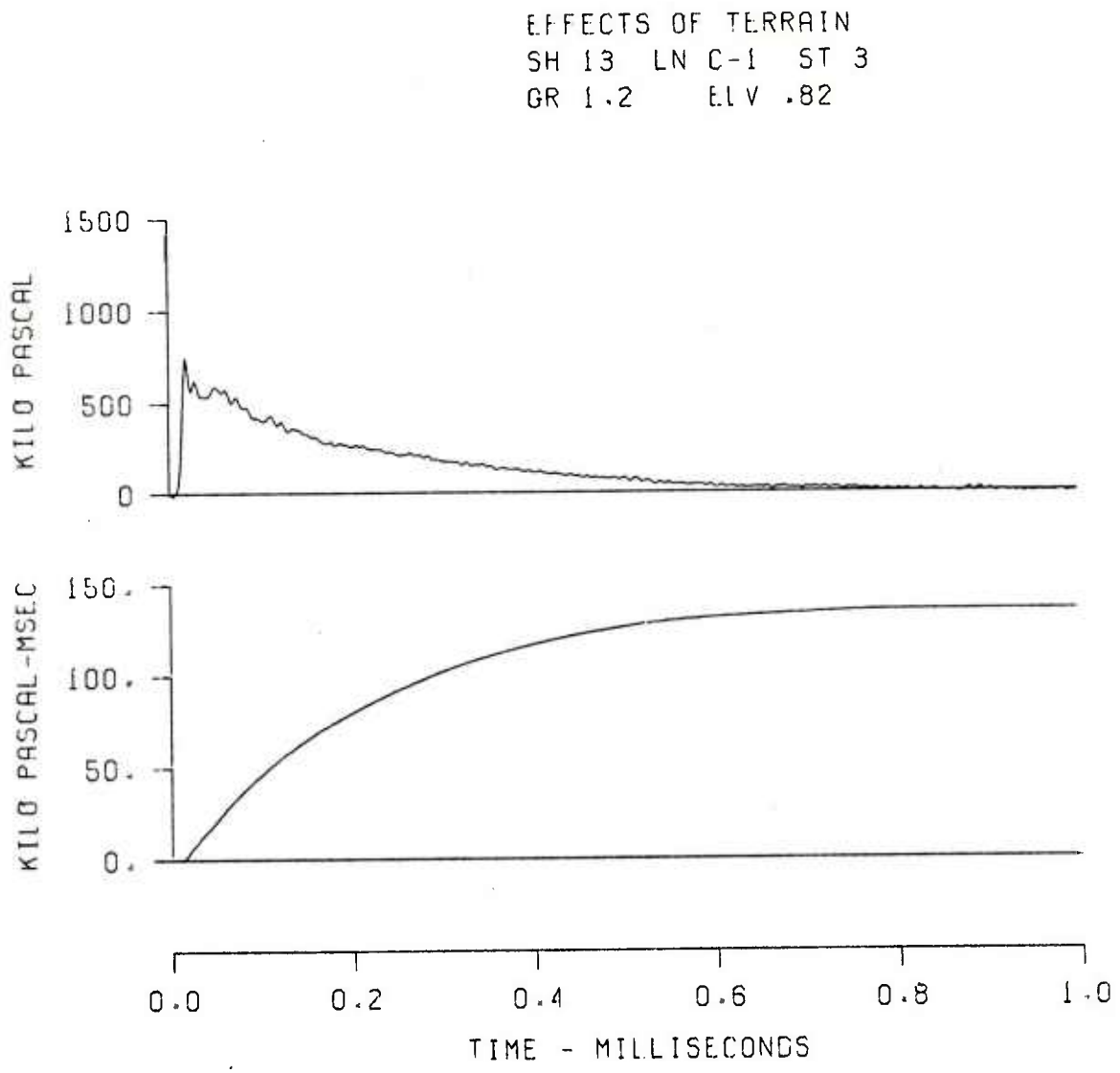

Figure A-4. Pressure-Time Traces for Lines C-1, C-4 and C-5

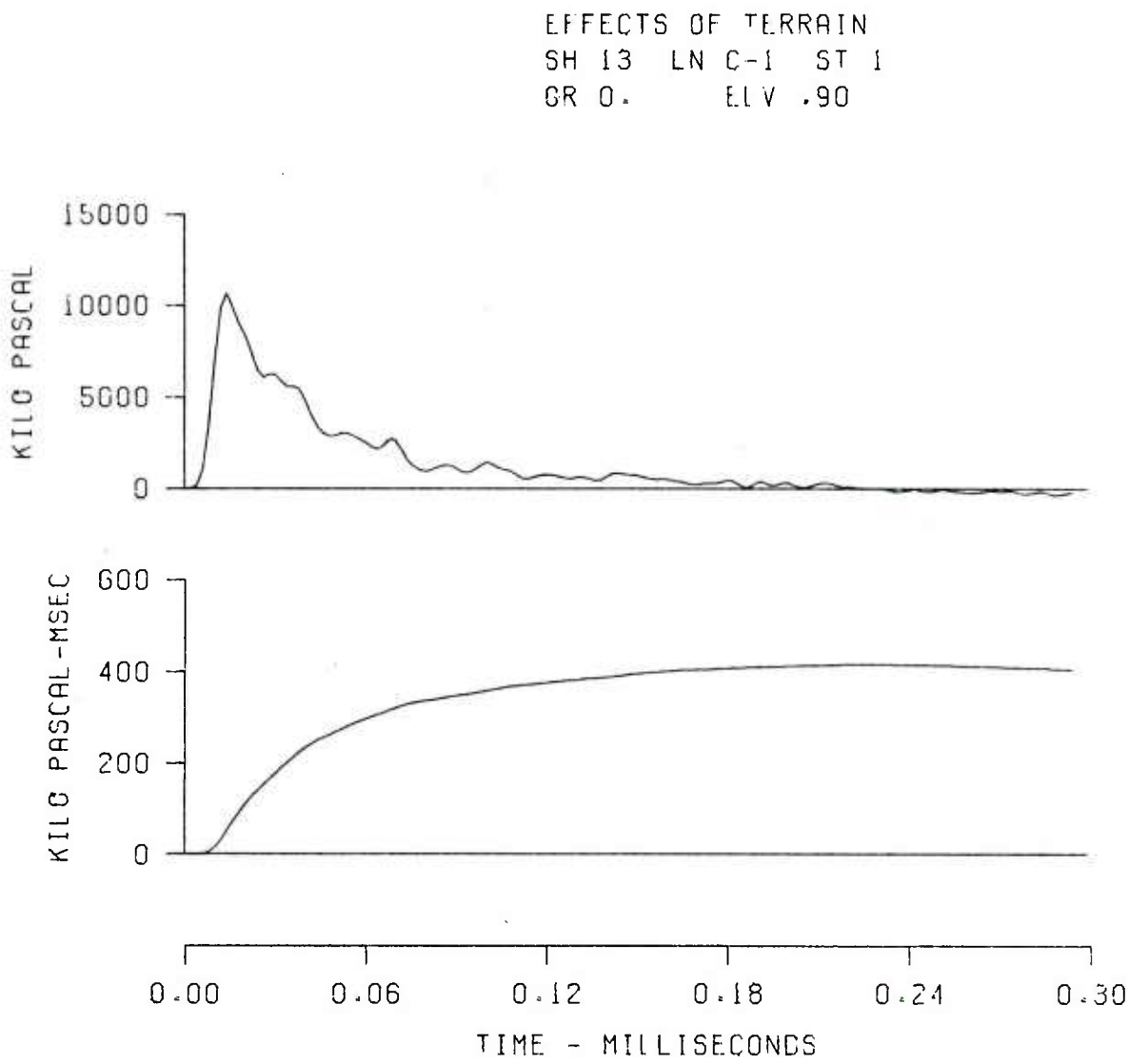

Figure A-4 (Cont). Pressure-Time Traces for Lines C-1, C-4 and C-5

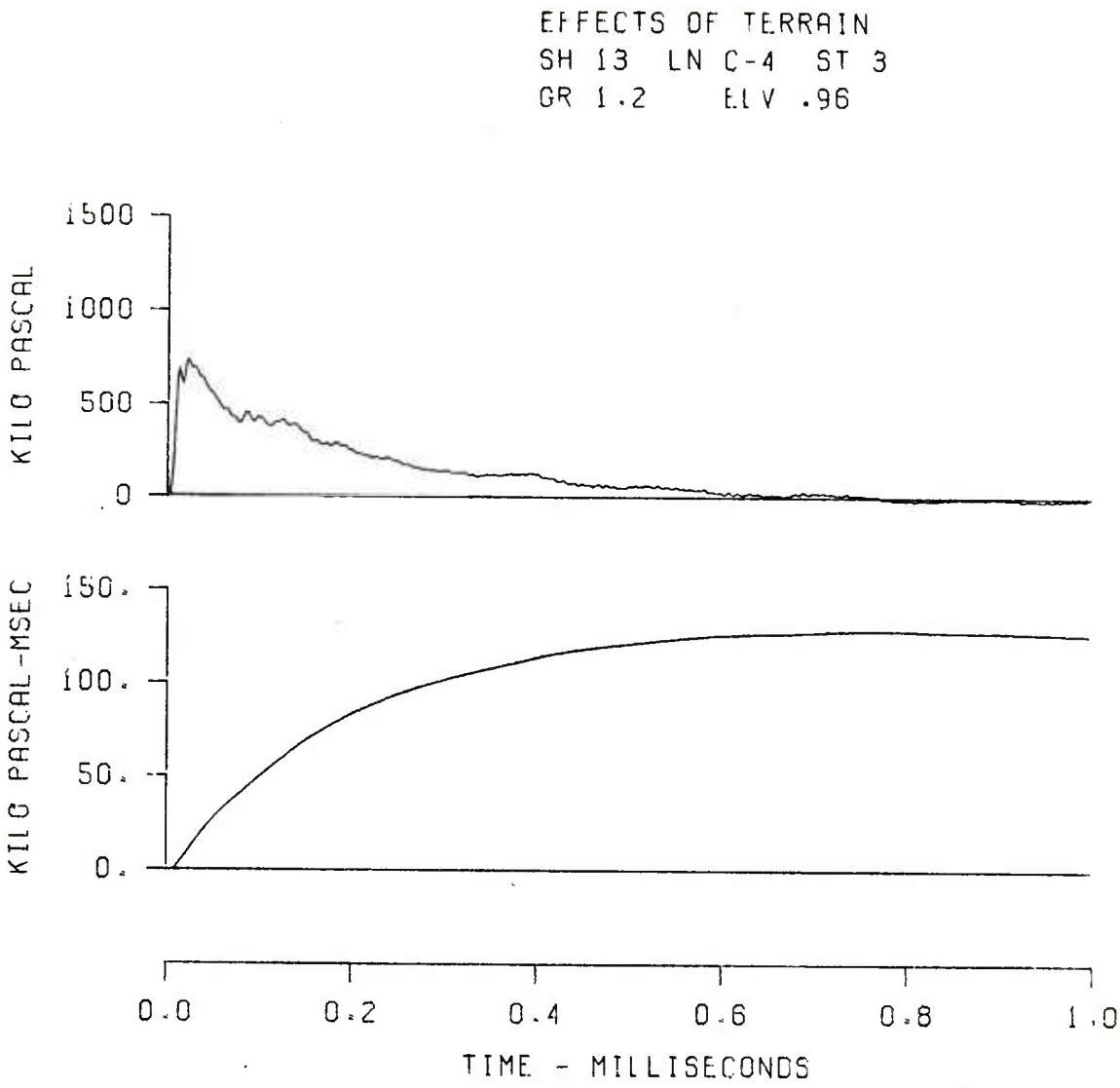

Figure A-4 (Cont). Pressure-Time Traces for Lines C-1, C-4 and C-5

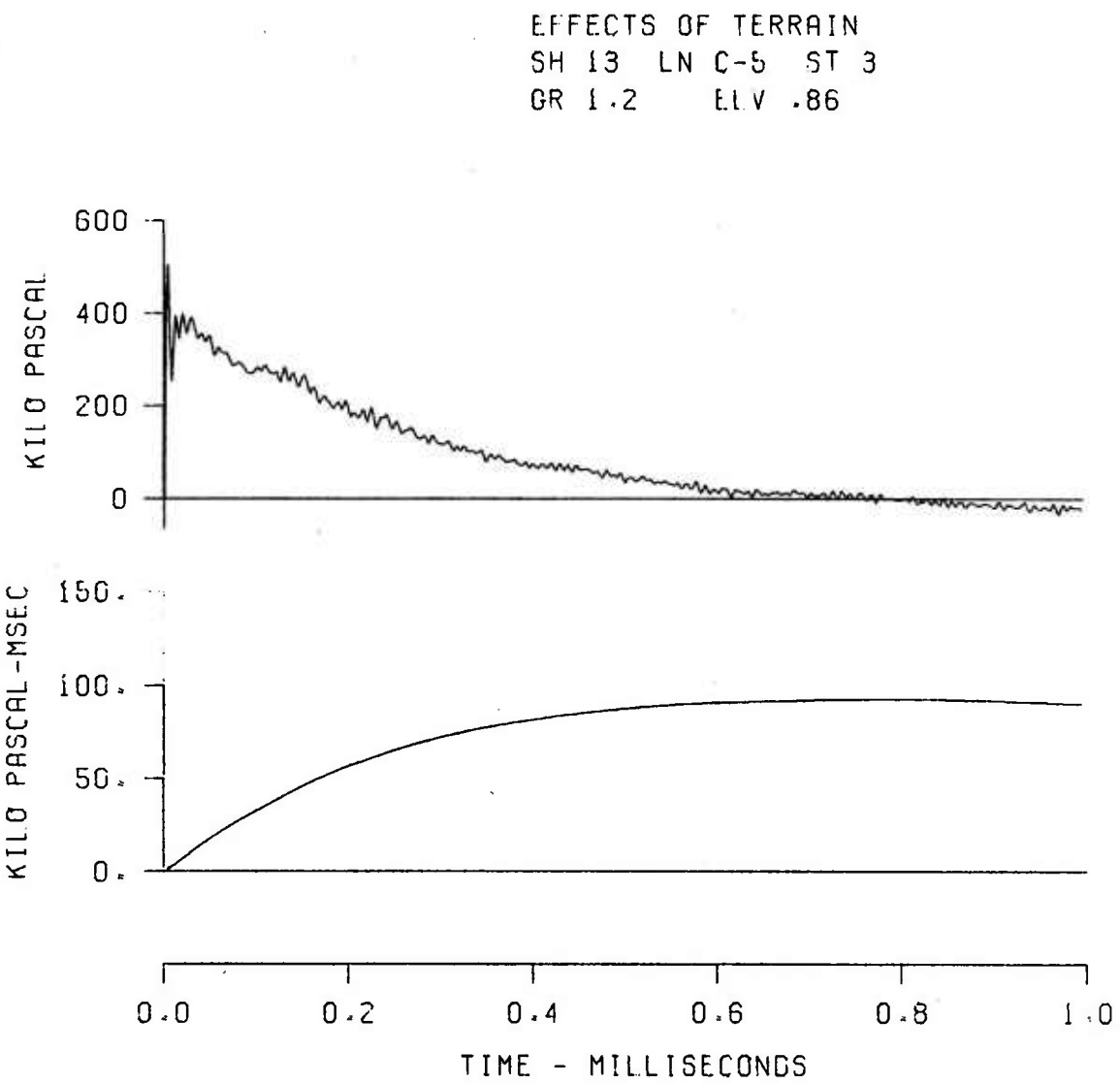

Figure A-4 (Cont). Pressure-Time Traces for Lines C-1, C-4 and C-5

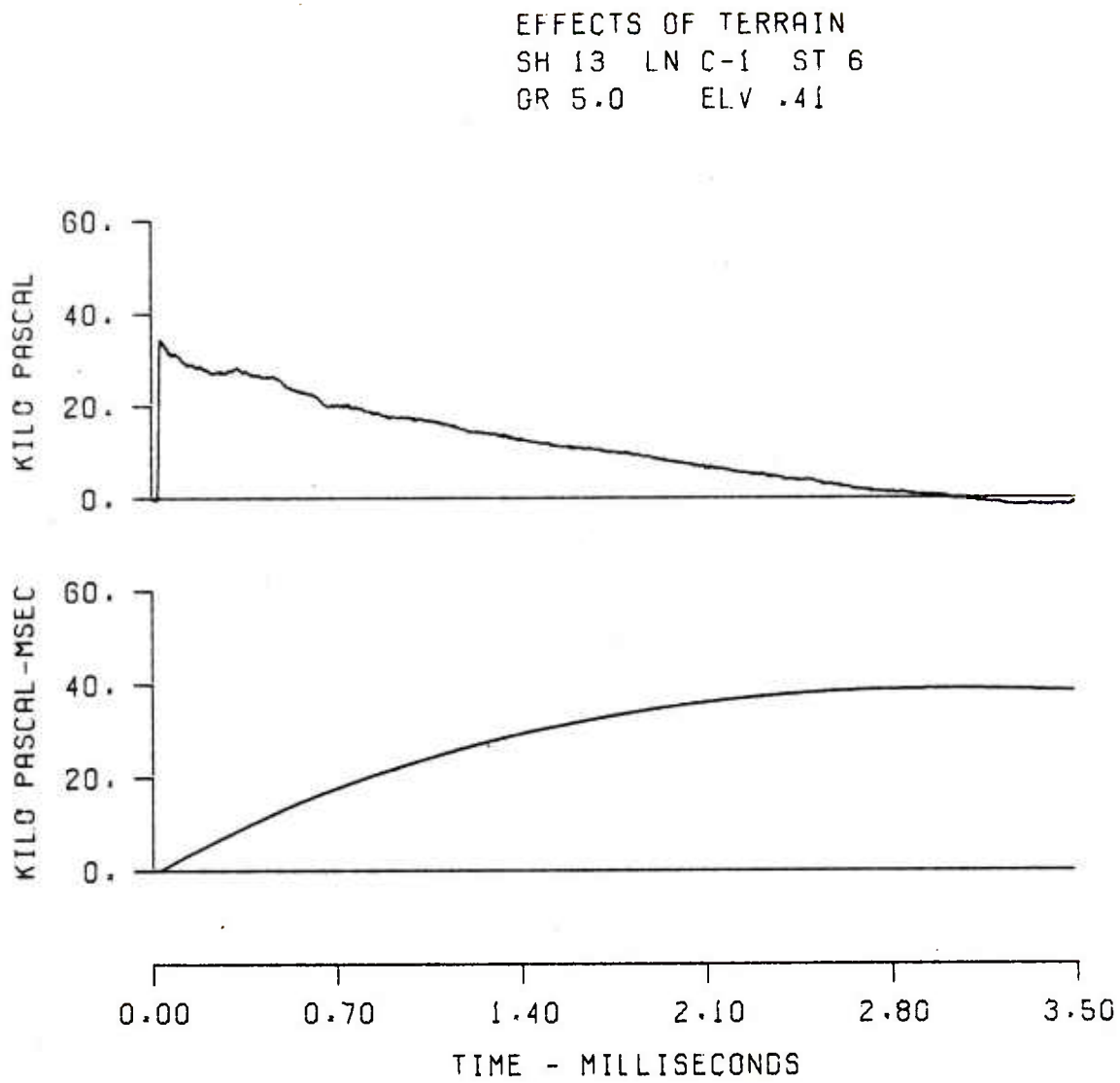

Figure A-4 (Cont). Pressure-Time Traces for Lines C-1, C-4 and C-5

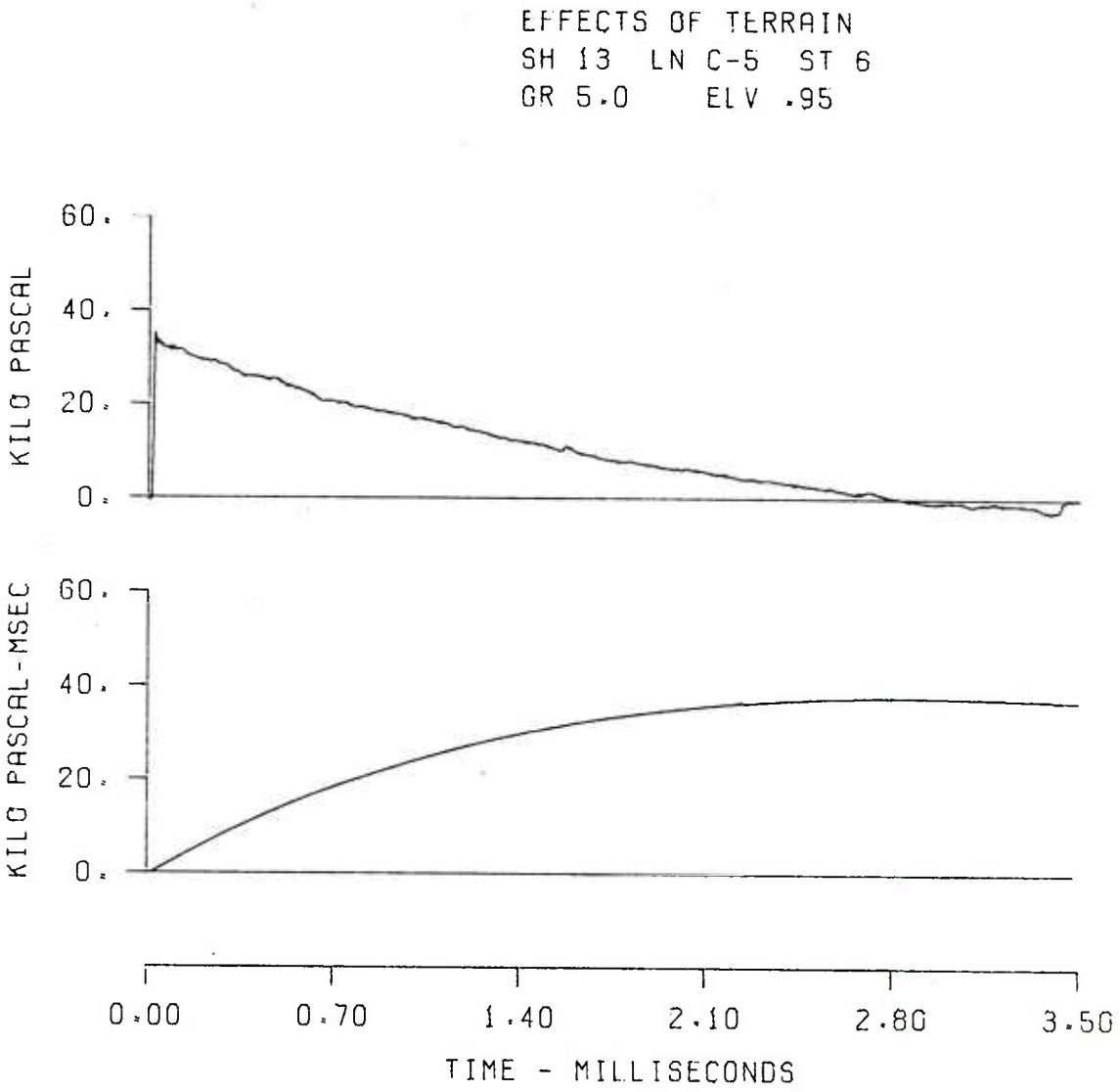

Figure A-4 (Cont). Pressure-Time Traces for Lines C-1, C-4 and C-5

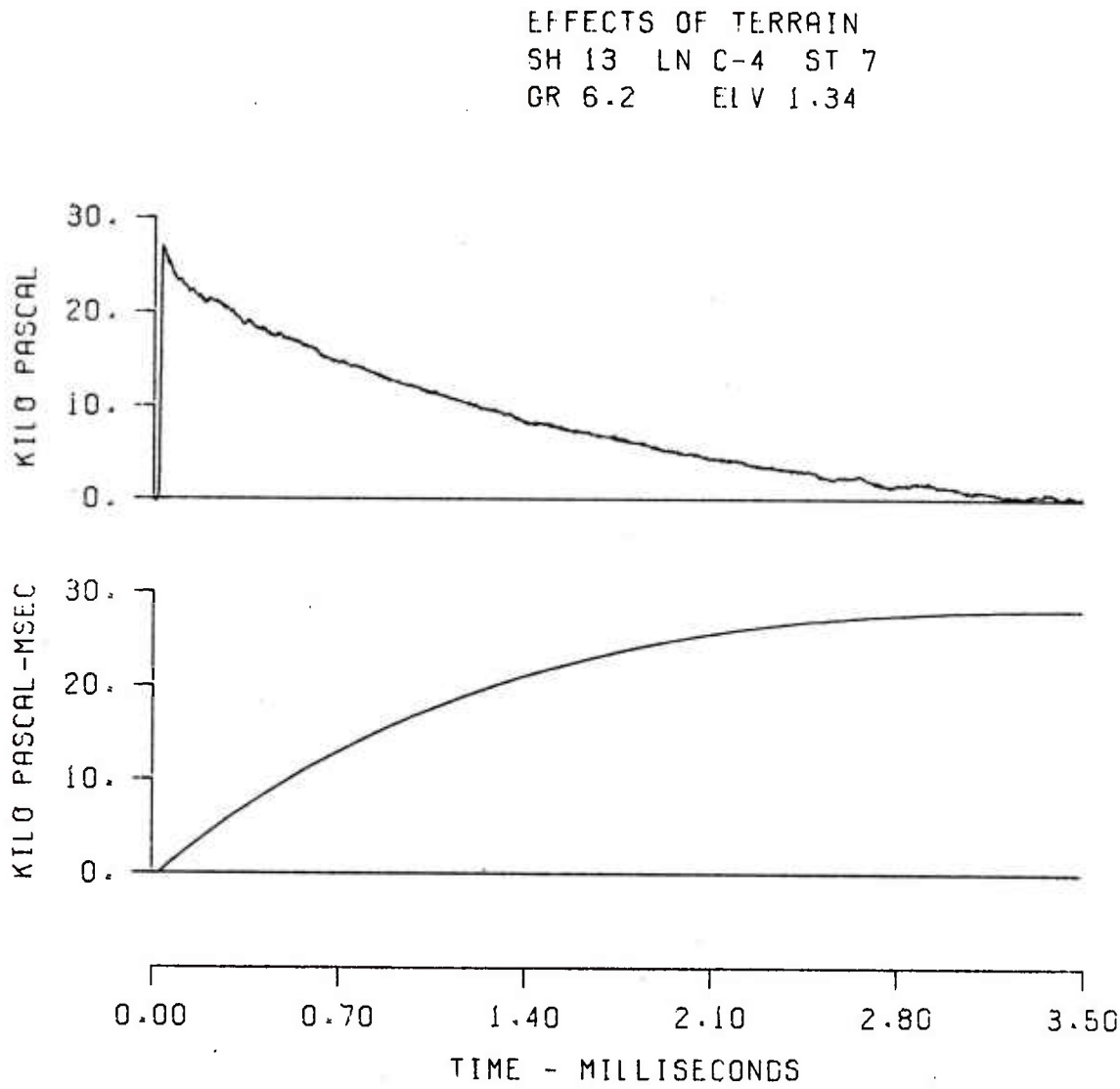

Figure A-4 (Cont). Pressure-Time Traces for Lines C-1, C-4 and C-5

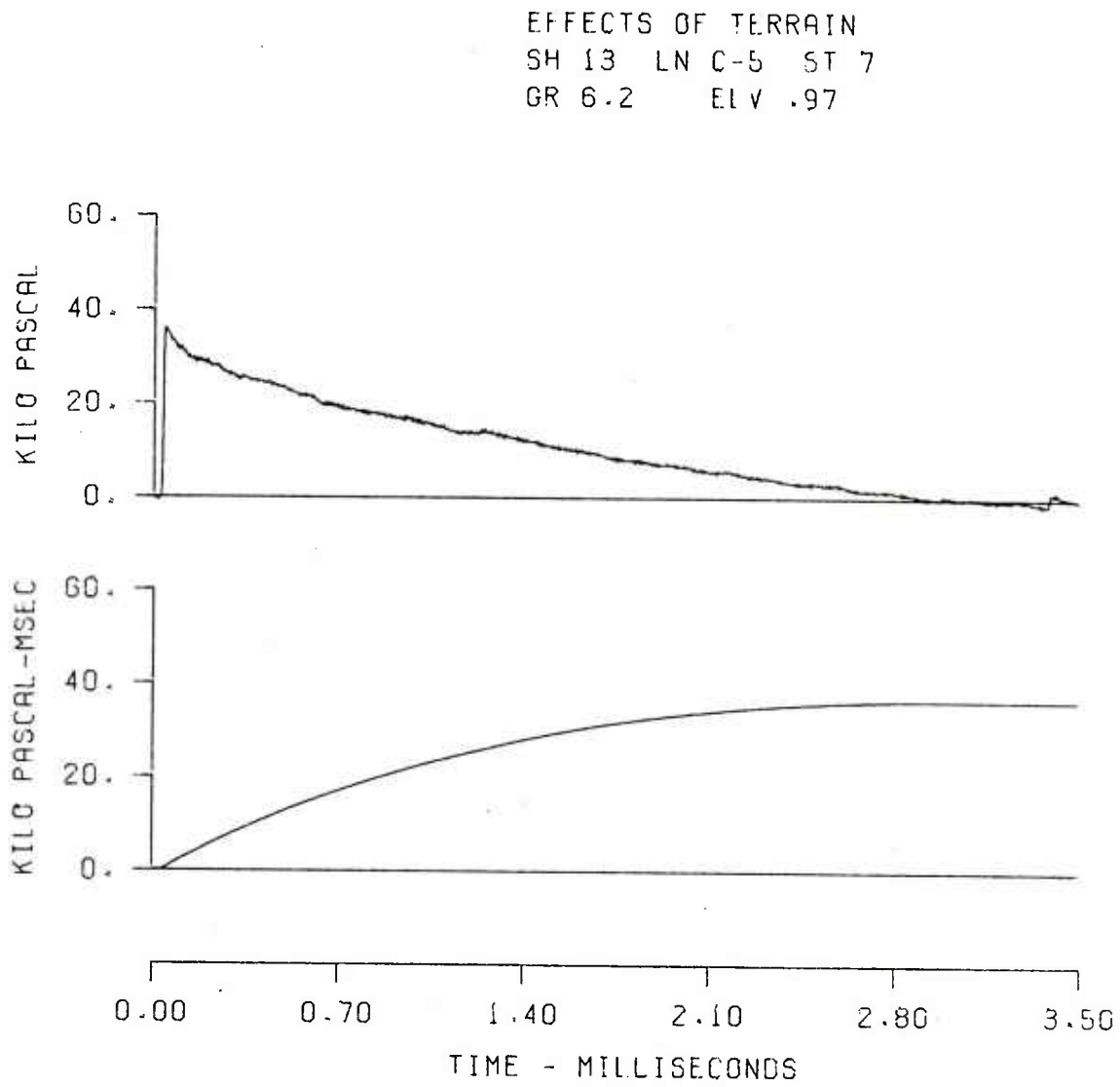

Figure A-4 (Cont). Pressure-Time Traces for Lines C-1, C-4 and C-5

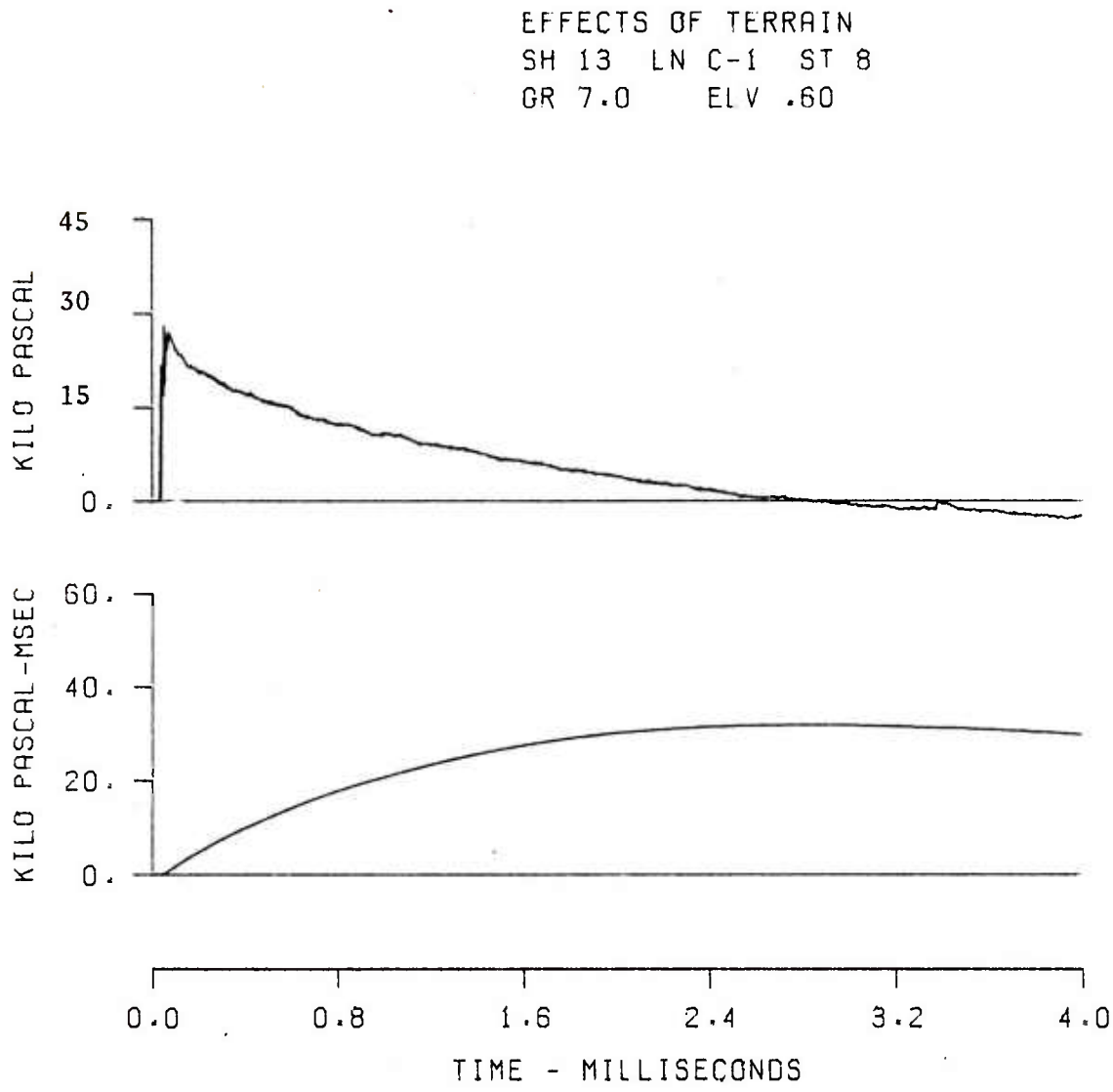

Figure A-4 (Cont). Pressure-Time Traces for Lines C-1, C-4 and C-5

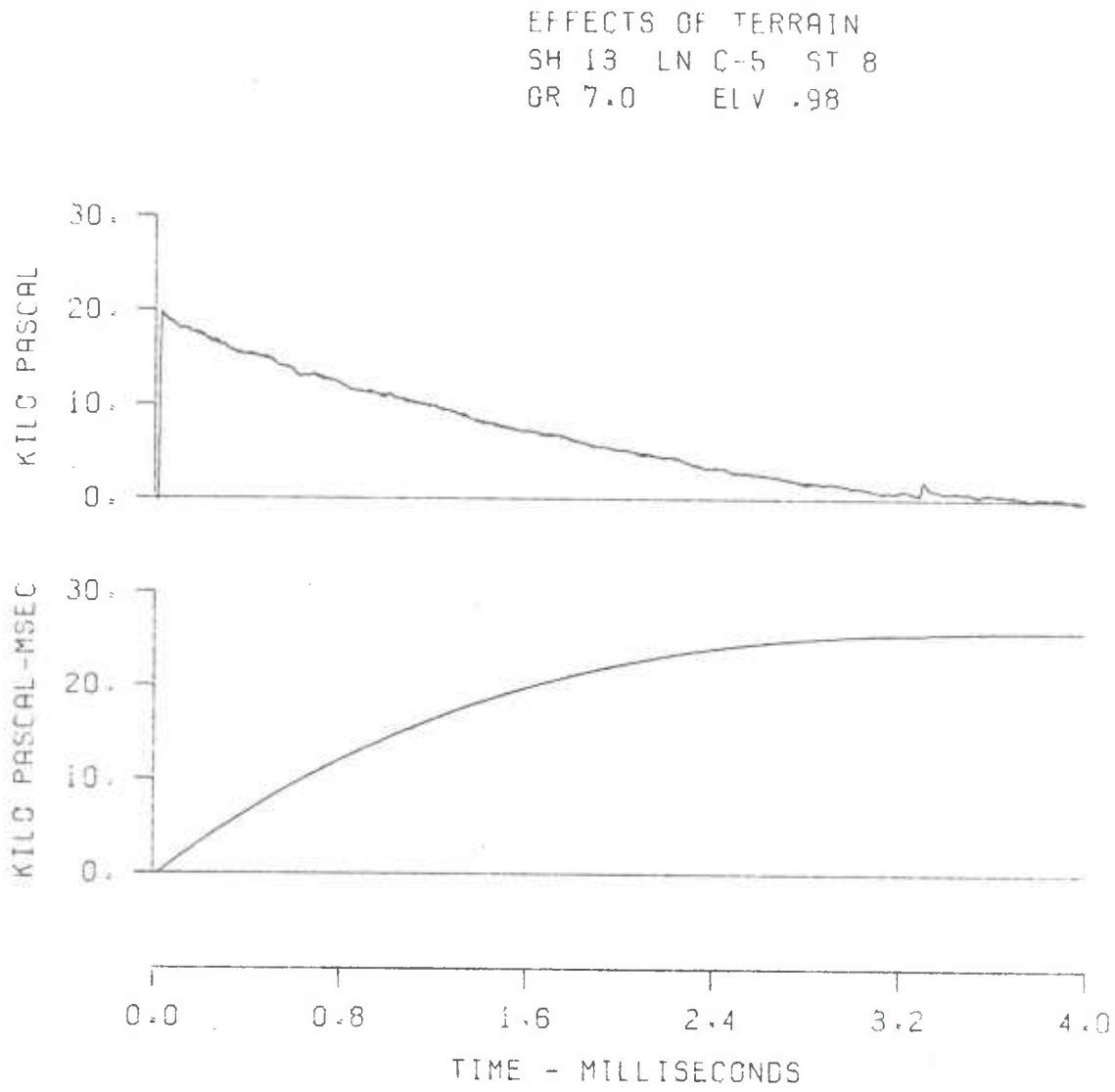

Figure A-4 (Cont). Pressure-Time Traces for Lines C-1, C-4 and C-5

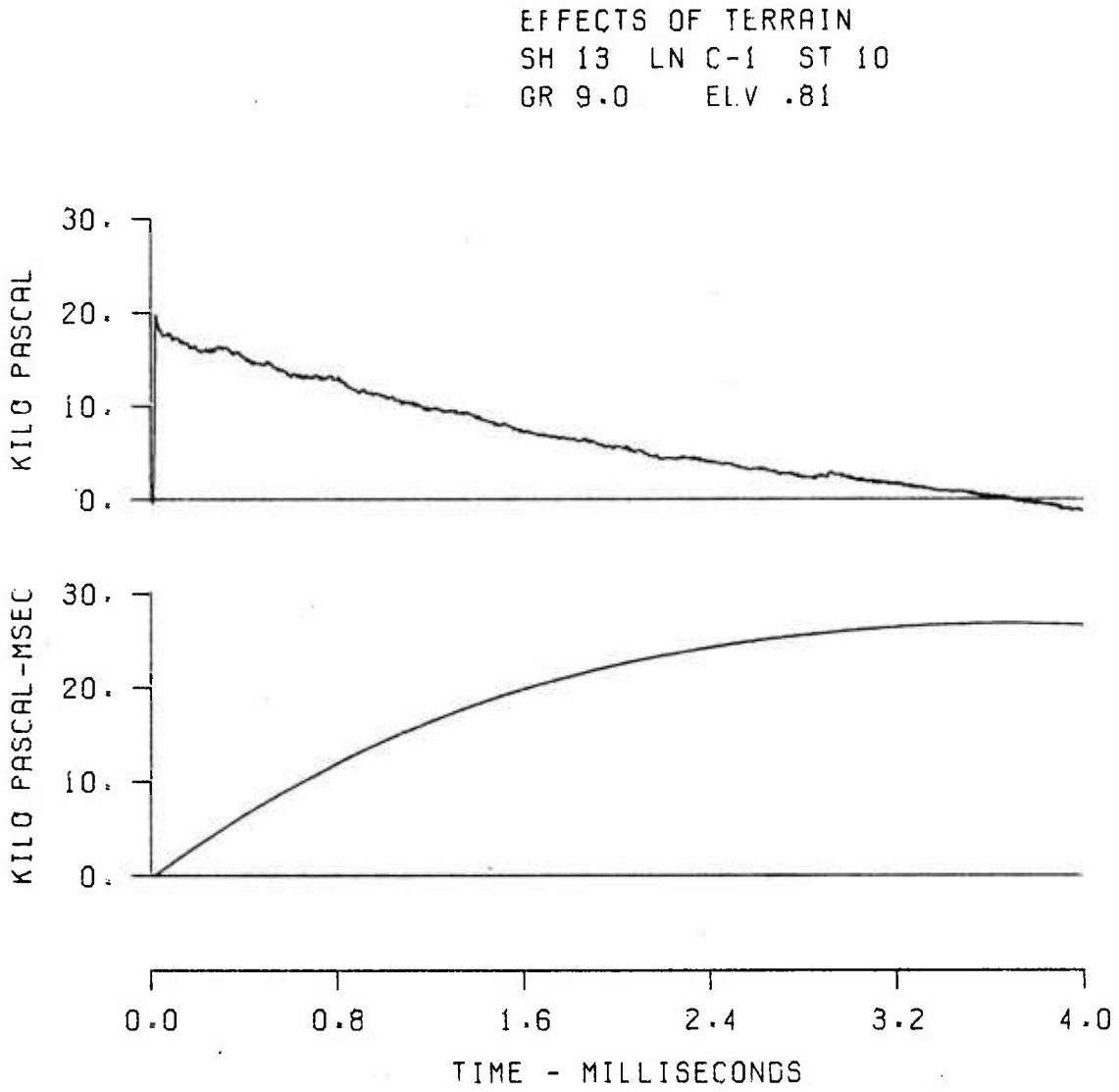

Figure A-4 (Cont). Pressure-Time Traces for Lines C-1, C-4 and C-5

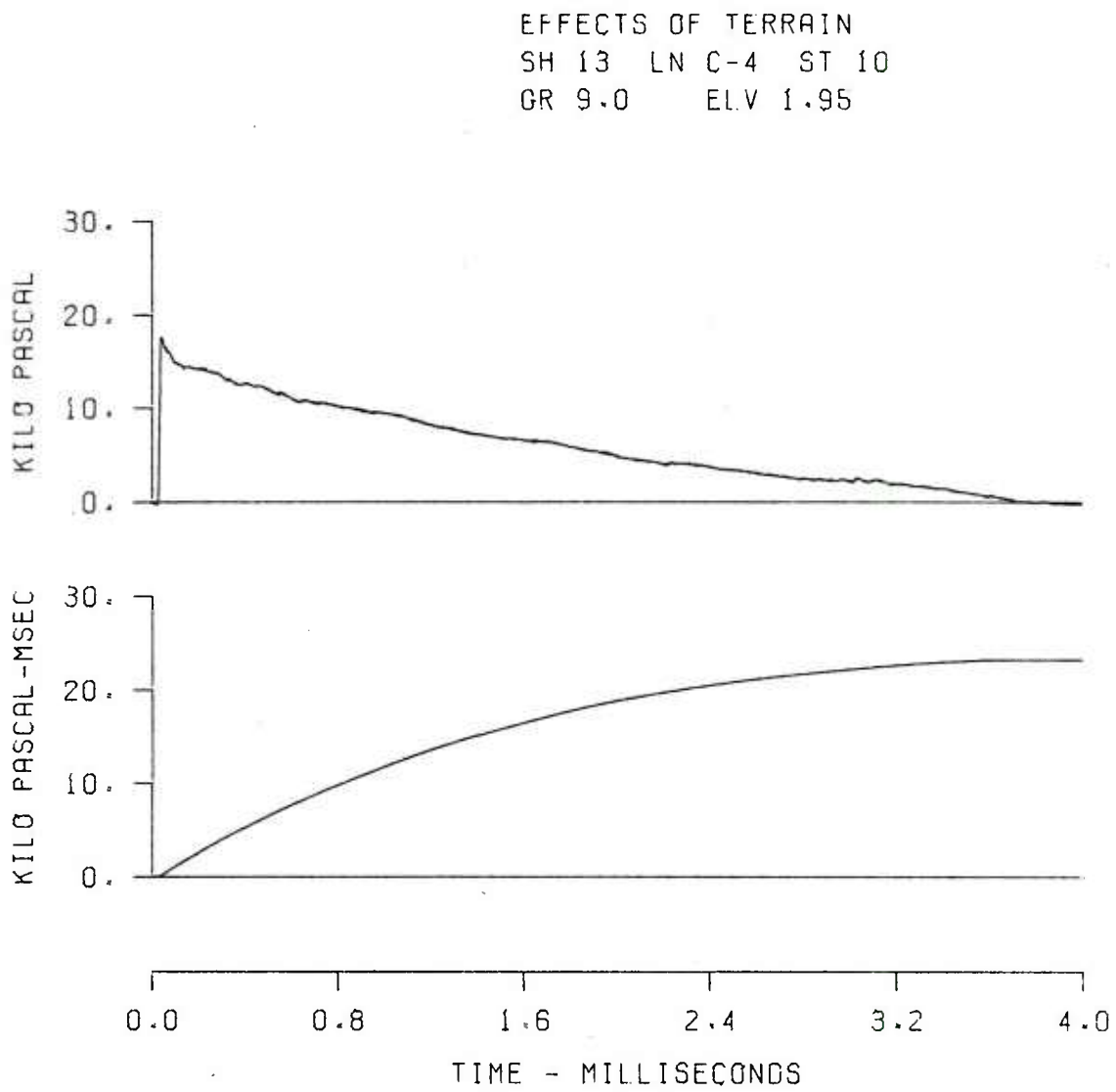

Figure A-4 (Cont). Pressure-Time Traces for Lines C-1, C-4 and C-5

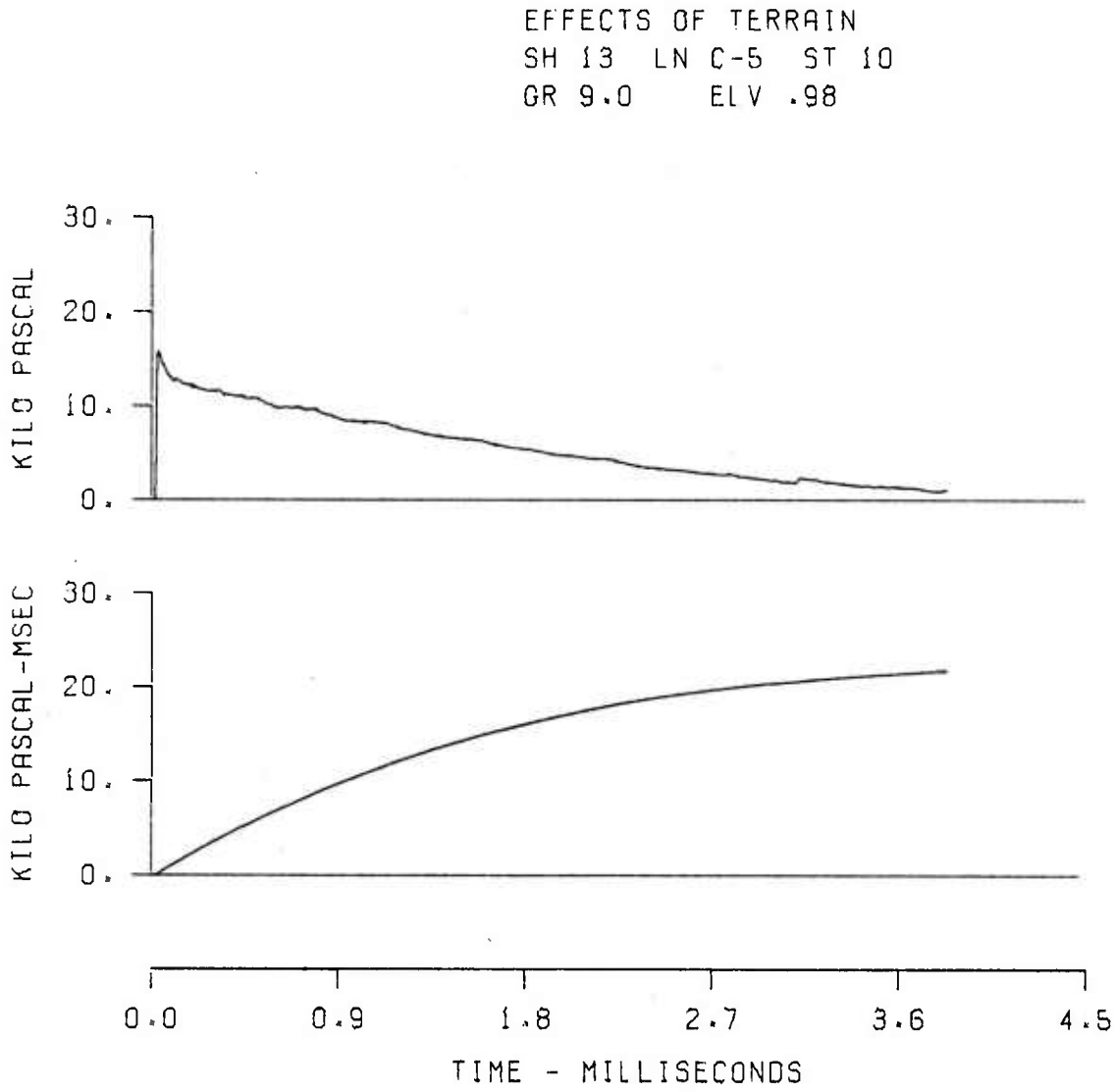

Figure A-4 (Cont). Pressure-Time Traces for Lines C-1, C-4 and C-5

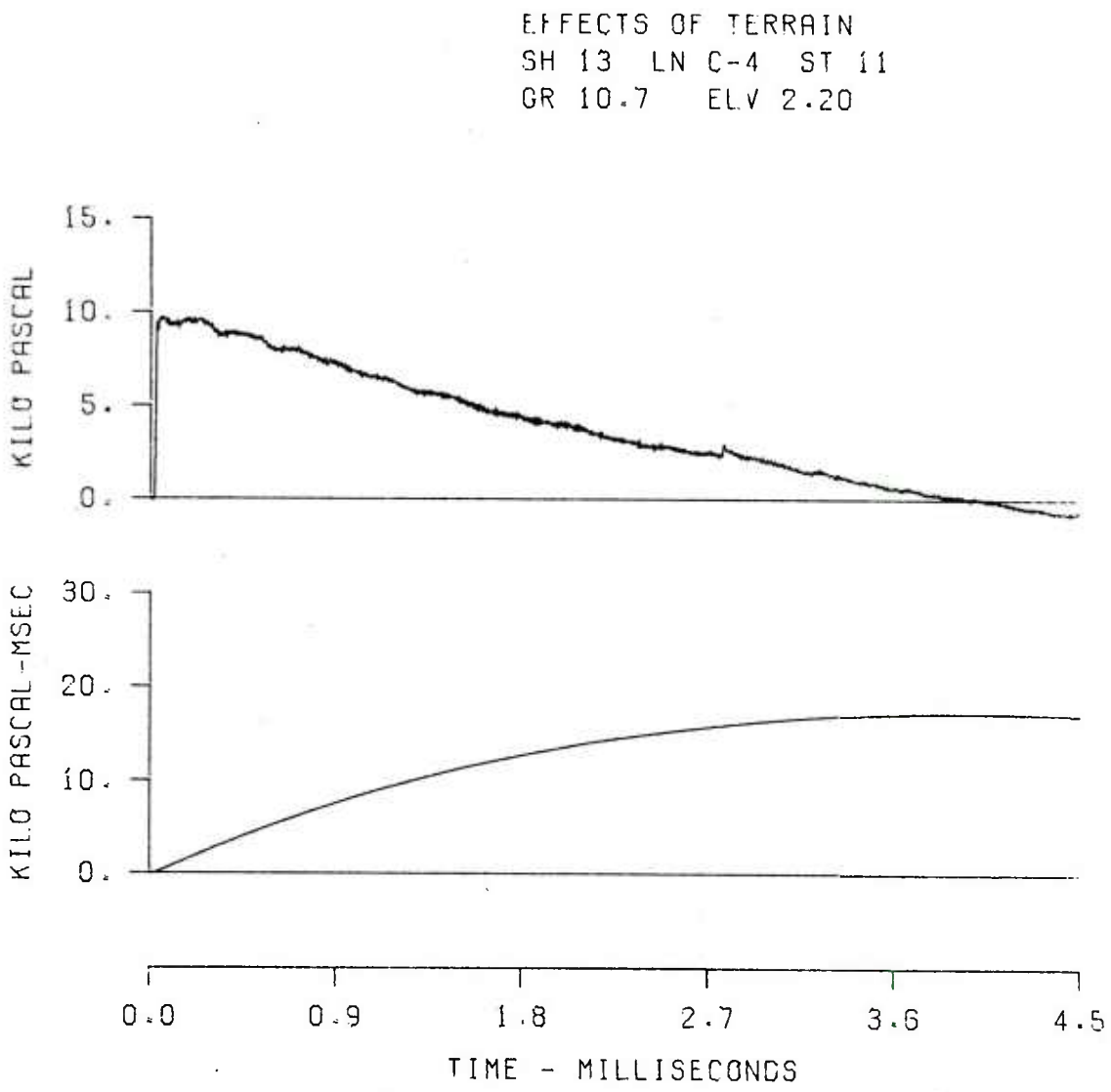

Figure A-4 (Cont). Pressure-Time Traces for Lines C-1, C-4 and C-5

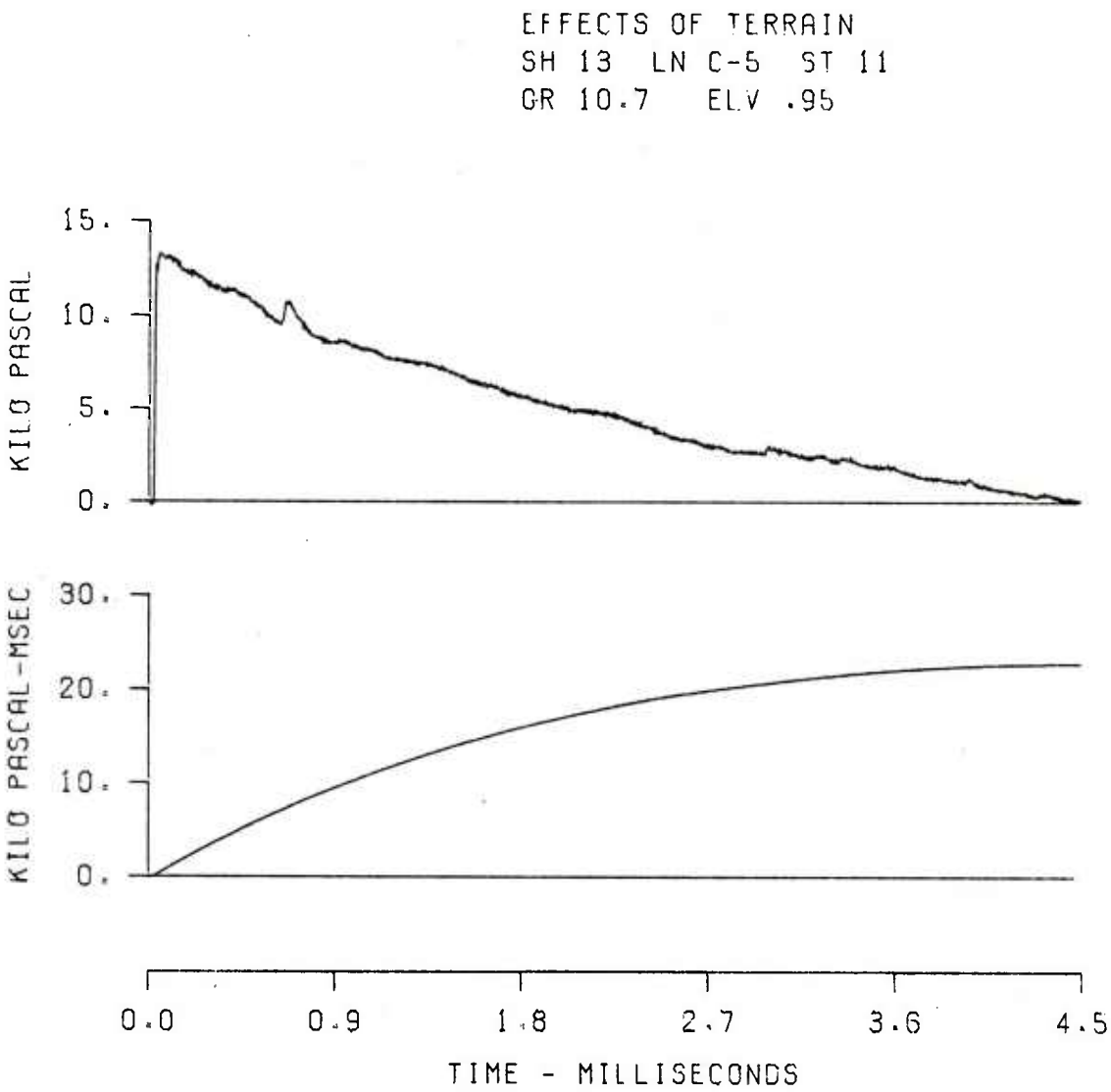

Figure A-4 (Cont). Pressure-Time Traces for Lines C-1, C-4 and C-5

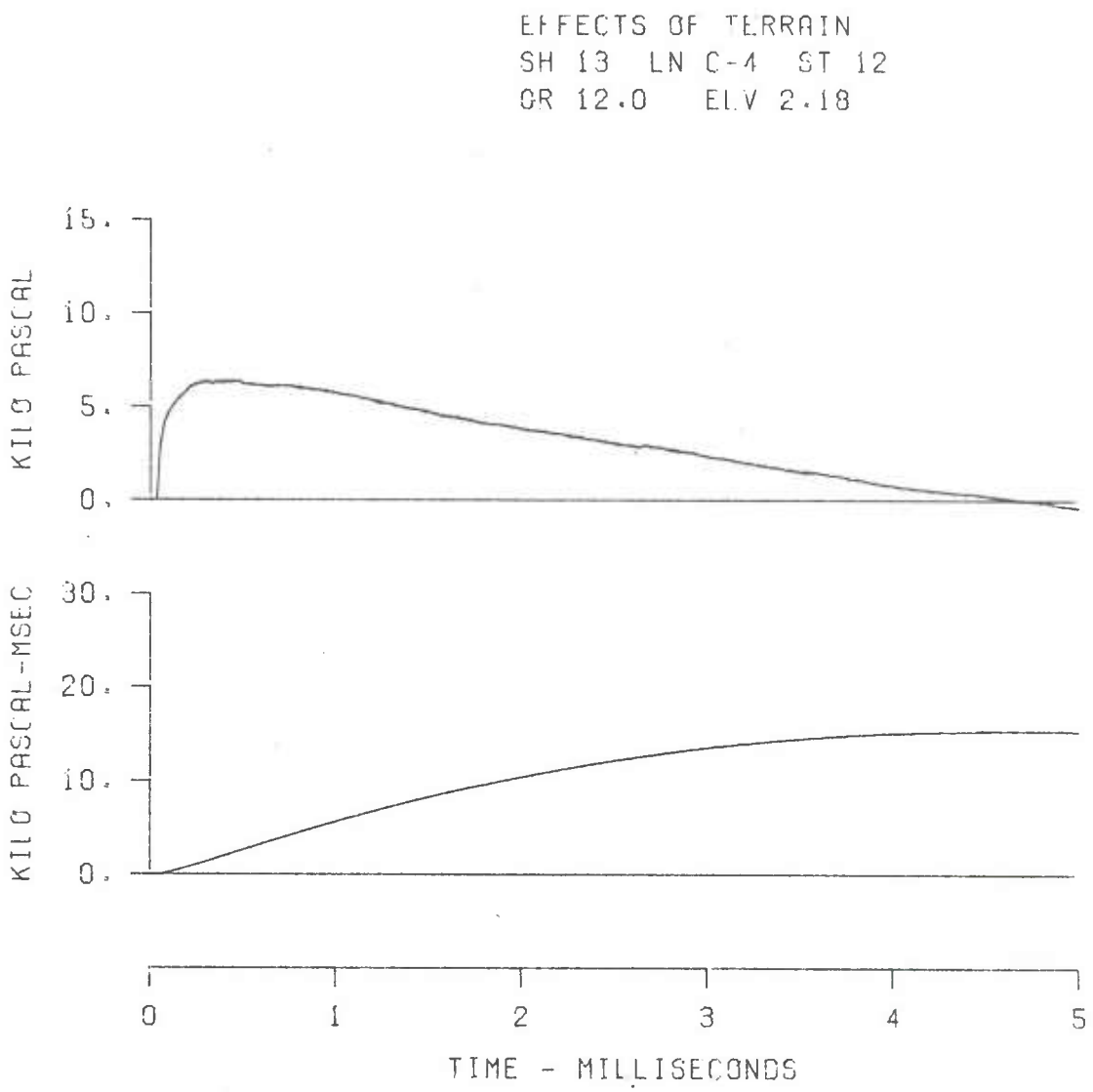

Figure A-4 (Cont). Pressure-Time Traces for Lines C-1, C-4 and C-5

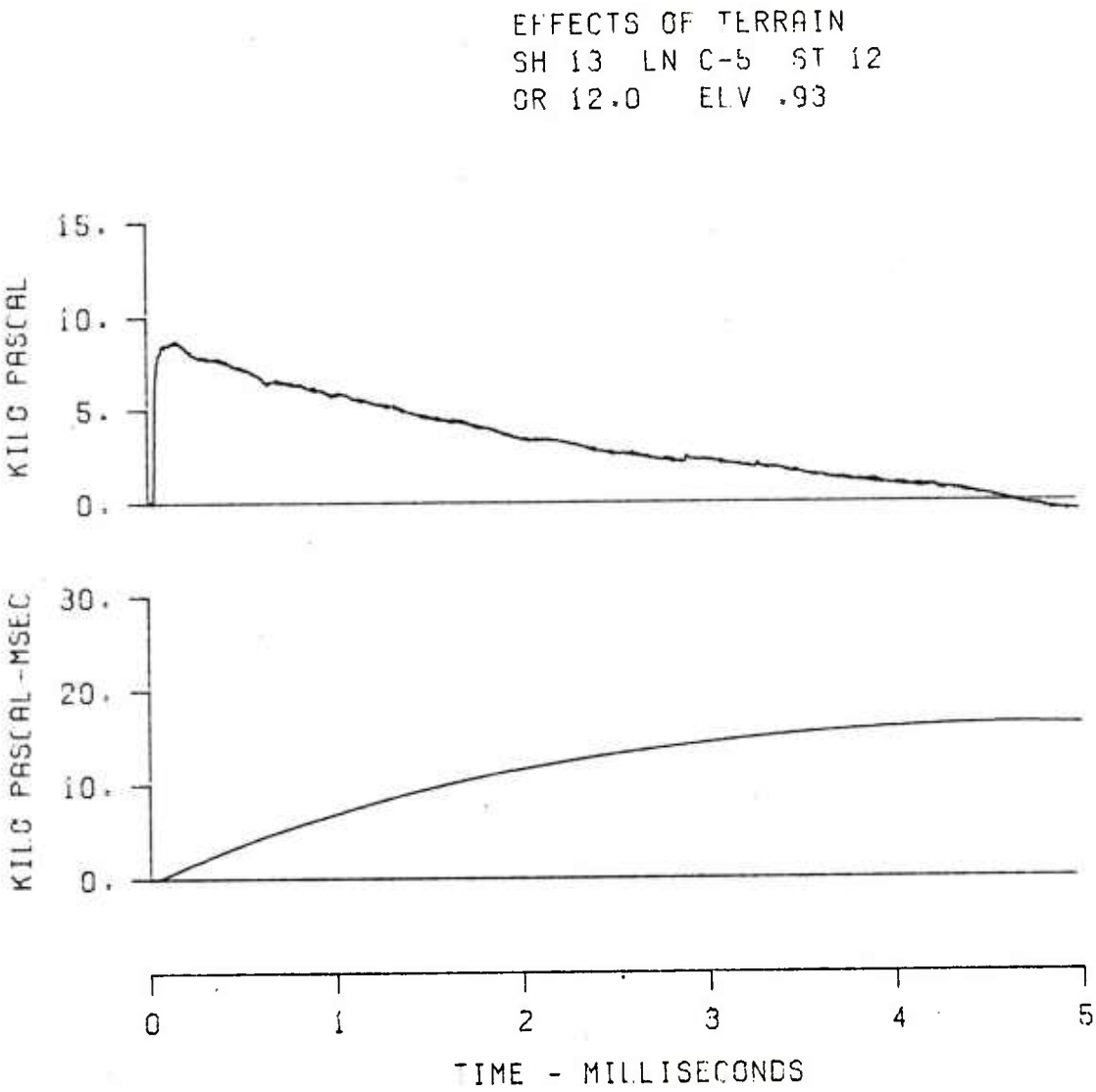

Figure A-4 (Cont). Pressure-Time Traces for Lines C-1, C-4 and C-5

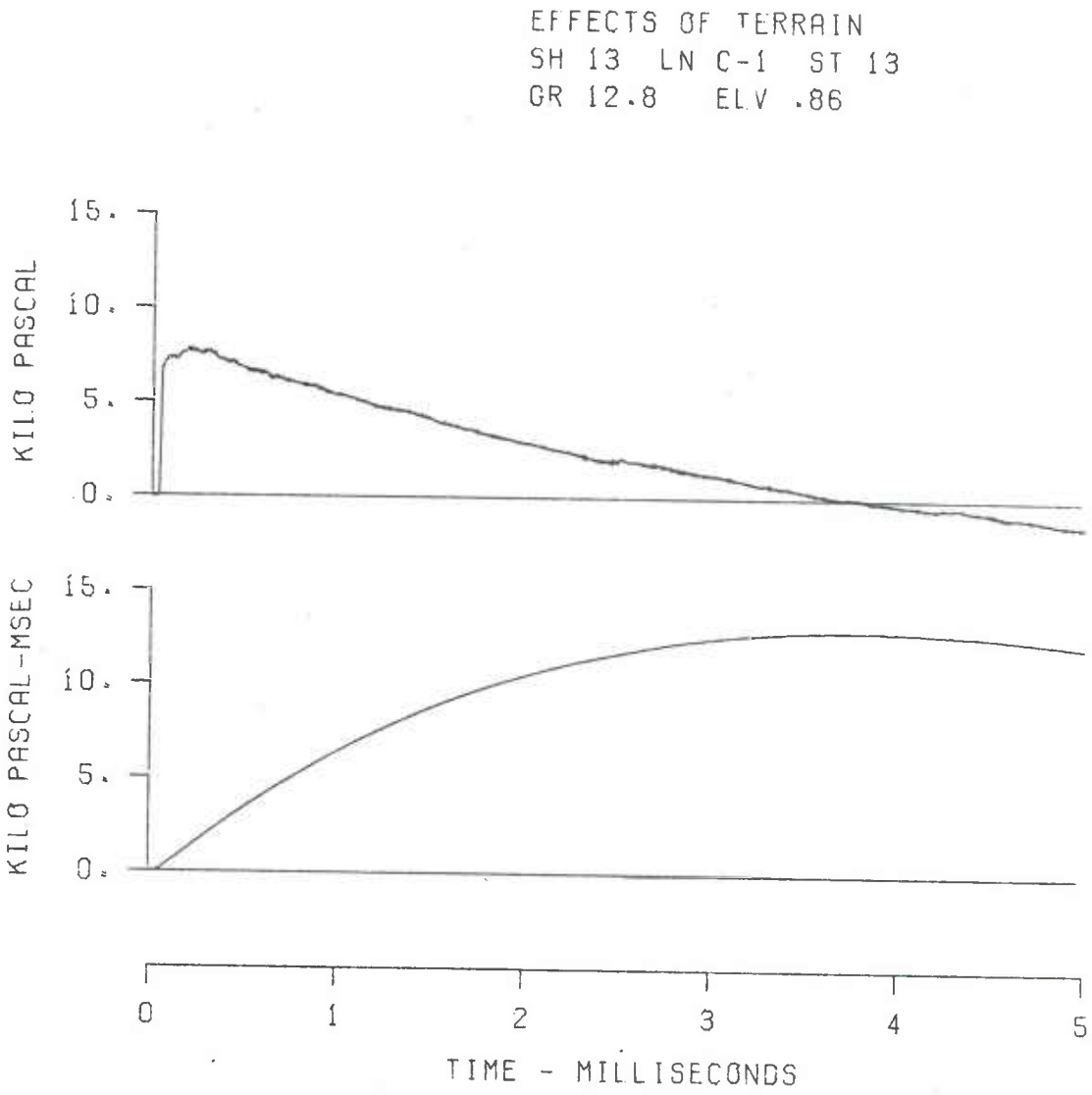

Figure A-4 (Cont). Pressure-Time Traces for Lines C-1, C-4 and C-5

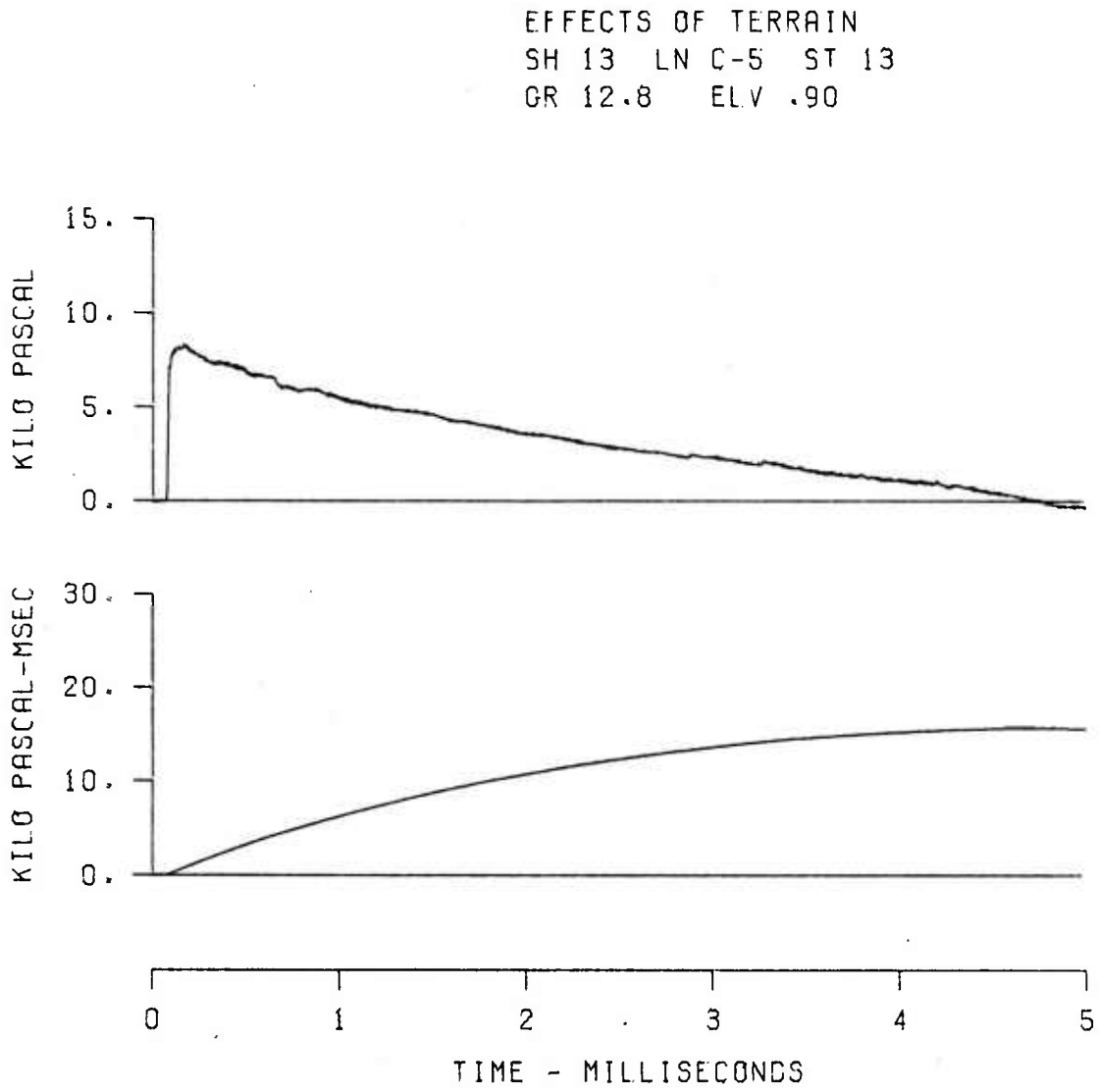

Figure A-4 (Cont). Pressure-Time Traces for Lines C-1, C-4 and C-5

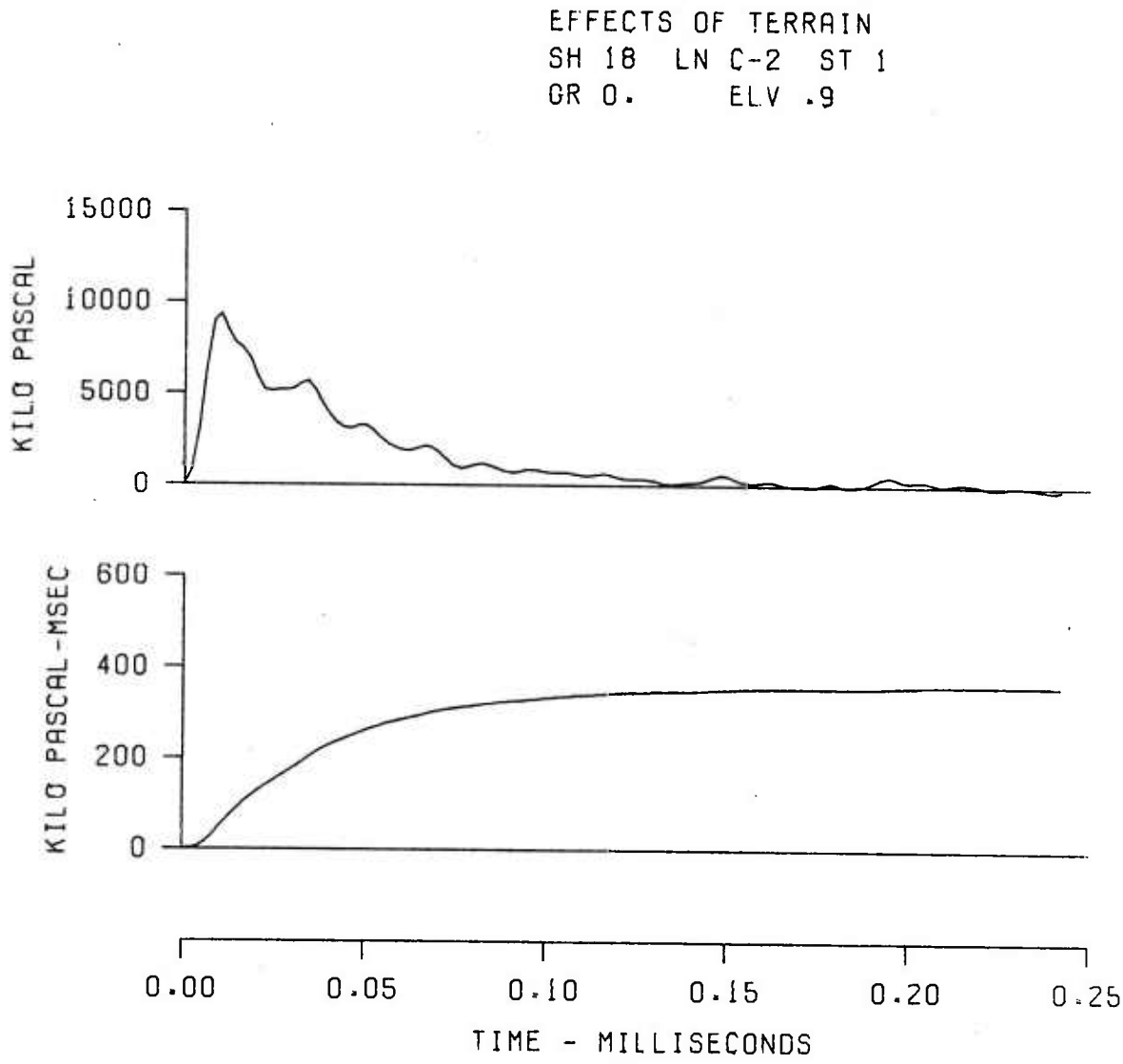

Figure A-5. Pressure-Time Traces for Lines C-2, C-3 and C-5

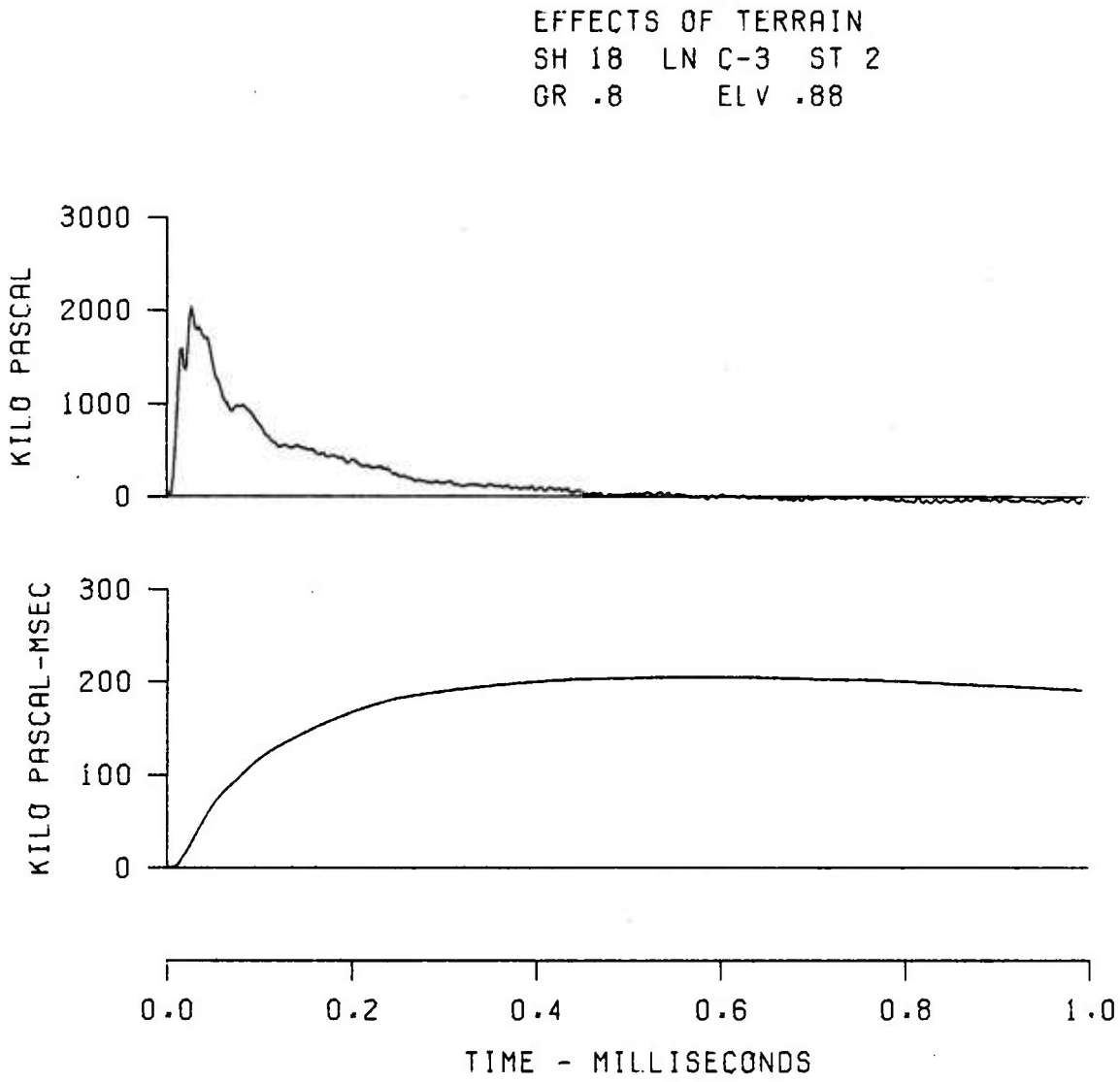

Figure A-5 (Cont). Pressure-Time Traces for Lines C-2, C-3 and C-5

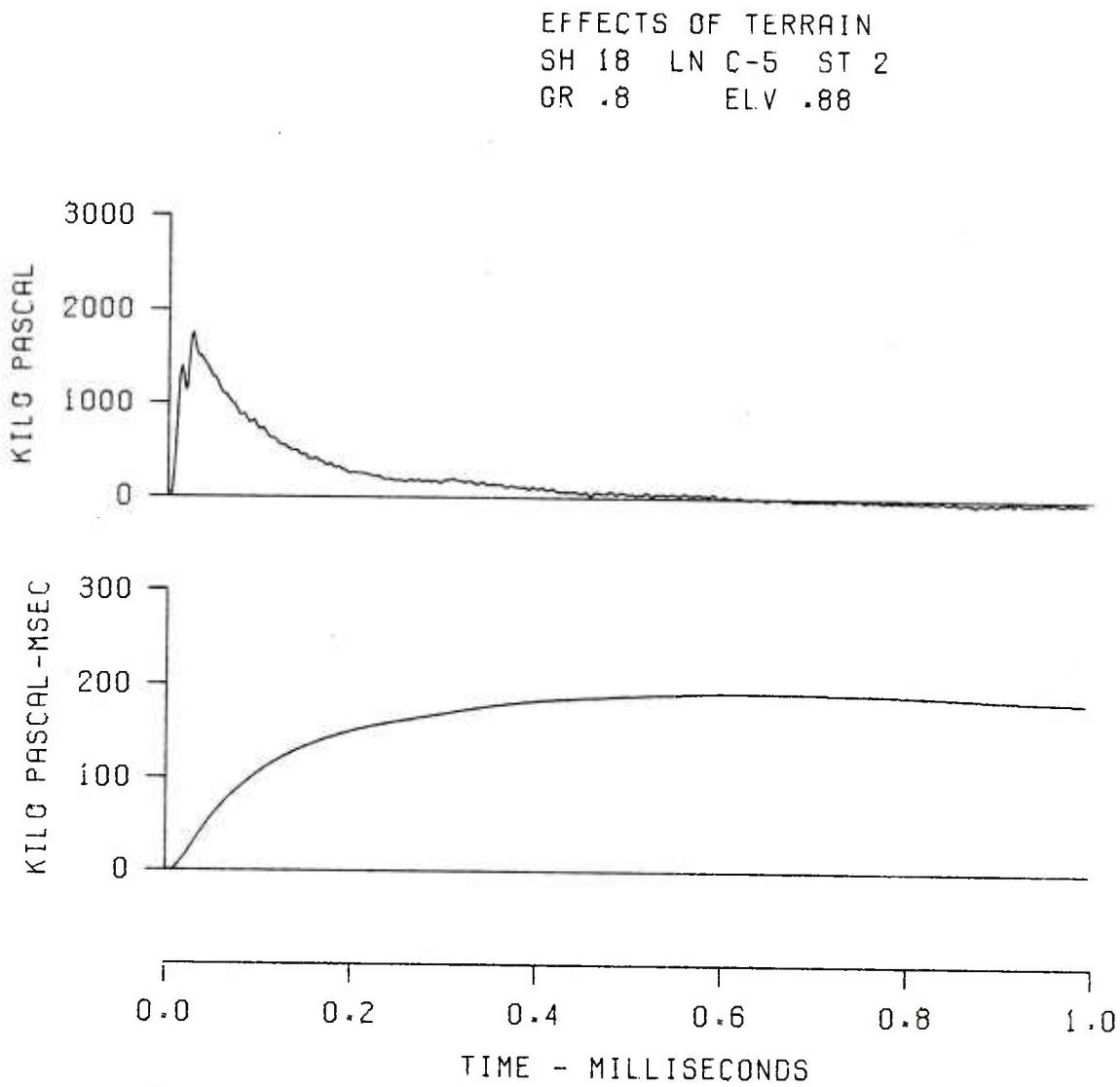

Figure A-5 (Cont). Pressure-Time Traces for Lines C-2, C-3 and C-5

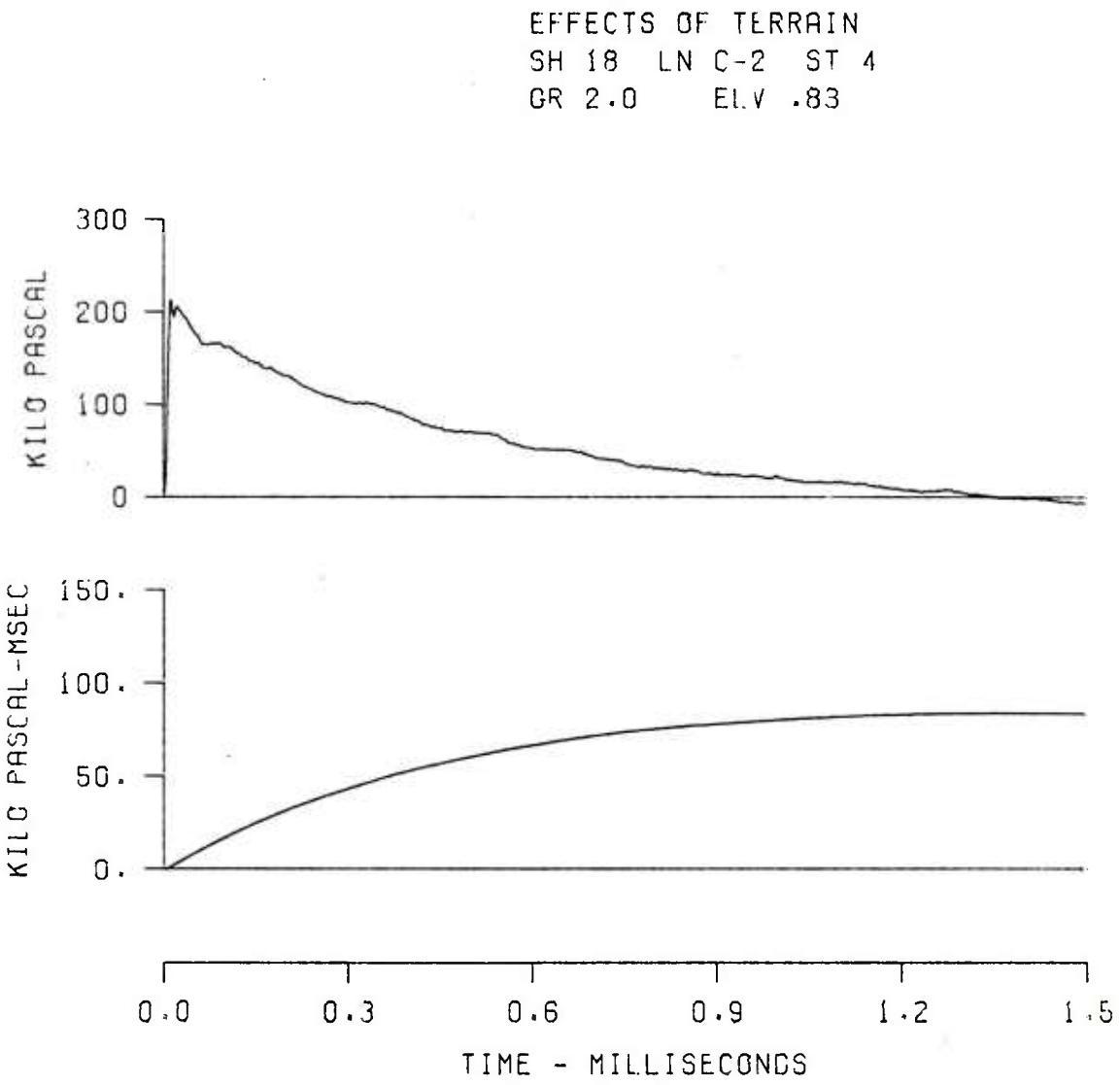

Figure A-5 (Cont). Pressure-Time Traces for Lines C-2, C-3 and C-5

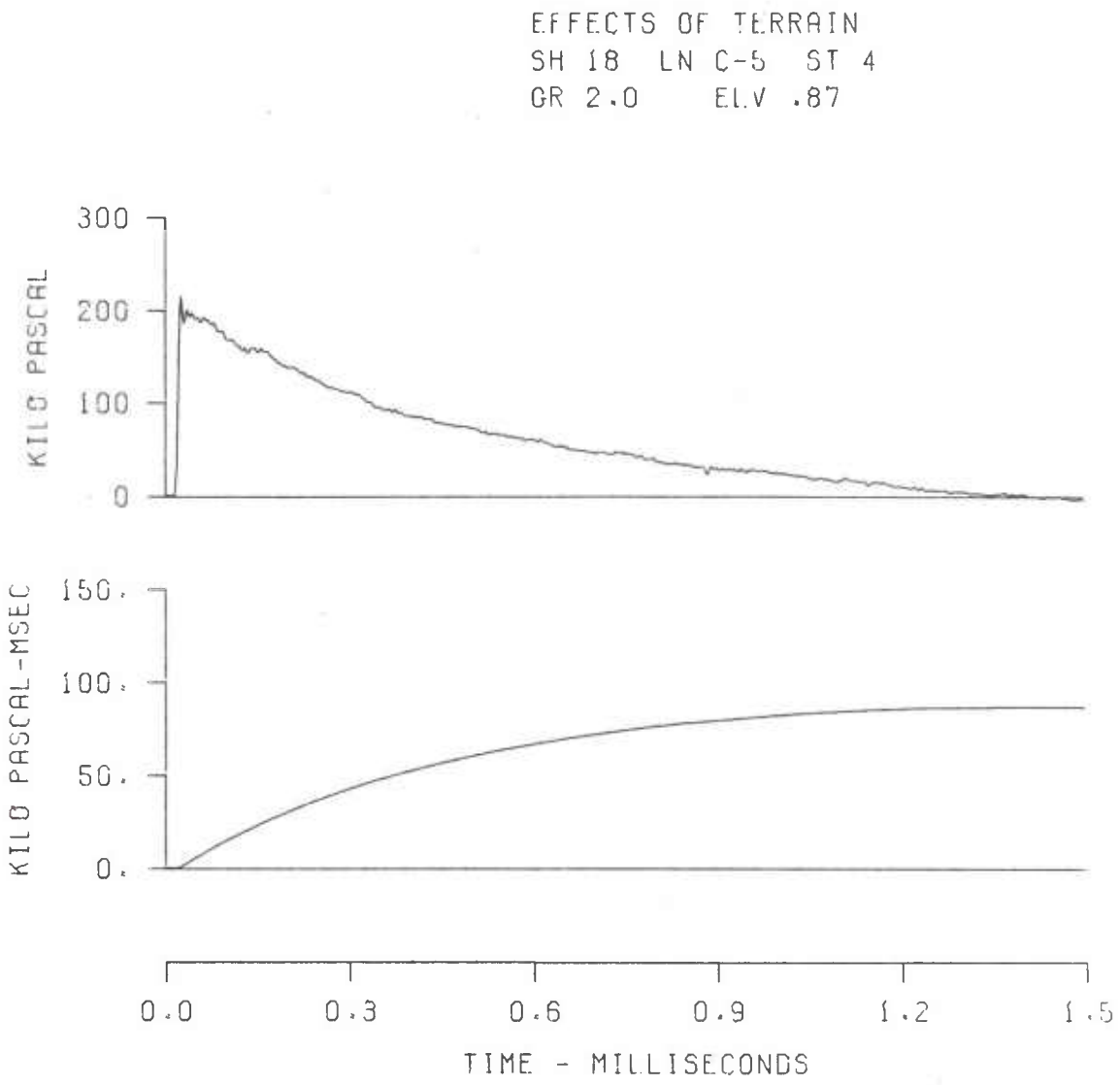

Figure A-5 (Cont). Pressure-Time Traces for Lines C-2, C-3 and C-5

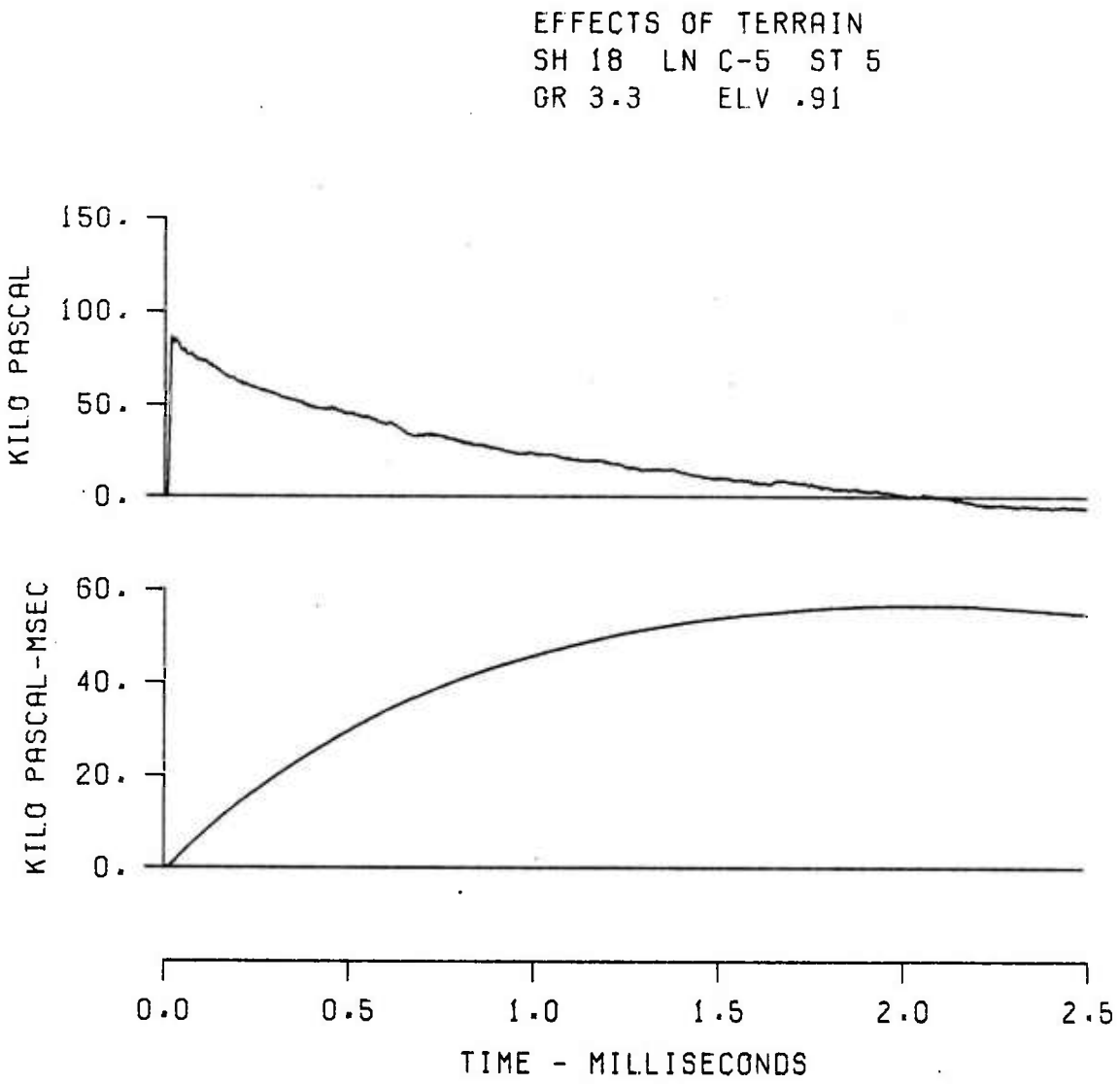

Figure A-5 (Cont). Pressure-Time Traces for Lines C-2, C-3 and C-5

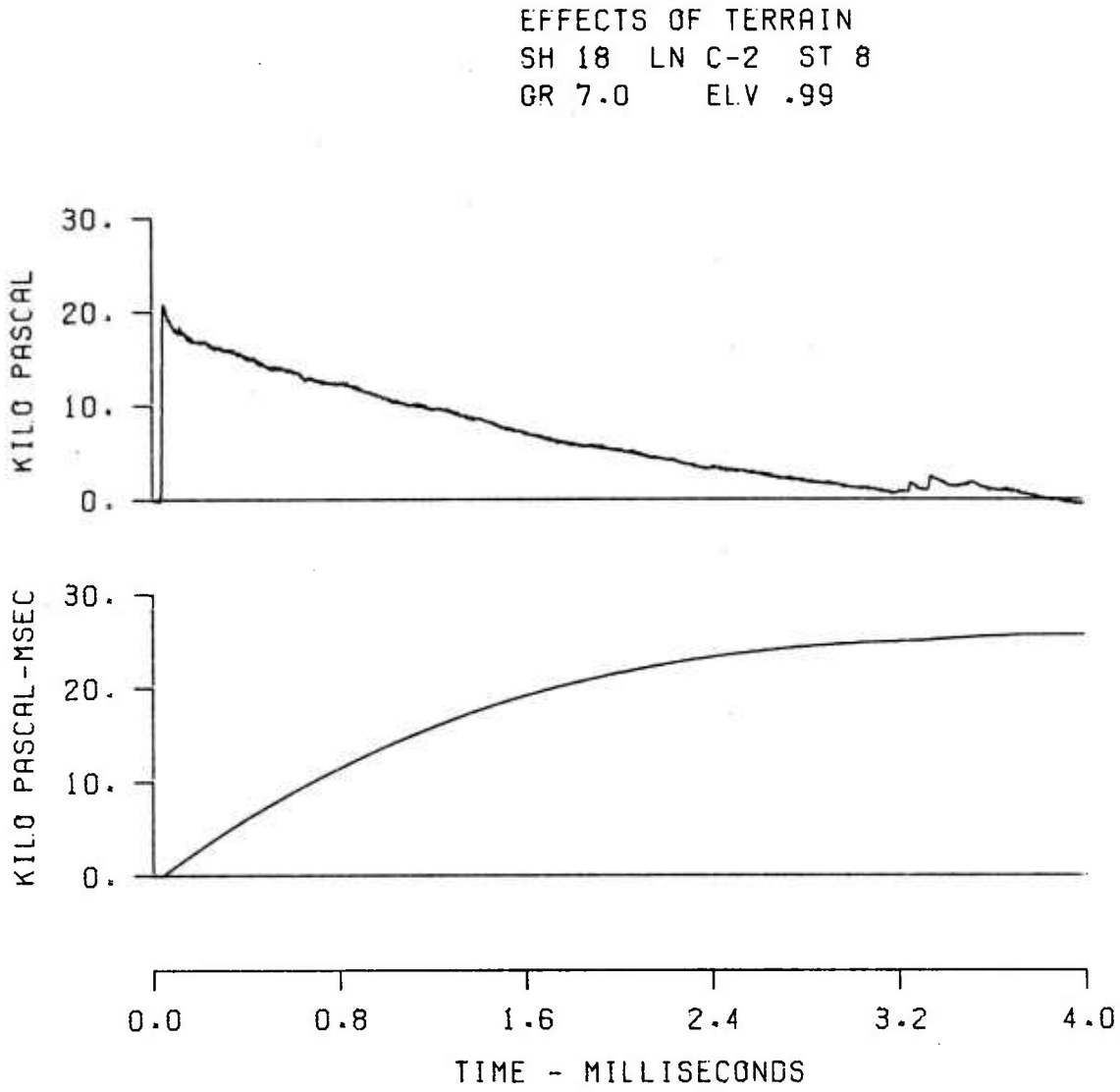

Figure A-5 (Cont). Pressure-Time Traces for Lines C-2, C-3 and C-5

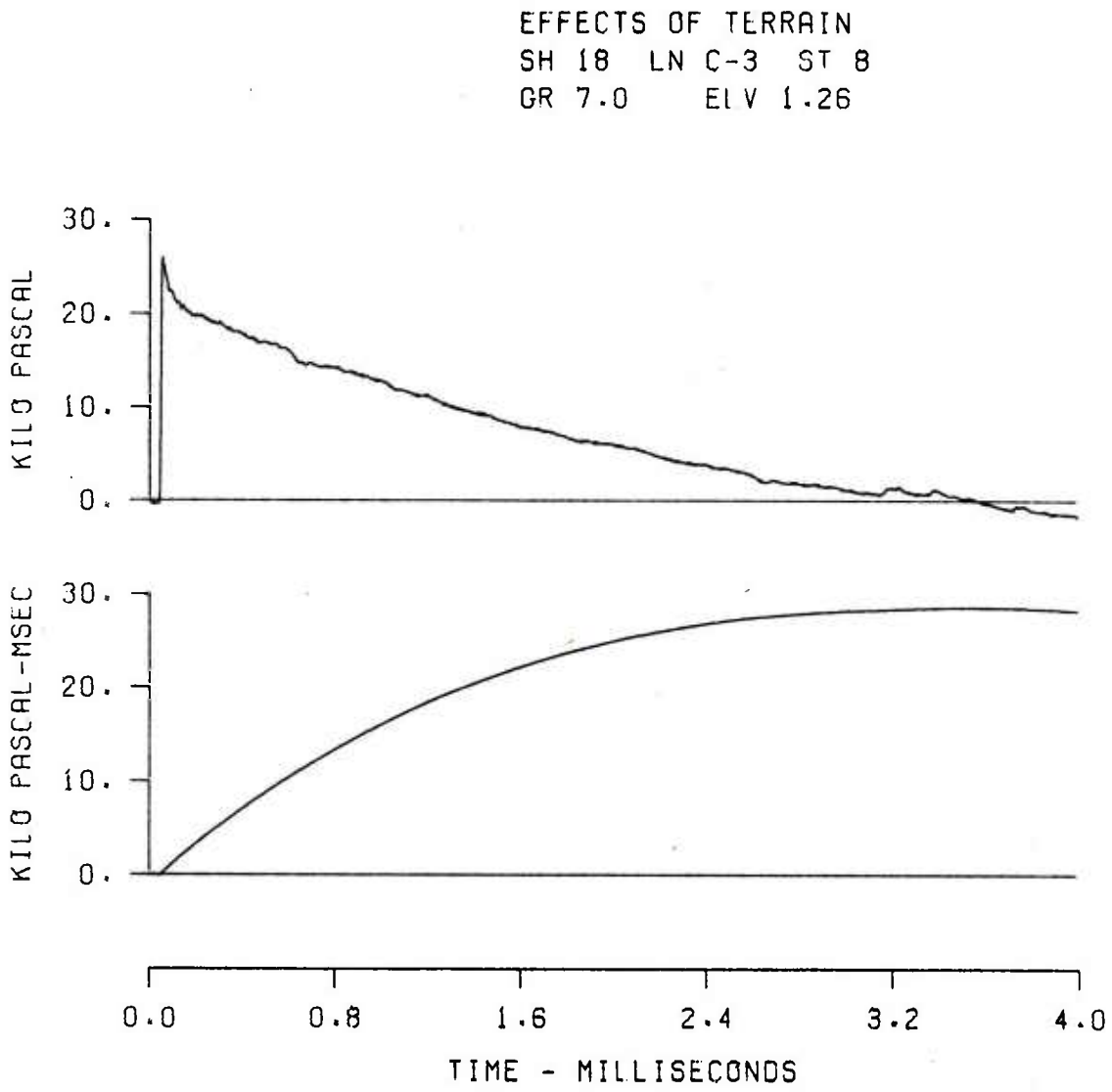

Figure A-5 (Cont). Pressure-Time Traces for Lines C-2, C-3 and C-5

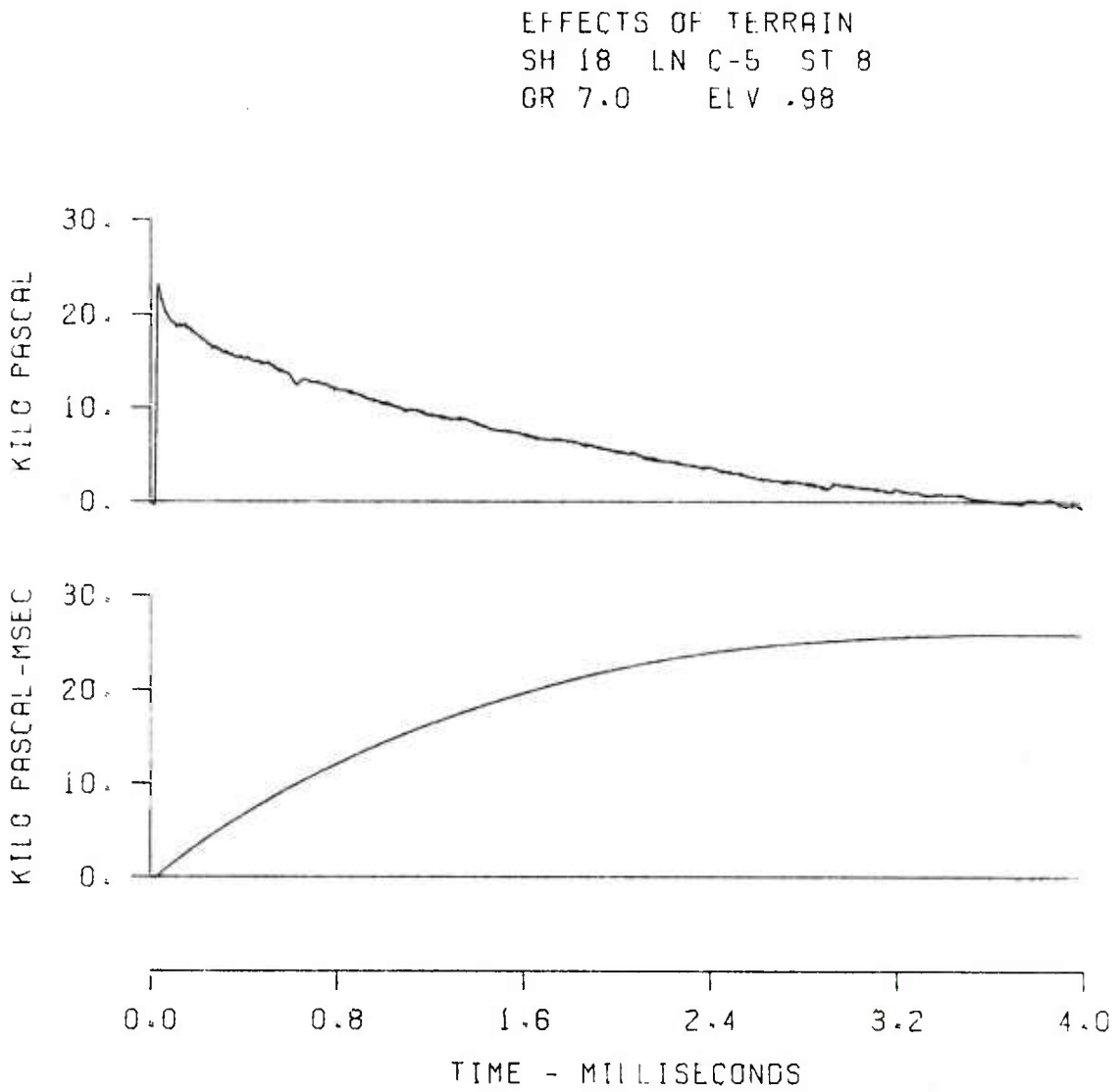

Figure A-5 (Cont). Pressure-Time Traces for Lines C-2, C-3 and C-5

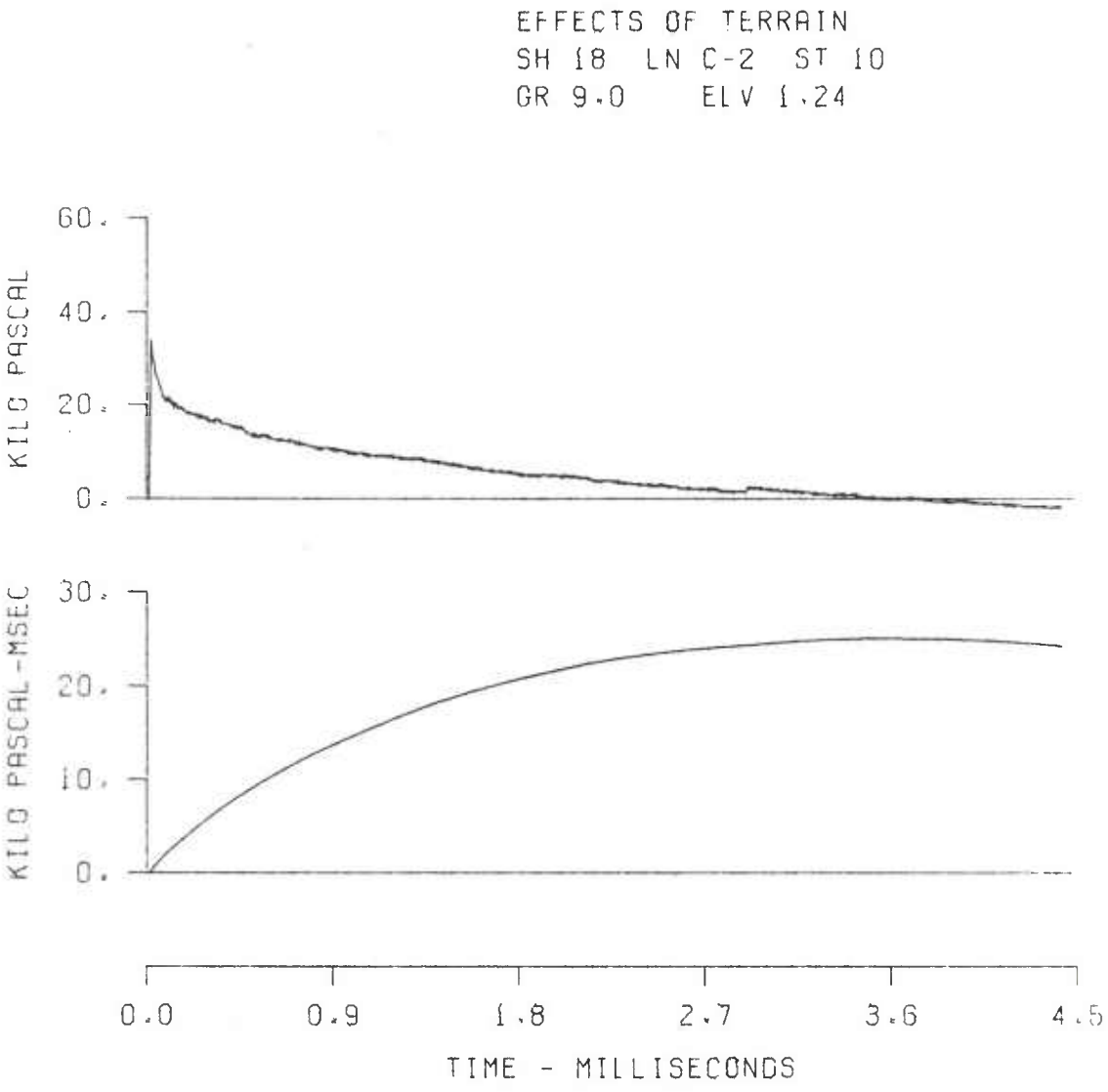

Figure A-5 (Cont). Pressure-Time Traces for Lines C-2, C-3 and C-5

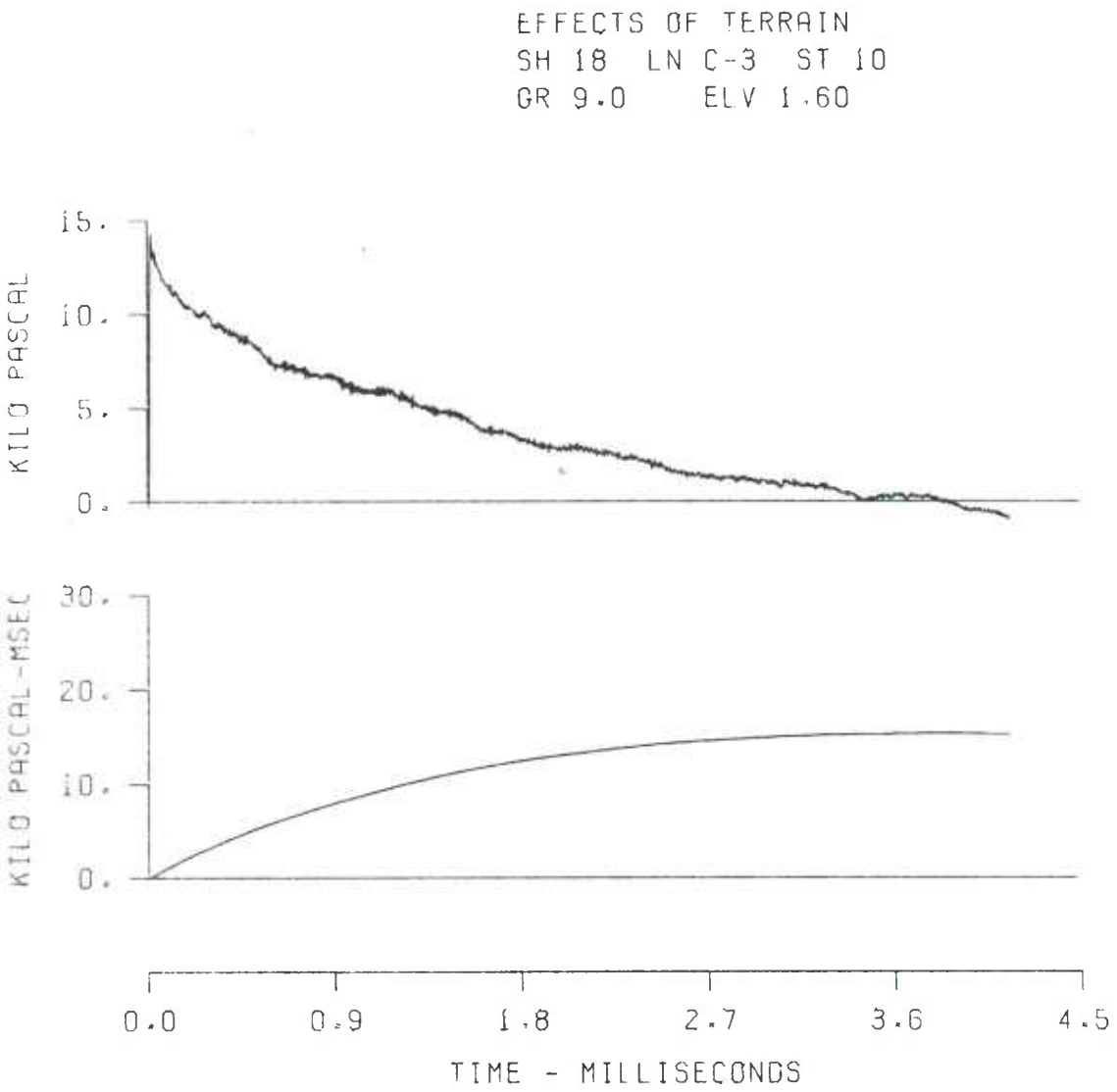

Figure A-5 (Cont). Pressure-Time Traces for Lines C-2, C-3 and C-5

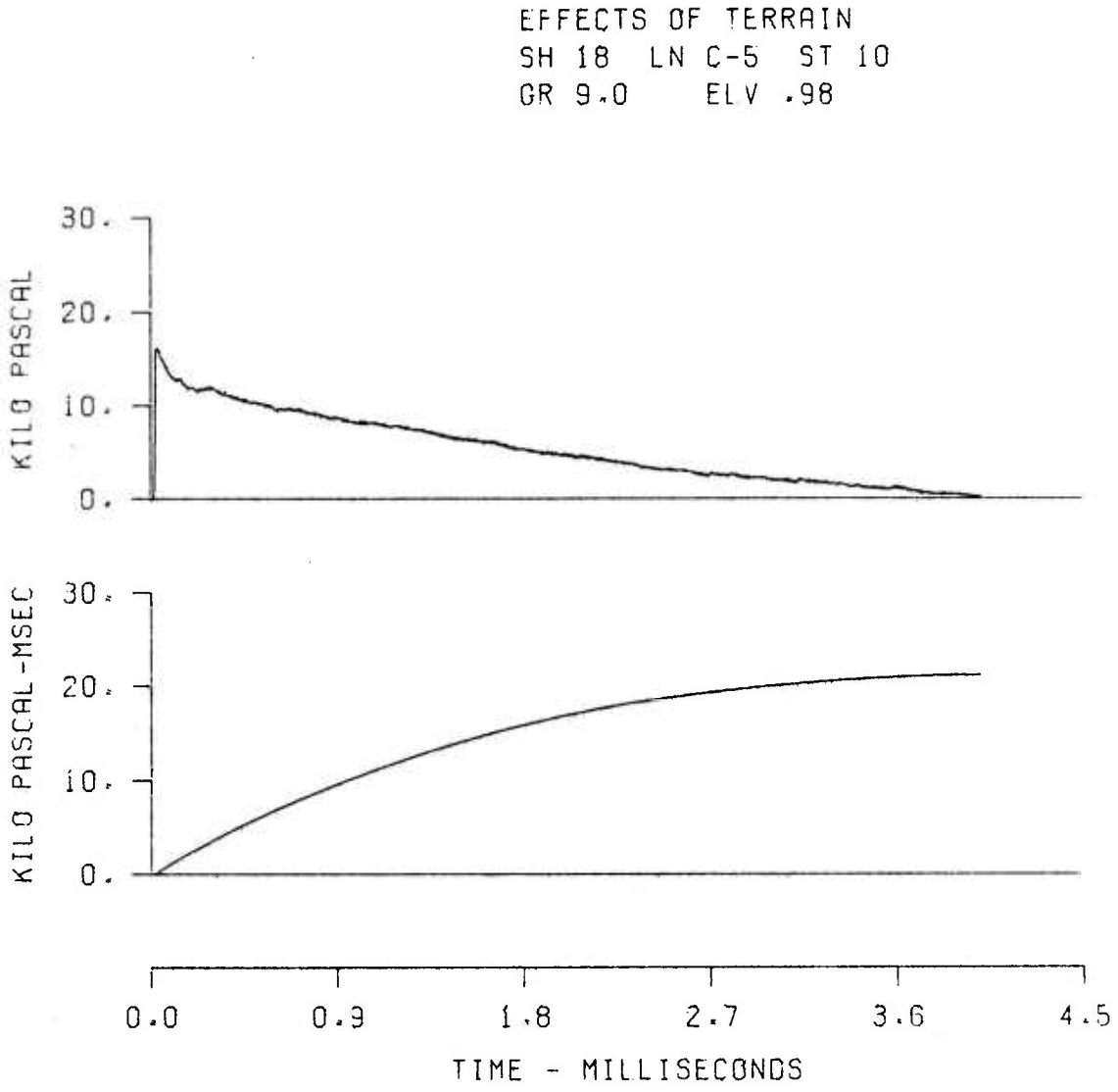

Figure A-5 (Cont). Pressure-Time Traces for Lines C-2, C-3 and C-5

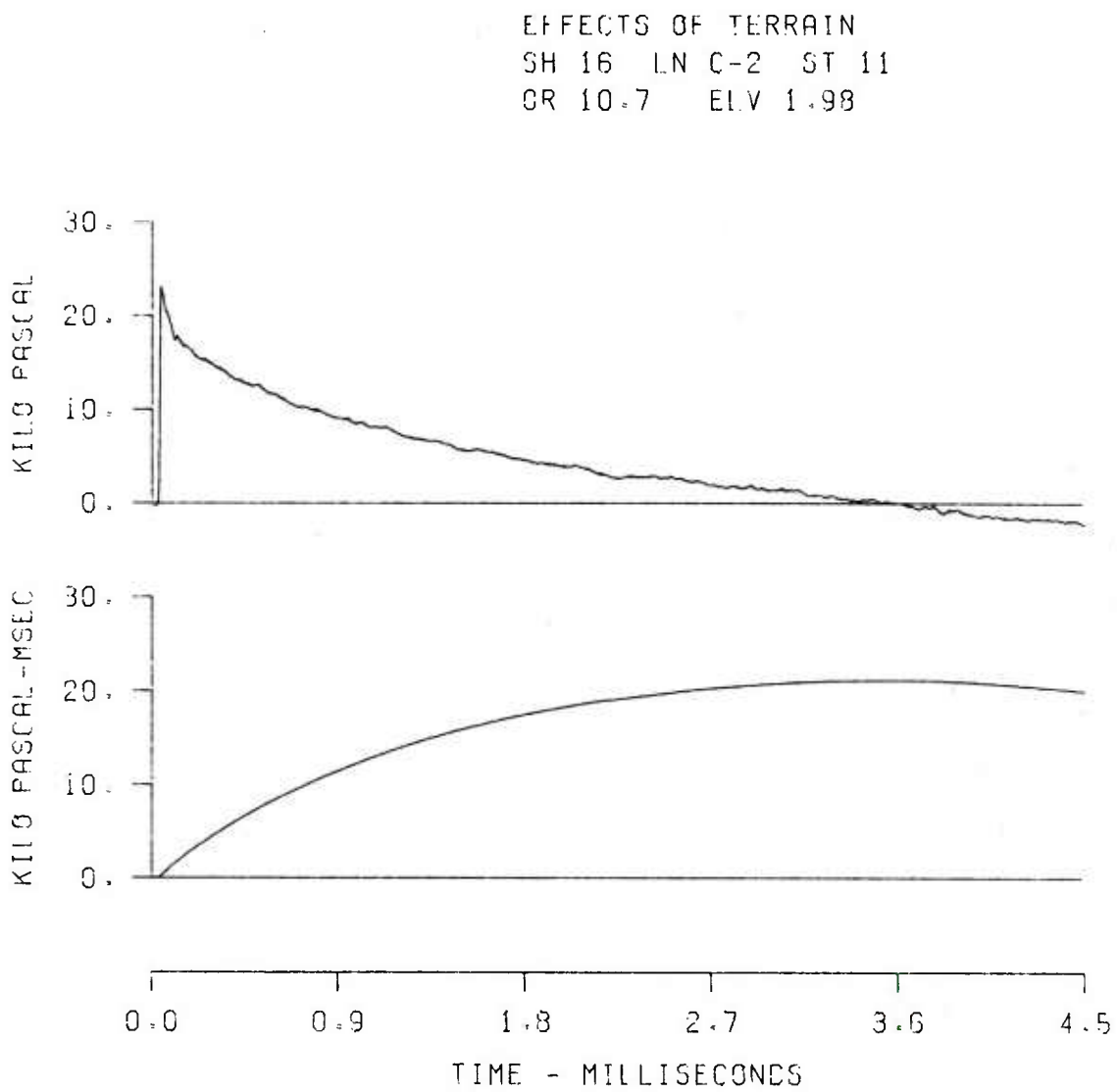

Figure A-5 (Cont). Pressure-Time Traces for Lines C-2, C-3 and C-5

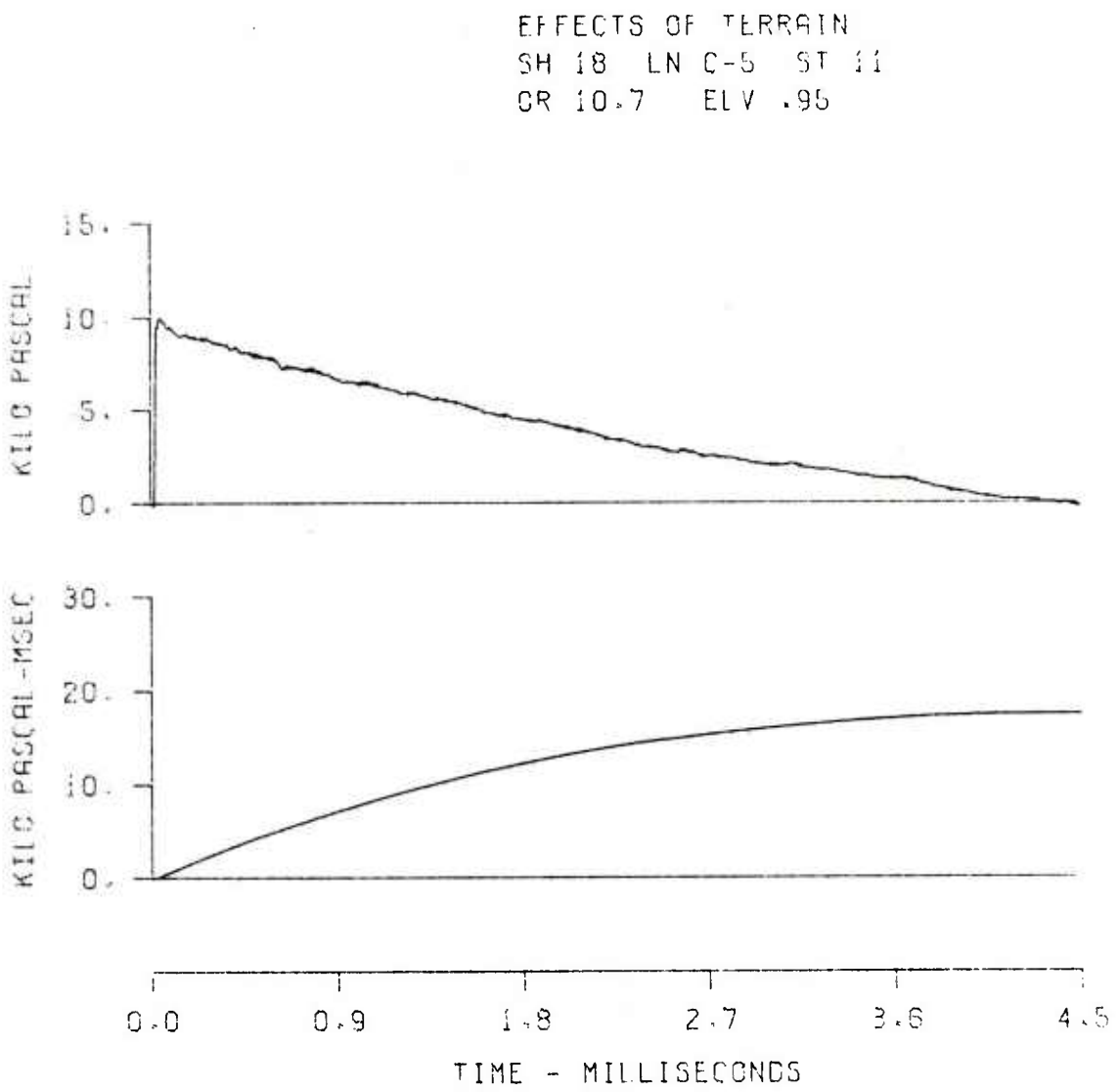

Figure A-5 (Cont). Pressure-Time Traces for Lines C-2, C-3 and C-5

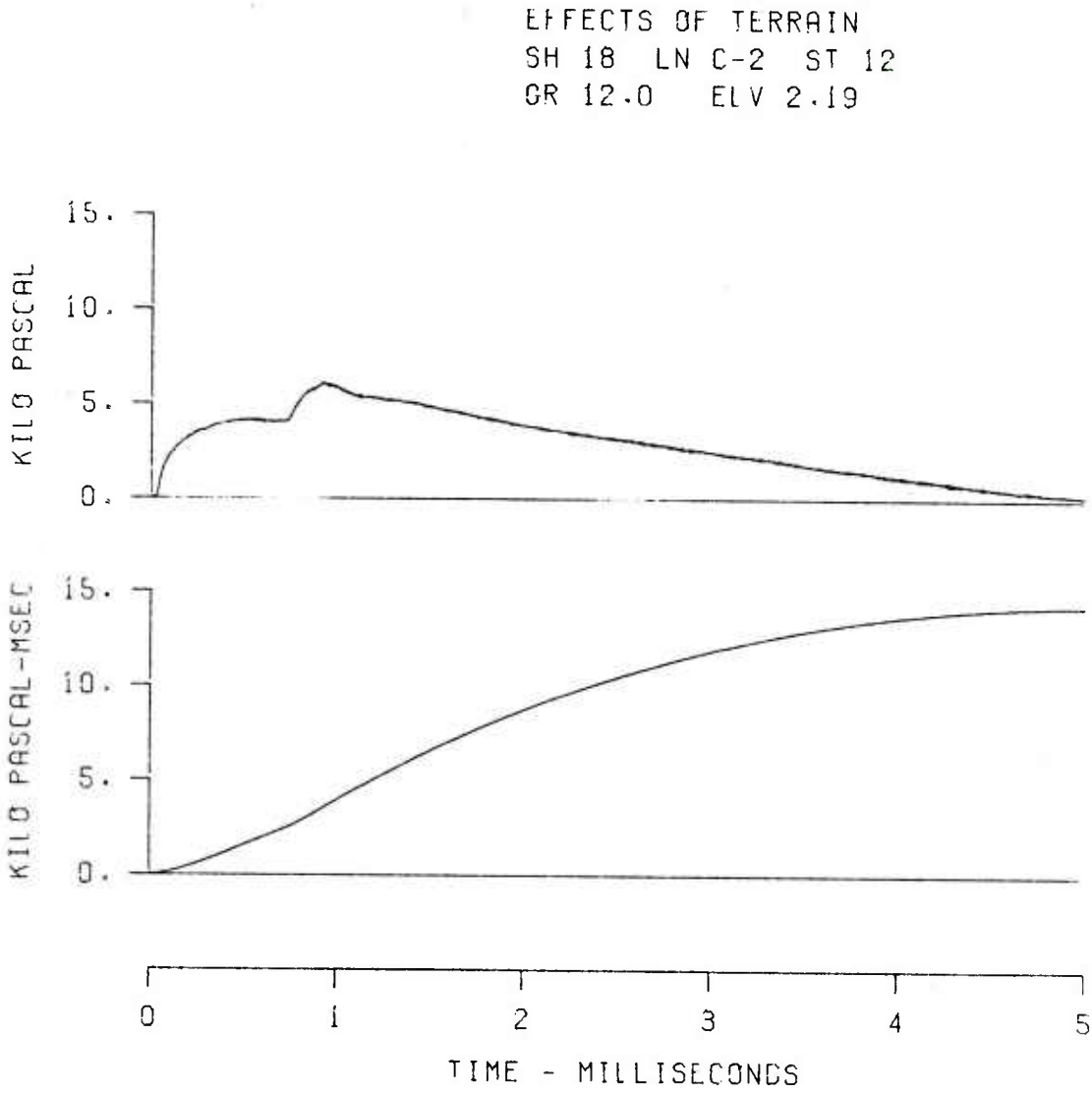

Figure A-5 (Cont). Pressure-Time Traces for Lines C-2, C-3 and C-5

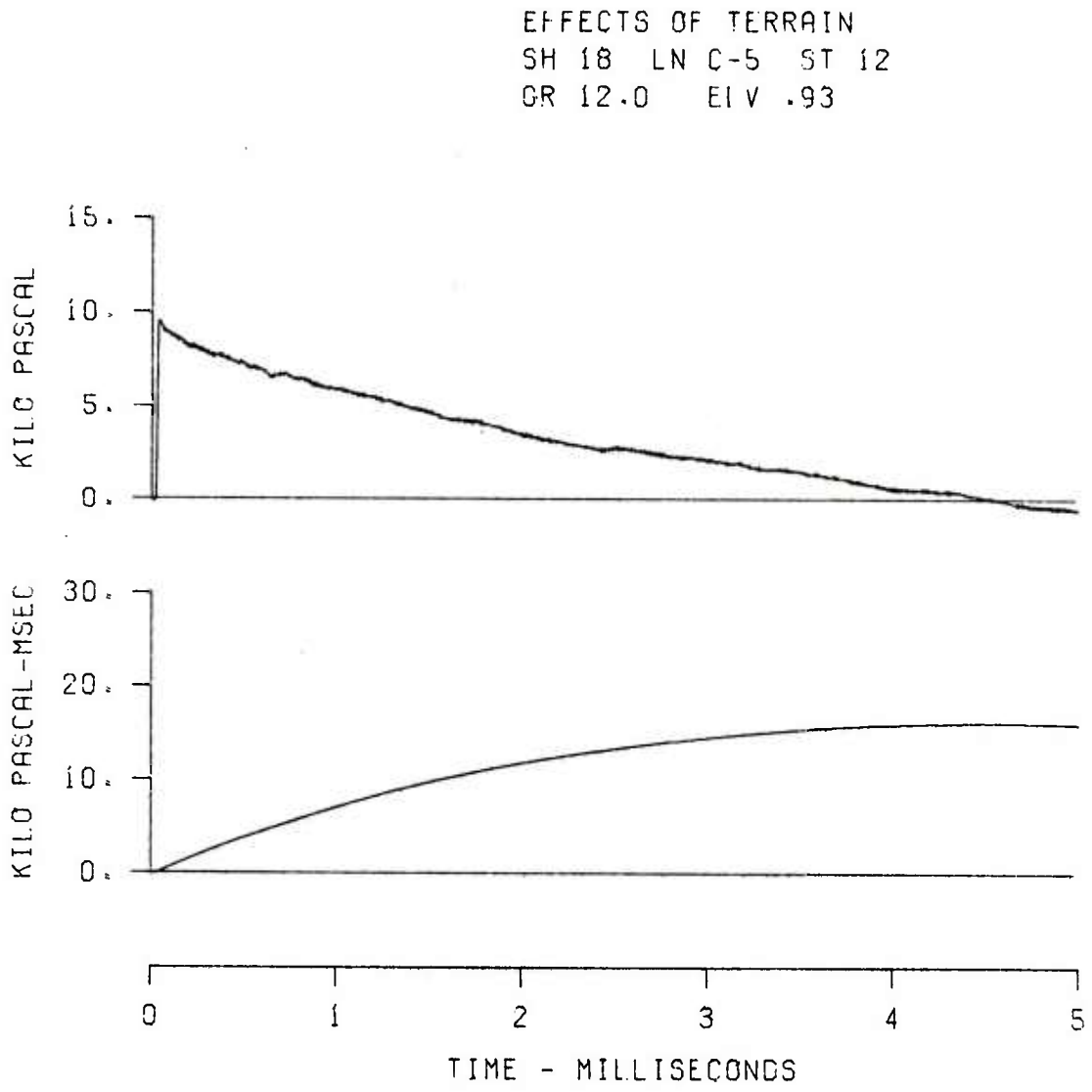

Figure A-5 (Cont). Pressure-Time Traces for Lines C-2, C-3 and C-5

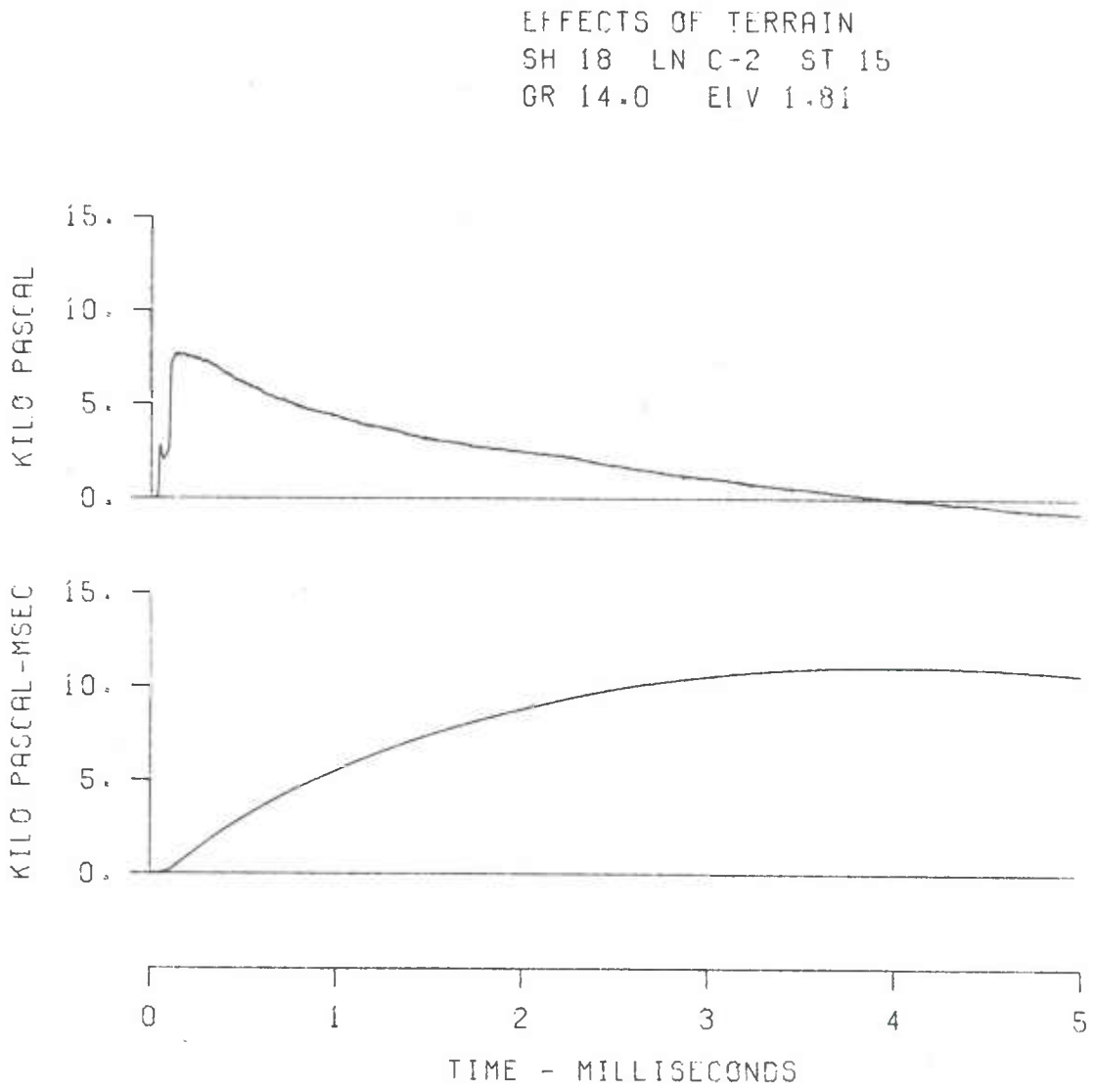

Figure A-5 (Cont). Pressure-Time Traces for Lines C-2, C-3 and C-5

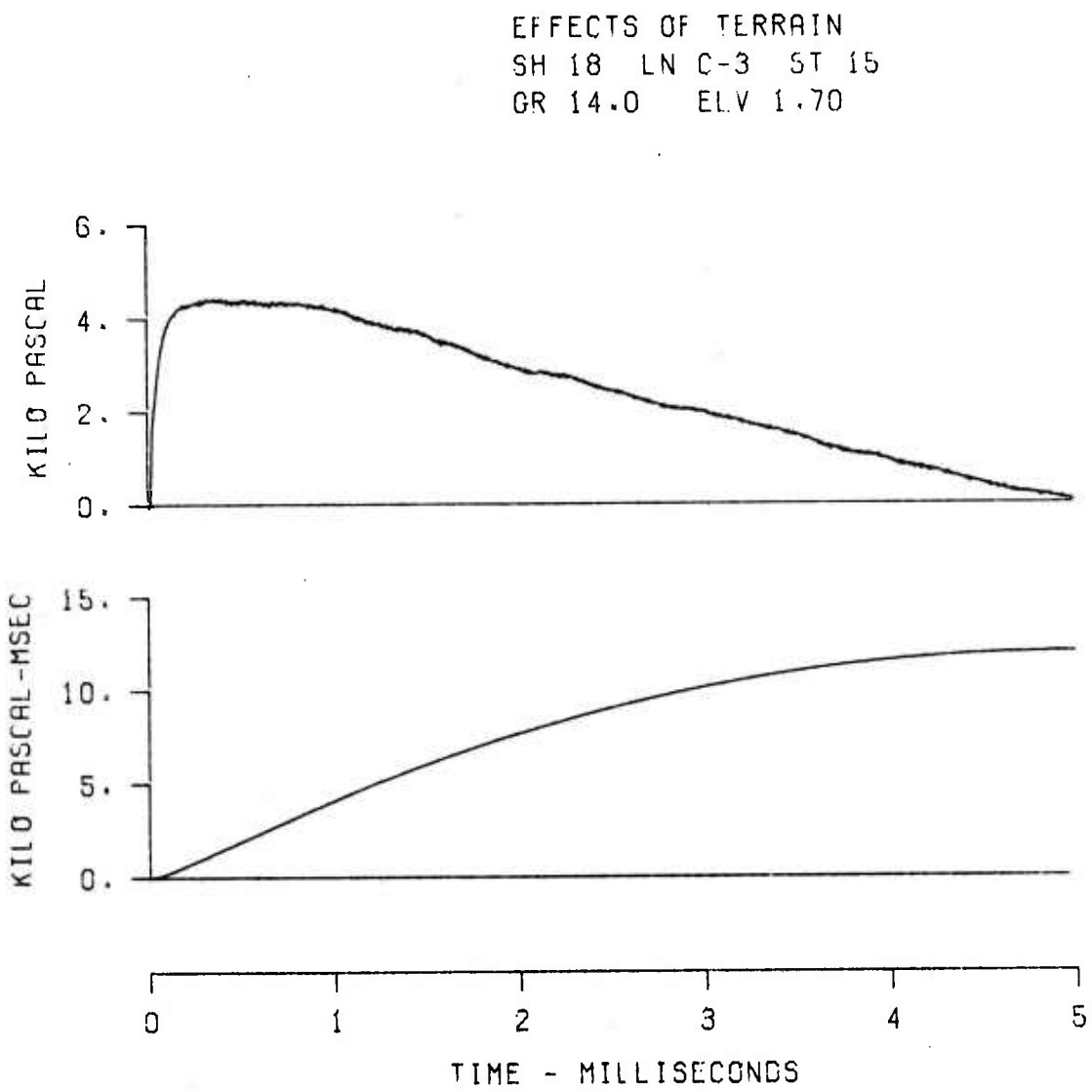

Figure A-5 (Cont). Pressure-Time Traces for Lines C-2, C-3 and C-5

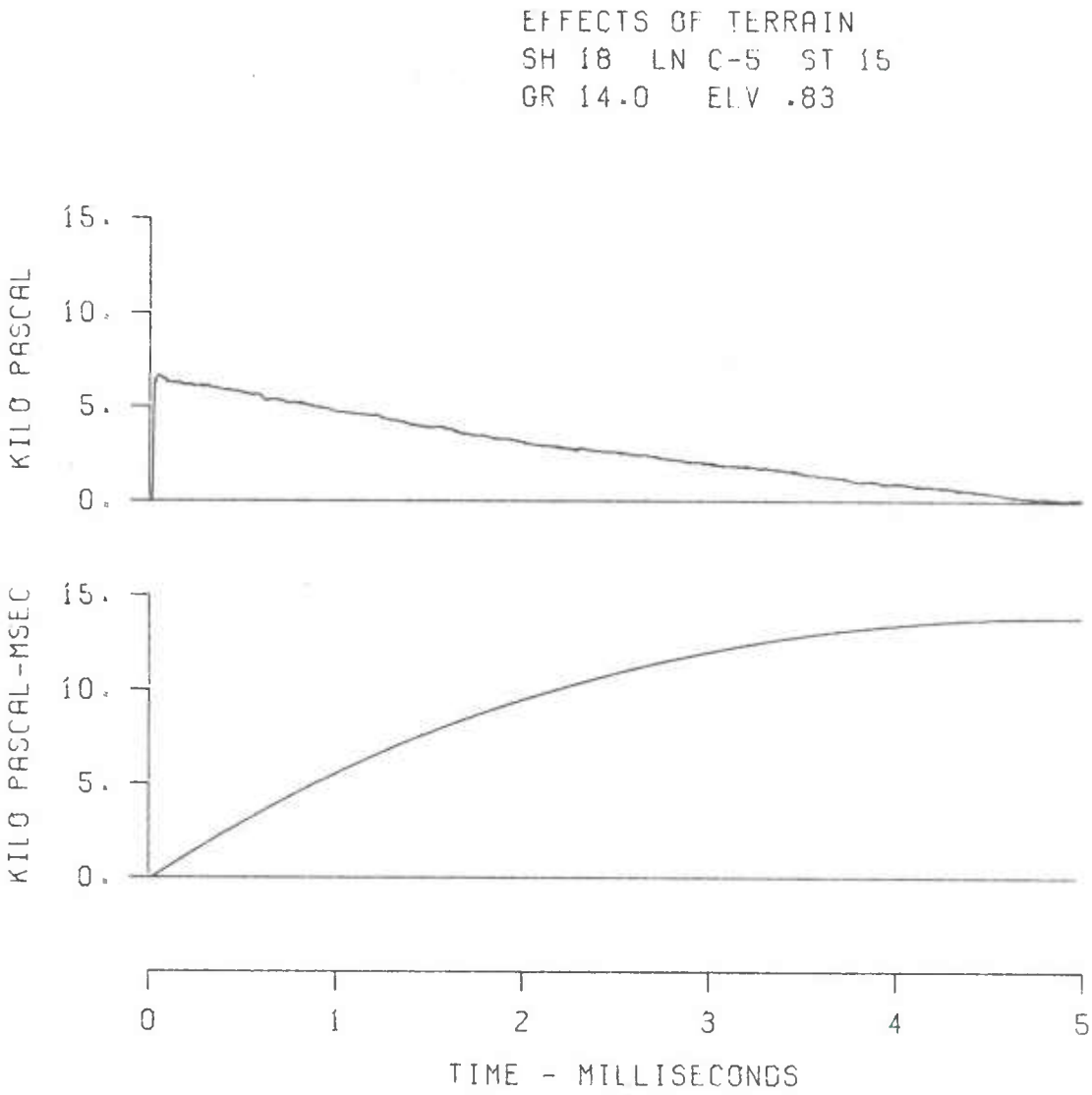

Figure A-5 (Cont). Pressure-Time Traces for Lines C-2, C-3 and C-5

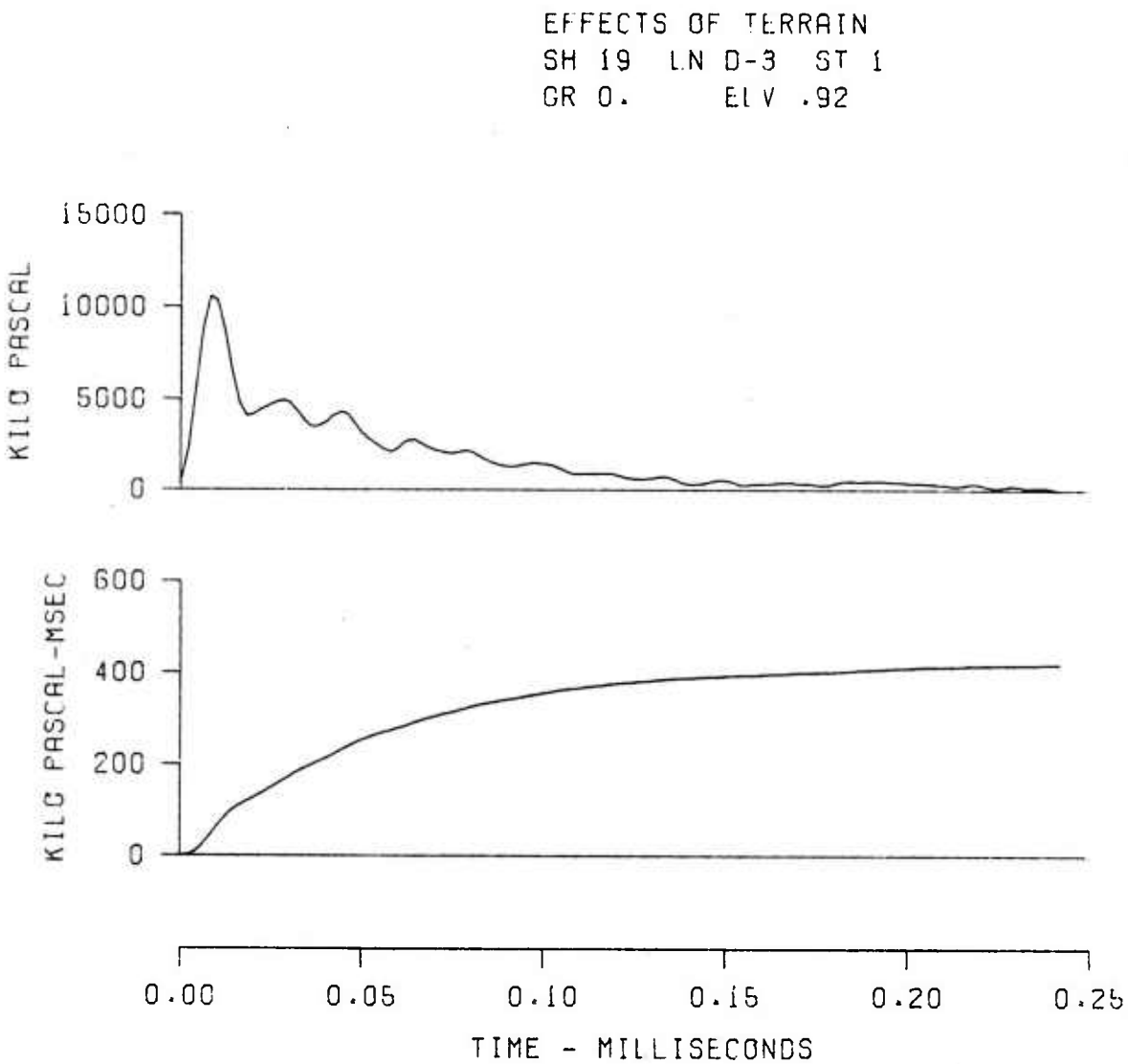

Figure A-6. Pressure-Time Traces for Lines D-2 and D-3

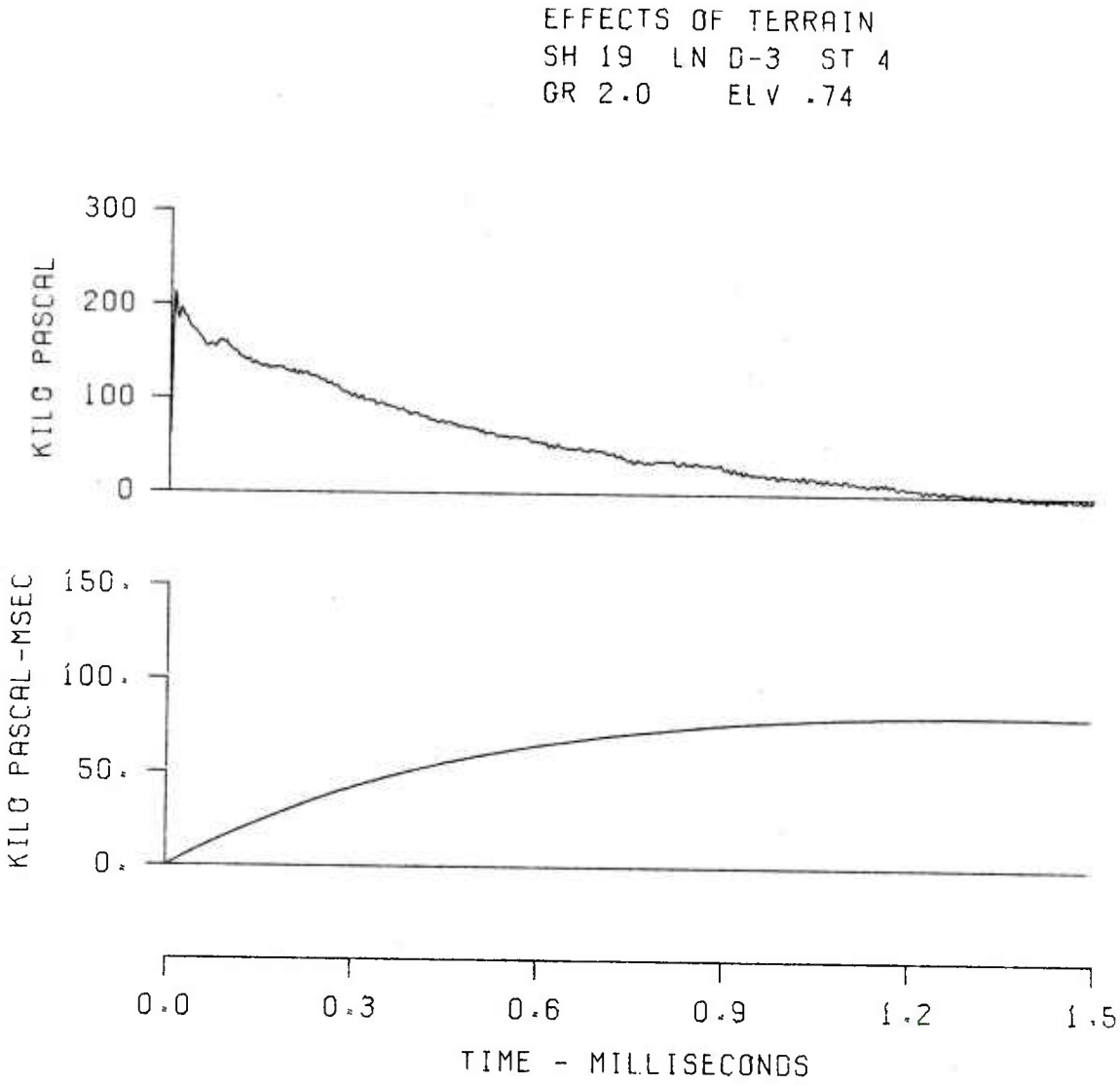

Figure A-6 (Cont). Pressure-Time Traces for Lines D-2 and D-3

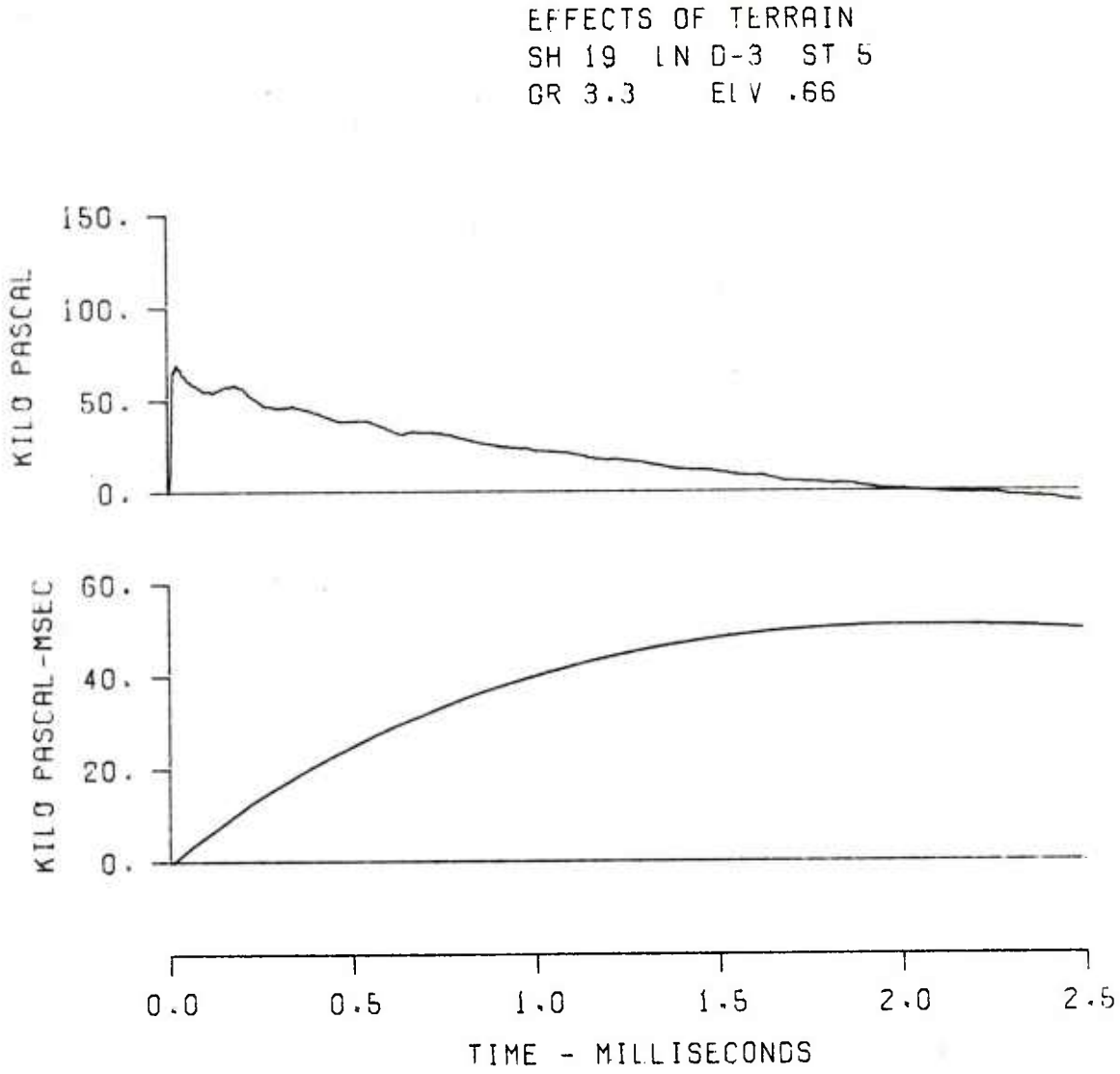

Figure A-6 (Cont). Pressure-Time Traces for Lines D-2 and D-3

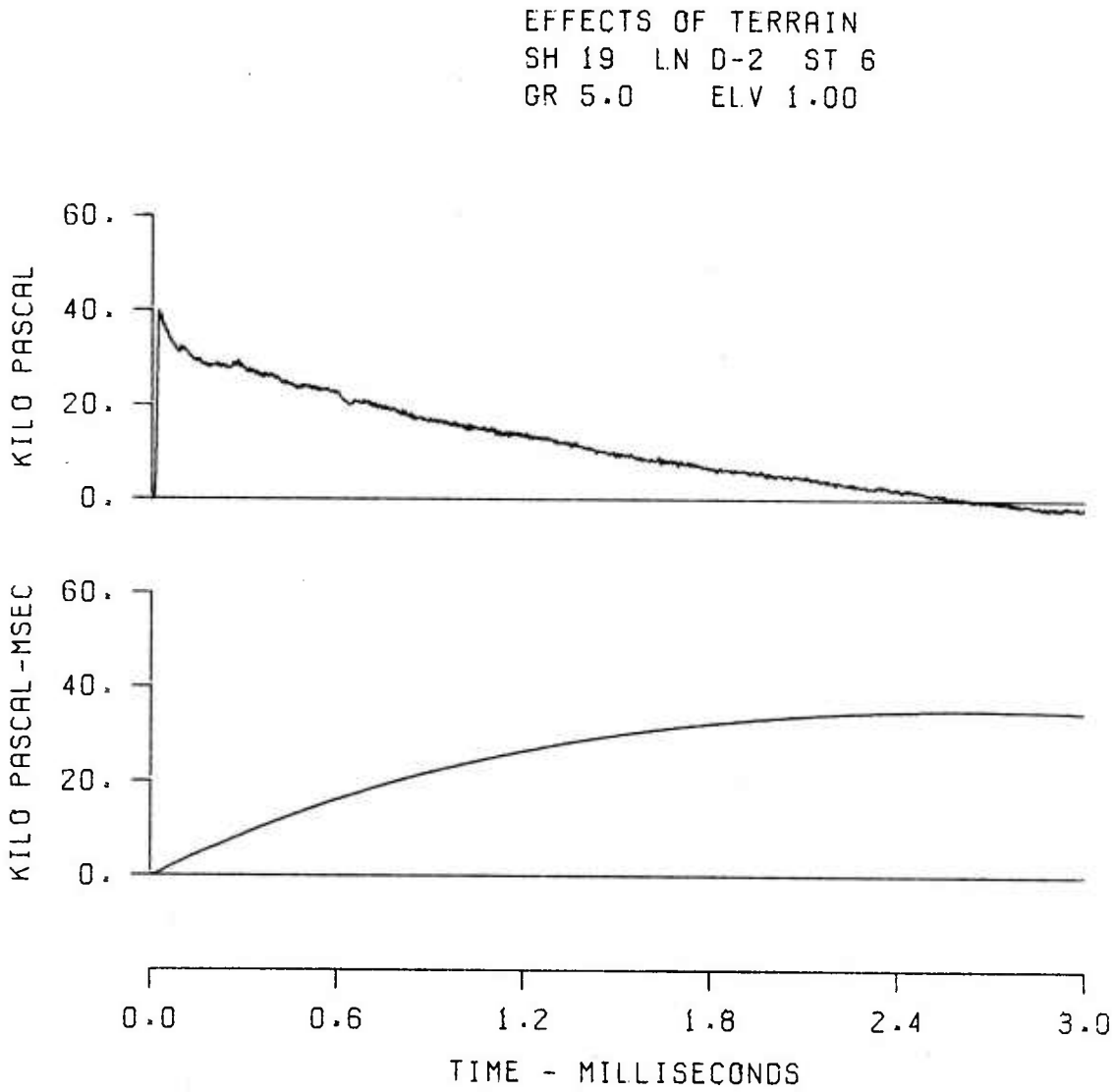

Figure A-6 (Cont). Pressure-Time Traces for Lines D-2 and D-3

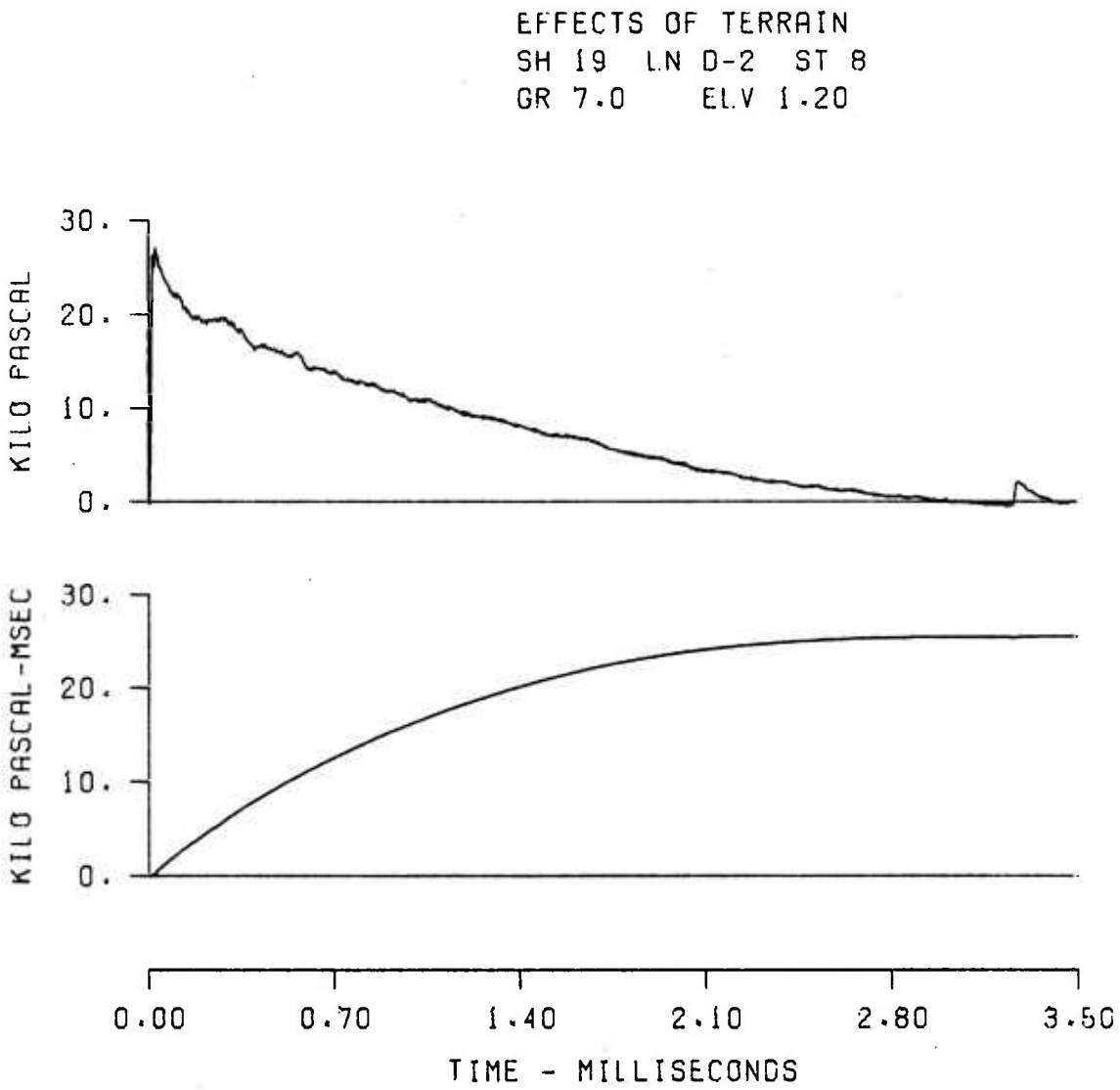

Figure A-6 (Cont). Pressure-Time Traces for Lines D-2 and D-3

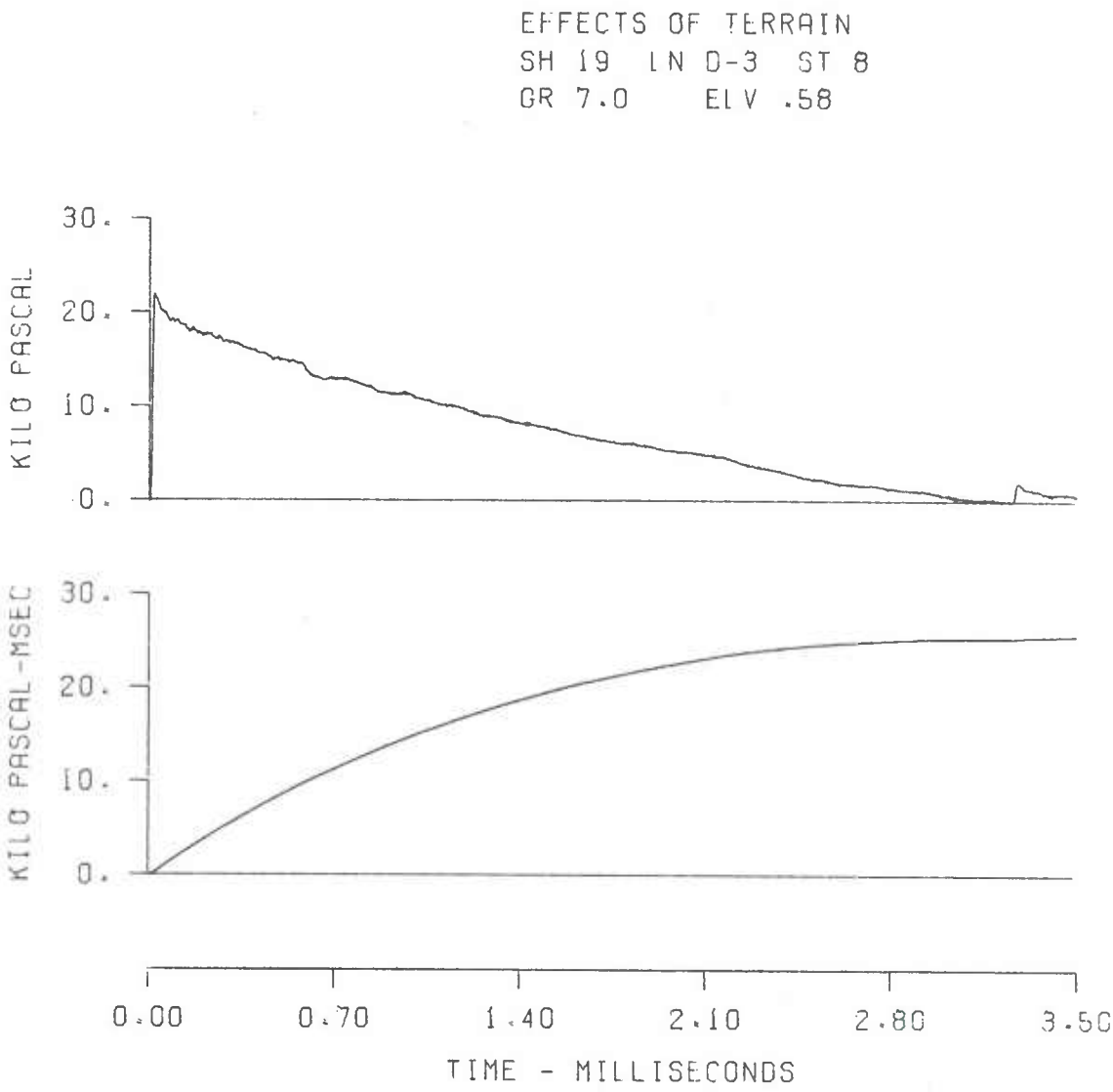

Figure A-6 (Cont). Pressure-Time Traces for Lines D-2 and D-3

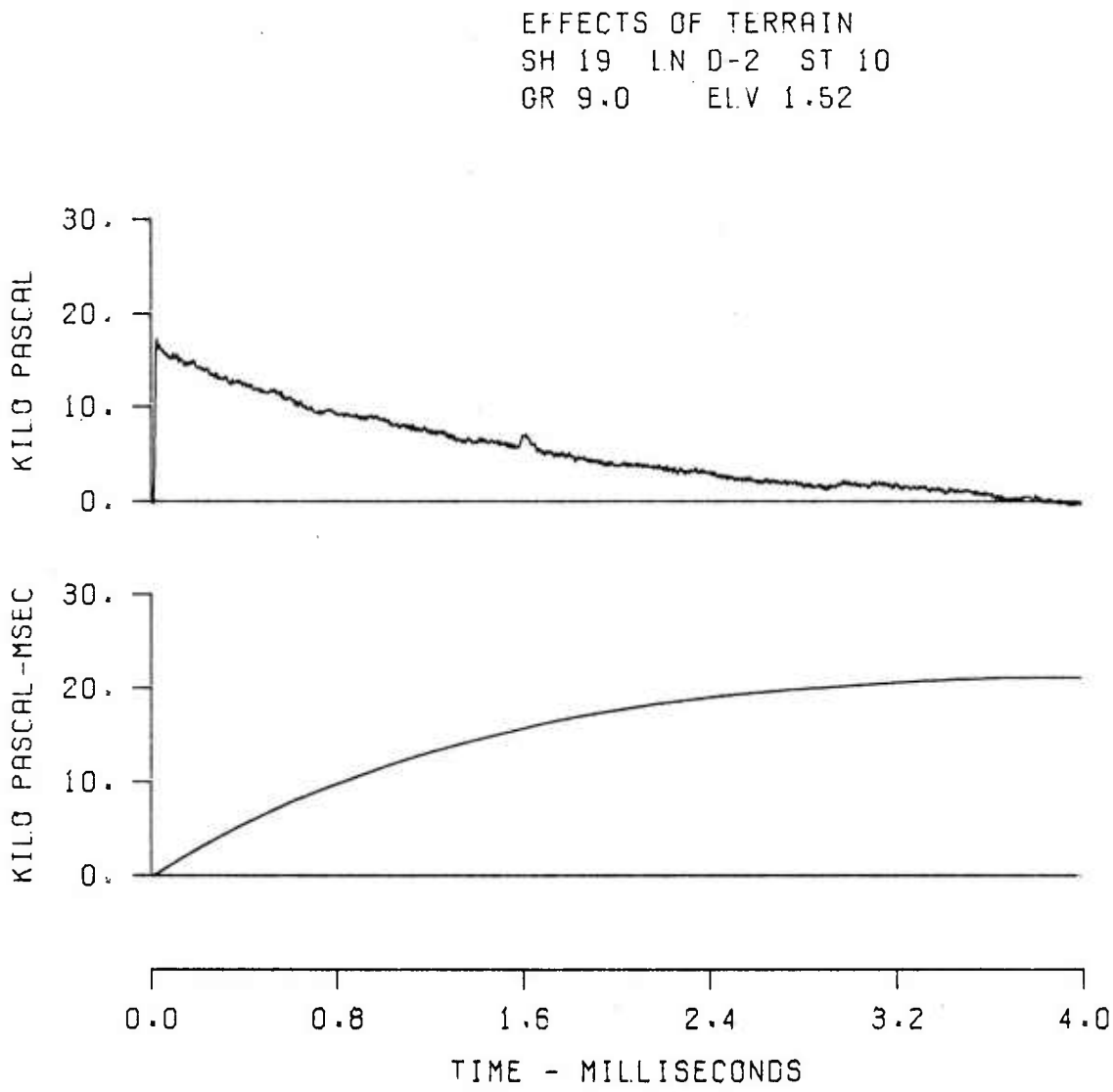

Figure A-6 (Cont). Pressure-Time Traces for Lines D-2 and D-3

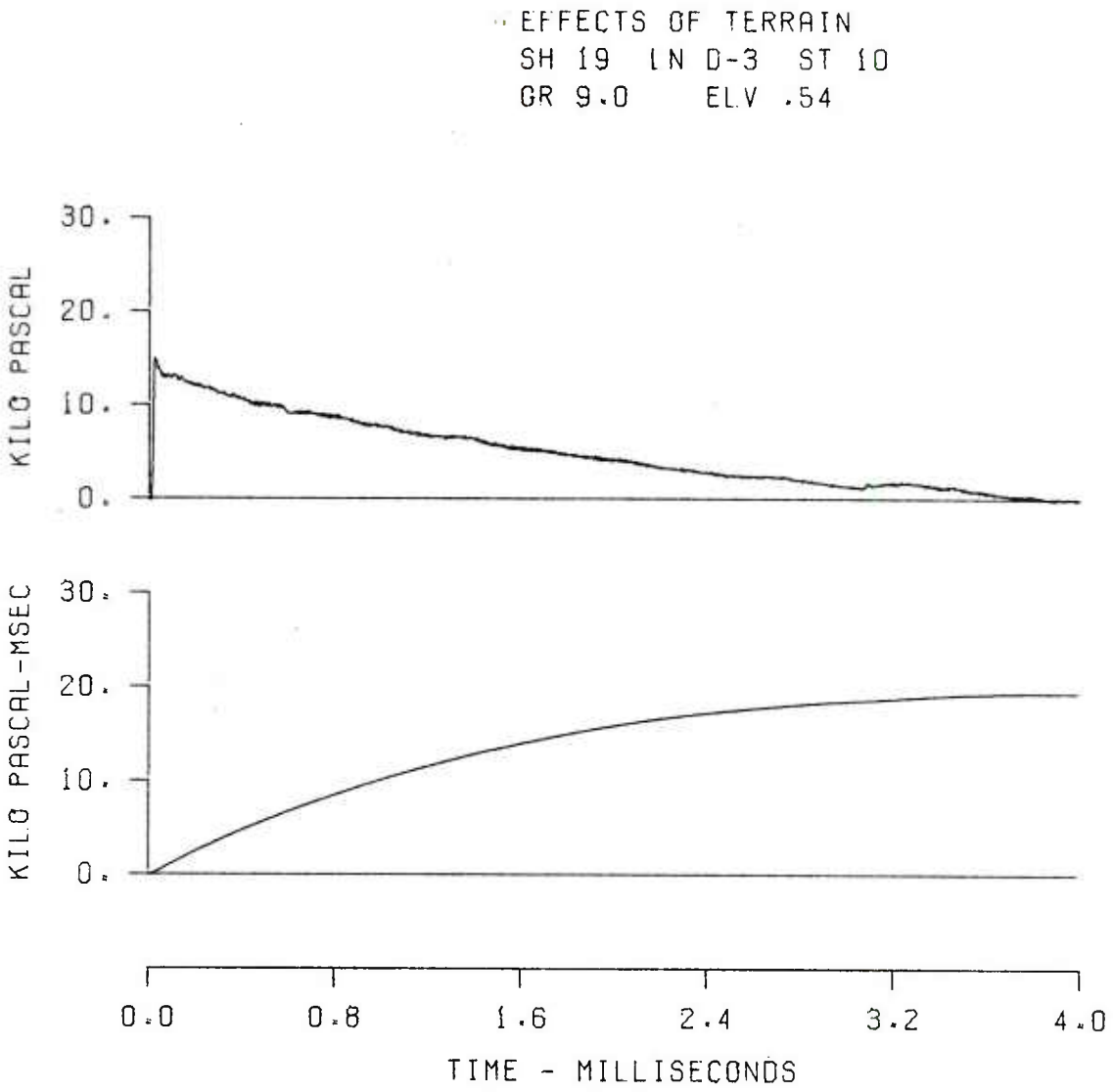

Figure A-6 (Cont). Pressure-Time Traces for Lines D-2 and D-3

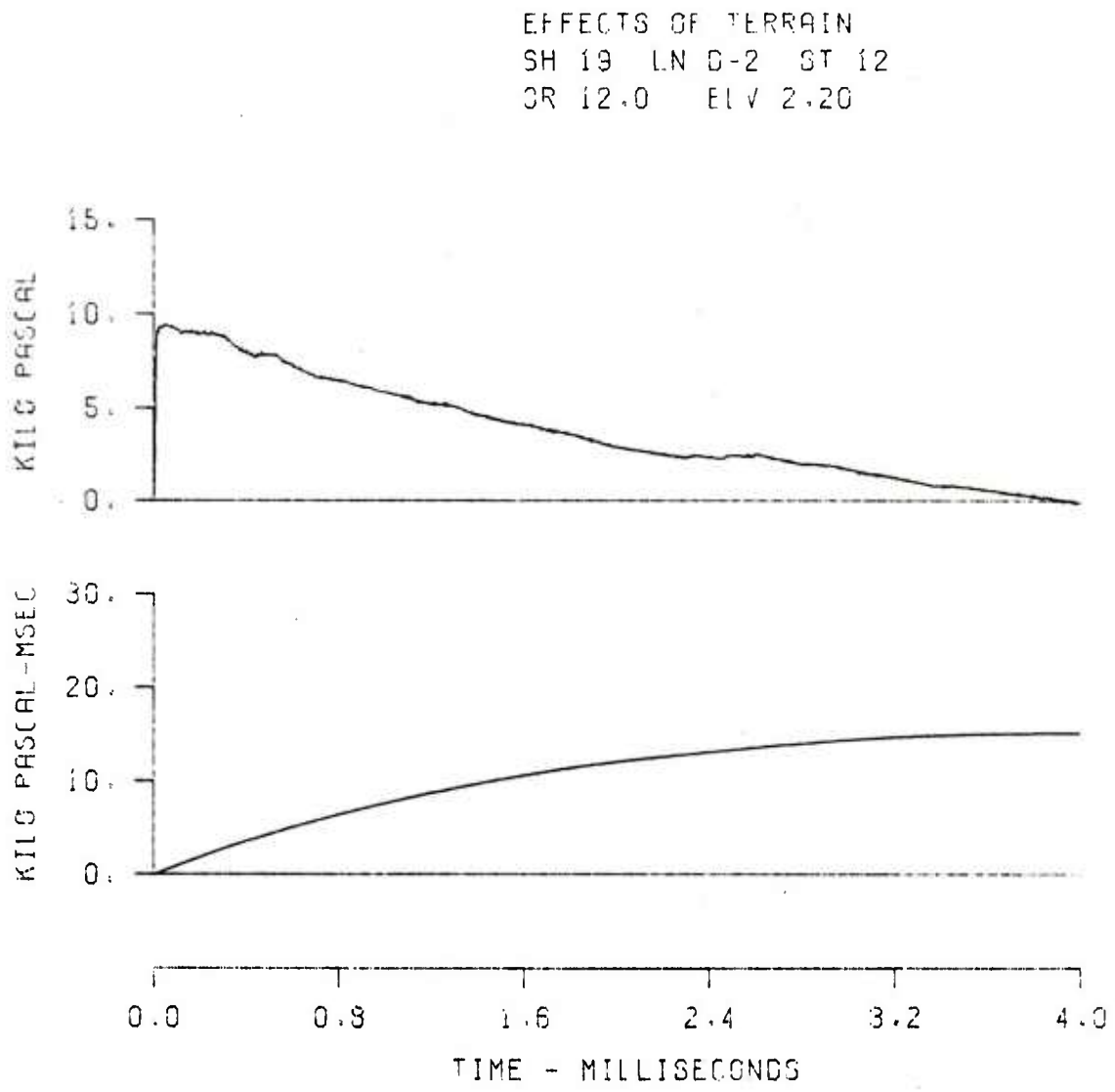

Figure A-6 (Cont). Pressure-Time Traces for Lines D-2 and D-3

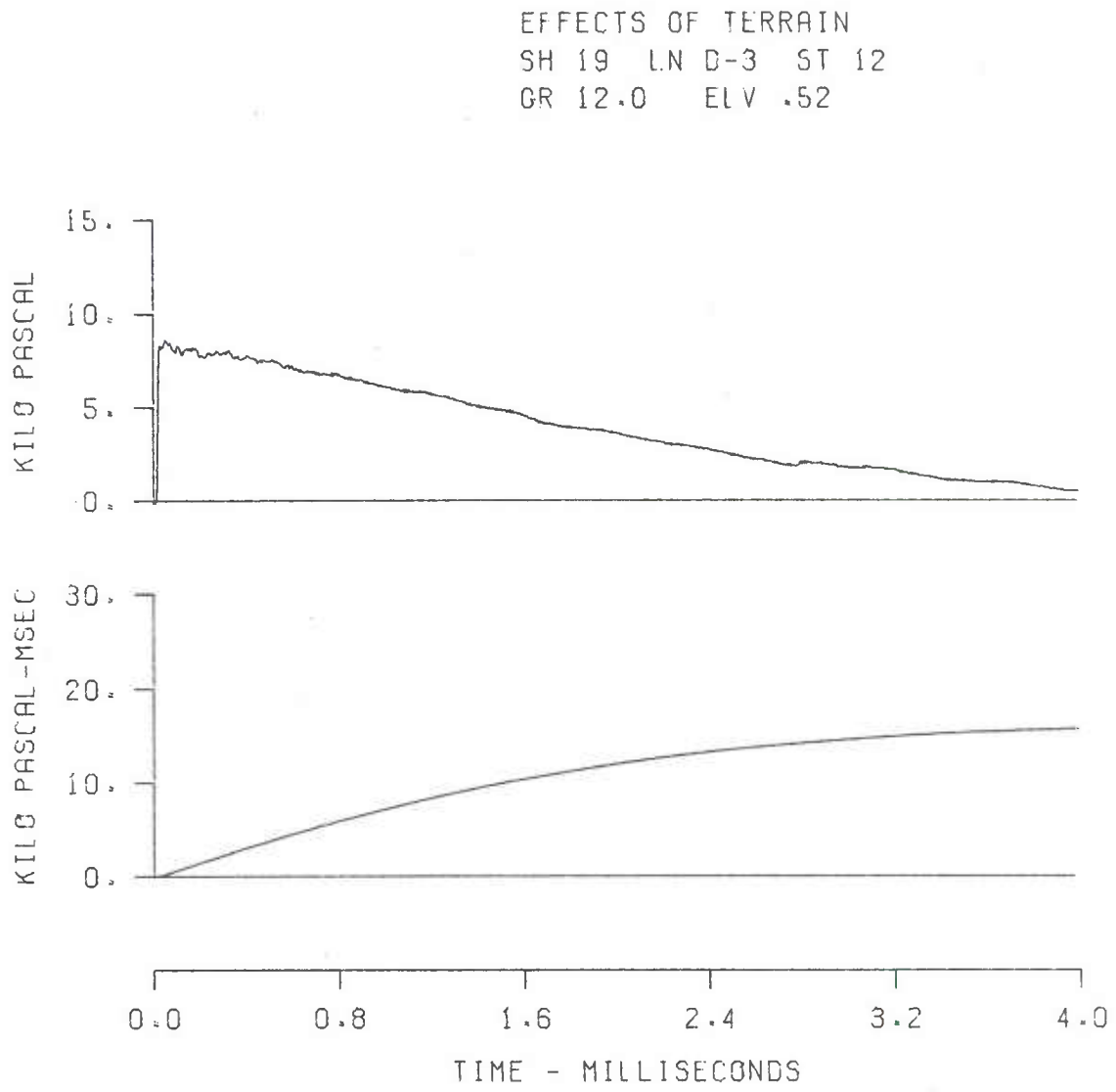

Figure A-6 (Cont). Pressure-Time Traces for Lines D-2 and D-3

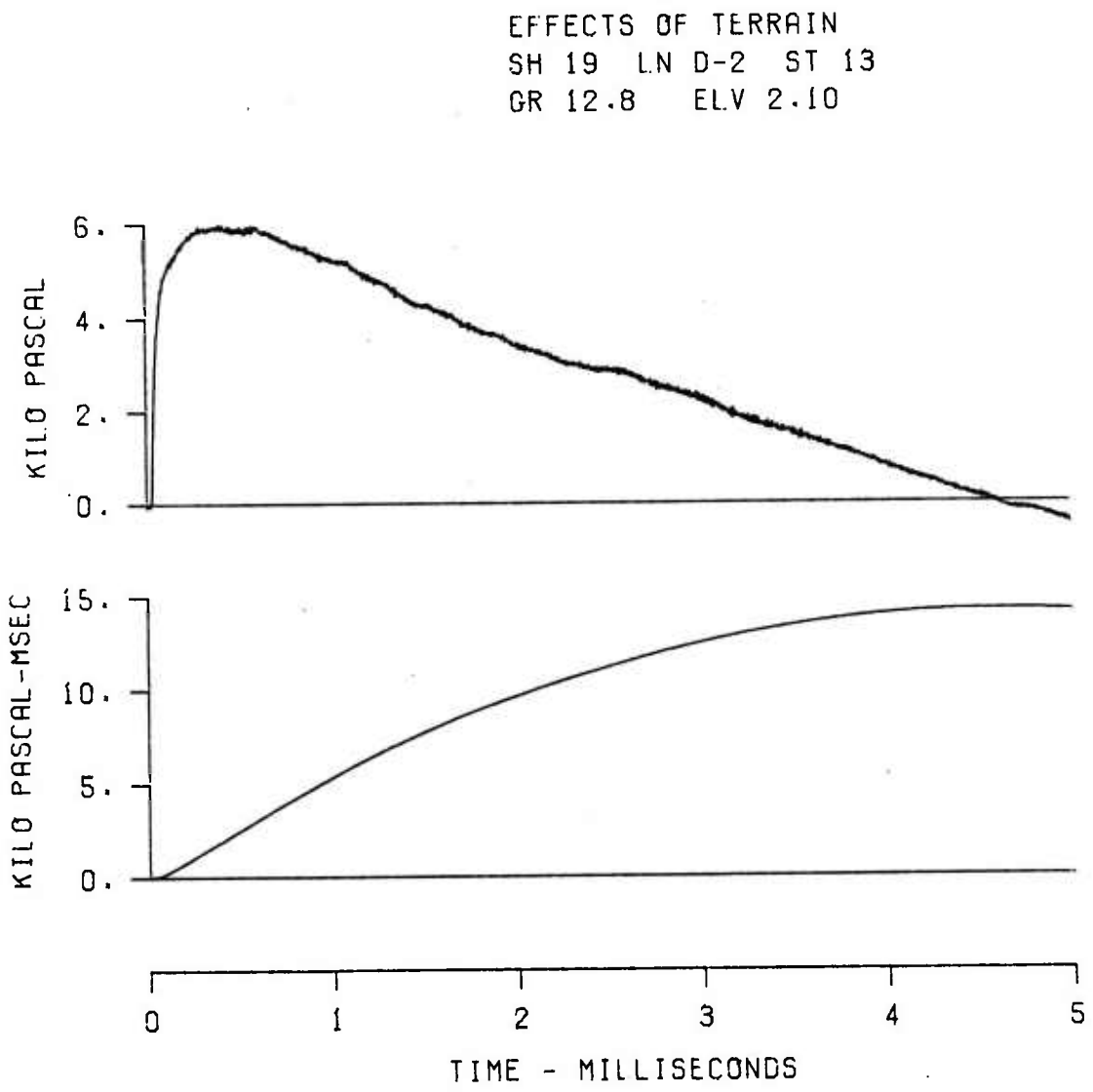

Figure A-6 (Cont). Pressure-Time Traces for Lines D-2 and D-3

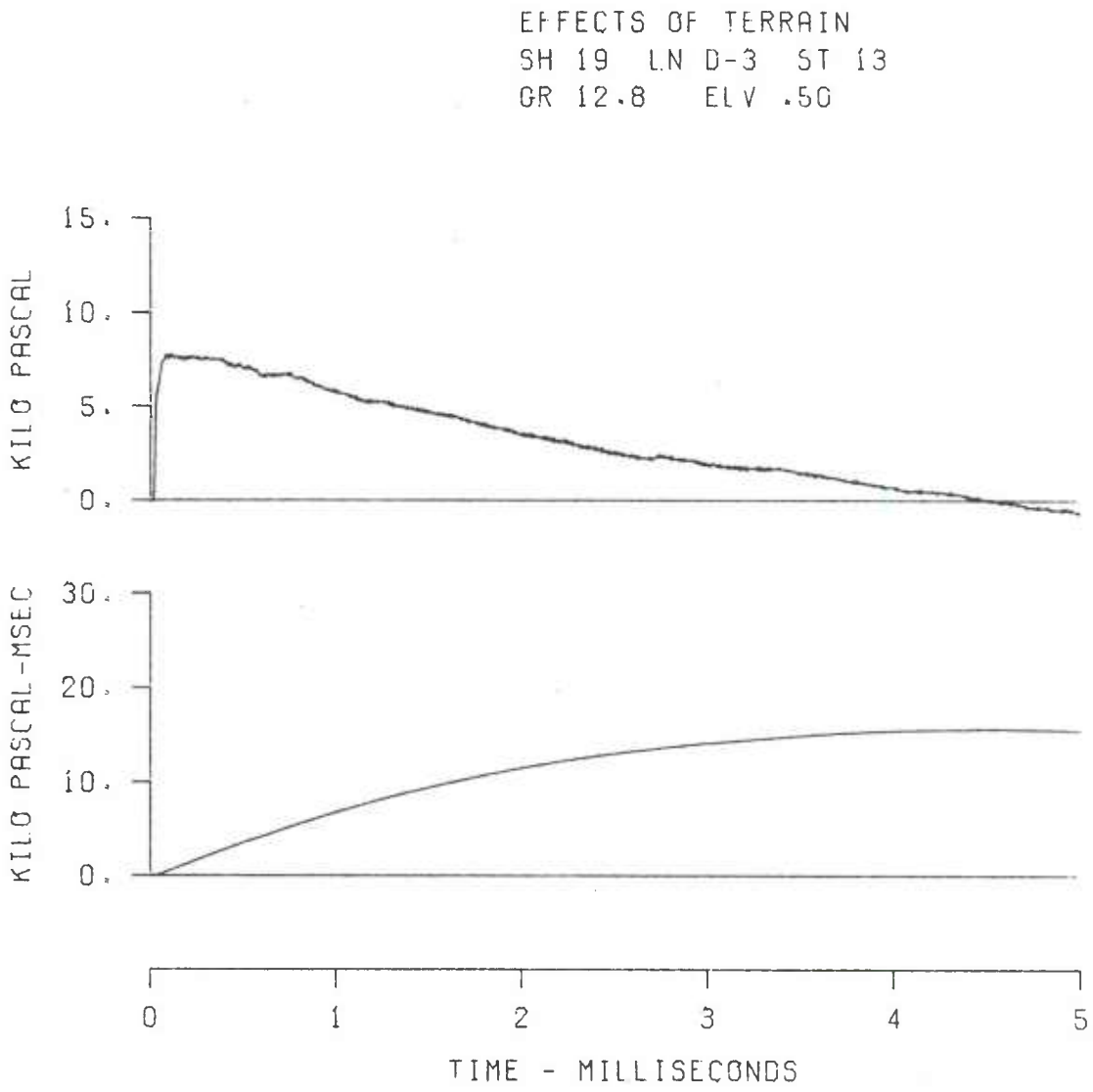

Figure A-6 (Cont). Pressure-Time Traces for Lines D-2 and D-3

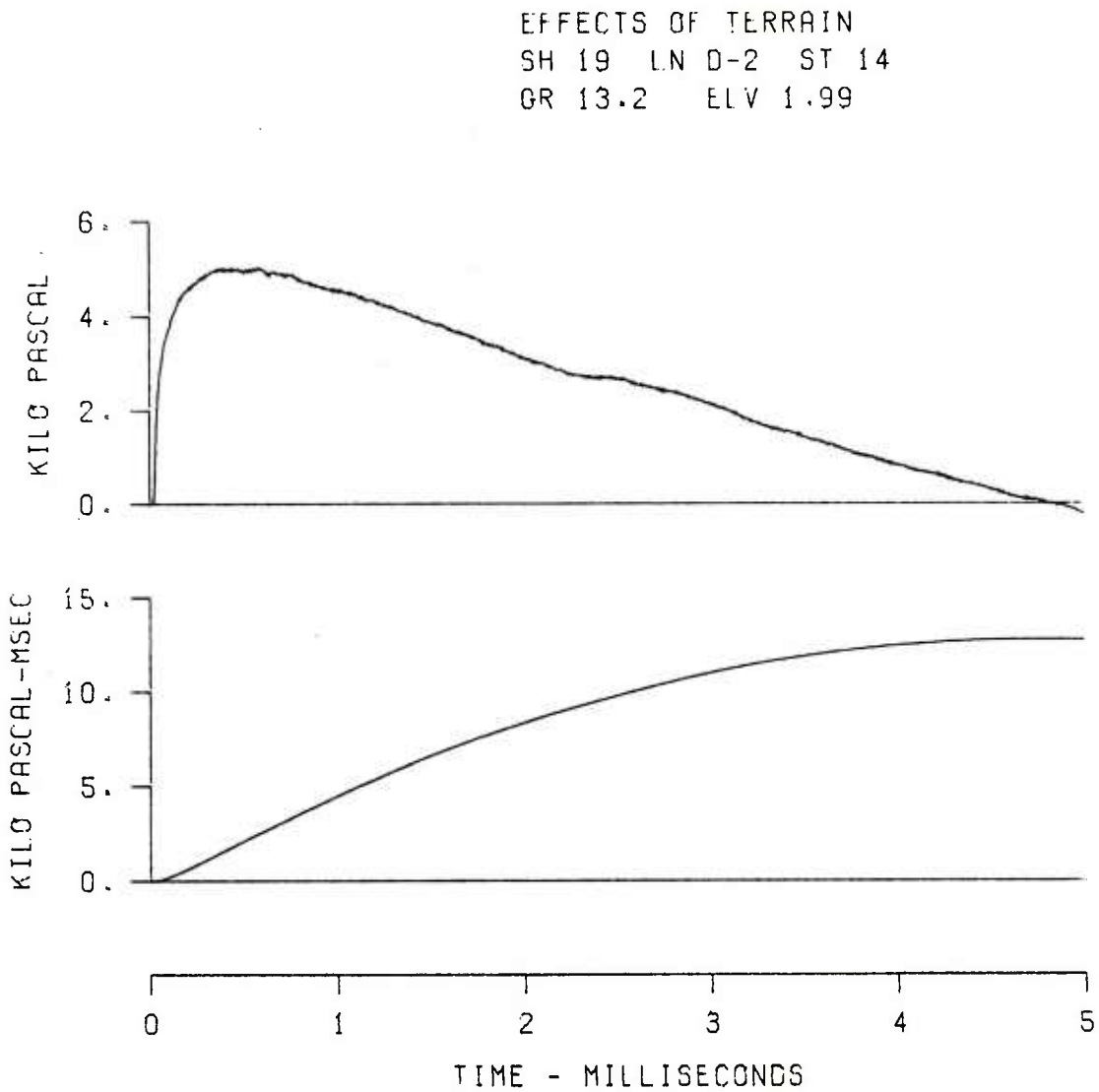

Figure A-6 (Cont). Pressure-Time Traces for Lines D-2 and D-3

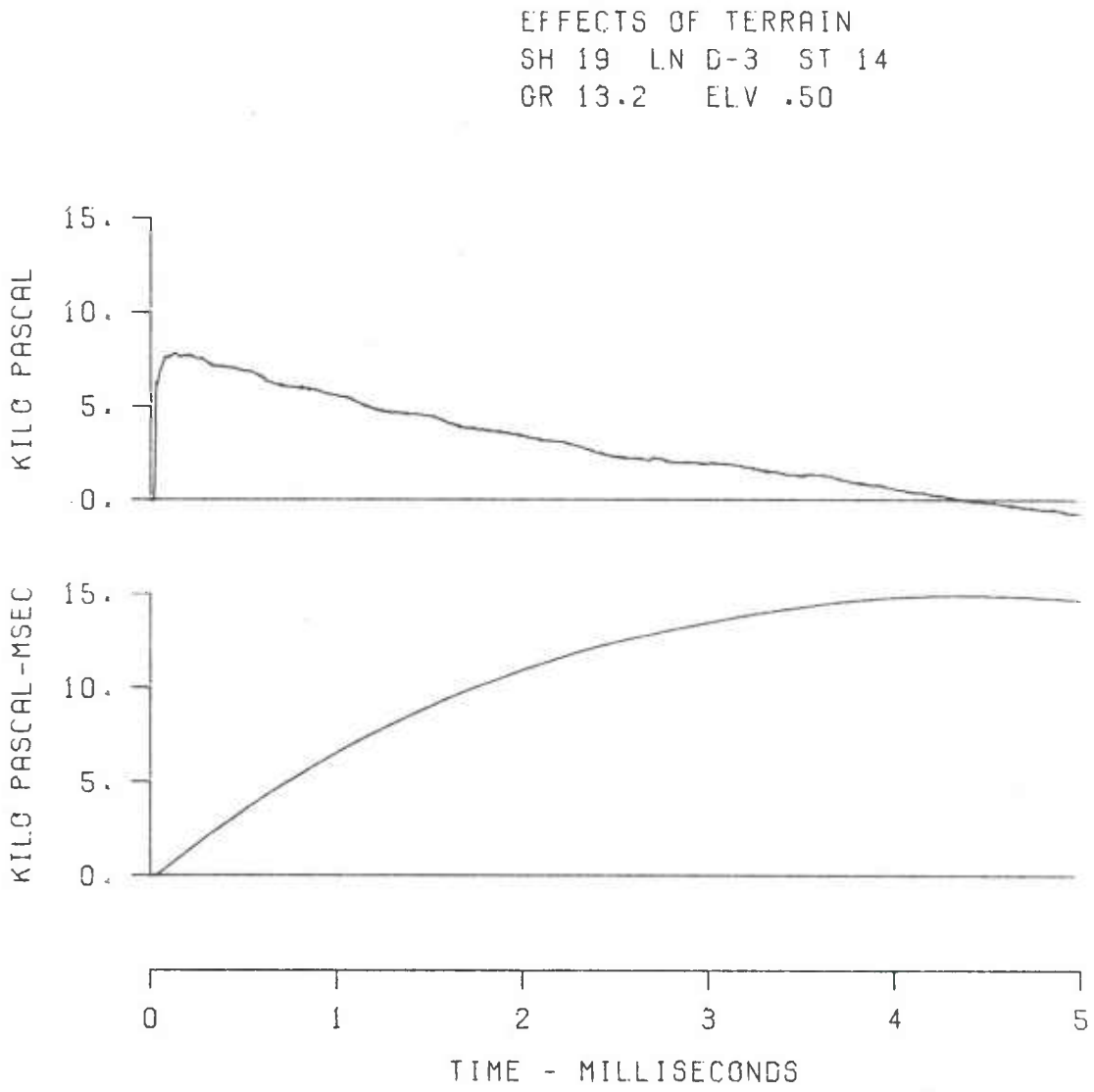

Figure A-6 (Cont). Pressure-Time Traces for Lines D-2 and D-3

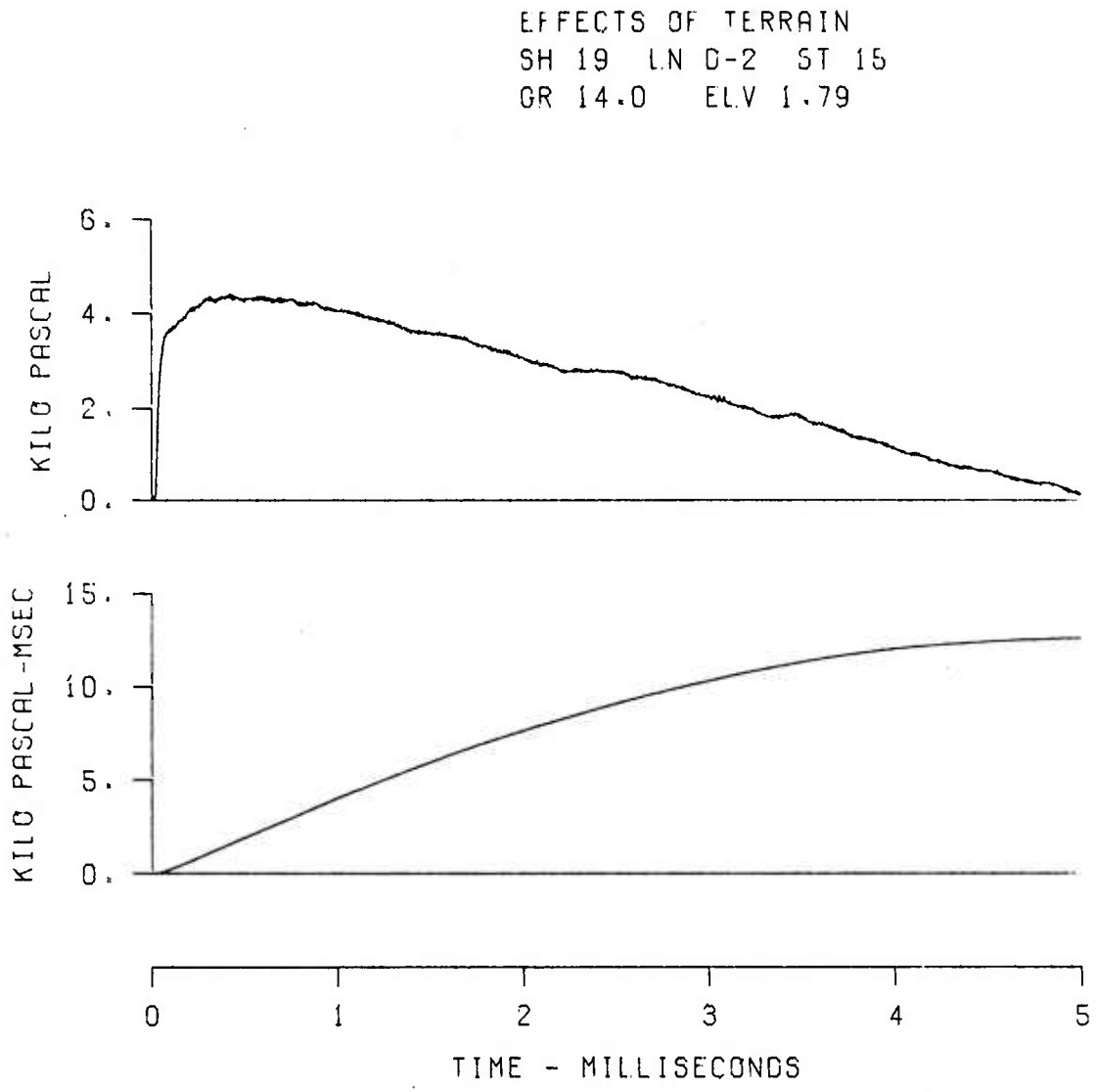

Figure A-6 (Cont). Pressure-Time Traces for Lines D-2 and D-3

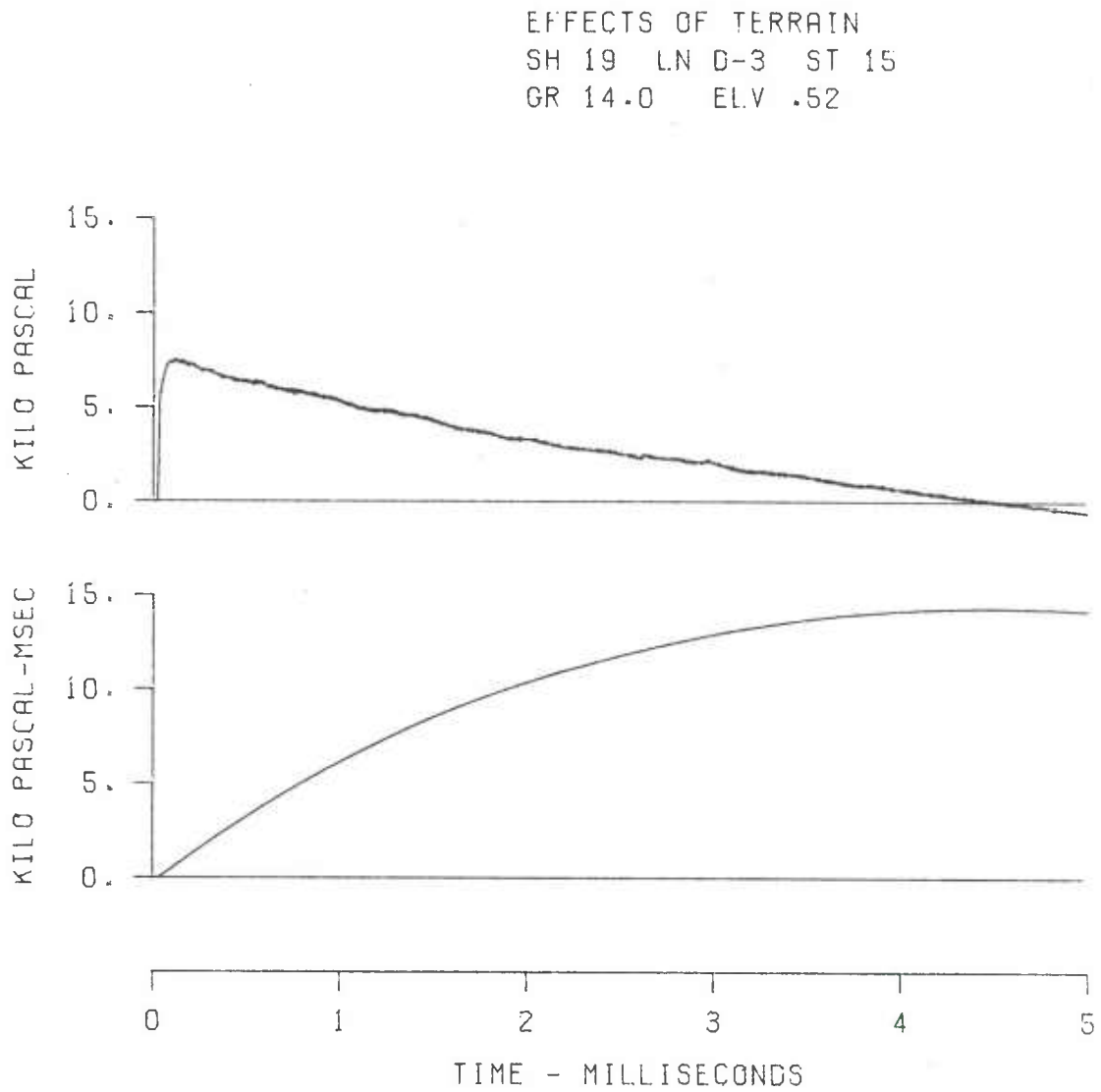

Figure A-6 (Cont). Pressure-Time Traces for Lines D-2 and D-3

APPENDIX B

HIGH SPEED PHOTOGRAPHS

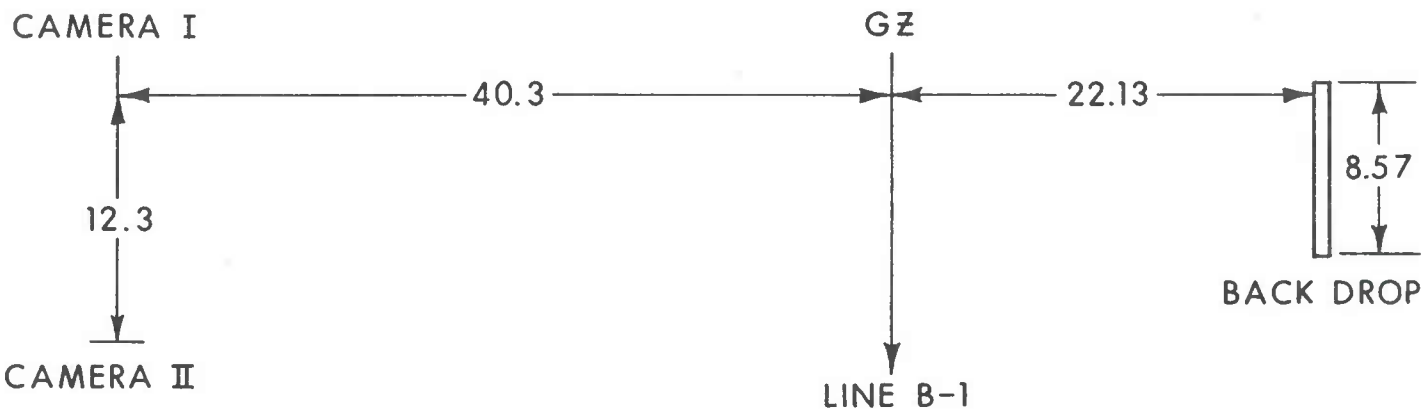

NOTE:
ALL DIMENSIONS IN METRES

Figure B-1. Sketch of Camera Locations

(A) TIME AFTER DETONATION - 1.0 ms

(B) TIME AFTER DETONATION - 1.9 ms

Figure B-2. Blast Wave Travel along Line B-1, Camera I

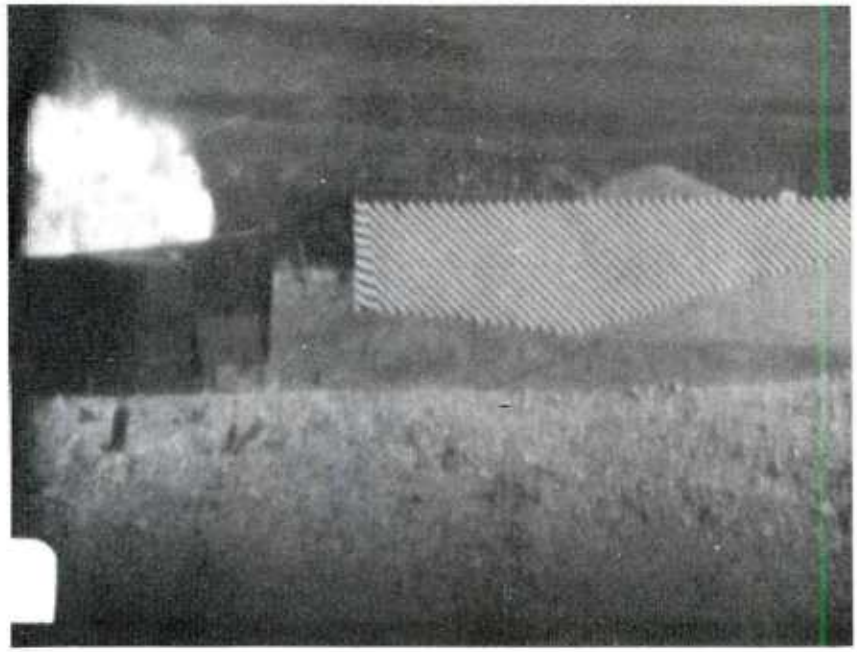

(A) TIME AFTER DETONATION - 3.5 ms

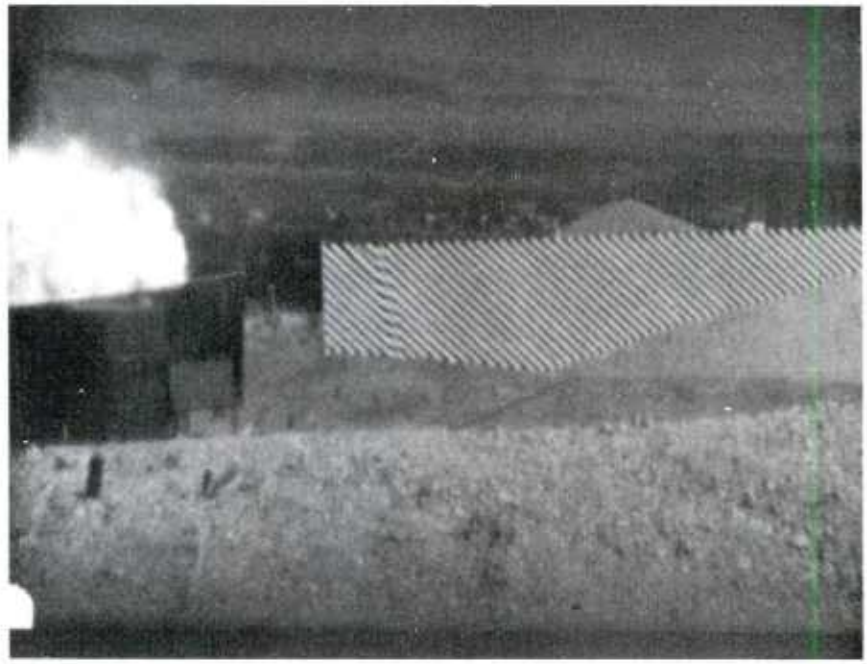

(B) TIME AFTER DETONATION - 4.4 ms

Figure B-3. Blast Wave Travel along Line B-1 Camera II

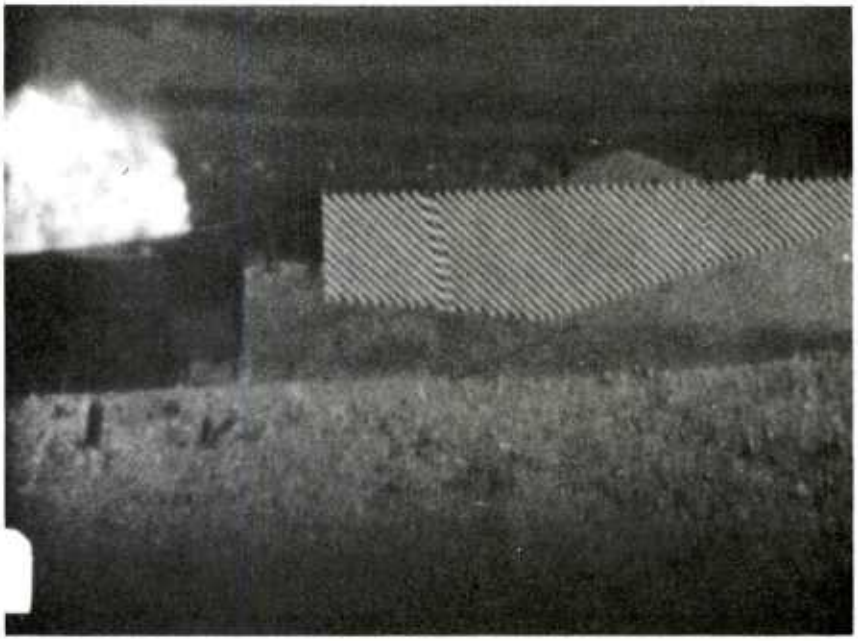

(C) TIME AFTER DETONATION - 5.3 ms

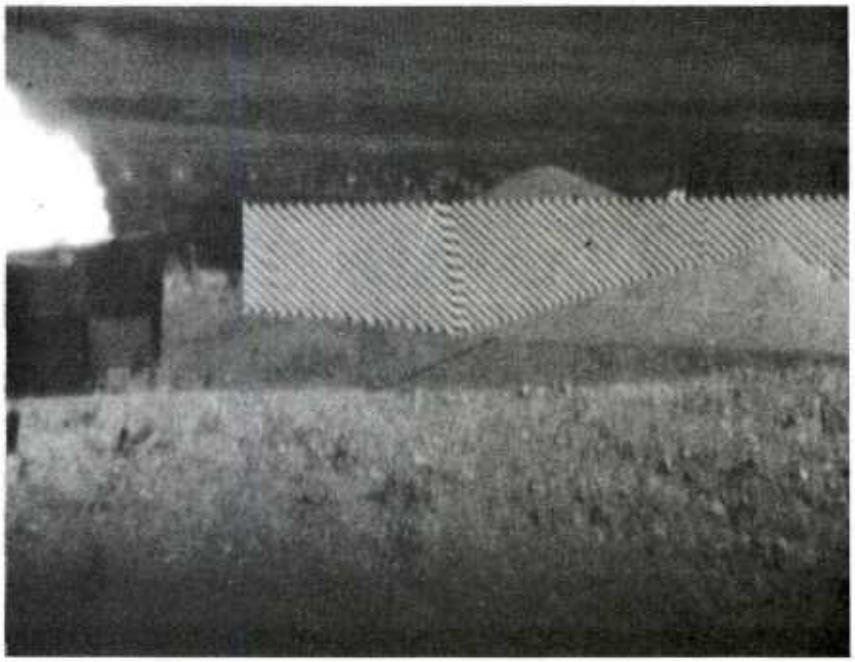

(D) TIME AFTER DETONATION - 7.0 ms

Figure B-3 (Cont). Blast Wave Travel along Line E-1 Camera II

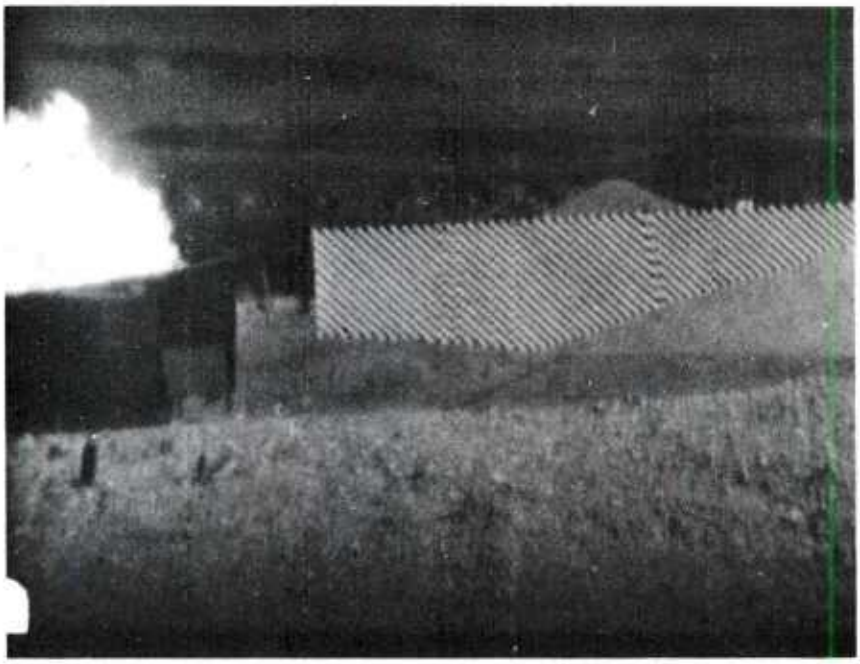

(E) TIME AFTER DETONATION - 9.7ms

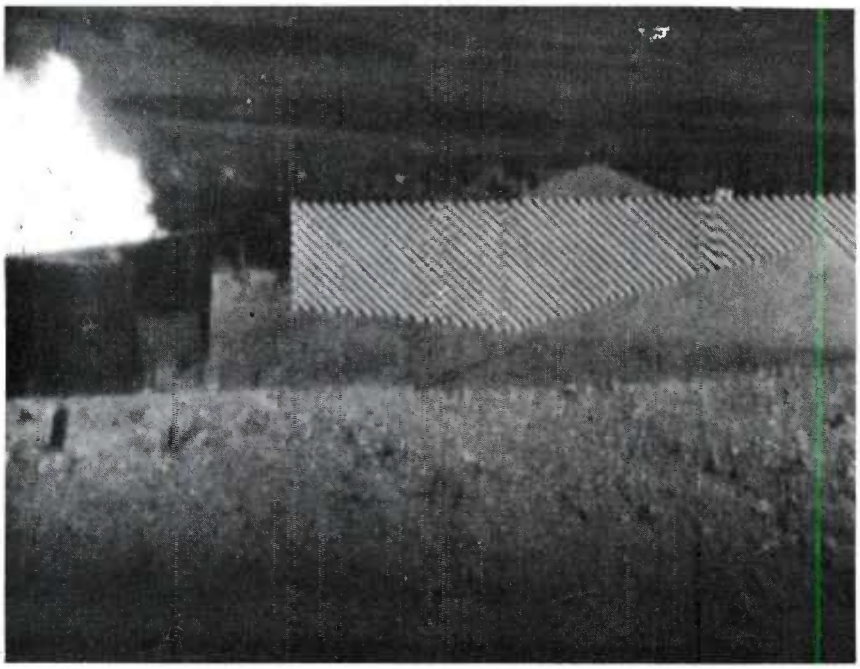

(F) TIME AFTER DETONATION - 11.4ms

Figure B-3 (Cont). Blast Wave Travel along Line B-1, Camera II

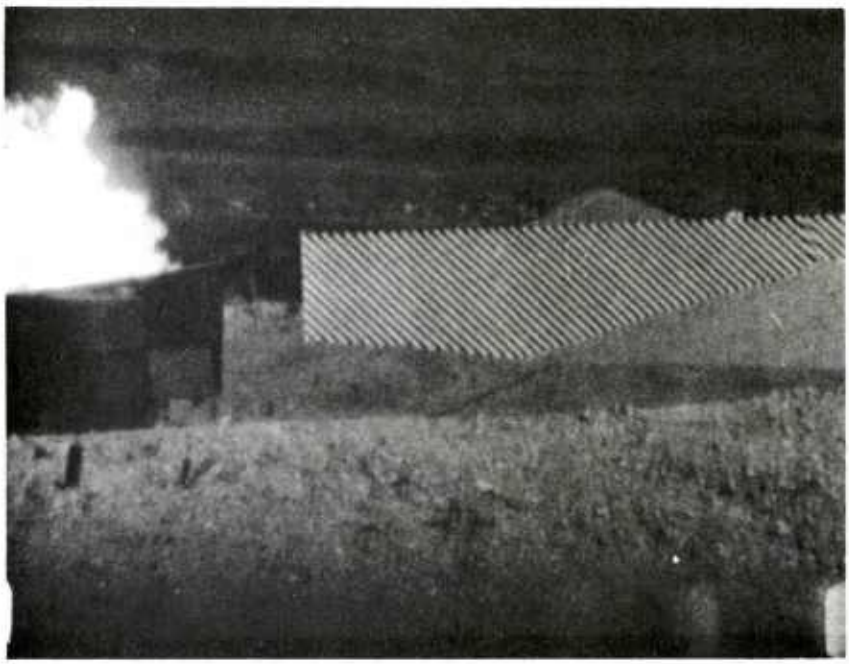

(G) TIME AFTER DETONATION - 13.2 ms

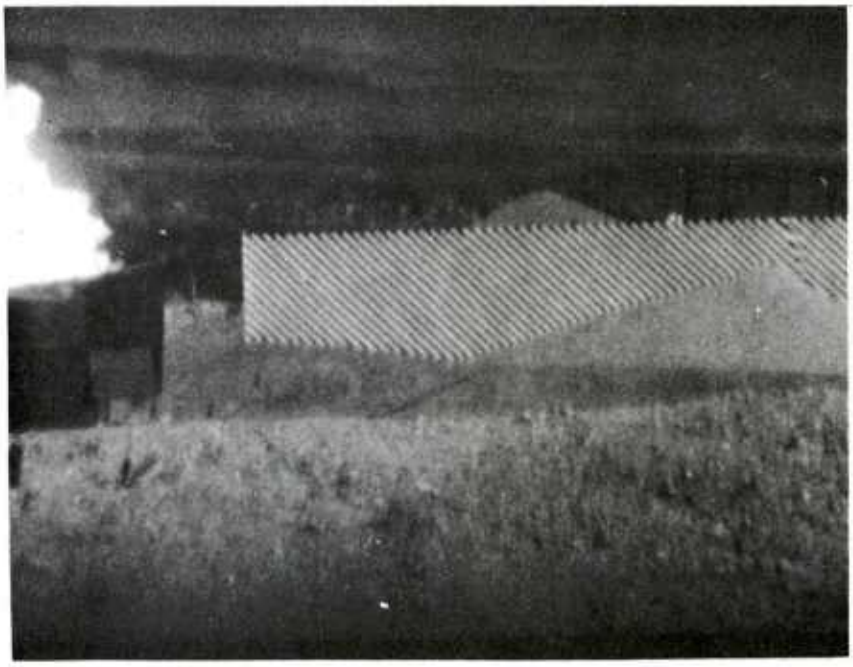

(H) TIME AFTER DETONATION - 14.1 ms

Figure B03 (Cont). Blast Wave Travel along Line B-1, Camera II

APPENDIX C

COMPARISON OF DATA WITH PREDICTED WAVEFORMS

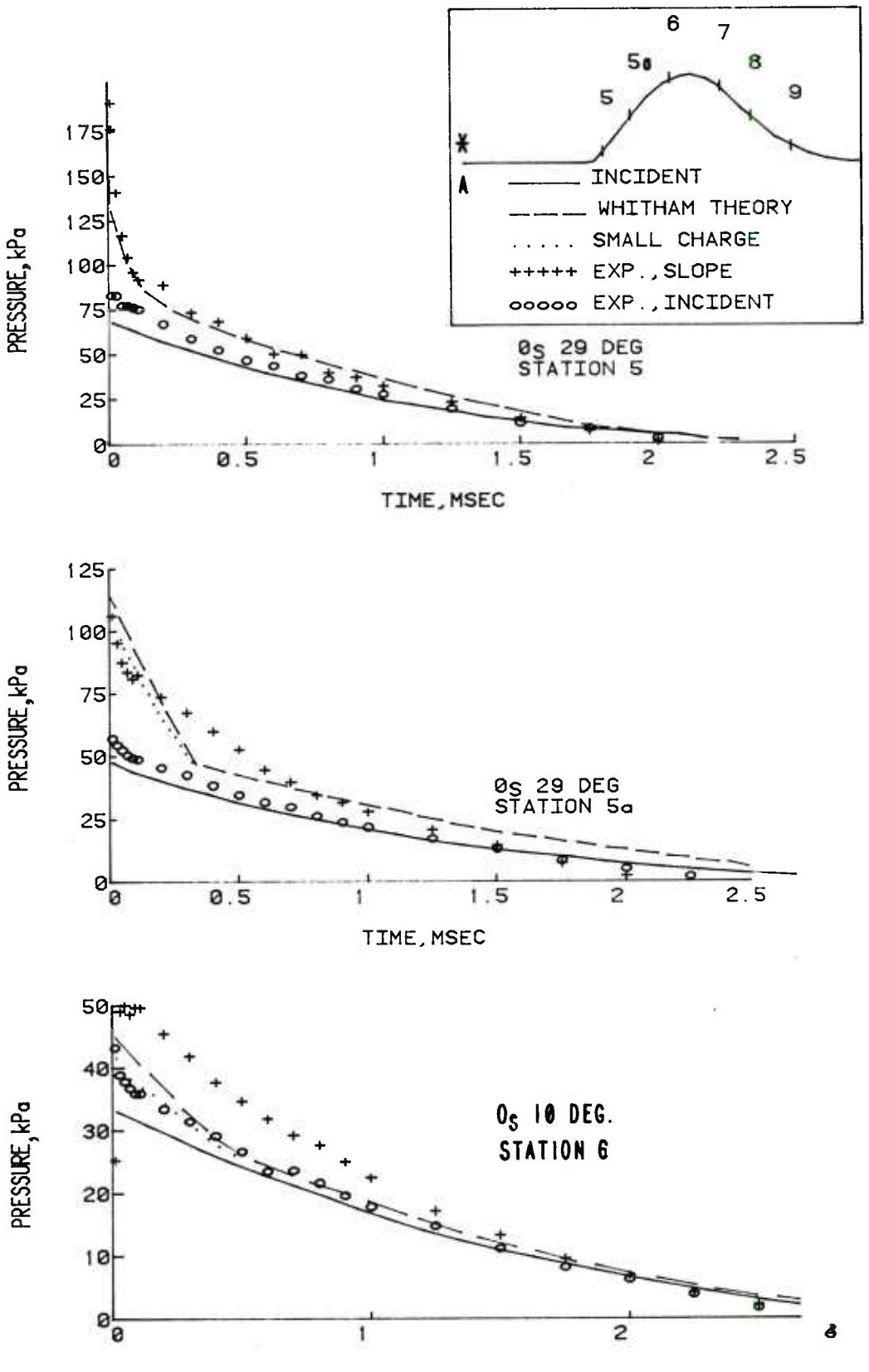

Figure C-1. Overpressure along Line A-1 from a Burst Over GZ-A

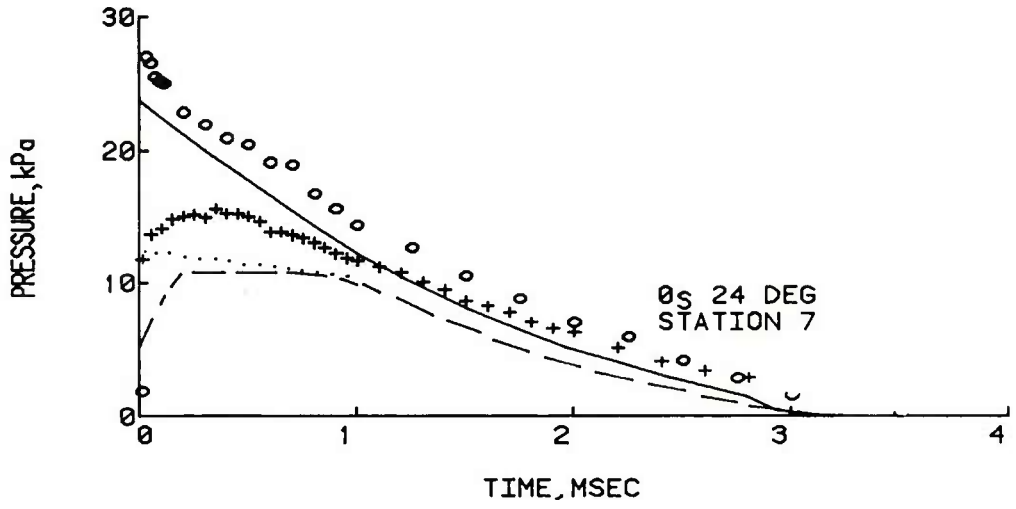

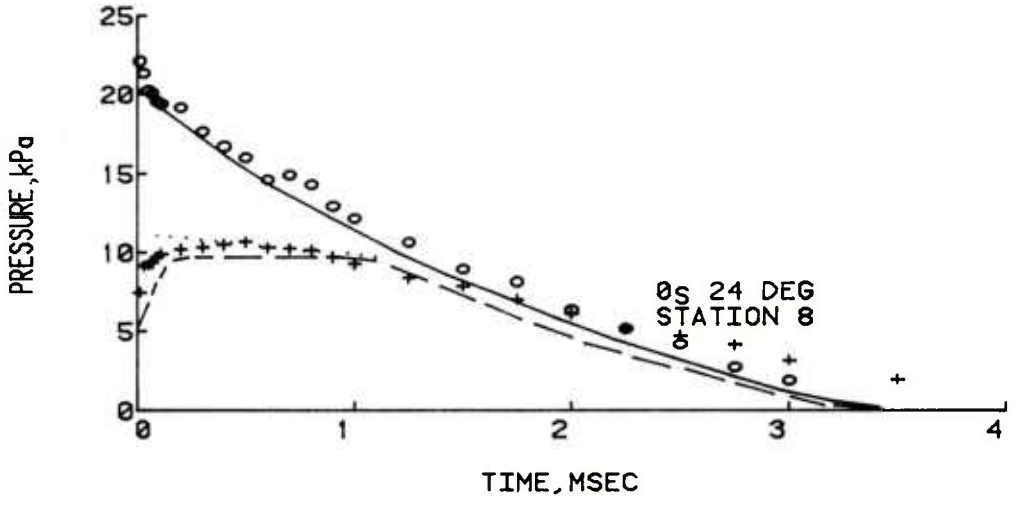

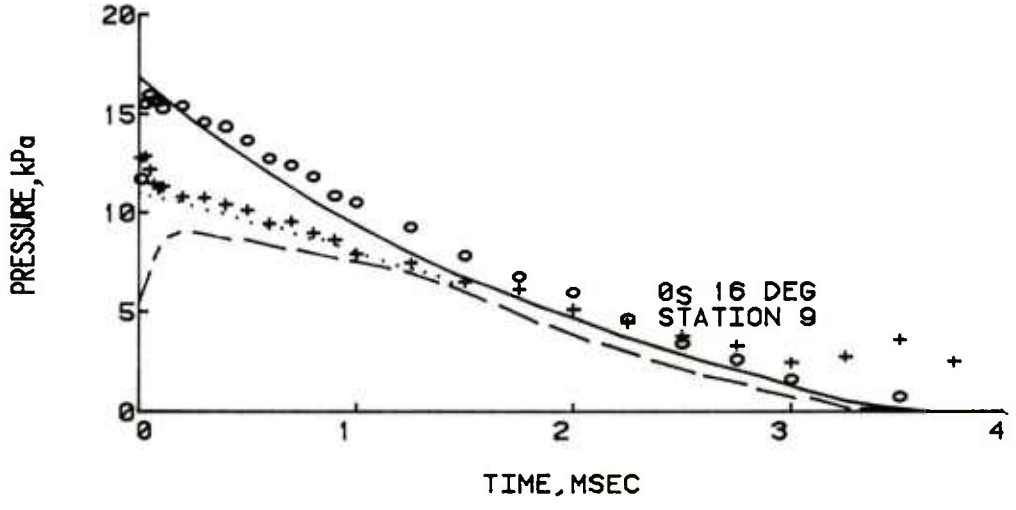

Figure C-1 (Cont). Overpressure along Line A-1 from a Burst Over GS-A

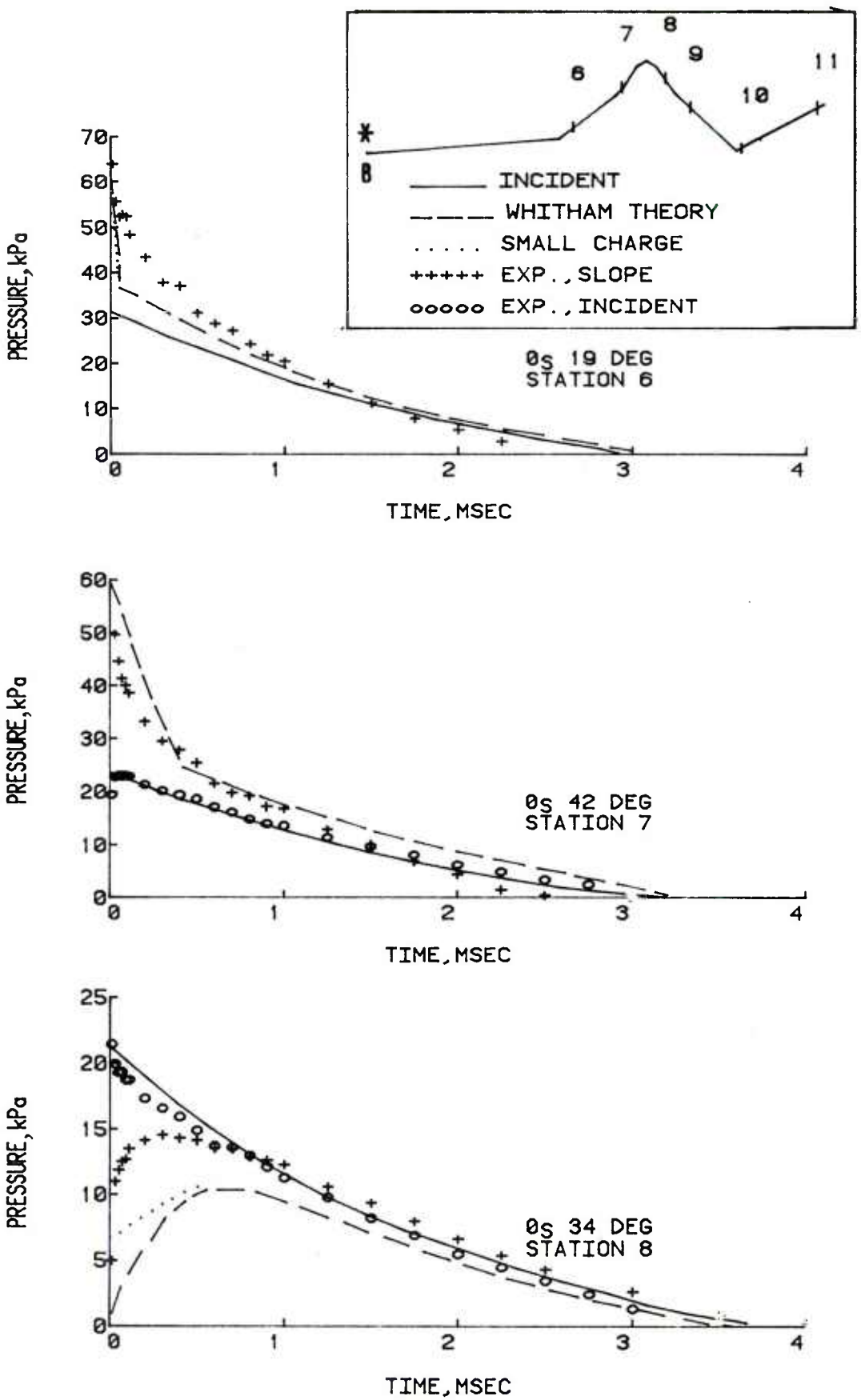

Figure C-2. Overpressure along Line B-1 from a Burst over GZ-B

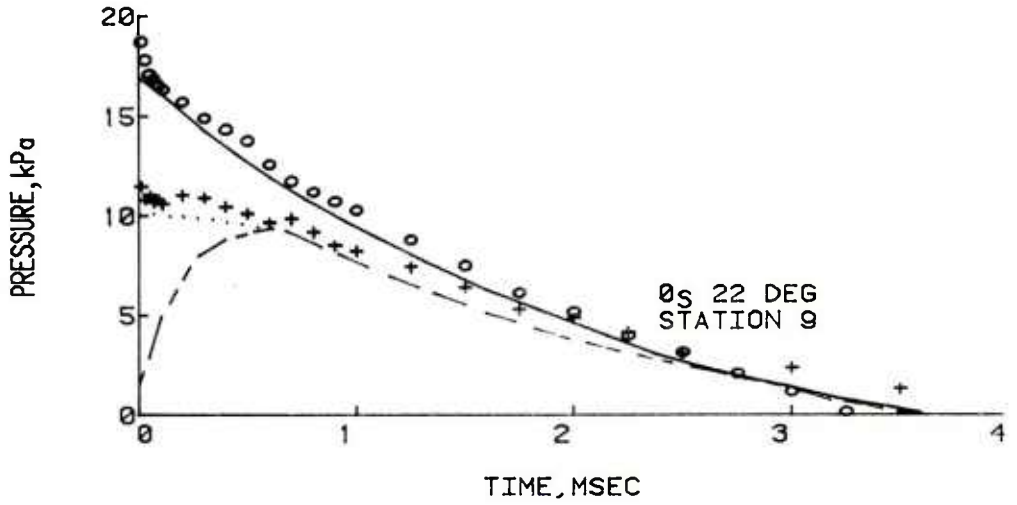

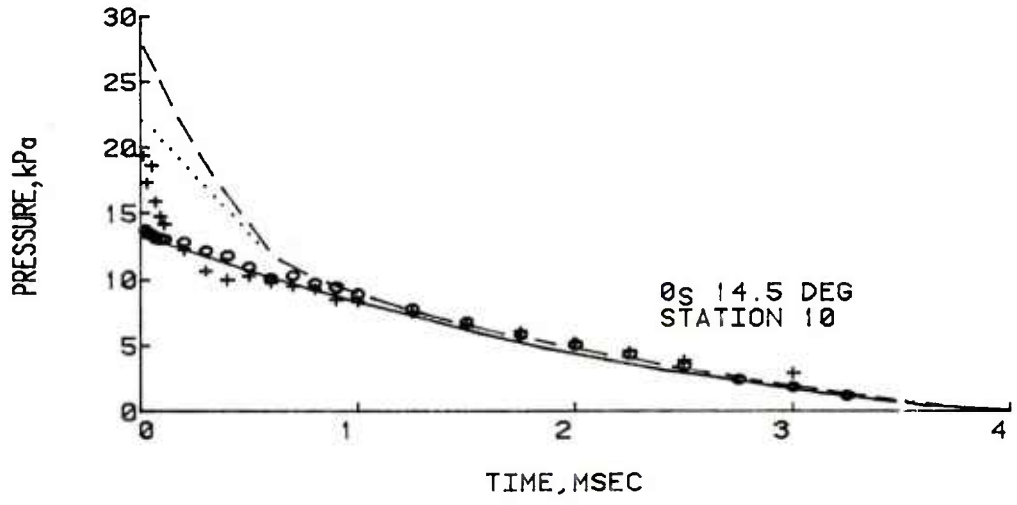

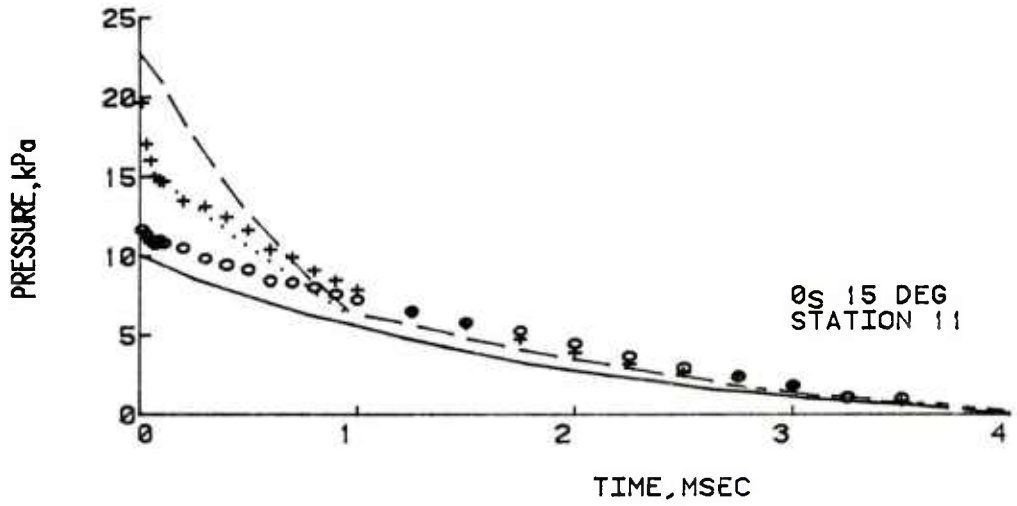

Figure C-2 (Cont). Overpressure along Line B-1 from a Burst over GZ-B

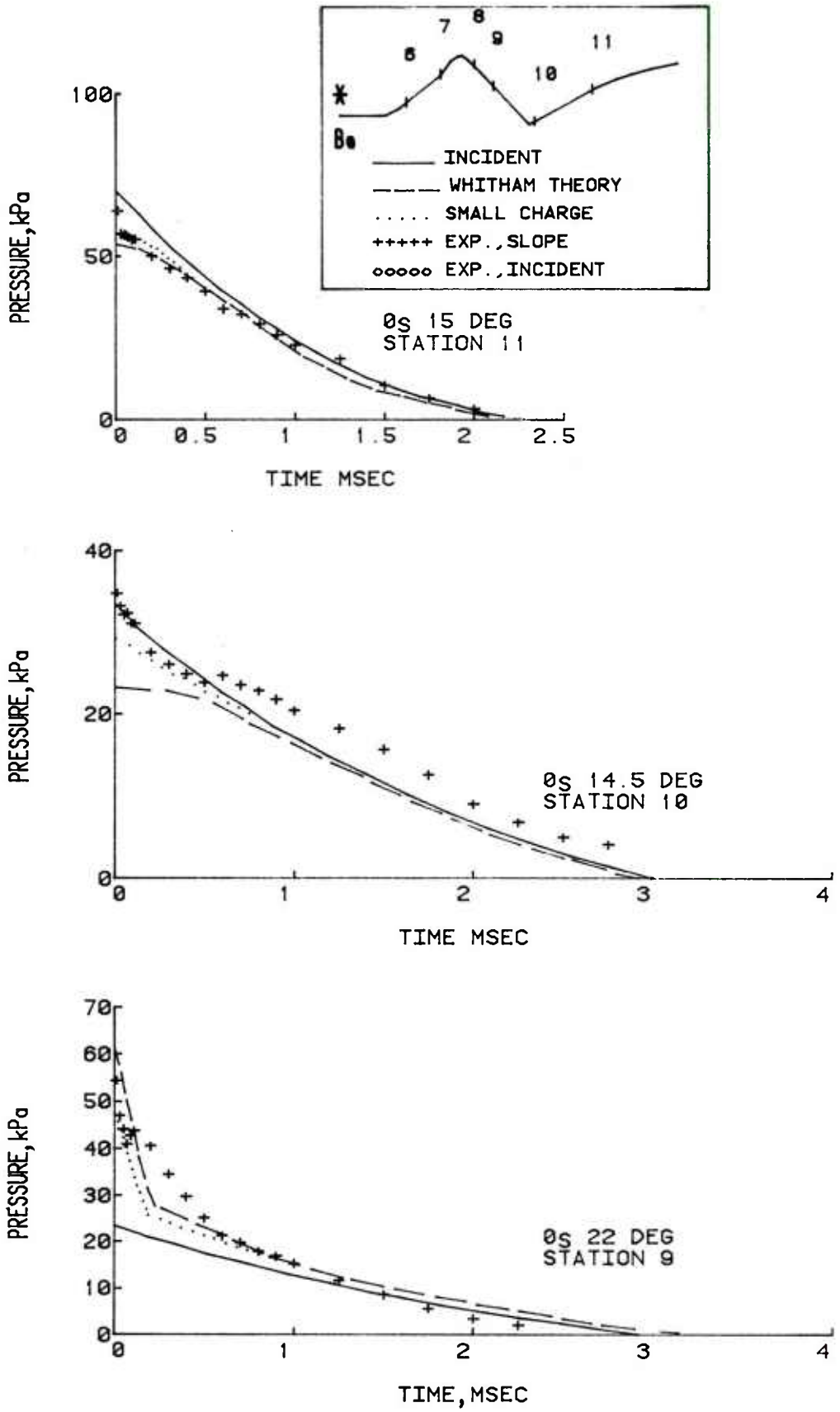

Figure C-3. Overpressure along Line B-1 from a Burst over GZ-B_a

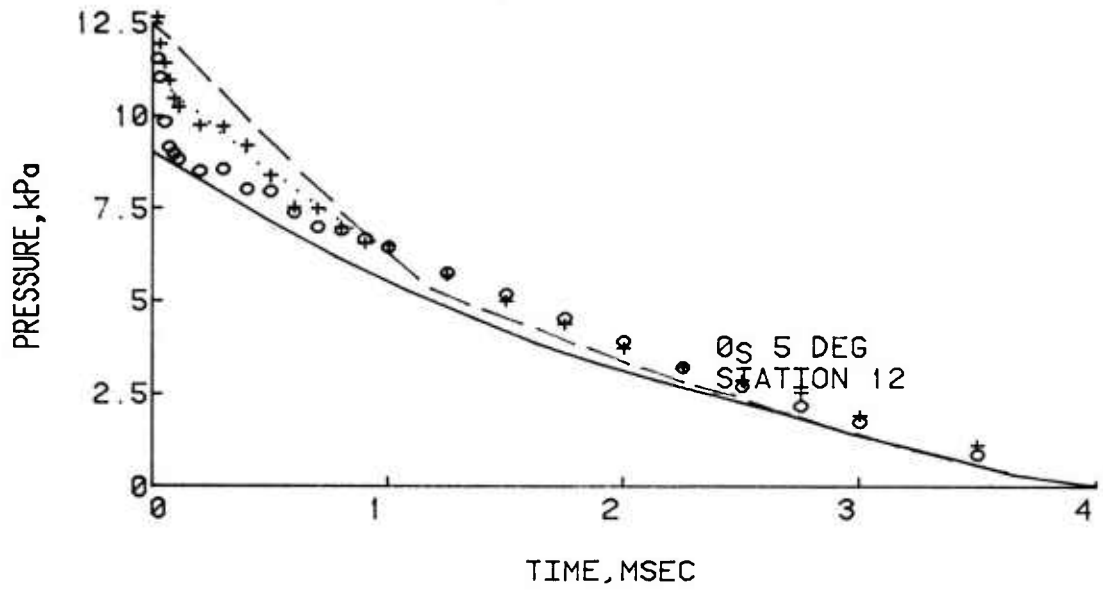

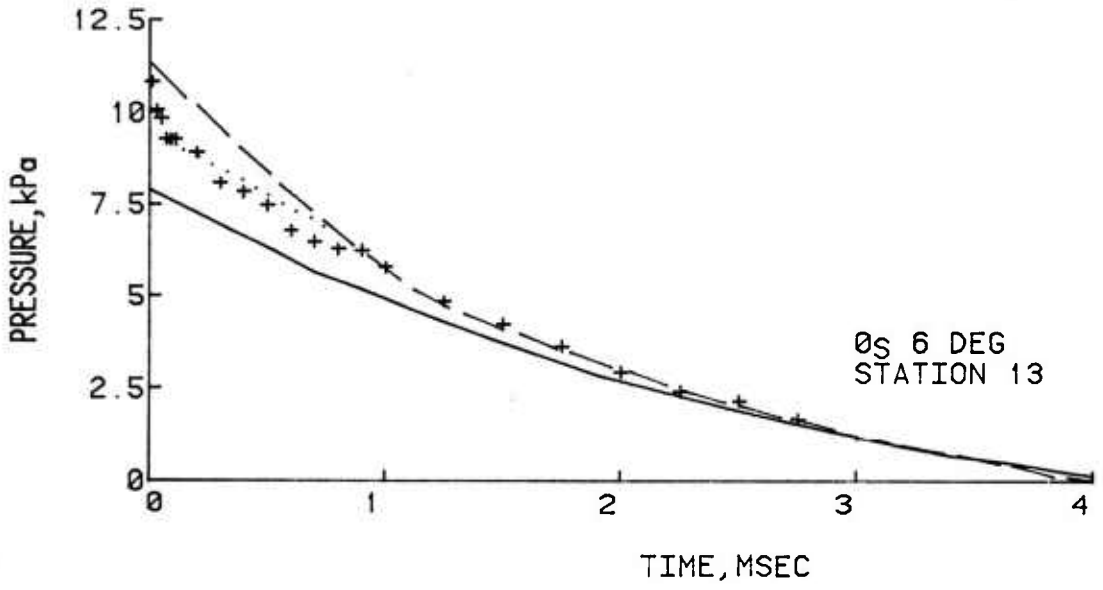

Figure C-3 (Cont). Overpressure along Line B-1 from a Burst over GZ-B_a

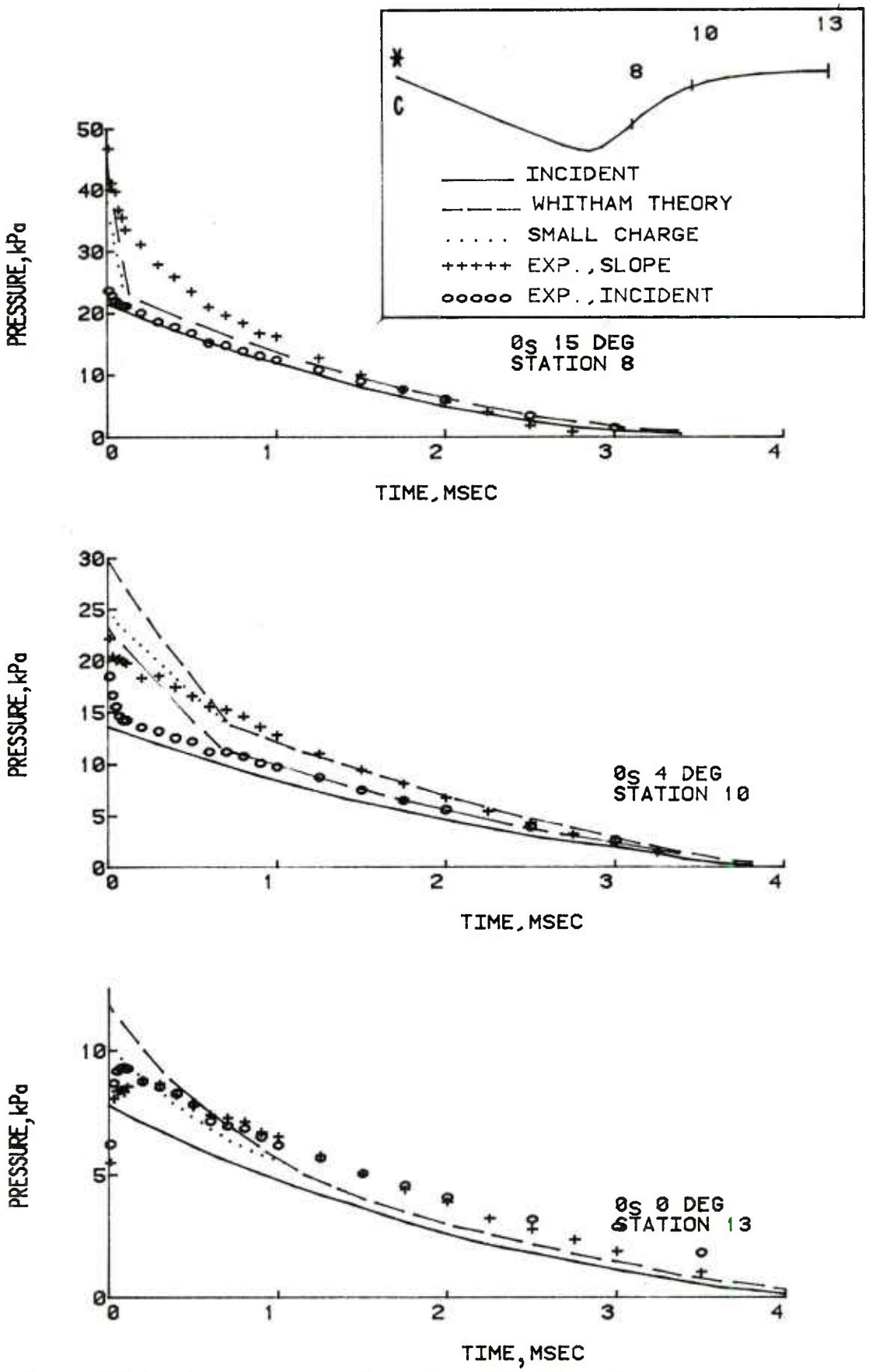

Figure C-4. Overpressure along Line C-1 from a Burst over GZ-C

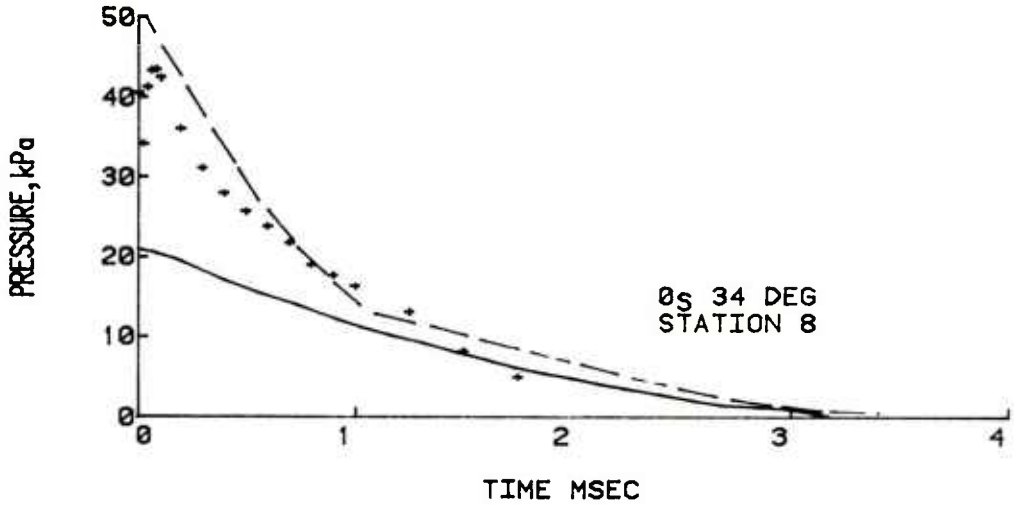

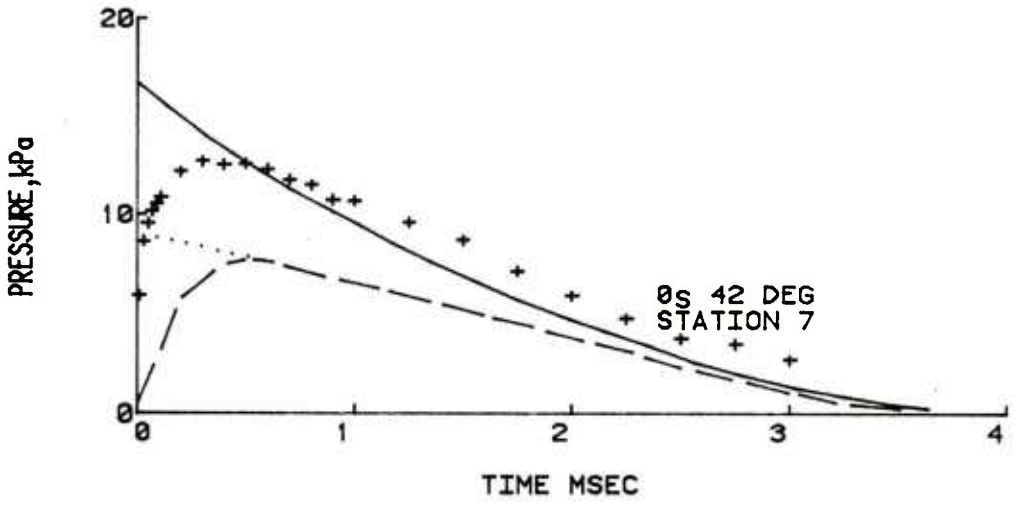

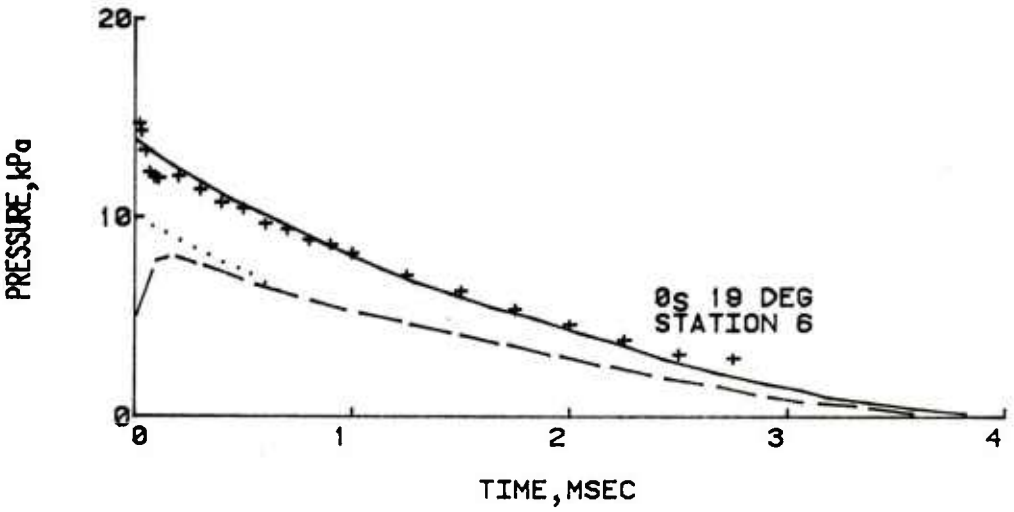

Figure C-4 (Cont). Overpressure along Line C-1 from a Burst over GZ-C

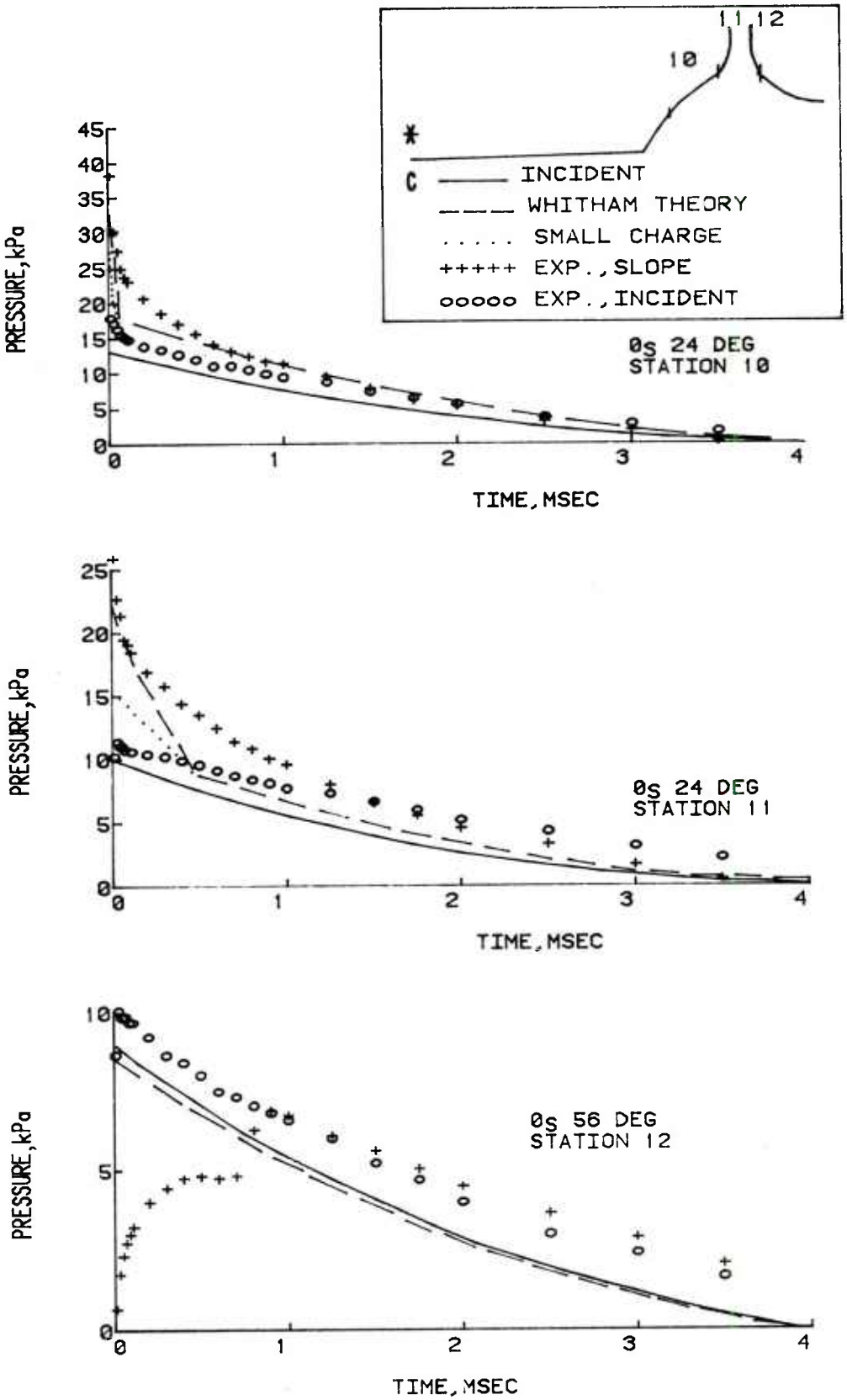

Figure C-5. Overpressure along Line C-2 from a Burst over GZ-C

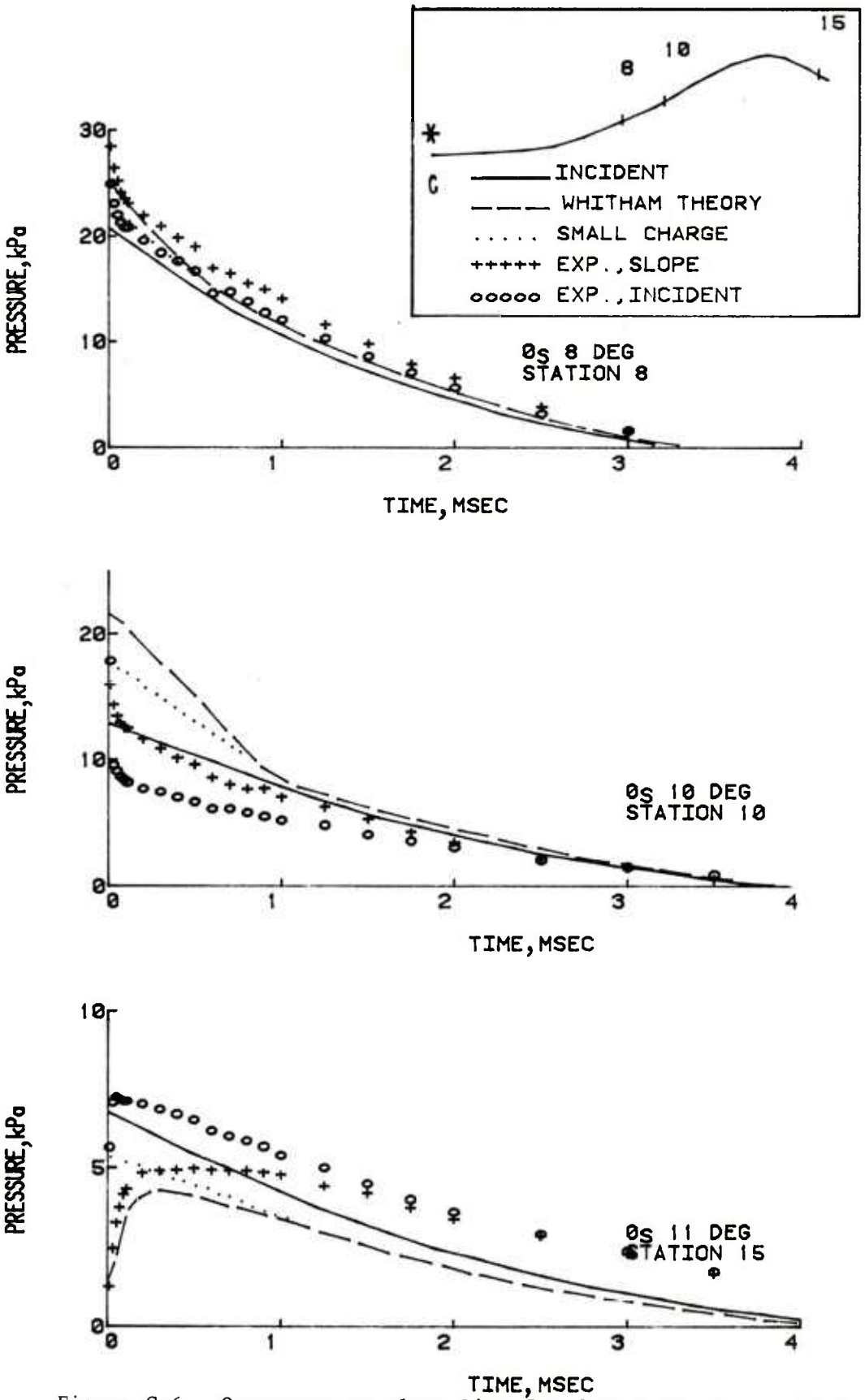

Figure C-6. Overpressure along Line C-3 from a Burst over GZ-C

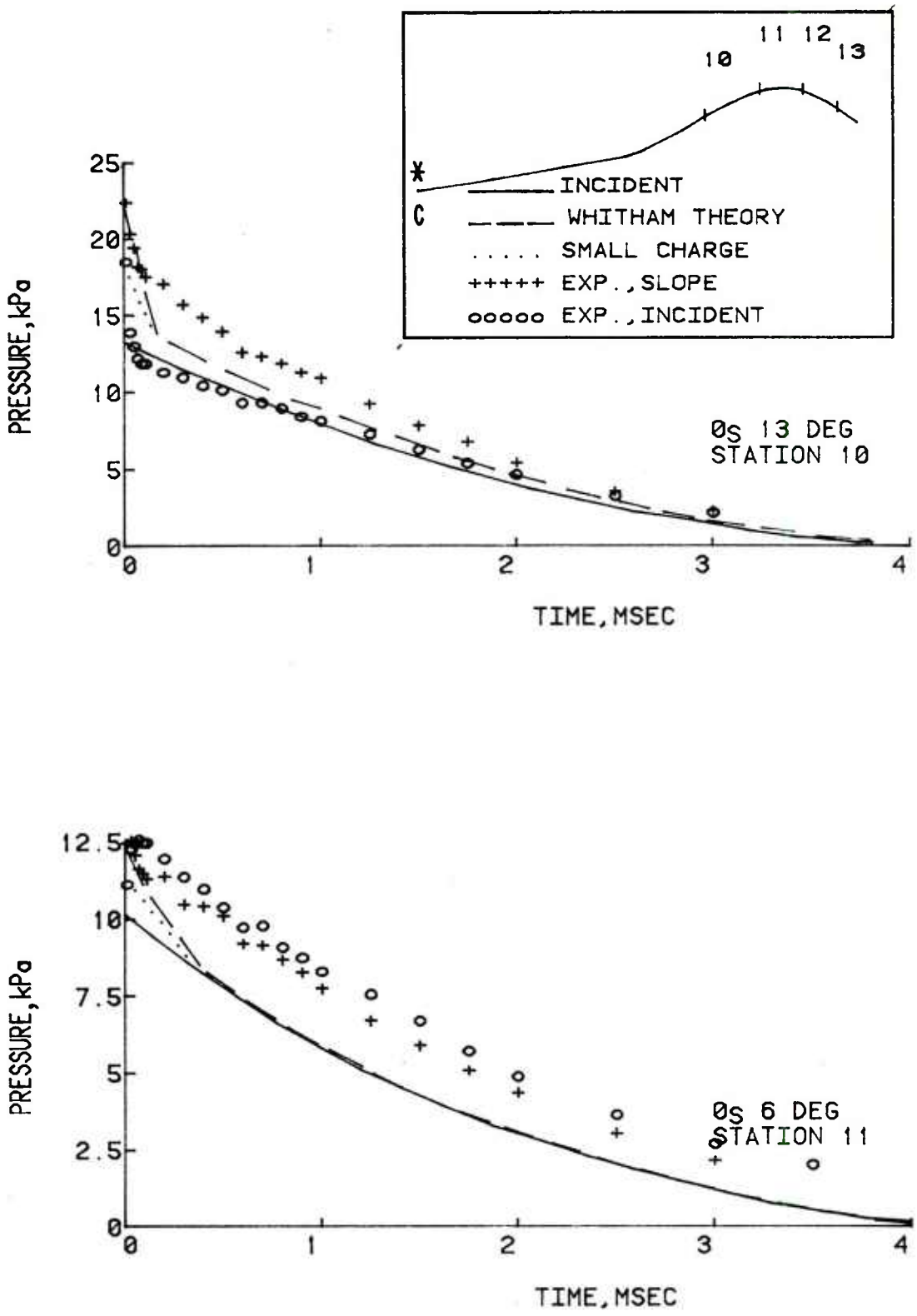

Figure C07. Overpressure along Line C-4 from a Burst over GZ-C

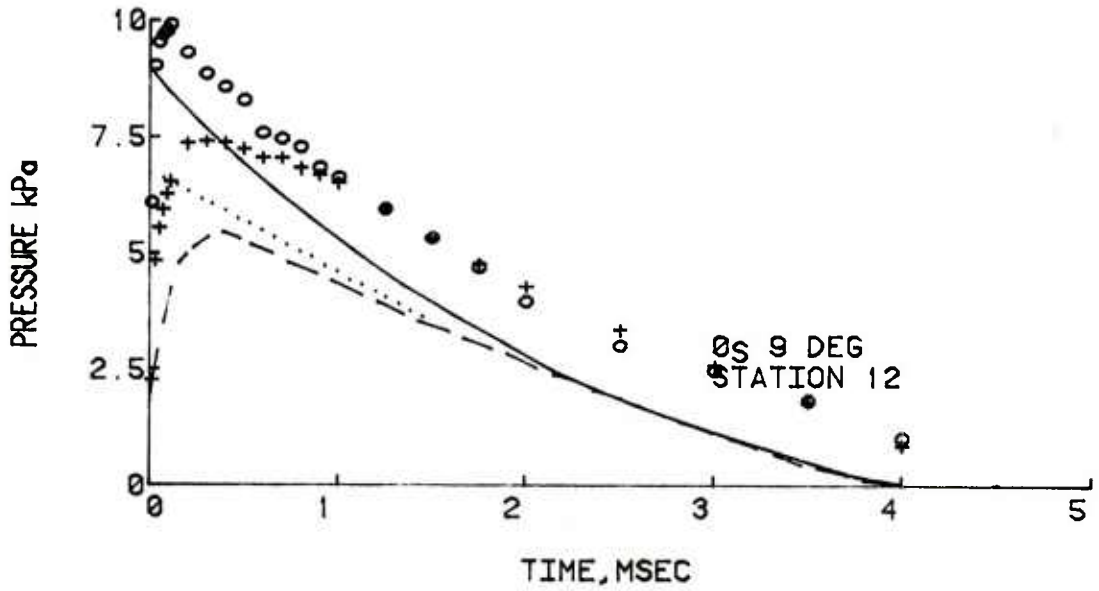

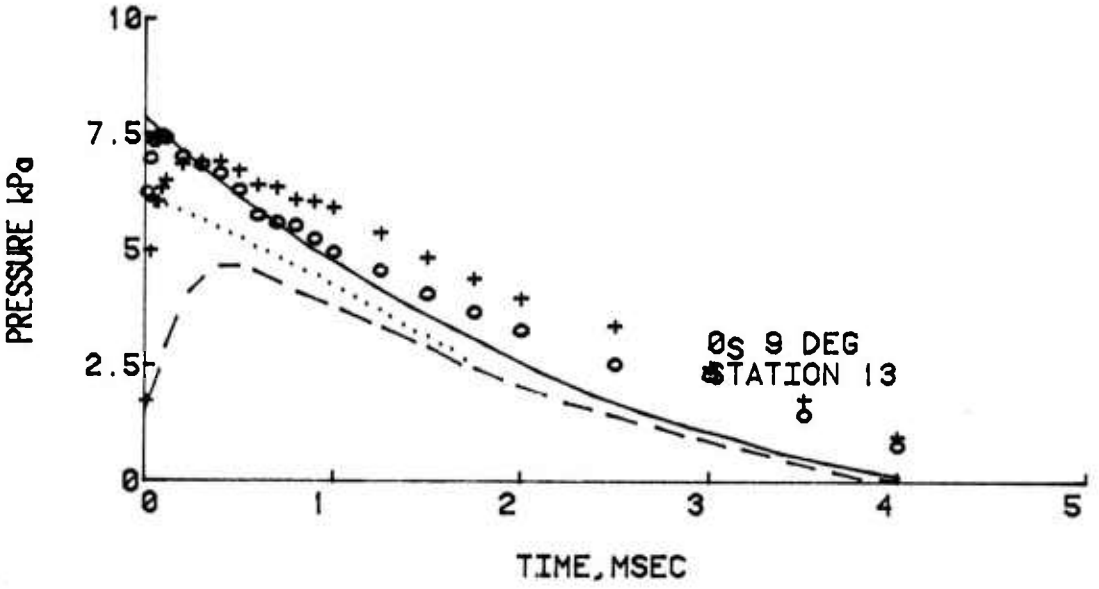

Figure C-7 (Cont). Overpressure along Line C-4 from a Burst over GZ-C

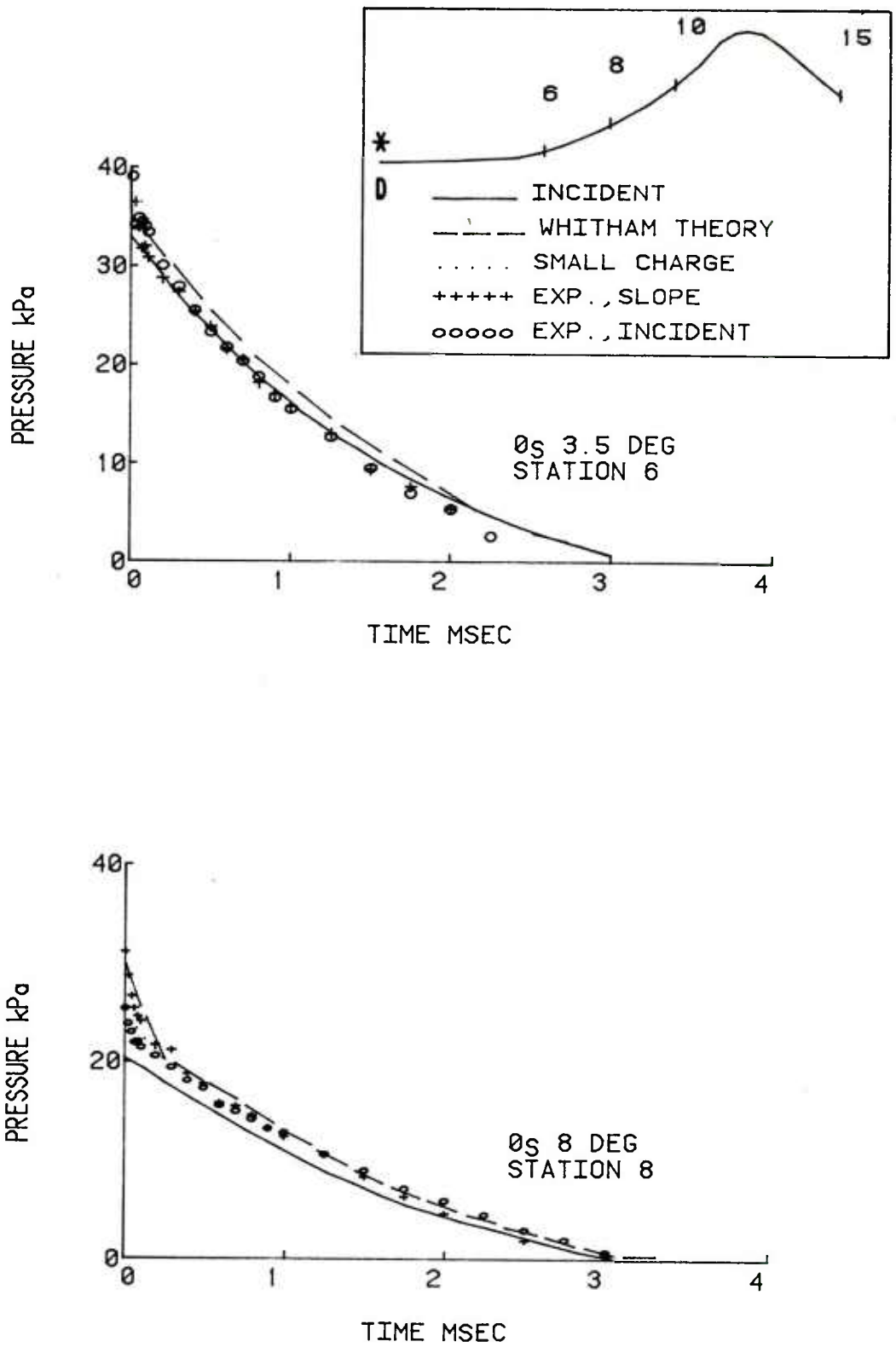

Figure C-8. Overpressure along Line D-2 from a Burst over GZ-D

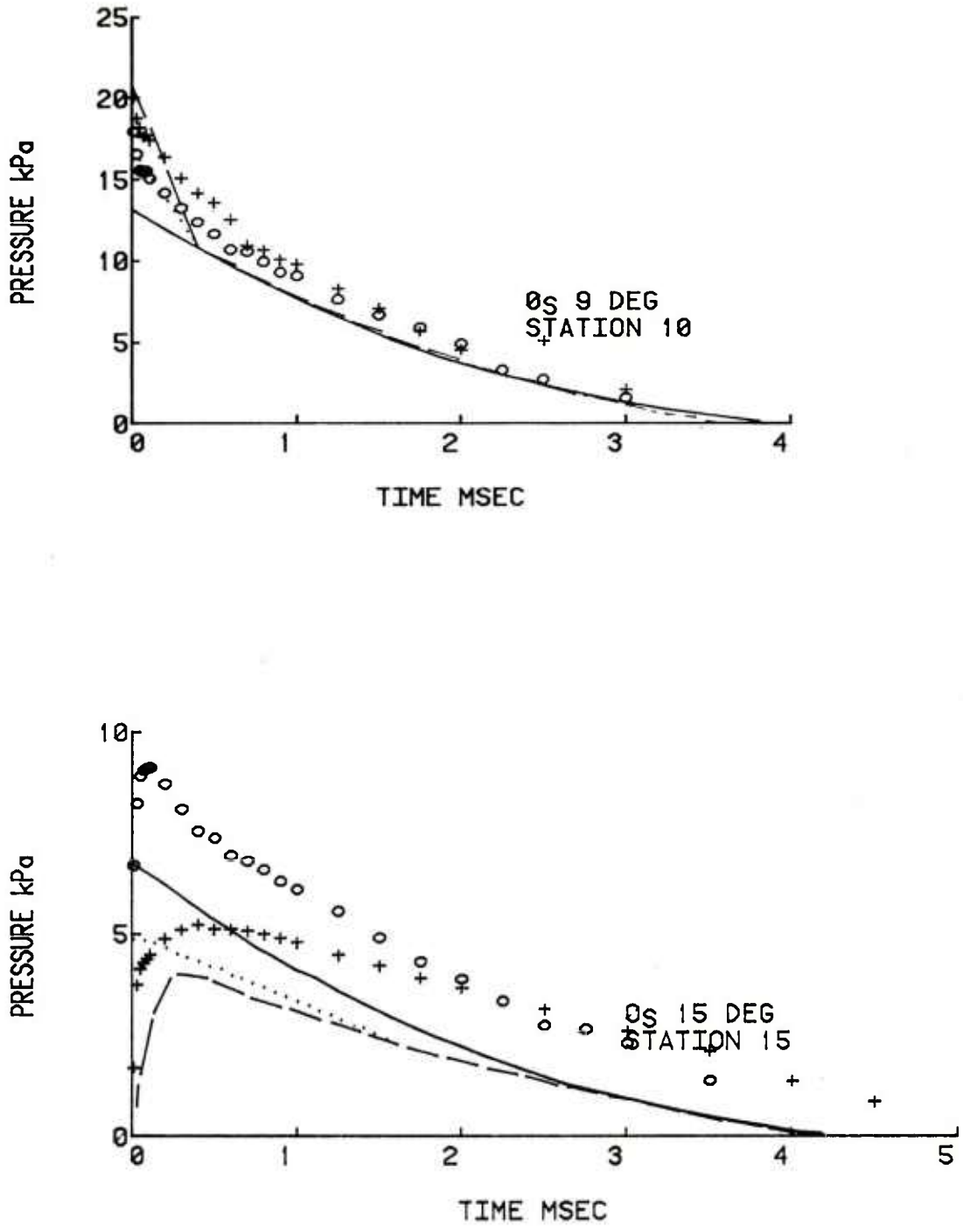

Figure C-8 (Cont). Overpressure along Line D-2 from a Burst over GZ-D

LIST OF SYMBOLS

D	Distance from ground zero
GZ	Ground zero
HOB	Height of burst, m
I	Impulse, kPa - ms
kPa	Kilopascal
kt	Kiloton (nuclear yield)
L	Distance along slope from first slope change, m
m	Metres
P_o	Ambient pressure, kPa
$P(0) = P_S$	Initial peak overpressure, kPa
P(t)	Blast overpressure behind front, kPa
s	Seconds
t	Time
T_A	Arrival time to reach station, s
T_O	Ambient temperature, $^{\circ}K$
W	Weight of explosive, kg
θ	Effective slope angle, deg
θ_s	Slope angle, deg
θ'	Modified effective slope angle, deg
ϕ	Blast wave approach angle, deg
τ	Positive duration, s
VDC	Volts direct current
pps	Pictures per second
Superscript (0)	Sea level conditions
Superscript (h)	Test conditions at altitude.

DISTRIBUTION LIST

No. of Copies	Organization
12	Commander Defense Documentation Center ATTN: DDC-DDA Cameron Station Alexandria, VA 22314
4	Director of Defense Research & Engineering ATTN: DD/TWP DD/S&SS DD/I&SS AD/SW Washington, DC 20301
3	Director Defense Advanced Research Projects Agency ATTN: Technical Library NMRO PMO 1400 Wilson Boulevard Arlington, VA 22209
6	Director Defense Nuclear Agency ATTN: STTL (Tech Lib, 2 cys) SPAS, Mr. J. Moulton DDST, Mr. P. H. Haas SPSS, Dr. George Ullrich SPAS, Mr. D. Kohler Washington, DC 20305
2	Commander Field Command, DNA ATTN: FCTMOF Kirtland AFB, NM 87115
2	Department of Defense Explosives Safety Board ATTN: R. Perkins Dr. Tom Zaker Room 856C, Hoffman Bldg. I 2461 Eisenhower Avenue Alexandria, VA 22331
1	Commander US Army Materiel Development and Readiness Command ATTN: DRCDMD-ST 5001 Eisenhower Avenue Alexandria, VA 22333
1	Commander US Army Aviation Research and Development Command ATTN: DRSAV-E 12th and Spruce Streets St. Louis, MO 63166
1	Director US Army Air Mobility Research & Development Laboratory Ames Research Center Moffett Field, CA 94035
1	Commander US Army Electronics Research & Development Command Tech Spt Activity ATTN: DELSD-L Fort Monmouth, NJ 07703
1	Commander US Army Communications Rsch and Development Command ATTN: DRDCO-PPA-SA Fort Monmouth, NJ 07703
3	Commander US Army Missile R&D Command ATTN: DRDMI-R DRDMI-YDL DRDMI-S, Chief Scientist Redstone Arsenal, AL 35809
2	Commander US Army Tank Automotive Research & Development Command ATTN: DRDTA-UL DRDTA-RHT, LT P. Hasek Warren, MI 48090

DISTRIBUTION LIST

No. of Copies	Organization
2	Commander US Army Armament Materiel Readiness Command ATTN: SARRI-LR, B. Morris DRSAR-LEP-L, Tech Lib Rock Island, IL 61229
4	Commander US Army Armament Research & Development Command ATTN: DRDAR-TSS (2 cys) P. Angelotti Mr. Demitrack Dover, NJ 07801
4	Commander US Army Harry Diamond Laboratories ATTN: DRXDO-TI/012 DRXDO-NP, F. Wimenitz DRXDO-NP, J. Gaul DRXDO-NP, J. Gwaltney 28 Powder Mill Road Adelphi, MD 20783
1	Director US Army Materials and Mechanics Research Center ATTN: Technical Library Watertown, MA 02172
1	Commander US Army Foreign Science and Technology Center ATTN: Research & Data Branch 220 7th Street, NE Charlottesville, VA 22901
3	Commander US Army Nuclear Agency ATTN: ATCN-W, CAPT M. Bowling CDINS-E Technical Library 7500 Backlick Road, Bldg 2073 Springfield, VA 22150
1	Director US Army TRADOC Systems Analysis Activity ATTN: ATAA-SL, Tech Library White Sands Missile Range New Mexico 88002
1	HGDA (DAMA-AR, NCB Division) Washington, DC 20310
3	Director US Army Advanced BMD Technology Center ATTN: Mr. B. E. Kelley Mr. M. Capps Mr. Marcus Whitfield P. O. Box 1500 Huntsville, AL 35807
1	Commander US Army Ballistic Missile Defense Systems Command ATTN: SSC-DH, H. Solomonson P. O. Box 1500 Huntsville, AL 35807
1	Commander US Army Ballistic Missile Defense Program Office ATTN: DACS-SAE-S, J. Shea 5001 Eisenhower Avenue Alexandria, VA 22333
2	Commander US Army Engineer Waterways Experiment Station ATTN: Library W. Flateau P. O. Box 631 Vicksburg, MS 39180

DISTRIBUTION LIST

No. of Copies	Organization
2	Chief of Naval Research Department of the Navy ATTN: T. Quinn, Code 461 J.L. Warner, Code 461 Washington, DC 20360
2	Commander Naval Ship Eng'g Center ATTN: J. R. Sullivan NSEC 6105-G Technical Library Hyattsville, MD 20782
4	Commander Naval Surface Weapons Center ATTN: Code 1224, Navy Nuclear Programs Office Code 241, J. Petes Code 730, Tech Library J. Pittman Silver Spring, MD 20910
1	Commander Naval Weapons Evaluation Fac ATTN: Document Control Kirtland AFB, NM 87117
1	Commander Naval Civil Engineering Lab ATTN: Dr. W. A. Shaw, Code L31 Port Hueneme, CA 93041
3	Director Naval Research Laboratory ATTN: M. Persechino G. Cooperstein Tech Lib, Code 2027 Washington, DC 20375
1	HQ USAFSC (DLCAW, Tech Library) Andrews AFB Washington, DC 20331
1	AFOSR (OAR) Bolling AFB, DC 20332
1	RADC (Document Lib, FMTLD) Griffis AFB, NY 13440
4	AFWL (CA, Dr. A. Guenther DYT, Charles Needham DYT, MAJ G. Gonong; S. Melzer) Kirtland AFB, NM 87117
1	AFCRL L. G. Hanscom Field Bedford, MA 01730
1	SAMSO (Library) P. O. Box 92960 Los Angeles, CA 90009
3	AFTC (K. Rosenlof R. McBride G. Leies) Patrick AFB, FL 32925
2	AFML (G. Schmitt, MAS; D. Schmidt) Wright-Patterson AFB, OH 45433
2	Energy Research & Development Administration Department of Military Application ATTN: R&D Branch Library Branch, G-043 Washington, DC 20545
2	Director Los Alamos Scientific Laboratory ATTN: Dr. J. Taylor Technical Library P. O. Box 1663 Los Alamos, NM 87554

DISTRIBUTION LIST

No. of Copies	Organization
1	Director, NASA ATTN: Code 04.000 Langley Research Center Langley Station Hampson, VA 23365
1	Director NASA Scientific & Technical Information Facility ATTN: SAK/DL P. O. Box 8757 Baltimore/Washington International Airport, MD 21240
1	National Academy of Sciences ATTN: Dr. Donald Groves 2101 Constitution Avenue, NW Washington, DC 20418
1	Aerospace Corporation ATTN: Tech Information Svcs, Bldg 105, Rm 2220 P. O. Box 92957 Los Angeles, CA 90009
1	Agbabian Associates ATTN: Dr. J. Malthan 250 N. Nash Street El Segundo, CA 90245
1	AVCO Government Products Group ATTN: Dr. W. Bade 201 Lowell Street Wilmington, MA 01887
1	AVCO-Everett Research Laboratory ATTN: Technical Library 2385 Revere Beach Parkway Everett, MA 02149
1	John A. Blume & Associates ATTN: Dr. John A. Blume Sheraton-Palace Hotel 100 Jessie Street San Francisco, CA 94105
1	CALSPAN Corporation ATTN: Library P. O. Box 235 Buffalo, NY 14221
1	Effects Technology, Inc. ATTN: E. Anderson 5383 Holister Avenue Santa Barbara, CA 93105
1	General Electric Co. - TEMPO ATTN: DASIAC 816 State Street, Drawer QQ Santa Barbara, CA 93102
1	General Electric Co.-TEMPO ATTN: Dr. Lynn Kennedy 7800 Marble Avenue, NE, Suite 5 Albuquerque, NM 87110
1	H-Tech Laboratories, Inc. ATTN: B. Hartenbaum P. O.Box 1686 Santa Monica, CA 90406
1	Hughes Aircraft Company Systems Development Laboratory ATTN: Dr. A. Puckett Centinela and Teale Streets Culver City, CA 92032
1	Ion Physics Corporation ATTN: Technical Library South Bedford Street Burlington, MA 01803

DISTRIBUTION LIST

No. of Copies	Organization
1	Kaman Sciences Corporation ATTN: Dr. D. Sachs 1500 Garden of the Gods Road Colorado Springs, CO 80907
1	Kaman Avidyne, Division of Kaman Sciences ATTN: Dr. J. Ray Ruetenik 83 2nd Ave, NW Industrial Park Burlington, MA 01803
1	KTECH Corporation ATTN: Dr. Donald V. Keller 911 Pennsylvania NE Albuquerque, NM 87110
1	Lockheed Missiles & Space Co, Inc. Division of Lockheed Aircraft Corp ATTN: J. Nickell P. O. Box 504 Sunnyvale, CA 94088
1	Management Science Associates ATTN: Kenneth Kaplan P. O. Box 239 Los Altos, CA 94022
1	Martin Marietta Aerospace Orlando Division ATTN: A. Ossin P. O. Box 5837 Orlando, FL 32805
1	Maxwell Laboratories, Inc. ATTN: A. Kolb 9244 Balboa Avenue San Diego, CA 92123
1	McDonnell Douglas Astronautics Corporation 5301 Bolsa Avenue Huntington Beach, CA 92647
1	Philco Ford Corporation Aeronutronic Division ATTN: L. K. Goodwin Newport Beach, CA 92663
2	Physics International Company ATTN: Document Control Fred Sauer 2700 Merced Street San Leandro, CA 94577
3	R&D Associates ATTN: Technical Library Jerry Carpenter Allen Kuhl P. O. Box 9695 Marina del Rey, CA 90291
1	Sandia Laboratories ATTN: Dr. J. Kennedy P. O. Box 5800 Albuquerque, NM 87115
2	Science Applications, Inc ATTN: Mr. J. W. Miller Dr. John Cockayne 8400 West Park Drive McLean, VA 22101
1	Shock Hydrodynamics, Inc. ATTN: L. Zernow 4710-16 Vineland Avenue N. Hollywood, CA 91602
1	Systems, Science & Software ATTN: Technical Library P. O. Box 1620 La Jolla, CA 92036
2	SRI International ATTN: Dr. H. Murphy J. Remple 333 Ravenswood Avenue Menlo Park, CA 94025

DISTRIBUTION LIST

No. of Copies	Organization
1	Teledyne-Brown Engineering ATTN: Dr. M. Batel Research Park Huntsville, AL 35807
1	Union Carbide Corporation Oak Ridge National Laboratory ATTN: Technical Library P. O. Box X Oak Ridge, TN 37830
1	URS Research Company ATTN: Technical Library 155 Bovet Road San Mateo, CA 94002
1	Battelle Memorial Institute ATTN: Technical Library 505 King Avenue Columbus, Ohio 43201
2	Denver Research Institute University of Denver ATTN: Mr. John Wisotski P. O. Box 10127 Denver, CO 90210
1	Director Applied Physics Laboratory The Johns Hopkins University Johns Hopkins Road Laurel, MD 20810
1	Lovelace Rsch Institute ATTN: Dr. D. Richmond P. O. Box 5890 Albuquerque, NM 87108
1	Massachusetts Institute of Technology Aerophysics Laboratory Cambridge, MA 02139
1	New Mexico Institute of Mining and Technology ATTN: Mr. P. McClain Socorro, NM 87801
1	Northwestern Michigan College ATTN: Prof. D. C. Kennard, Jr. Traverse City, MI 49584
1	Southwest Research Institute ATTN: Dr. W. Baker 8500 Culebra Road San Antonio, TX 78206
1	Stevens Institute of Technology Dept of Electrical Engineering ATTN: Prof. R. Geldmacher Castle Point Station Hoboken, NJ 07039
1	Research Institute of Temple University ATTN: Technical Library Philadelphia, PA 19144
1	Texas Tech University Dept of Civil Engineering ATTN: Mr. Joseph E. Minor Lubbock, TX 79409
1	University of Arkansas Department of Physics ATTN: Prof. O. Zinke Fayetteville, AR 72701
1	University of California Lawrence Livermore Laboratory Technical Information Division ATTN: Technical Library Dr. Donald N. Montan P. O. Box 808 Livermore, CA 94550

DISTRIBUTION LIST

No. of Copies	Organization
1	University of Illinois Consulting Engineering Services ATTN: Nathan M. Newmark 1211 Civil Engineering Building Urbana, IL 61801
1	University of Maryland Department of Physics ATTN: Dr. E. Oktay College Park, MD 20742
1	The university of Michigan Gas Dynamics Laboratory ATTN: Z. Gabrijel Aerospace Engineering Building Ann Arbor, MI 48109
1	The University of New Mexico Eric H. Wang Civ Eng'g Res Fac ATTN: Technical Library University Station, Box 188 Albuquerque, NM 87131
1	University of Oklahoma Department of Physics ATTN: Prof. R. Fowler Norman, OK 73069

Aberdeen Proving Ground

Director, USAMSAA
ATTN: Dr. J. Sperrazza
Mr. R. Norman, GWD
DRXSY-MP, H. Cohen
Cdr, USATECOM
ATTN: DRSTE-TO-F
Dir, Wpns, Sys Concepts Team
Bldg E3516, EA
ATTN: DRDAR-ACW

USER EVALUATION OF REPORT

Please take a few minutes to answer the questions below; tear out this sheet and return it to Director, US Army Ballistic Research Laboratory, ARRADCOM, ATTN: DRDAR-TSB, Aberdeen Proving Ground, Maryland 21005. Your comments will provide us with information for improving future reports.

1. BRL Report Number _____

2. Does this report satisfy a need? (Comment on purpose, related project, or other area of interest for which report will be used.)

_____

_____

_____

3. How, specifically, is the report being used? (Information source, design data or procedure, management procedure, source of ideas, etc.) _____

_____

_____

4. Has the information in this report led to any quantitative savings as far as man-hours/contract dollars saved, operating costs avoided, efficiencies achieved, etc.? If so, please elaborate.

_____

_____

5. General Comments (Indicate what you think should be changed to make this report and future reports of this type more responsive to your needs, more usable, improve readability, etc.) _____

_____

_____

_____

6. If you would like to be contacted by the personnel who prepared this report to raise specific questions or discuss the topic, please fill in the following information.

Name: _____

Telephone Number: _____

Organization Address: _____

_____

_____